To the Graduate Council:

I am submitting herewith a dissertation written by Mark C Burleigh entitled "Molecular Imprinting of Organofunctionalized Sol-gel Materials for Metal Ion Separations." I have examined the final copy of this dissertation for form and content and recommend that it be accepted in partial fulfillment of the requirements for the degree of Doctor of Philosophy, with a major in Chemistry.

Dr Ziling Ben Xue, Major Professor

We have read this dissertation
and recommend its acceptance

Dr Sheng Dai

Dr. Mark Dadmun

Dr Craig Barnes

Dr Paul Bienkowski

Accepted for the Council

Associate Vice Chancellor and
Dean of The Graduate School

MOLECULAR IMPRINTING OF ORGANOFUNCTIONALIZED SOL-GEL MATERIALS FOR METAL ION SEPARATIONS

A Dissertation

Presented for the

Doctor of Philosophy

Degree

The University of Tennessee, Knoxville

Mark Charles Burleigh

August 2000

ACKNOWLEDGMENTS

Many people provided technical assistance in the progress of this work. First of all I would like to thank Dr. Sheng Dai [Chemical Technology Division, Oak Ridge National Laboratory (ORNL)], for his expert guidance during the course of this work. Special thanks go to my committee for their careful reading of this dissertation. For technical assistance, I wish to thank Dr. Jar-Shyong Lin (Solid State Division, ORNL) for help with the small angle x-ray scattering experiments, and Dr. Edward Hagaman (Chemical and Analytical Sciences Division, ORNL) for his help with solid-state NMR experiments.

I am grateful for the friendships that I have made during my graduate studies. I would like to thank Dr. David Beach (Chemical and Analytical Sciences Division) for his technical assistance and advice throughout my four years at ORNL. I would also like to thank fellow group member Dr. Jonathan Diminnie (Olin Corporation) for his help and guidance. This research would not have been possible without the support of my many co-workers. Special thanks go to fellow lab mates Dr. Said Waesada and Dr. Rajendra Makote.

Most importantly, I am grateful to my family for their support and patience through these years of higher education. I am thankful for the many members of my

extended family who have given much inspiration and encouragement during the difficult times.

This work was supported by the U. S. Department of Energy, Division of Basic Energy Sciences, Office of Science, under contract No. DE-AC05-96OR22464, and the Environmental Management and Science Program, under contract No. DE-FG07-97ER14817 and was performed at the Oak Ridge National Laboratory.

ABSTRACT

This dissertation describes the synthesis and characterization of new metal ion sorbent materials. These materials exhibit many favorable properties such as high metal ion capacities, metal ion selectivity, fast kinetics, and easy regeneration. Sorbents have been developed to selectively adsorb Cu(II), Zn(II), and Ni(II) cations.

A combination of four primary synthetic techniques were used to create mesoporous sorbents with specific adsorption characteristics. The hydrolysis and condensation of silicon alkoxide precursors via sol-gel reactions leads to the formation of a solid matrix. Bifunctional reagents were used to graft amine moeities to the solid support and give the sorbent a high affinity for metal ions. Molecular imprinting techniques were used to create metal ion binding sites that are designed to bind to a specific metal ion. The surfactant template approach was used to engineer the porosity of the sorbents.

Four new methodologies have been developed and described herein: imprint coating, stepwise assembly, double imprinting, and organic-inorganic polymer imprinting. The imprint coating technique involves grafting of metal ion complexes of bifunctional reagents to the surface of mesoporous silica. Acid leaching of the metal ion template results in the formation of selective binding sites in which the ligands are

arranged in a conformation well suited to rebind the template. In stepwise assembly, the bifunctional reagent is first grafted to mesoporous silica, followed by metal ion complex formation and the addition of more bifunctional reagent. In the double imprinting methodology, metal ion complexes of bifunctional reagents undergo copolymerization with silicon alkoxide precusors in the presence of supramolecular assemblies of surfactant molecules in a single step synthesis. Surfactant extraction gives a porous matrix with a large surface area. Hybrid organic-inorganic sorbents were synthesized using a protocol similar to double imprinting, except that the sol-gel precursor used was a bridged silicon alkoxide containing an ethylene group.

These sorbent materials have been characterized by a variety of techniques including: ^{29}Si solid-state nuclear magnetic resonance spectroscopy, N_2 adsorption, powder X-ray diffraction, UV/visible spectroscopy, and batch testing with subsequent ICP/OES analysis. These organofunctionalized sol-gel materials exhibit a number of favorable properties including: enhanced capacities for the target metal ion, selective adsorption of the target metal ion from mixed solutions containing competitor species, fast metal ion uptake kinetics, and easy regeneration.

TABLE OF CONTENTS

CHAPTER PAGE

1. INTRODUCTION 1

2. SYNTHESIS OF MESOPOROUS SILICA 11

I. Introduction 11

II. Analytical Methods 14

III. Synthesis and Characterization of Mesoporous Silica 15

III.1. MCM-41 15

III.1.1. Synthesis 15

III.1.2. Characterization 16

III.2. CTAB/mesitylene Silica 19

III.2.1. Synthesis 19

III.2.2. Characterization 21

III.3. CTAB/H^+ Silica 21

III.3.1. Synthesis 23

III.3.2. Characterization 23

III.4. HMS 25

III.4.1. Synthesis 28

III.4.2. Characterization 28
III.5. Tween 80 Silica 30
III.5.1. Synthesis 33
III.5.2. Characterization 33
III.6. Pluronic Surfactants 36
III.6.1. Pluronic F127 Silica 37
III.6.1.1. Synthesis 37
III.6.1.2. Characterization 38
III.6.2. Pluronic P85 Silica 41
III.6.2.1. Synthesis 41
III.6.2.2. Characterization 42
III.6.3. Pluronic P123 Silica 42
III.6.3.1. Synthesis 42
III.6.3.2. Characterization 44
II.7. Reproducibility 47
IV. Conclusions 47
3. IMPRINT COATING OF MESOPOROUS SILICA 52
I. Introduction 52
II. Preliminary Experiments 63

II.1. Synthesis 64

II.1.1. Cu(II)/TMSen/MCM-41 64

II.1.2. Cu(II)/TMSA/MCM-41 65

II.2. Batch Tests 65

II.3. Analytical Techniques 66

II.4. Metal(II) Sorption Calculations 66

II.5. Results and Discussion 67

III. Imprint Coating of Amorphous Silica 72

III.1. Synthesis 73

III.1.1. Cu(II)/TMSen/SG/MeOH 73

III.1.2. Cu(II)/TMSen/SG/H_2O 74

III.1.3. Cu(II)/TMSA/SG/H_2O 74

III.2. Results and Discussion 75

IV. Imprint Coating of BTMSen on CTAB/H^+ Silica 80

IV.1. Synthesis 81

IV.1.1. Cu(II)/BTMSen/CTAB/H^+ Silica 81

IV.2. Copper(II) Adsdorption 83

IV.3. Copper(II) vs. Zinc(II) Selectivity 85

IV.4. Discussion 85

V. Imprint Coating of TMSen on MCM-41 89

V.1. Synthesis 89

V.1.1. Cu(II)/TMSen/MCM-41 90

V.2. Copper(II) Adsorption 90

V.3. Copper(II) vs. Zinc(II) Selectivity 93

V.4. Adsorption of Divalent Cations on Calcined MCM-41 93

VI.4. Discussion 95

VI. Ethylenediamine as a Competitor Species 98

VI.1. Synthesis 98

VI.2. Copper(II) vs. Zinc(II) Selectivity with Free Ethylenediamine 99

VI.3. Discussion 101

VII. Stability of TMSen MCM-41 Imprint Coated Sorbents 104

VII.1. Synthesis 105

VII.2. Copper(II) Adsorption 106

VII.3. Copper(II) vs. Zinc Selectivity 108

VII.4. N_2 Adsorption Analysis 108

VII.5. Discussion 113

VIII. Imprint Coating of TMSen on Pluronic P123 Silica 114

VIII.1. Synthesis 114

VIII.2. Copper(II) Adsorption 115

VIII.3. Copper(II) vs. Zinc(II) Selectivity 115

VIII.4. Adsorption of Divalent Cations on Calcined Pluronic P123 Silica 118

VIII.5. Discussion 120

IX. Imprint Coating of TMSen on Pluronic P123 Silica with Low Ligand Loading 121

IX.1. Synthesis 122

IX.2. Ligand Loading Capacity via Cu(II) Leaching 123

IX.3. Copper(II) Adsorption 124

IX.4. Copper Adsorption as a Function of pH 127

IX.5. Discussion 128

X. Ion Exchange Properties of Imprint Coated Sorbents 133

X.1. Synthesis 133

X.1.1. Zn(II)/TMSen/MCM-41/EtOH 133

X.1.2. Ni(II)/TMSen/MCM-41/EtOH 134

X.2. Ion Exchange Batch Tests 134

X.3. Discussion 138

XI. Ligand Loading Capacity via Solid-State NMR 139

XI.1. Synthesis 139

XI.2. Analytical Method 140

XI.3. Results and Discussion 141

4. STEPWISE ASSEMBLY OF SURFACE IMPRINT SITES ON MESOPOROUS SILICA 150

I. Introduction 150

II. Experimental 151

II.1. Synthesis of the MCM-41 Mesoporous Support 151

II.2. Functionalization and Imprinting 153

II.3. Post-synthetic Treatment 153

II.4. Batch Procedures 154

II.5. Analyses 154

III. Results and Discussion 155

III.1. MCM-41 Characterization 155

III.2. Stepwise Methodology 155

III.3. Copper(II) Adsorption 157

III.4. Copper(II) vs. Zinc(II) Selectivity 160

III.5. Solid-State ^{29}Si NMR Analyses of Sorbents 162

IV. Conclusions 165

5. DOUBLE IMPRINTING OF AN ORGANOFUNCTIONALIZED SOL-GEL FOR SELECTIVE METAL ION SEPARATIONS 167

I. Introduction 167

II. Synthesis 169

III. Copper(II) Adsorption 174

IV. Copper(II) Adsorption Kinetics 174

V. Copper(II) vs. Zinc(II) Selectivity 174

VI. Copper(II) vs. Zinc(II) Selectivity as a Function of pH 177

VII. N_2 Adsorption 177

VIII. Ligand Loading Capacity 180

IX. Zinc(II) Imprinted Sorbent 181

X. Conclusions 181

6. MOLECULAR IMPRINTING OF AN ORGANIC-INORGANIC HYBRID POLYMER FOR THE ENHANCED RECOGNITION OF METAL IONS 184

I. Introduction 184

II. Experimental 186

II.1. Synthesis 186

II.1.1. Blank Hybrid 186

II.1.2. Nonimprinted Hybrid 187

II.1.3. Copper(II) Imprinted Hybrid 187

II.1.4. Nickel(II) and Zinc(II) Imprinted Hybrids 187

II.2. Post-synthetic Processing 188

II.3. Batch Procedures 188

II.3. Analytical Techniques 189

III. Results and Discussion 189

III.1. Synthesis 189

III.2. Functionalization 190

III.3. Surfactant Templating 190

III.4. Molecular Imprinting 191

III.5. Metal Ion Sorption 192

III.5.1. Metal(II) Uptake Capacity 192

III.5.1.1. Copper(II) Imprinted Hybrid 192

III.5.1.2. Nickel(II) Imprinted Hybrid 192

III.5.1.3. Zinc(II) Imprinted Hybrid 195

III.5.2. Metal(II) Selectivity 200

III.5.2.1. Cu(II) vs. Zn(II) Selectivity 201

III.5.2.2. Ni(II) vs. Zn(II) Selectivity 207

III.5.2.3. Divalent Cation Mixture 207

III.6. Adsorption Kinetics 210

III.7. Multiple Use Cycles 210

III.8 Small Angle X-ray Scattering 215

III.9 N_2 Adsorption 215

III.10. UV-Visible Spectroscopy 220

III.10.1. Nonimprinted hybrid 223

III.10.2. Copper(II) Imprinted Hybrid 223

IV. Conclusions 226

4. CONCLUSIONS 228

I. Introduction 228

II. Mesoporous Silica 229

III. Imprint Coating 231

IV. Stepwise Assembly 236

V. Double Imprinting 237

VI. Organic-Inorganic Hybrid 237

VII. Future Studies 239

LIST OF REFERENCES 241

VITA 248

LIST OF TABLES

TABLE		PAGE
2.1	Surface Areas of Synthesized Mesoporous Silicas	49
3.1	Cu(II) Uptake Capacity of Cu(II) Imprint Coated and Nonimprinted Sorbents	68
3.2	Competitive Loading of Cu(II) and Zn(II) by Cu(II) Imprinted and Nonimprinted Sorbents	70
3.3	Cu(II) Uptake Capacity of Cu(II) Imprinted and Nonimprinted Sorbents Coated on Amorphous Silica	76
3.4	Competitive Loading of Cu(II) and Zn(II) by Cu(II) Imprinted and Nonimprinted Sorbents Coated on Amorphous Silica	77
3.5	Competitive Loading of Cu(II) and Zn(II) by Cu(II) Imprinted and Nonimprinted Sorbents Coated on Amorphous Silica	78
3.6	Cu(II) Uptake capacity of BTMSen/CTAB/H^+ Sorbents	84
3.7	Competitive Loading of Cu(II) and Zn(II) by BTMSen/CTAB/H^+ Sorbents	86
3.8	Cu(II) Uptake Capacity of TMSen/MCM-41 Sorbents	91
3.9	Competitive Loading of Cu(II) and Zn(II) by TMSen/MCM-41 Sorbents	94
3.10	Adsorption of Divalent Cations on Calcined MCM-41 at pH = 5.0	96
3.11	Competitive Loading of Cu(II) and Zn(II) by TMSen/MCM-41 Sorbents in the Presence of Ethylenediamine	100
3.12	Cu(II) Uptake Capacity of TMSen/MCM-41 Sorbents	107
3.13	Competitive Loading of Cu(II) and Zn(II) by TMSen/MCM-41 Sorbents	109

3.14 Porosity data of Imprint Coated Sorbents 112

3.15 Cu(II) Uptake Capacity of TMSen/P123 Sorbents 116

3.16 Competitive Loading of Cu(II) and Zn(II) by TMSen/P123 Sorbents 117

3.17 Adsorption of Cu(II), Zn(II), and Ni(II) on Calcined Pluronic P123 Silica . 119

3.18 Cu(II) Uptake Capacity of TMSen/P123 Sorbents with Low Ligand Loading 125

3.19 Cu(II) Uptake Capacity of TMSen/P123 Sorbents as a Function of pH 129

3.20 Ion Exchange Properties of Ni(II) Loaded TMSen/MCM-41 135

3.21 Ion Exchange Properties of Zn(II) Loaded TMSen/MCM-41 137

4.1 Cu(II) Uptake of Cu(II) Imprinted and Nonimprinted Sorbents 158

4.2 Sorbent Metal Ion Selectivity [Cu(II) vs. Zn(II)] 161

5.1 Cu(II) Uptake of Cu(II) Imprinted and Nonimprinted Sorbents prepared via Double Imprinting 175

5.2 Porosity Data for Cu(II) Imprinted and Nonimprinted Sorbents Prepared via Double Imprinting 175

5.3 Porosity Data for Cu(II) Imprinted and Nonimprinted Sorbents Prepared via Double Imprinting 182

5.4 Cu(II) vs. Zn(II) Selectivity of Nonimprinted, Cu(II) Imprinted, and Zn(II) Imprinted Sorbents 182

6.1 Copper(II) Uptake of Cu(II) Imprinted and Nonimprinted Hybrid Sorbents 193

6.2 Nickel(II) Uptake of Cu(II) Imprinted and Nonimprinted Hybrid Sorbents . 196

6.3 Zinc(II) Uptake of Cu(II) Imprinted and Nonimprinted Hybrid Sorbents .. 198

6.4 Cu(II) vs. Zn(II) Selectivity of Cu(II) Imprinted and Nonimprinted Hybrid Sorbents 202

6.5 Cu(II) vs. Zn(II) Selectivity of Cu(II) Imprinted and Nonimprinted Hybrid Sorbents 203

6.6 Ni(II) vs. Zn(II) Selectivity of Cu(II) Imprinted and Nonimprinted Hybrid Sorbents 208

6.7 Small Angle X-ray Scattering Data of Hybrid Sorbents 219

6.8 Porosity Data of Hybrid Sorbents 219

LIST OF FIGURES

FIGURE		PAGE
2.1	Mechanism for the Formation of MCM-41	13
2.2	The Structure of Cetyltrimethylammonium Bromide	17
2.3	N_2 Adsorption/Desorption Isotherm of Calcined MCM-41	17
2.4	Pore Size Distribution of Calcined MCM-41	18
2.5	Powder X-ray Diffraction Pattern of As-synthesized MCM-41	18
2.6	Powder X-ray Diffraction Pattern of Calcined MCM-41	20
2.7	Mechanism of Mesitylene Pore Expander	20
2.8	N_2 Adsorption/Desorption Isotherm of CTAB/mesitylene Silica	22
2.9	Pore Size Distribution of Calcined CTAB/mesitylene Silica	22
2.10	Powder X-ray Diffraction Pattern of CTAB/mesitylene Silica	24
2.11	N_2 Adsorption/Desorption Isotherm of CTAB/H^+ Silica	24
2.12	Pore Size Distribution of Calcined CTAB/H^+ Silica	26
2.13	N_2 Adsorption/Desorption Isotherm of Extracted CTAB/H^+ Silica	26
2.14	Pore Size Distribution of Extracted CTAB/H^+ Silica	27
2.15	Powder X-ray Diffraction Pattern of Calcined CTAB/H^+ Silica	27
2.16	Powder X-ray Diffraction Pattern of As-synthesized CTAB/H^+ Silica	29
2.17	Structure of Dodecylamine	29

2.18 N_2 Adsorption/Desorption Isotherm of HMS 31

2.19 Pore Size Distribution of HMS 31

2.20 Powder X-ray Diffraction Pattern of As-synthesized HMS 32

2.21 Powder X-ray Diffraction Pattern of Calcined HMS 32

2.22 Structure of Tween 80 34

2.23 N_2 Adsorption/Desorption Isotherm of Tween 80 Silica 34

2.24 Pore Size Distribution of Tween 80 Silica 35

2.25 Powder X-ray Diffraction Pattern of Tween 80 Silica 35

2.26 General Structure of Pluronic Surfactants 39

2.27 N_2 Adsorption/Desorption Isotherm of Pluronic F127 Silica 39

2.28 Pore Size Distribution of Pluronic F127 Silica 40

2.29 Powder X-ray Diffraction Pattern of Pluronic F127 Silica 40

2.30 N_2 Adsorption/Desorption Isotherm of Pluronic P85 Silica 43

2.31 Pore Size Distribution of Pluronic P85 Silica 43

2.32 Powder X-ray Diffraction Pattern of Pluronic P85 Silica 45

2.33 N_2 Adsorption/Desorption Isotherm of Pluronic P123 Silica 45

2.34 Pore Size Distribution of Pluronic P123 Silica 46

2.35 Powder X-ray Diffraction Pattern of Pluronic P123 Silica 46

2.36 TEM Image of Calcined Pluronic P123 Silica 48

3.1 Mechanism of Ligand Grafting to Silica Surface 53

3.2 Cross-sectional Views of Ordered and Amorphous Silicas 56

3.3 Schematic Representation of Molecular Imprinting 58

3.4 Mechanism of Imprint Coating Functionalization 60

3.5 Conventional Surface Functionalization Procedure 61

3.6 Binding Cavaties Created by Conventional Coating and Imprint Coating . . . 62

3.7 UV/Visible Spectra of Imprint Coated Complexes 71

3.8 Structure of Bis[(3-trimethoxysilyl)propyl]ethylenediamine 82

3.9 Flexibility of Grafted TMSen and BTMSen 82

3.10 Copper(II) Adsorption Isotherms of TMSen/MCM-41 Sorbents 92

3.11 Copper(II) Adsorption on Imprint Coated Sorbent and Entropy Change . . . 103

3.12 N_2 Adsorption/Desorption Isotherm of Calcined MCM-41 110

3.13 N_2 Adsorption/Desorption Isotherm of StabSN Sorbent 110

3.14 N_2 Adsorption/Desorption Isotherm of StabHN Sorbent 111

3.15 N_2 Adsorption/Desorption Isotherm of StabFN Sorbent 111

3.16 Copper(II) Adsorption of TMSen/Pluronic P123 Silica with Low Ligand Loading 126

3.17 Copper(II) Adsorption of TMSen/Pluronic P123 Silica as a Function of pH 130

3.18 Possible Bonding Modes of ^{29}Si in Imprint Coated Sorbents 142

3.19 Solid-state ^{29}Si SPE/MAS NMR Spectrum of Calcined MCM-41 143

3.20 Solid-state ^{29}Si SPE/MAS NMR Spectrum of Cu(II) Imprint Coated for 4h 144

3.21 Solid-state ^{29}Si SPE/MAS NMR Spectrum of Nonimprint Coated for 4h .. 145

3.22 Solid-state ^{29}Si SPE/MAS NMR Spectrum of Cu(II) Imprint Coated for 8h 147

3.23 Solid-state ^{29}Si SPE/MAS NMR Spectrum of Nonimprint Coated for 8h .. 148

4.1 Preparation of the Mesoporous Support 152

4.2 Mechanism of Stepwise Assembly 156

4.3 Structures of Imprinted and Nonimprinted TMSen Sorbents 159

4.4 Solid-state ^{29}Si SPE/MAS NMR Spectrum of Cu(II) Imprinted Stepwise Sorbent 163

4.5 Solid-state ^{29}Si SPE/MAS NMR Spectrum of Stepwise Sorbent 164

5.1 Preparation of Cu(II) Imprinted Sorbent via Double Imprinting 171

5.2 Post-synthetic Processing of Sorbents Created via Double Imprinting 173

5.3 Copper(II) Uptake Kinetics of Sorbent Prepared via Double Imprinting ... 176

5.4 Metal Ion Selectivity of Sorbents Prepared via Double Imprinting 178

5.5 N_2 Adsorption Isotherms of Cu(II) Imprinted and Nonimprinted Sorbents . 179

6.1 Copper(II) Percentage Sorption Isotherm 194

6.2 Copper(II) K_d Sorption Isotherm 194

6.3 Nickel(II) Percentage Sorption Isotherm 197

6.4 Nickel(II) K_d Sorption Isotherm 197

6.5 Zinc(II) Percentage Sorption Isotherm 199

6.6 Zinc(II) K_d Sorption Isotherm 199

6.7 Cu(II) vs. Zn(II) Selectivity of Cu(II) Imprinted and Nonimprinted Sorbents 205

6.8 Cu(II) vs. Zn(II) Adsorption Percentage of Hybrid Sorbents 206

6.9 Ni(II) vs. Zn(II) Uptake on Ni(II) Imprinted Hybrid 209

6.10 Ni(II) vs. Zn(II) Uptake on Zn(II) Imprinted Hybrid 209

6.11 Metal Ion Adsorption on Copper(II) Imprinted Hybrid 211

6.12 Copper(II) Adsorption Kinetics of Hybrid Sorbent 212

6.13 Recycleability of Hybrid Sorbents 214

6.14 SAXS Plots of Hybrid Sorbents 216

6.15 N_2 Adsorption Isotherms of Hybrid Sorbents 217

6.16 Arrangement of TMSen Ligands in Hybrid Sorbents 221

6.17 UV-Visible Spectra of Cu(II):TMSen Sorbents 222

6.18 UV-Visible Spectra of Nonimprinted Hybrid Sorbent 224

6.19 UV-Visible Spectra of Copper(II) Imprinted Hybrid Sorbent 225

LIST OF ABBREVIATIONS

BET	method of Brunauer, Emmett, and Teller
BJH	method of Barrett, Joyner, and Halenda
BTMSen	bis[(3-trimethoxysilyl)propyl]ethylenediamine
BTSE	bis(trimethoxysilyl)ethane
CTAB	cetyltrimethylammonium bromide
CTAC	cetyltrimethylammonium chloride
D_{max}	pore size distribution maxima
EPR	electron paramagnetic resonance spectroscopy
HMS	hexagonally packed mesoporous silica
ICP/OES	inductively coupled plasma optical emmission spectroscopy
IUPAC	International Union of Pure and Applied Chemistry
K_d	distribution coefficient
k	selectivity coefficient
k'	relative selectivity coefficient
MCM-41	mesoporous silica
M41S	family of mesoporous silicas
PET	polyethylene terephthalate

SAXS	small angle X-ray scattering
SG	silica gel
TEM	transmission electron microscopy
TEOS	tetraethyl orthosilicate
TMSA	3-(trimethoxysilyl)propylamine
TMSen	N-[3-(trimethoxysilyl)propyl]ethylenediamine
XRD	X-ray diffraction

LIST OF CHEMICALS

FORMULA	VENDOR
$CH_3(CH_2)_{15}N(CH_3)_3Br$ (CTAB)	Aldrich
$CH_3(CH_2)_{15}N(CH_3)_3Cl$ (CTAC)/25% in water	Aldrich
Tween 80	Aldrich
$EO_{106}PO_{70}EO_{106}$ (Pluronic F127)	BASF
$EO_{26}PO_{39}EO_{26}$ (Pluronic P85)	BASF
$EO_{20}PO_{70}EO_{20}$ (Pluronic F123)	BASF
$C_6H_3(CH_3)_3$/99.5%+ (mesitylene)	Fluka
$Cu(NO_3)_2$ $3H_20$/98%+	Aldrich
$Zn(NO_3)_2$ $6H_20$/98%+	Aldrich
$Ni(NO_3)_2$ $6H_20$/98%+	Aldrich
$Cd(NO_3)_2$ $4H_20$/98%+	Aldrich
$C_8H_{22}O_6Si_2$ (BTSE)	Gelest
$C_{14}H_{36}N_2O_6Si_2$ (BTMSen)/62% in methanol	Gelest
$C_8H_{22}N_2O_3Si$ (TMSen)	Gelest
$C_6H_{17}NO_3Si$ (TMSA)	Gelest
$Si(OC_2H_5)_4$ (TEOS)	Aldrich

MeOH/99.8%+	J.T. Baker
EtOH/99.5%+	J.T. Baker
$C_6H_5CH_3$/99.5%+ (toluene)	J.T. Baker
NH_4OH/7.7 M	J.T. Baker
HCl/37%	J.T. Baker
HNO_3/70%	J.T. Baker

CHAPTER 1

INTRODUCTION

Men have harnessed the unique properties of metals since ancient times. Durability, ductility, malleability, and conductivity are some of the specific properties which make metals useful for a wide variety of applications. The mining, industrial processing and widespread use of metal-containing products has led to a redistribution of metals from geologic deposits to nearly every corner of the globe. While mankind has enjoyed the many benefits of metal applications, this redistribution has led to increased levels of many metals in aquatic, marine, and terrestrial ecosystems throughout the world.

Another property exhibited by many metals is a high toxicity to a wide variety of plant and animal life. The finite size of the Earth coupled with the proliferation of human populations has led to widespread environmental changes. Whether one considers garbage dumps, runoff from mining operations, industrial effluents, smokestack particulates, or sewage nearly all forms of pollution contain concentrations of metals which are toxic to most life forms. Little has been done to control pollution despite the destruction of entire ecosystems. The basic needs of the human population require that men coexist with the natural world that fulfills these needs. Pollutants eventually end up in human foodstuffs and water supplies. For these reasons, the development of efficient separation technologies is a requirement for the environmental and economic health of society.

The benefits of efficient metal separations go far beyond pollution control and environmental remediation. The advantages for the mining and chemical industries may seem obvious. Improved purification techniques lower production costs. These benefits filter down to all other industries in the form of cheaper, purer raw materials, which lead to the development of better products and economic growth. It is in this environment of economic growth that new technologies are developed which provide the many "modern conveniences" people enjoy.

Two techniques developed for the separation of metal ions from aqueous solutions are solvent extraction and ion exchange. In general, solvent extraction involves the incorporation of a compound (extractant) with a high affinity for the target metal ion into an organic solvent. When the organic phase is contacted with the aqueous phase, the metal ion moves to the organic phase to form a complex with the extractant. Separation of the organic and aqueous phases results in an aqueous phase with a lower concentration of the target metal ion. Treatment of the organic phase with an appropriate stripping solution results in the recovery of the metal ions, which can be recycled (1). Advantages of the solvent extraction technique include fast extraction kinetics and the high degree of metal ion selectivity, which can be obtained. The disadvantages of solvent extraction include the high cost of the relatively large volumes of organic solvents needed to treat dilute metal ion solutions (2). Even a low solubility of the extractant and the organic solvent in the aqueous phase can lead to various problems with this technique. Toxic extractants (i.e. crown ethers) and solvents can be released into the aqueous phase, which not only add to the cost of the

technique due to the loss of these compounds, but also introduce new dangers which may be worse than those caused by metal ions.

The covalent grafting of the extractant to a solid support is a concept used to synthesize ion exchange materials. Due to its covalent attachment, loss of the extractant is avoided. In general, the solid supports have taken the form of organic polymers due in large part to their ease of preparation. The synthesis of organic polymers containing a wide variety of functional groups is well known. Also, well developed techniques such as emulsion polymerization can be used to create these "resins" in the convenient form of spherical beads. As the name implies, ion exchange involves the exchange of the target metal ion for a metal ion from the support such as H^+ or Na^+. The aqueous phase can be passed through a column containing the ion exchange material which absorbs the target metal ion and releases an innocuous ion such as a proton (3). This exchange is due to the larger coulombic interaction between the target metal species and the support. Also, a wide variety of chelating resins have been developed which function via complex formation with the target metal ion (4). Advantages of ion exchange over solvent extraction include the retention of extractant, ease of separation due to the heterogeneous nature of the system, and good performance with dilute solutions. Disadvantages of ion exchange with repect to solvent extraction include relatively slow kinetics due primarily to the hydrophobicity of the organic support, and lower selectivities for target metal ions.

A metal ion sorbent that combines the favorable characteristics of solvent extraction (fast kinetics, selectivity) with those of ion exchange materials (solid

support, good for dilute systems) would be ideal for many applications. The development of ion exchange materials that use a support with more favorable characteristics than organic polymers is one alternative. Among the many possible substrates on which to immobilize ligands, silica gel has been of particular interest. Silica does not swell like many organic supports, has good mechanical strength, and excellent thermal stability (5). The silicon dioxide matrix is also very stable and resistant to chemical degradation. Silica is particularly promising as a support for metal ion sorbents in aqueous media, due to its hydrophilic character.

Many researchers have grafted ligands to amorphous silica gel in order to synthesize selective metal ion sorbents. For example, Izatt and co-workers have immobilized numerous crown ether ligands, each with a unique selectivity for specific metal ions (6-8). Thermodynamic studies have shown that the equilibrium constants for the association of metal cations with the silica gel-bound crown ethers are comparable to log K (H_2O) values for the association of the same cations with the unbound ligands (9). Koklu et al. grafted 3-aminopropyltriethoxysilane to amorphous silica for the removal of Cu(II) and Cd(II) from aqueous solutions (10-11). Airoldi and co-workers reacted silica gel with 3-mercaptopropyltrimethoxysilane to produce a thiol-modified silica material which was shown to remove a wide variety of metal cations [i.e. Hg(II), Ag(I), Cu(II), Ni(II), and Zn(II)] from aqueous solutions (12-13). Although these results have been promising, the overall metal ion capacity of these materials is relatively low. For reasons described in greater detail in Chapter 3, the morphology of the silica prevents metal ion access to many of the functionalized sites.

A hydrophilic material with larger, ordered pores may perform better as a sorbent support.

Since this dissertation describes the synthesis and characterization of a variety of porous materials, a short description of the classification system for naming pores according to their size is warranted. In 1985, The International Union of Pure and Applied Chemistry (IUPAC) set specific guidelines for the reporting of data describing porosity (14). Pores in solids are classified in three broad catagories: (i) micropores (<2 nm), (ii) mesopores (2-50 nm), and (iii) macropores (>50 nm) (15). The recommendations of the IUPAC committee are followed throughout this text.

The discovery of a new family of mesoporous silicon oxides (M41S) by scientists at Mobil Oil Research and Development (16-20) has led to great interest in this area of materials science. The synthetic methodology involves the formation of supramolecular assemblies of sufactants and the subsequent polymerization of silicon alkoxides around them via a sol-gel reaction. The resulting gel consists of silica with regular arrays of cylindrical surfactant assemblies encapsulated within it. Removal of the surfactant template by extraction or calcination leaves a porous silica. These materials exhibit large internal surface areas and narrow pore size distributions similar to those found in microporous zeolites. Unlike zeolite materials, with maximum pore dimensions <20 Å, the pores of M41S can be engineered with diameters from 15-100 Å. The relatively large pore sizes, ordered pore structure, and hydrophilic nature of these materials make them ideal candidates for sorbent supports. The synthesis and characterization of this type of mesoporous silica is the focus of Chapter 2.

In order to develop metal ion sorbents that are selective for specific metal ions, we have used molecular imprinting strategies. The technique of molecular imprinting involves the incorporation of a template into a host matrix by combining it with polymerizable functional groups, which are copolymerized with host monomers, surrounding the template. Subsequent removal of the template results in a material that contains imprints with the ideal size, shape, and chemical environment to rebind the template. The imprinting approach based on organic polymer hosts was first developed by Wulff and Sarhan (21) who used this technique to produce polymers for the resolution of racemic mixtures. It has since been utilized in the development of artificial enzymes (22), and antibodies (23-4), chromatographic resins (25), and metal ion sorbents (26). In the context of our present work, the templates are metal ions and the polymerizable functional groups take the form of bifunctional reagents which contain both alkoxysilyl and amine groups. The amine groups form complexes with the metal ion templates via dative bonding. The alkoxysilyl groups undergo condensation reactions with the silanol groups on the silica surface.

The objective of the research described in this dissertation is to use the concepts and methods of sol-gel chemistry, the surfactant template approach, organofunctionalization of silica, and molecular imprinting to design, develop, and synthesize new metal ion sorbents. These sorbents will be used to remove metal ions from aqueous media and should exhibit the following properties:

(1) high capacities for the metal ion template

(2) selectivity for the target metal ion when in the presence of competitor species

(3) fast uptake kinetics of metal ion species

(4) efficient regeneration/long term durability

Chapter 2 describes the preparation of various mesoporous silicas via the surfactant template method. A wide variety of surfactants were used to engineer the porosity of these materials. The removal of the surfactant templates was achieved by either calcination in air or ethanol extraction. The syntheses of porous silicas were investigated using both acid and base catalyzed methods. The as-synthesized mesoscopic materials and mesoporous silicas were characterized primarily by N_2 adsorption and powder X-ray diffraction.

The mesosporous silicas synthesized in Chapter 2 were used in Chapter 3 as the solid support for the synthesis of imprint coated sorbents. Imprint coating is a new technique we have developed to create selective metal ion sorbents and sensors (27-8). Bifunctional reagents containing both alkoxysilyl and amine groups were used to functionalize the mesoporous silica. The alkoxysilyl groups undergo hydrolysis and condensation reactions with the surface silanol groups, thereby covalently grafting the ligand to the solid support. The amine groups form stable complexes with many metal ions via dative bonding. The formation of a metal ion complex with the bifunctional reagent prior to grafting gives the resulting sorbent special properties. The ligands become grafted to the solid matrix in the conformation controlled by the metal ion complex. Removal of the metal ion templates results in the formation of imprint sites

ideally suited for rebinding the metal ion template. The usefulness of these organofunctionalized silicas as metal ion sorbents was investigated by batch testing with buffered aqueous metal ion solutions. The effect of changes in experimental parameters such as solution concentration, pH, porosity of support, and bifunctional reagent were investigated.

In Chapter 4 the technique of stepwise functionalization was used to synthesize metal ion sorbents. We found that the ligand loading of metal ion imprinted and nonimprinted sorbents prepared via imprint coating were not equivalent. The technique of stepwise functionalization was thus developed in an attempt to eliminate this discrepancy (29). Instead of forming the complex between the metal ion and the bifunctional reagent prior to grafting (imprint coating), it is formed *in situ.* The mesoporous support is first coated with the bifunctional reagent and then placed in a solution containing the metal ion template. The resulting metal ion complexes act as catalysts for the adsorption of more bifunctional reagent, which graft to the silica surface following metal complex formation.

Chapter 5 describes the synthesis of metal ion sorbents by the double imprinting technique (30). Unlike the techniques used in Chapters 3 and 4, double imprinting does not involve the coating of a mesoporous support with organic ligands. Instead, the bifunctional reagent is placed in the original reaction mixture and undergoes hydrolysis and condensation reactions with the sol-gel precursor, thereby forming an organically modified polysiloxane. The inclusion of surfactants in the reaction mixture allows one to engineer the porosity of the resulting sorbent by solvent

extraction. The concepts behind our multi-level imprinting are as follows. Surfactant micelles and metal ions both act as templates in these hierarchically imprinted sorbents (31). The metal ion and the surfactant are removed from the matrix via acid leaching and ethanol extraction, respectively. This results in the formation of different sized imprints within the sorbent, each with a specific function. On the microporous level, the removal of the metal ion from the complex leaves cavities (1-3 Å) that exhibit ionic recognition. These pores give the sorbent enhanced selectivity for the target ion. On the mesoporous level, the removal of the surfactant micelles results in the formation of relatively large, cylindrical pores (20 Å) which give the gel an overall porosity which includes large surface areas and excellent metal ion transport kinetics. This combination of high capacity and selectivity, coupled with fast kinetics, makes these materials ideal candidates for many applications. Because the whole process utilizes template or imprinting synthesis twice and on different length scales, it can be viewed as a hierarchical double imprinting process. This technique is especially convenient because the "single pot synthesis" is much less time consuming than the multi-step syntheses described for both imprint coating and stepwise functionalization.

Chapter 6 describes the synthesis of organic-inorganic hybrid polymers via hydrolytic sol-gel reactions of an organic poly(alkoxysilyl) monomer (32). These materials are distinguished from the organically functionalized inorganic polymers synthesized in Chapters 3 and 4, since the organic moeity is part of the crosslinked network and not simply a side chain. Unlike the sorbent prepared by double imprinting in Chapter 5, all precursors contain organic moeities. What makes this

family of materials particularly exciting, is the ability to engineer polymeric materials, which exhibit the right combination of organic and inorganic properties for a particular application. Since the bifunctional reagent and surfactant are added to the precursor solution in a "one pot synthesis", the formation of the hybrid sorbents described herein is analogous to the double imprinting technique. Although the synthetic techniques are similar the products are not. While the backbone of the sorbents prepared via double imprinting is primarily inorganic, the backbone of these hybrid materials is a true organic-inorganic polymer with a 1:1 carbon to silicon ratio. Selective sorbents were synthesized for Cu(II), Ni(II), and Zn(II).

CHAPTER 2

SYNTHESIS OF MESOPOROUS SILICA

2-I. Introduction

The discovery of a new family of mesoporous silicon oxides (M41S) by scientists at Mobil Oil Research and Development (16-20) has led to great interest in this area of materials science. These materials exhibit large internal surface areas and narrow pore size distributions similar to those found in microporous zeolites. Unlike zeolite materials, with maximum pore dimensions <20 Å, the pores of M41S can be engineered with diameters from 15-100 Å. The relatively large pore sizes in these materials make them very attractive for applications such as catalysts, catalytic supports, and sorbents, especially when the molecules involved are too large to fit in the microporous channels of conventional zeolites.

The synthesis of various M41S materials is based on the ability of surfactant molecules to form supramolecular assemblies in solution. These self-assembled structures act as templates for the formation of the metal oxide materials. Removal of the organic template via calcination or extraction results in the mesoporous metal oxide. The final structure of the M41S material depends on many factors such as surfactant chain length and charge, solution pH, temperature, and ratios of the various precursors. A unique member of the M41S family, MCM-41, has a hexagonal arrangement of cylindrical mesopores. A proposed mechanism for the formation of

MCM-41 is shown in **Figure 2.1** (33). Rodlike organic micelles are formed in aqueous solution and interact with the silicate precursors to yield a more stable structure, with a few monolayers of silica around the outside walls. Spontaneous agglomeration of these composite species into a hexagonally packed arrangement is followed by further condensation of the silicate species to form the mesoscopic material with long range order. Removal of the surfactant molecules by calcination or extraction results in the formation of silica with hexagonal arrays of tubular pores.

Stucky and co-workers (34) have reported the synthesis of mesoporous silicas exhibiting a wide variety of structures. Quaternary ammonium surfactants with different alkyl chain lengths were used in order to control the pore sizes of the resulting mesoporous structure. Based on the general formula $C_nH_{2n+2}(CH_3)_3NBr$, where n = 10-18 the longer chain surfactants produced larger pore sizes. Surfactants with different sized head groups, mixed surfactants, and varying reaction conditions (i.e., pH, temperature) were also used in order to see the overall effect on the final product. In addition to the hexagonal phase, cubic and lamellar phases were also synthesized.

Pinnavaia and co-workers (35-7) reported the first synthesis of mesoporous moleular sieves through a neutral assembly pathway. Unlike all previous mechanistic pathways which employed coulombic interactions between charged surfactant head groups, counterions, and inorganic precursors to promote self-assembly, their neutral assembly approach employed weaker nonionic interactions such as hydrogen bonding. Neutral alkyl amine surfactants were used as the structure directing agents. They were

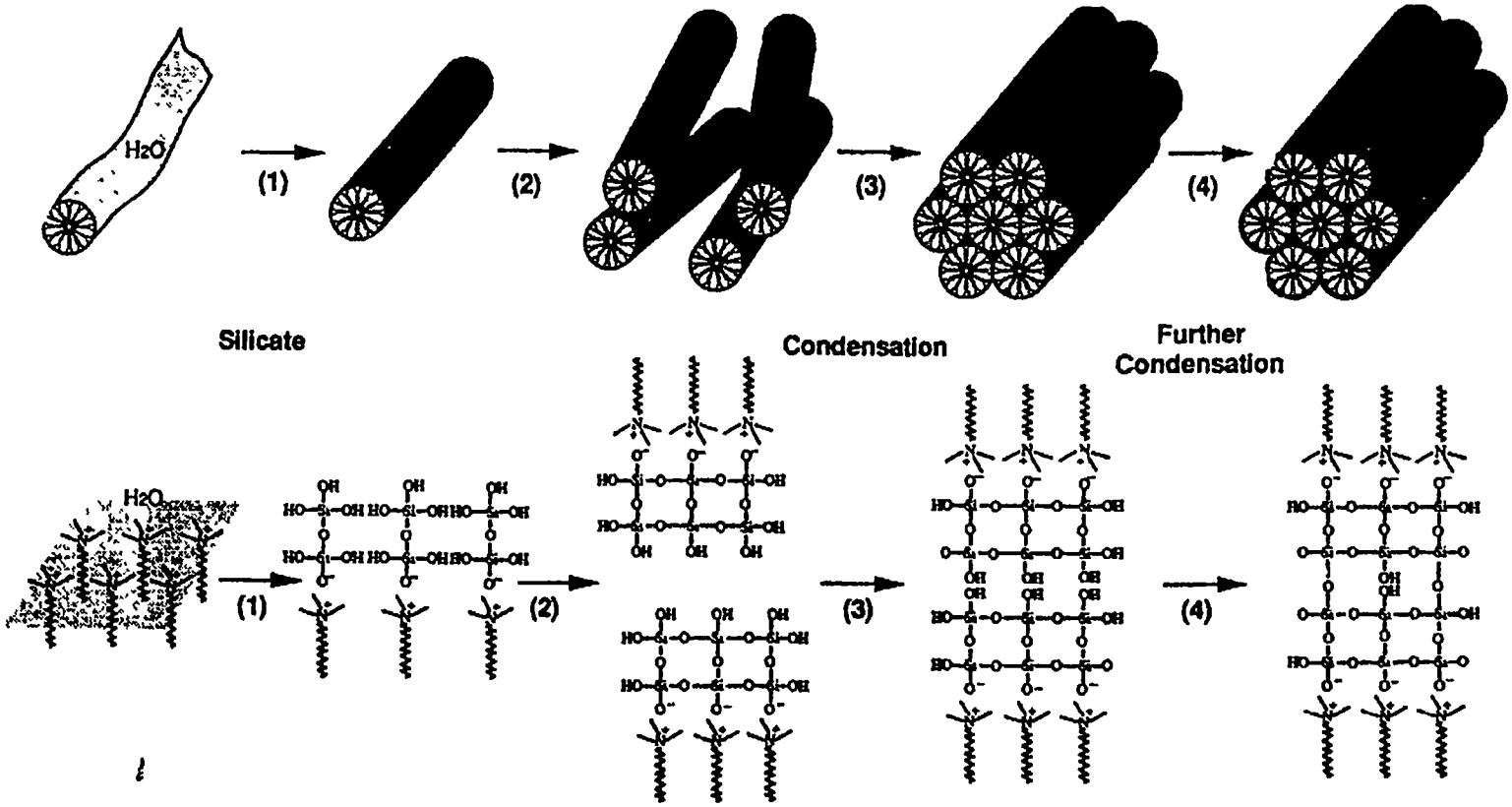


Figure 2.1 Mechanism for the formation of MCM-41 (33).

reported as having larger d-spacings, smaller pore sizes and therefore, thicker pore walls than their MCM-41 counterparts. This material was dubbed HMS for hexagonally packed mesoporous silica. Although the cylindrical pores in these materials are hexagonally packed, they are not "right" cylinders and they meander throughout the material. Surfactant removal results in a pore structure that has been described as a "wormhole motif." For this reason, they do not exhibit the long-range order associated with MCM-41 type materials.

More recently, Zhao *et al.* (38) reported the synthesis of a wide variety of silica mesophases using nonionic poly(alkylene oxide) surfactants and block copolymers as the organic templates. These reactions were carried out in strongly acidic media. The self assembly mechanism appears to occur by a hydrogen bonding $(S^0H^+)(XT^+)$ pathway, where S^0 and I^+ represent the surfactant and silicate species, respectively. Higher concentrations of acid (H^+X^-) resulted in an increase in the assembly rate of these materials.

2-II. Analytical Methods

Gas sorption experiments were carried out with a Micromeritics Gemini III 2375 surface area analyzer. Nitrogen (N_2) was used as the adsorbent. Adsorption and desorption isotherms were measured at 77 K after degassing the samples at 80 °C for 6 h. Surface areas were calculated from the isotherms using the method of Brunauer, Emmett, and Teller (39). Pore size distributions were derived by the procedure of Barrett, Joyner, and Halenda (40).

Powder X-ray scattering patterns were measured on a Siemens D5005 diffractometer equipped with a copper anode (K_α = 1.542 Å). The scan parameters were 50 kV accelerating voltage, 30 mA filament current, 0.03° step size, and 1 sec dwell time. The 2-theta maxima of the diffraction patterns were used to calculate d-spacings via the Bragg relationship (41).

2-III. Synthesis and Characterization of Mesoporous Silica

2-III.1 MCM-41

Since its discovery in 1992 by the Mobil Oil research and development team, MCM-41 has been the focus of great interest in the research community (16-20). This has led to the development of many different synthetic methods for the synthesis of mesoporous molecular sieves, which employ a wide variety of structure directors and reaction conditions. Despite these recent advances, the base catalyzed pathway originally reported by the Mobil researchers (16) remains the most widely used procedure. A similar protocol was employed here.

2-III.1.1 Synthesis

Cetyltrimethylammonium bromide (CTAB, 36 g, **Figure 2.2**) was added to 485 mL of deionized water. The mixture was heated gently and stirred at 60 °C to dissolve all surfactant. The clear solution obtained was then allowed to cool to room temperature. Concentrated NH_4OH (7.7 M, 109 mL) was gradually added to the

stirred solution. Tetraethyl orthosilicate (TEOS, 82.0 g) was then added. The resulting molar ratios of the reaction mixture were as follows:

1.0 TEOS : 0.25 CTAB : 2.13 NH_4OH : 83.8 H_2O

The mixture was then refluxed for 16 h. The solid product was recovered by filtration, washed with deionized water and ethanol, and air-dried. A portion of this as-synthesized material was used for powder X-ray (XRD) analysis. In order to remove the surfactant template, the remainder of the product was calcined in air. It was placed in a crucible in a furnace and the temperature was ramped by 2 °C/min to 550 °C, at which temperature it was calcined for 4 h.

2-III.1.2 Characterization

The nitrogen adsorption/desorption isotherm for the calcined material is shown in **Figure 2.3.** The very large, sharp step located in the relative pressure range of 0.2-0.6 is typical of MCM-41 type materials, and indicates that this sample is primarily mesoporous. This sample has a calculated surface area of 1,034 m^2/g, no micropore volume, and a total pore volume of 1.01 cm^3/g. The pore size distribution (**Figure 2.4)** illustrates that nearly all the pores in this material are in the range of 20 to 50 Å. The maximum of the pore size distribution (D_{max}) is located at 28.5 Å.

Powder X-ray diffraction patterns for the as-synthesized (**Figure 2.5**) and calcined (**Figure 2.6**) samples are remarkably similar. Both show a sharp peak located at $2\theta = 1.99°$, which corresponds to a d-spacing of 49.4 Å. The difference between the

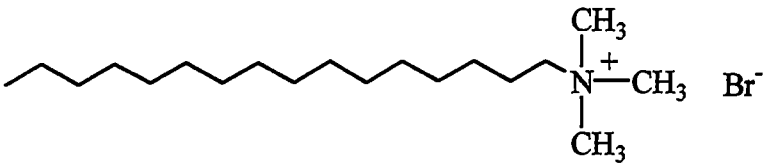


Figure 2.2. The structure of cetyltrimethylammonium bromide.

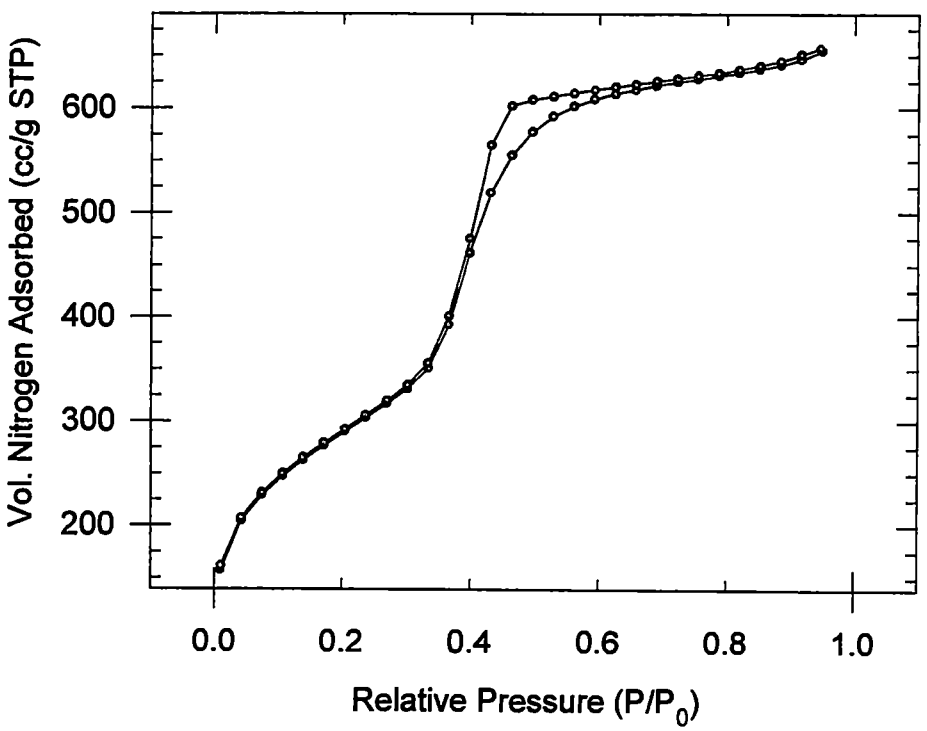


Figure 2.3. N_2 adsorption/desorption isotherm of calcined MCM-41.

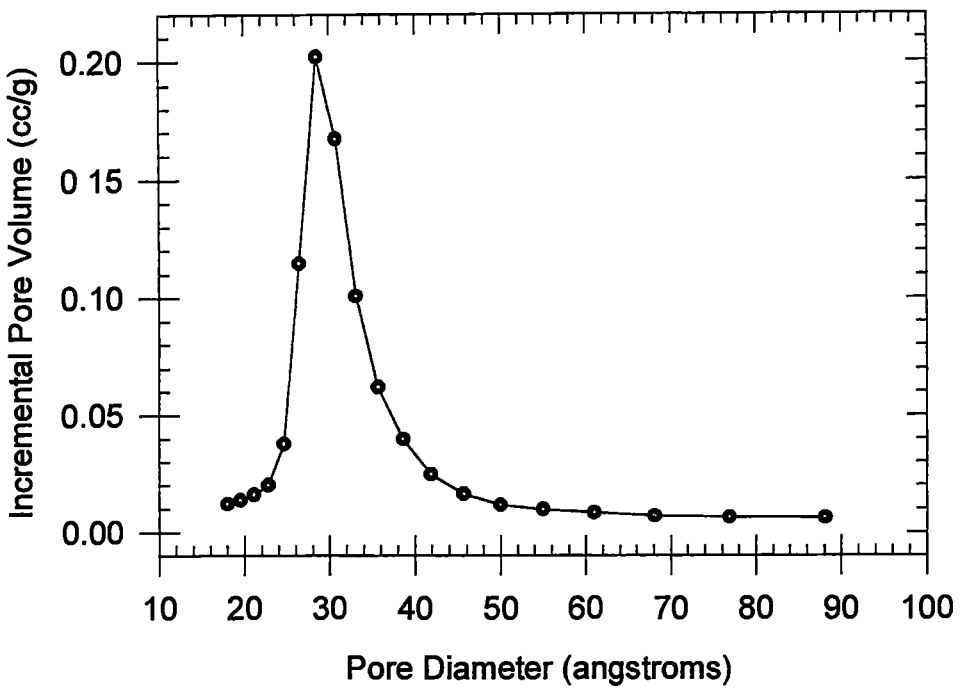


Figure 2.4. Pore size distribution of calcined MCM-41.

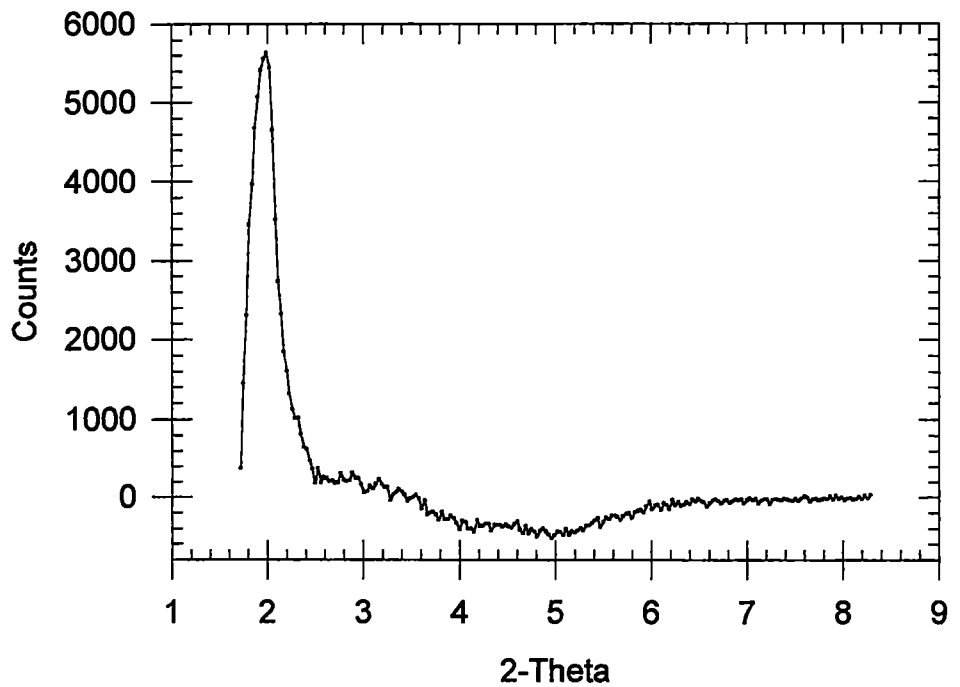


Figure 2.5. Powder X-ray diffraction pattern of as-synthesized MCM-41.

d-spacing and the average pore diameter gives an approximate wall thickness of 20.9 Å.

2-III.2 CTAB/mesitylene Silica

In addition to discovering the surfactant template approach in 1992, Beck and co-workers patented (42) a creative way to increase the size of the pores in the resulting metal oxide framework. 1,3,5-trimethylbenzene (mesitylene) was used to expand the size of the micellar rods in the surfactant solution. When placed in a micellar solution, the mesitylene molecules move to the hydrophobic core of the micelles, causing them to expand in size (**Figure 2.7**). After the formation of the mesoscopic material and micelle removal, the resulting metal oxide framework was reported to have substantially larger pore sizes, while still keeping its long range order. A similar protocol was followed here using mesitylene as the pore expander and CTAB surfactant in basic media.

2-III.2.1 Synthesis

CTAB (3.6 g) was added to 100 mL of deionized water and heated to 60 °C under stirring in order to dissolve all surfactant. Mesitylene (8.4 mL) was added gradually and the solution was stirred for 15 min. After the addition of 20 mL of concentrated (7.7 M) NH_4OH, the solution was stirred for an additional 10 min. and TEOS (8.8 mL) was then added gradually. This mixture was then refluxed for 16 h. The solid product was recovered by filtration, washed with deionized water and

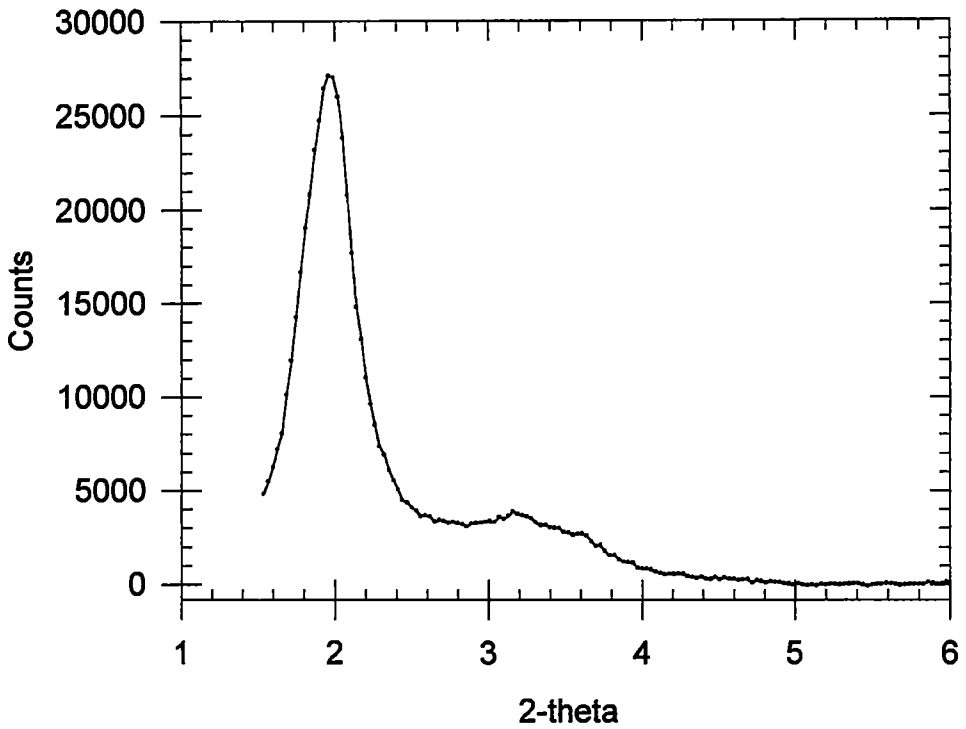


Figure 2.6. Powder X-ray diffraction pattern of calcined MCM-41.

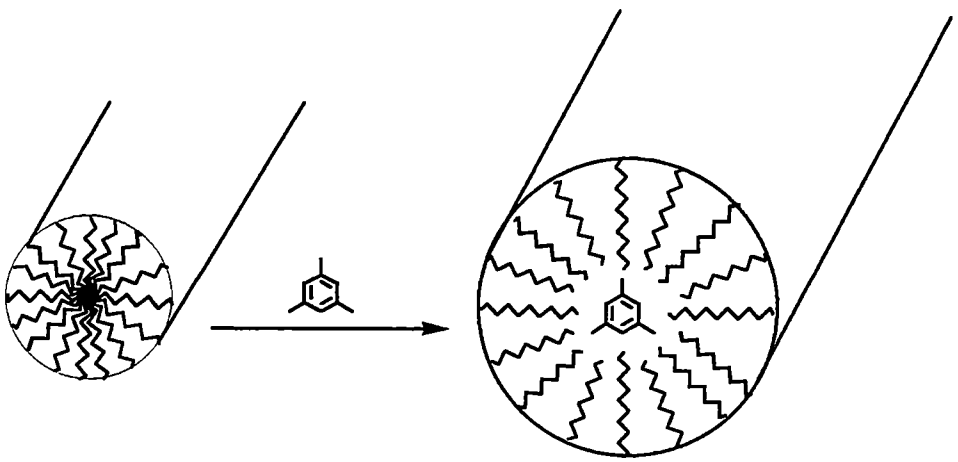


Figure 2.7. Mechanism of mesitylene pore expander.

absolute ethanol, and air-dried. The surfactant and pore expander was removed by calcination in air at 550° C.

2-III.2.2 Characterization

The nitrogen adsorption/desorption isotherm for the calcined CTAB/mesitylene material is shown in **Figure 2.8**. This isotherm exhibits multiple steps, but none of them are sharp. This is indicative of a porous material with a rather broad distribution of pore sizes. The very large amount of N_2 (700 cm^3/g S.T.P.) adsorbed gives evidence for large pores. This material has a calculated surface area of 949 m^2/g, no micropore volume, and a total pore volume of 1.1 cm^3/g. The pore size distribution (**Figure 2.9**) is broad, with a D_{max} of 52.9 Å. **Figure 2.10** shows the powder X-ray diffraction pattern for the calcined CTAB/mesitylene material. A peak at $2\theta = 1.81°$ corresponds to a d-spacing of 54.2 Å. This result does not agree with the nitrogen adsorption data, which gave a D_{max} of 52.9 Å. Another peak may be present at an even lower value of 2θ, but could not be resolved.

2-II.3 CTAB/H^+ Silica

Recently, Stucky and co-workers (34) reported the synthesis of mesoporous silica based materials in which the surfactant cetyltrimethylammonium bromide was used as the template in acidic media. Different reactant molar ratios and reaction temperatures were employed in order to determine what effect they have on the pore

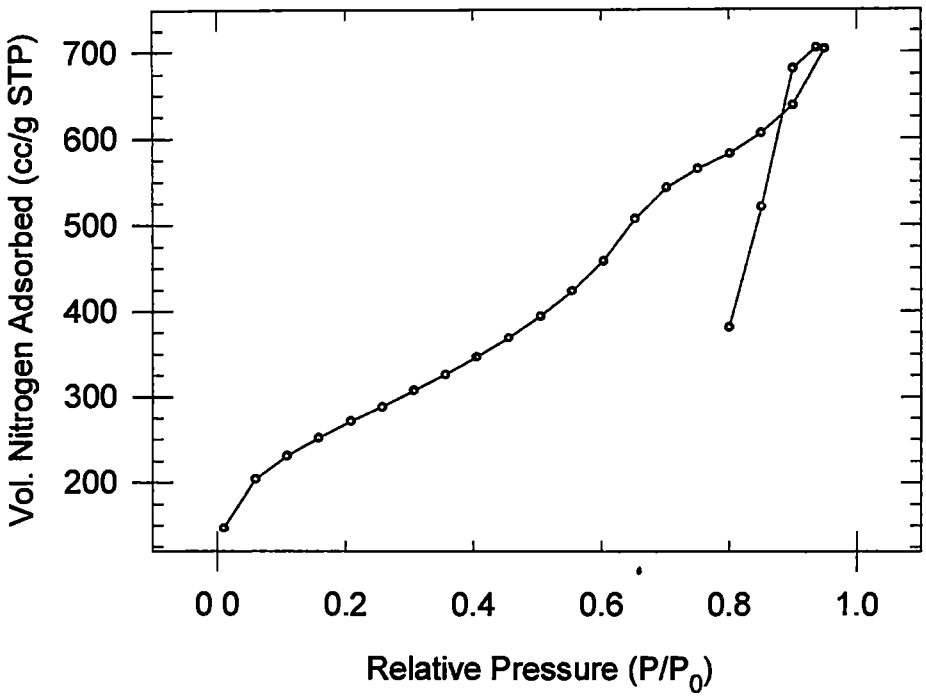


Figure 2.8. Nitrogen adsorption/desorption isotherm of CTAB/mesitylene.

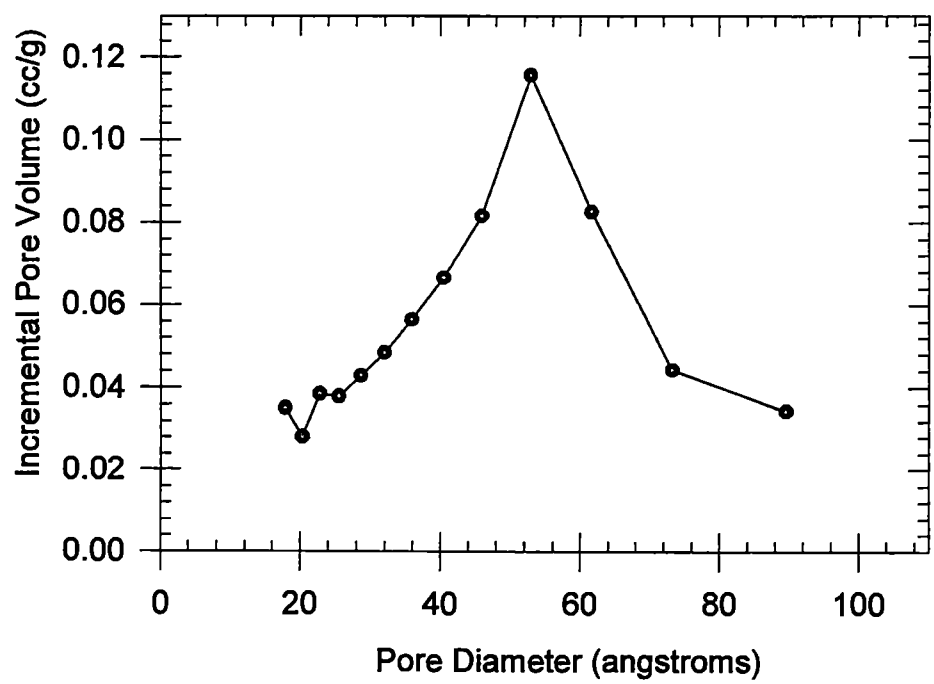


Figure 2.9. Pore size distribution of CTAB/mesitylene silica.

structure of the final product. A similar protocol at ambient temperature was followed here.

2-III.3.1 Synthesis

Concentrated HCl (12.2M, 37.5 mL) and 2.185 g of CTAB were added to 79.5 mL deionized water and stirred for 10 min. To this clear solution, 11.15 mL of TEOS was added. The molar ratios of the reaction mixture were as follows:

1.0 TEOS : 0.12 CTAB : 8.5 HCl : 83 H_2O

The mixture was covered, and vigorously stirred for 1 h. The solid product was recovered by filtration and washed with deionized water, and air-dried. A portion of this as-synthesized product was then separated and characterized. The remaining product was split into two equal portions. For the first portion, the surfactant was removed by calcination in air. The remaining portion was placed in 250 mL of an ethanol/HCl solution (1 M HCl), covered, and stirred at 50 °C for 6 h. in order to extract the CTAB. The product was then recovered by filtration and the extraction procedure was repeated. The final product was then recovered and air-dried.

2-III.3.2 Characterization

The nitrogen adsorption/desorption isotherm for the calcined CTAB/H^+ material is shown in **Figure 2.11**. The constant slope in the relative pressure range of 0.1-0.3 indicates the presence of a large number of supermicropores (10-17 Å) in this material. This is consistent with the pore size distribution (**Figure 2.12**) which has a

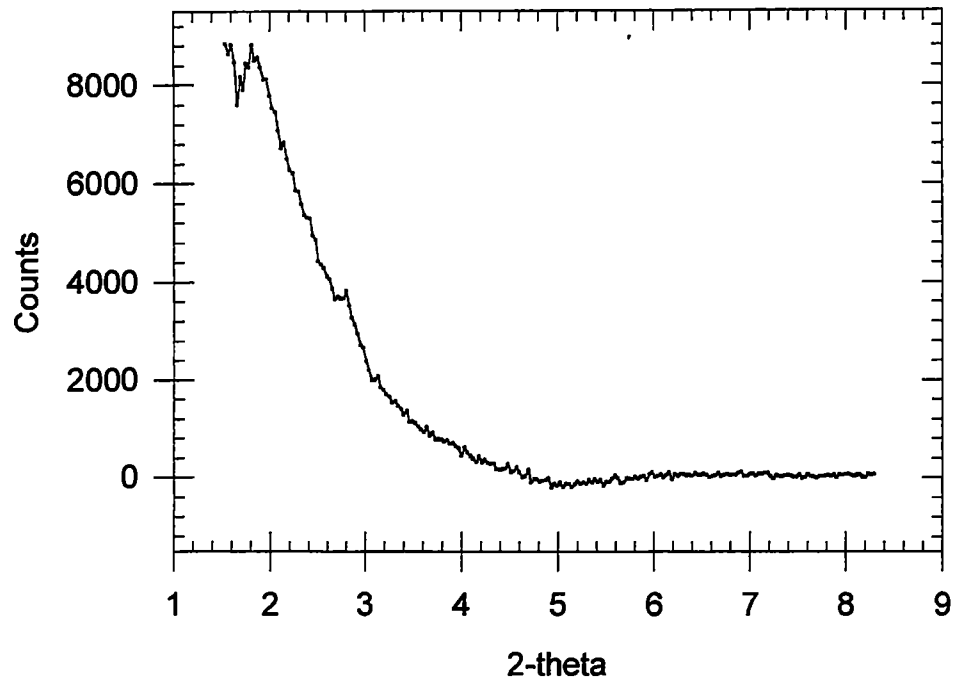


Figure 2.10. Powder X-ray diffraction pattern for CTAB/mesitylene silica.

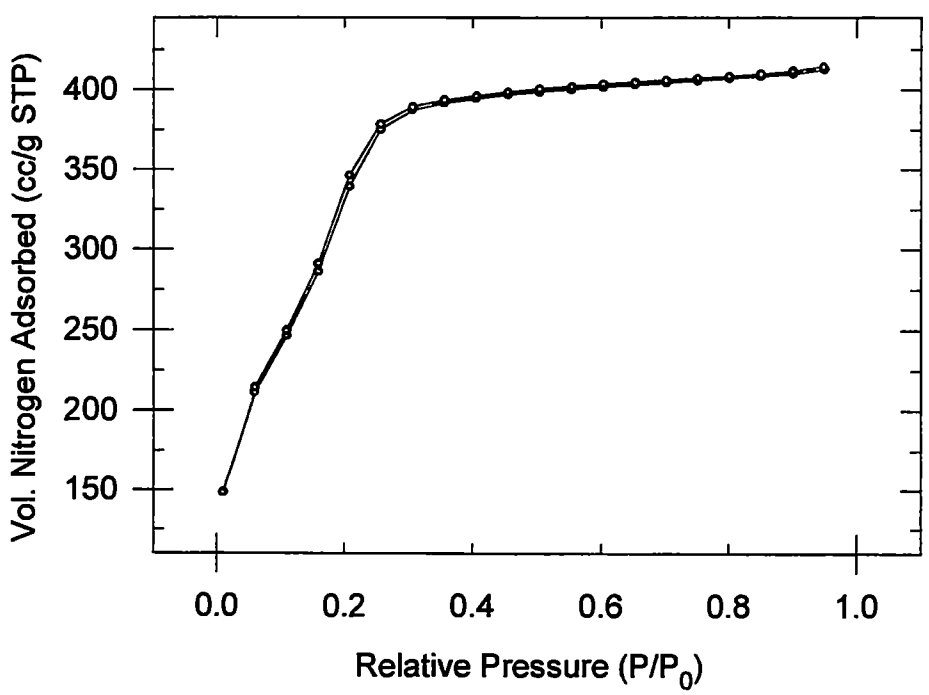


Figure 2.11. N_2 adsorption/desorption isotherm for CTAB/H^+ silica.

D_{max} at the low end. The calcined material has a calculated surface area of 1294 m^2/g, a micropore volume of 0.31 cm^3/g, and a total pore volume of 0.64 cm^3/g. **Figure 2.13** shows the nitrogen adsorption/desorption isotherm for the extracted CTAB/H^+ material. Unlike the calcined sample, this does not show any evidence of supermicroporosity. This is a typical isotherm exhibited by microporous solids. The pore size distribution (**Figure 2.14**) shows very little pore volume attributable to pores greater than 17 Å. A N_2 adsorption experiment was conducted on the as-synthesized material, and indicated that the solid had no porosity. The calculated surface area of 0.2 m^2/g is a typical value for nonporous powders. **Figure 2.15** shows the powder X-ray diffraction pattern for the calcined CTAB/H^+ material. A sharp peak at $2\theta = 2.56°$ corresponds to a d-spacing of 38.3 Å. The X-ray diffraction pattern for the as-synthesized sample shown in **Figure 2.16** displays a sharp peak at $2\theta = 2.41°$, which corresponds to a d-spacing of 40.7 Å.

2-III.4 HMS

Pinnavaia and co-workers (35) have used nonionic surfactants to synthesize mesoporous silica with wormhole motifs based on hydrogen bonding interacions at the organic/inorganic interface. Neutral alkyl amine surfactants were used as the structure directing agents. The synthesis is believed to proceed through a S^0I^0 assembly pathway, where S^0 and I^0 represent the neutral sufactant and inorganic silicate,

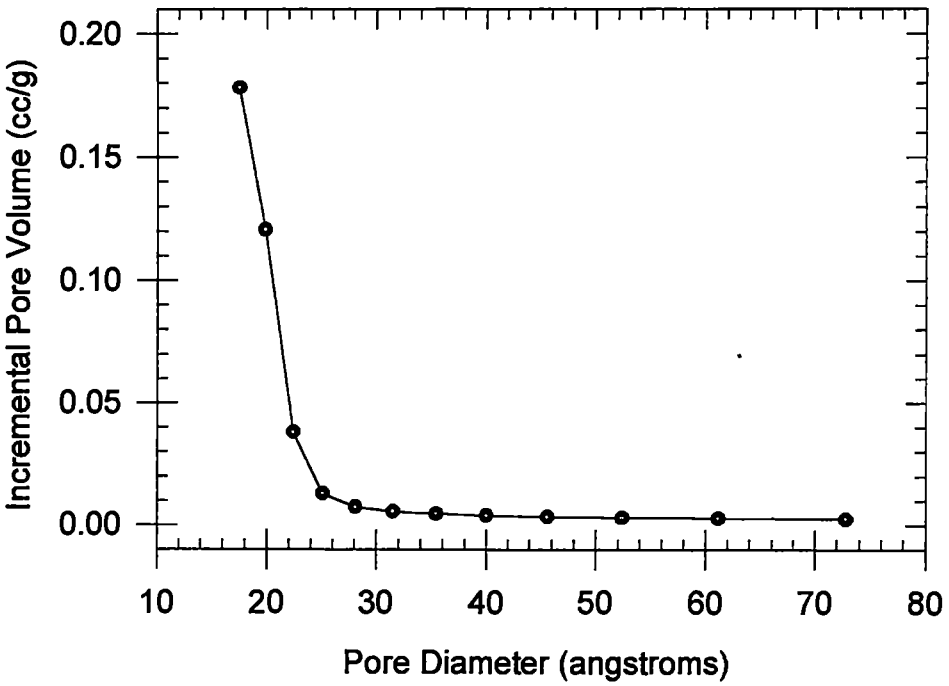


Figure 2.12. Pore size distribution of calcined CTAB/H^+ silica.

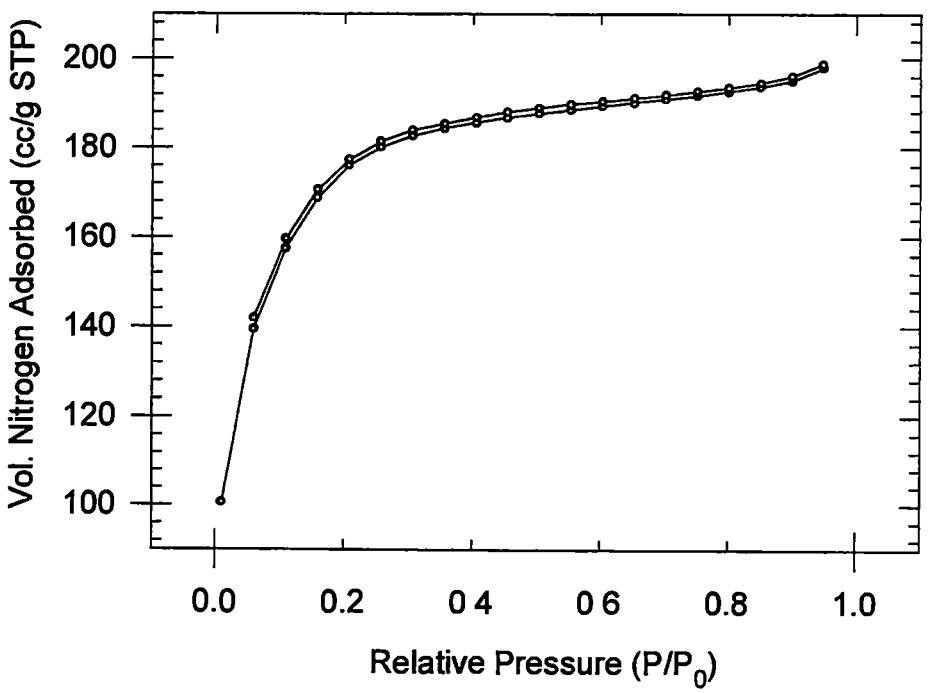


Figure 2.13. N_2 adsorption/desorption isotherm of extracted CTAB/H^+ silica.

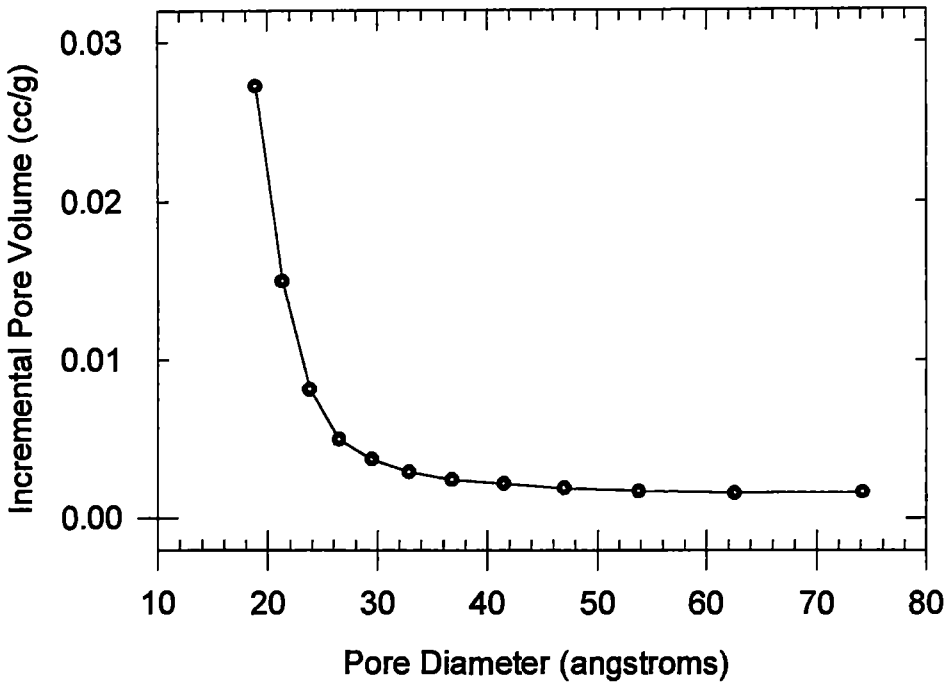


Figure 2.14. Pore size distribution of extracted CTAB/H^+ silica.

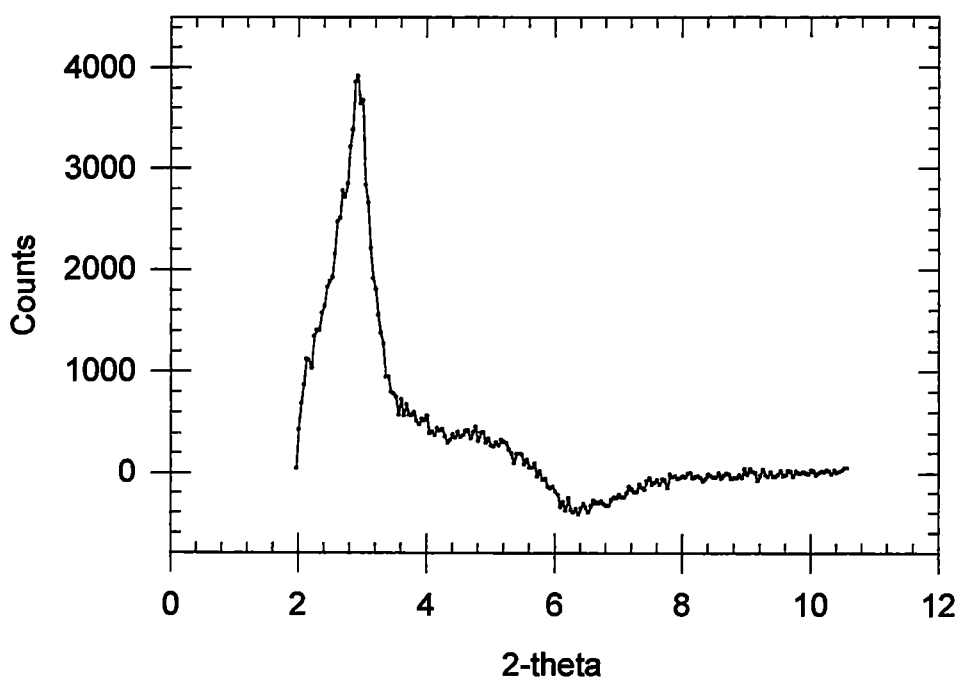


Figure 2.15. Powder X-ray diffraction pattern of calcined CTAB/H^+ silica.

respectively. A protocol similar to that employed by Pinnavaia and co-workers was employed here. Dodecylamine (**Figure 2.17**) was used as the surfactant.

2-III.4.1 Synthesis

Dodecylamine (2.41 g) was added to a solution containing 20 mL of deionized water and 26 mL of absolute ethanol and stirred vigorously for 10 min. in order to dissolve all the surfactant. TEOS (10 mL) was gradually added to the stirred solution to give the following molar ratios in the reaction mixture:

1.0 TEOS : 0.27 DDA : 9.1 EtOH : 29.6 H_2O

The reaction vessel was covered, and the reaction mixture was aged at room temperature without stirring for 24 h. The solid product was recovered by filtration, washed with deionized water, and air-dried. A portion of this as-synthesized material was used for powder X-ray analysis. In order to remove the surfactant template, the remainder of the product was calcined in air at 550 °C.

2-III.4.2 Characterization

The nitrogen adsorption/desorption isotherm for the calcined material is shown in **Figure 2.18**. The large, sharp step located in the relative pressure range of 0.2-0.4 indicates a large amount of mesoporosity in this material. This isotherm is very similar those observed in MCM-41 type materials. It is interesting to note that the desorption branch does not exhibit the hysteresis shown by MCM-41 materials. This perhaps indicates a general lack of strong capillary effects and therefore the possibility

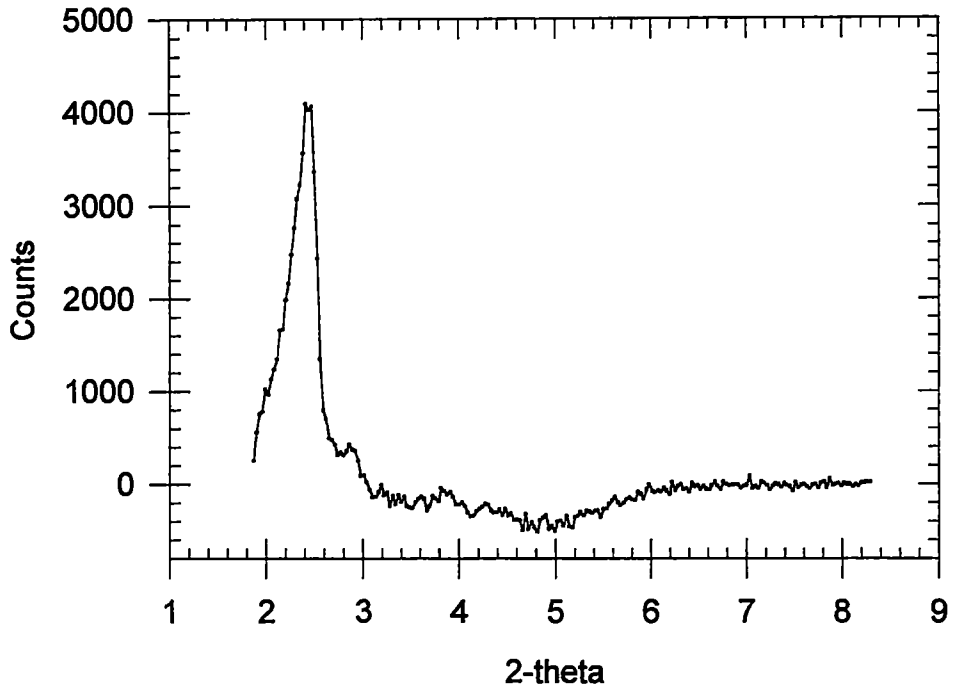


Figure 2.16. Powder X-ray diffraction pattern of as-synthesized CTAB/H^+ silica.

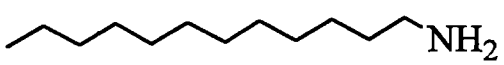


Figure 2.17 Structure of dodecylamine.

of better kinetics in the HMS material. The pore size distribution (**Figure 2.19**) shows a narrow peak with a D_{max} of 24.8 Å. **Figure 2.20** shows the powder X-ray diffraction pattern for the as-synthesized material. A sharp peak at $2\theta = 1.96°$ corresponds to a d-spacing of 50.0 Å. A similar pattern is shown by the calcined product (**Figure 2.21**). A peak at $2\theta = 2.05°$ corresponds to a d-spacing of 48.0 Å. As in the case of the acid catalyzed MCM-41 material, the calcination step resulted in a small contraction of the matrix. No evidence for any loss of localized order is seen in the diffraction patterns. The difference between the d-spacing and the average pore diameter gives an approximate wall thickness of 23.2 Å.

2-III.5 Tween 80 Silica

Tween 80 is a nonionic alkyl poly(oxyethylene) surfactant commonly used as an emulsifier and dipersing agent. When used as a food additive in such products as vegetable shortenings, baked goods, and ice cream, it is referred to as polysorbate 80. This amber-colored, viscous liquid has an approximate molecular weight of 1310 a.m.u. **Figure 2.22** shows the chemical structure of tween 80. Recently, Zhao et al. (38) reported the synthesis of mesoporous silica with a cubic pore structure by using Tween 80 as the structure directing agent and TEOS as the metal oxide precursor. A similar protocol was followed at room temperature in acidic media.

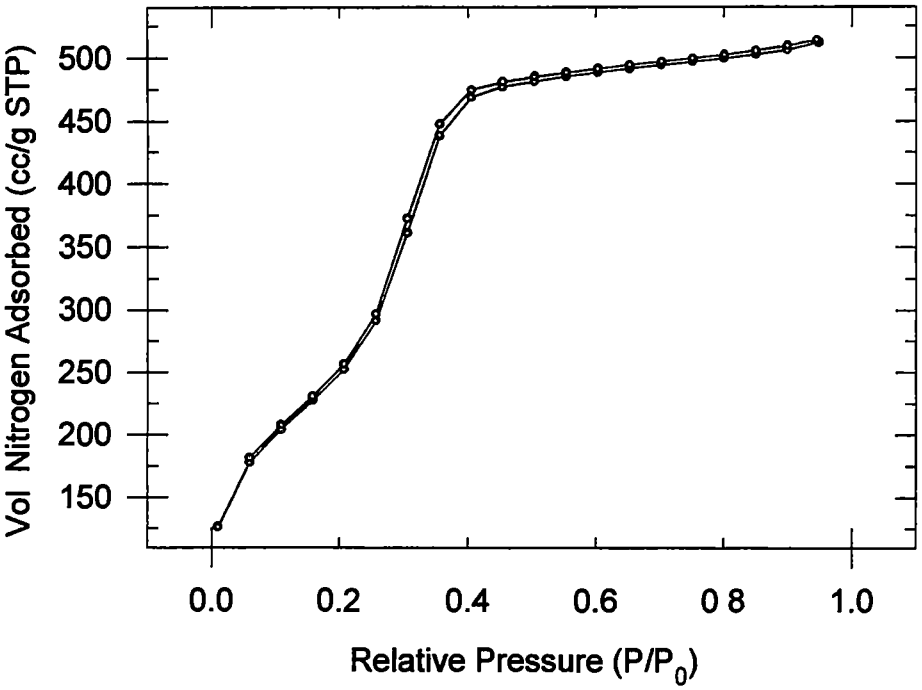


Figure 2.18 N_2 adsorption/desorption isotherm of HMS.

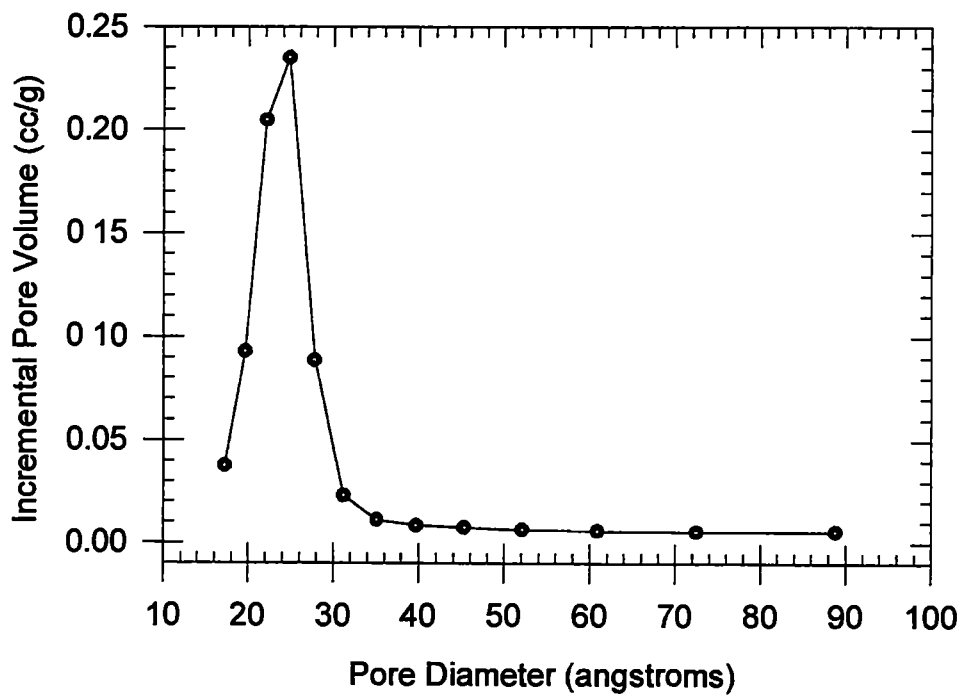


Figure 2.19 Pore size distribution of HMS.

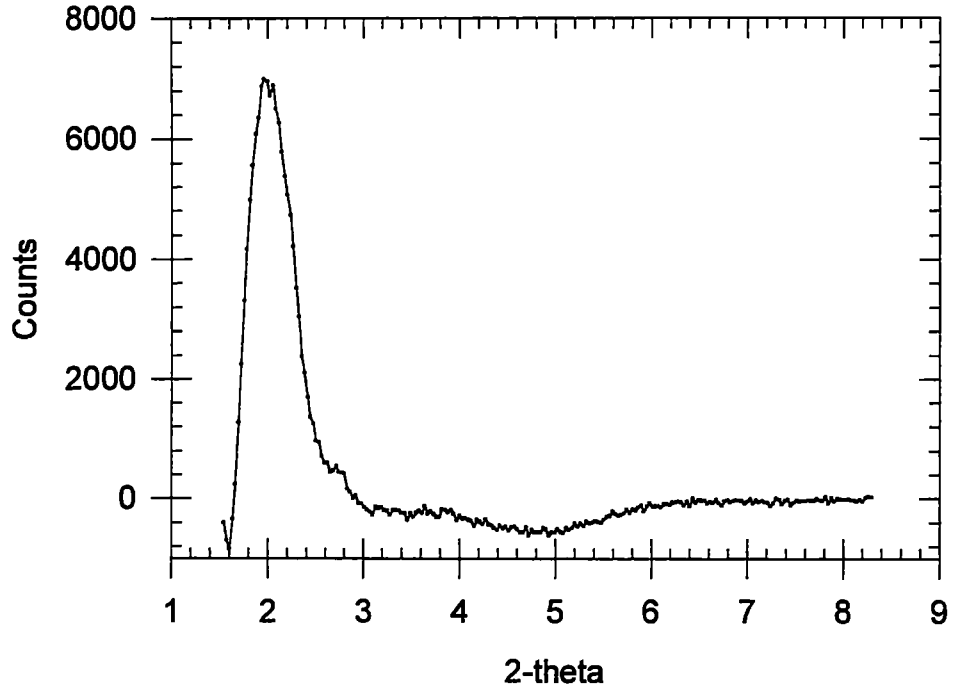


Figure 2.20 Powder X-ray diffraction pattern of as-synthesized HMS.

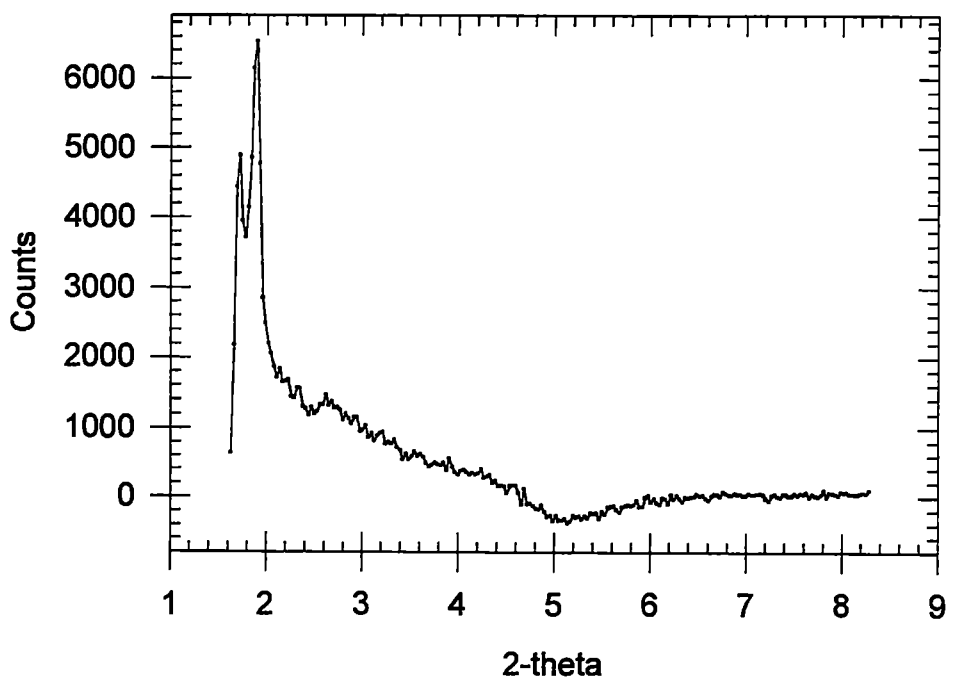


Figure 2.21 Powder X-ray diffraction pattern for calcined HMS.

2-III.5.1 Synthesis

In a typical preparation, 6.9 mL of Tween 80 was dissolved in 20 mL of deionized water and 80 mL of 2 M HCl solution while stirring. 9.4 grams of TEOS was then gradually added. The molar ratios of the reaction mixture were as follows:

1.0 TEOS : 0.13 Tween : 3.79 HCl : 131.5 H_2O

The vessel was then covered and the reaction mixture was stirred at room temperature for 24 h. The white solid product was then recovered by filtration and washed with deionized water and air-dried. The surfactant was removed by calcination in air at 550 °C.

2-III.5.2 Characterization

The nitrogen adsorption/desorption isotherm for the calcined material is shown in **Figure 2.23**. The constant slope throughout the relative pressure range of ca. 0.1-0.3 is typical of supermicroporosity (pore sizes of 10-17 Å) within the material. The large micropore volume of 0.13 cm^3/g supports this result. The significant hysteresis shown by the desorption branch of the isotherm gives evidence for the presence of relatively narrow pore openings in the larger pores of the matrix. This material has a B.E.T. surface area of 620 m^2/g , and a total pore volume of 0.46 cm^3/g. The B.J.H. pore size distribution (**Figure 2.24**) shows a D_{max} of 21.0 Å.

Figure 2.25 shows the powder X-ray diffraction pattern for the calcined product. A sharp peak at $2\theta = 1.63°$ corresponds to a d-spacing of 60.2 Å. The difference between the d-spacing and the average pore diameter gives an approximate

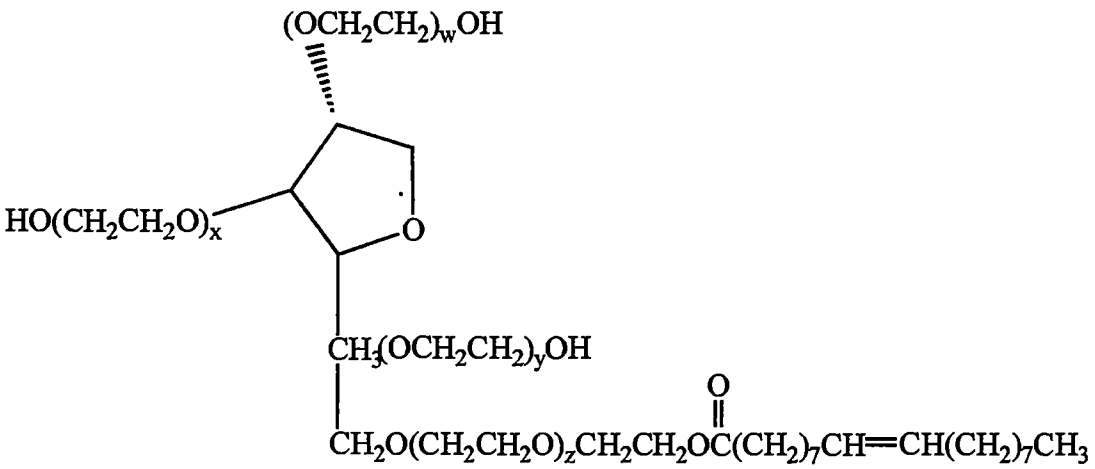


Figure 2.22 Structure of Tween 80

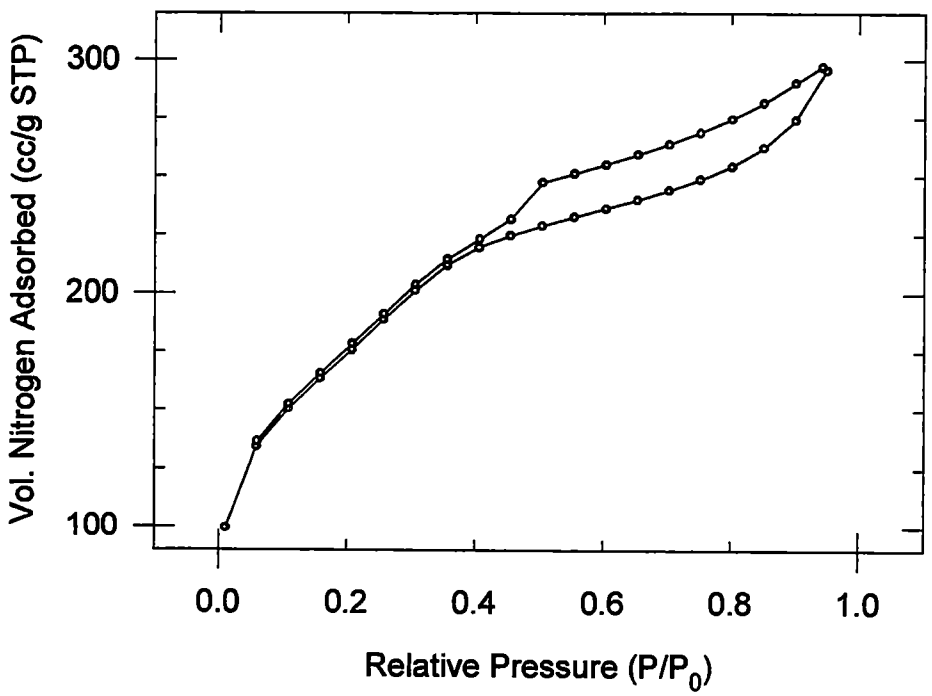


Figure 2.23 N_2 adsorption/desorption isotherm for Tween 80 silica.

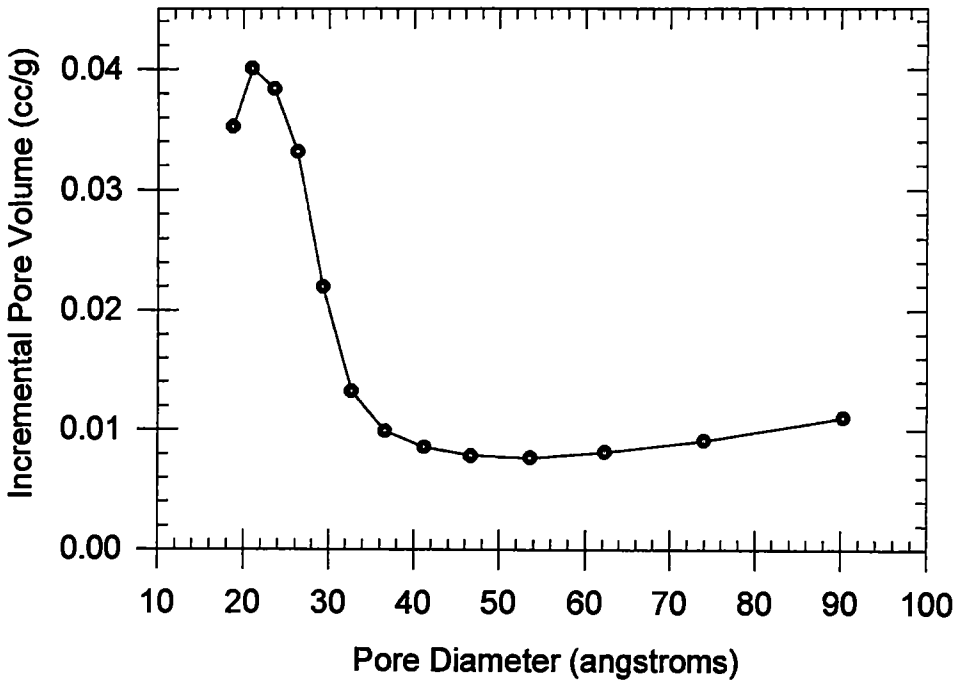


Figure 2.24 Pore size distribution of Tween 80 silica.

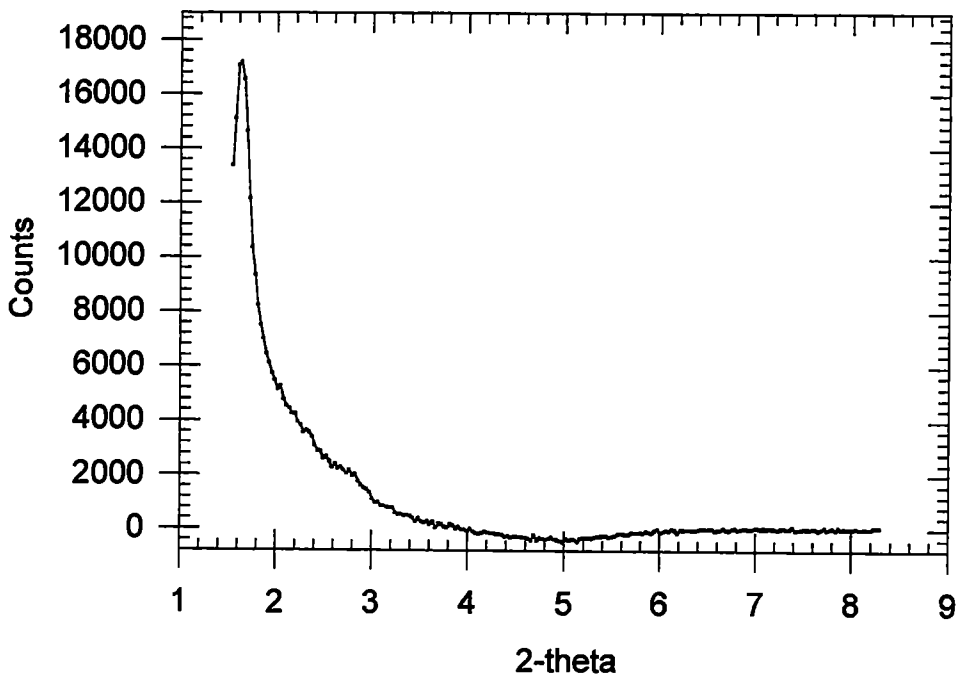


Figure 2.25. Powder X-ray diffraction pattern of Tween 80 silica.

wall thickness of 39.2 Å. There is no evidence for a cubic pore structure in this material.

2-III.6 Pluronic Surfactants

Pluronic nonionic surfactants are block copolymers of propylene oxide and ethylene oxide. The propylene oxide block is sandwiched between the two ethylene oxide blocks. The general structure of Pluronic surfactants is illustrated in **Figure 2.26**. Recently, Stucky and co-workers (38) have reported the synthesis of a number of highly ordered mesoporous silica structures using pluronic surfactants as the structure directing agents. Although a wide variety of surfactants were used to produce many different mesophases (hexagonal, cubic, and lamellar structures of various sizes), three are of particular interest here. Pluronic F127 was reported to produce a cubic mesostructure with a pore size of approximately 54 Å. Pluronic P85 and P123 were used to synthesize mesoporous silica with hexagonal structures having pore sizes of 60 and 90 Å, respectively. Both of these are significantly larger than those achieved with either quaternary ammonium surfactants or neutral amine surfactants described earlier.

The general interest in cubic structures lies in the fact that a sorbent synthesized with a cubic support may display better overall kinetics than the hexagonal analog. Ions and molecules moving through the sorbent may travel in three dimensions instead of just one, as is the case with the cylindrical pores of the hexagonal supports. Clogging of the pore structure of a cubic system is less likely to

occur than in the hexagonal arrangement. For example, if one of the cylindrical pores of an MCM-41 type material is blocked, the rest of the pore and all the internal surface area is no longer accessible, except from the opposite end. Each pore can be viewed as a very long chamber with a door at each end. This same chamber, in a cubic structure, is surrounded by six doors that are all adjacent to it. If one pore opening is blocked, five other openings still allow access.

If a support with a hexagonal arrangement is used as a sorbent, the larger pore spaces achieved with Pluronic P85 and P123 may result in better kinetics and less blockage. It should be noted here that the bifunctional reagents commonly used to functionalize silica are generally 10-25 Å in length. These reagents supply the electron donating functional groups, which give the sorbent material a high affinity for metal ions. If the pore size of the silica support is too small, the covalent grafting of these ligands to the silica surface by condensation reactions with the silanol groups may lead to pore blockage before the sorbent material is ever used.

2-III.6.1 Pluronic F127 Silica

2-III.6.1.1 Synthesis

Pluronic F127 has the general formula $EO_{106}PO_{70}EO_{106}$ and an average molecular weight of 12,600 a.m.u. It is a white solid powder at S.T.P. Porous silica was synthesized using F127 by the following procedure. Pluronic F127 (30 g) and 100 mL of concentrated (12.2 M) HCl were added to 650 mL of deionized water. The mixture was covered, stirred, and heated at 70 °C for 6 h., resulting in a clear solution.

The solution was cooled to room temperature and 46 mL of TEOS was gradually added upon stirring. The molar ratios of the reaction mixture were:

1.0 TEOS : 0.012 F127 : 5.9 HCl : 202 H_2O

This mixture was covered and stirred at room temperature for 24 h. The mixture was then heated to 80 °C and stirred for 72 h. The white solid product was recovered by filtration and washed with deionized water and absolute ethanol. The surfactant template was removed by calcination in air at 550 °C.

2-III.6.1.2 Characterization

The nitrogen adsorption/desorption isotherm for the calcined F127 material is shown in **Figure 2.27**. This unusual isotherm contains three very pronounced steps. This indicates the presence of micro, meso, and macroporosity. The hysteresis shown in the desorption branch of the isotherm may indicate some bottlenecking in the mesoporous range. This material has a calculated surface area of 510 m^2/g, micropore volume of 0.11 cm^3/g, and a total pore volume of 0.40 cm^3/g. Although the pore size distribution (**Figure 2.28**) has a D_{max} of 41.8 Å in the mesoporous range, it also gives evidence for the presence of both micro and macropores. The powder X-ray diffraction pattern is shown in **Figure 2.29**. The relatively broad peak at 2θ = 1.8-3.0° indicates that although this material contains short range order, it is not homogeneous in nature, and therefore not a cubic structure. The peak maximum located at 2θ = 2.17° corresponds to a d-spacing of 45.3 Å. The difference between the d-spacing and

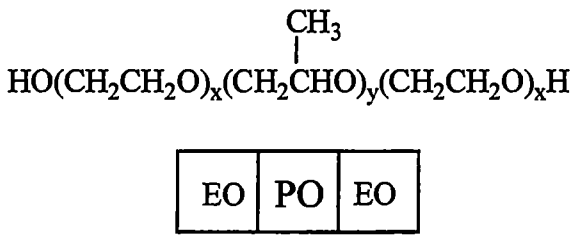


Figure 2.26 General structure of Pluronic surfactants.

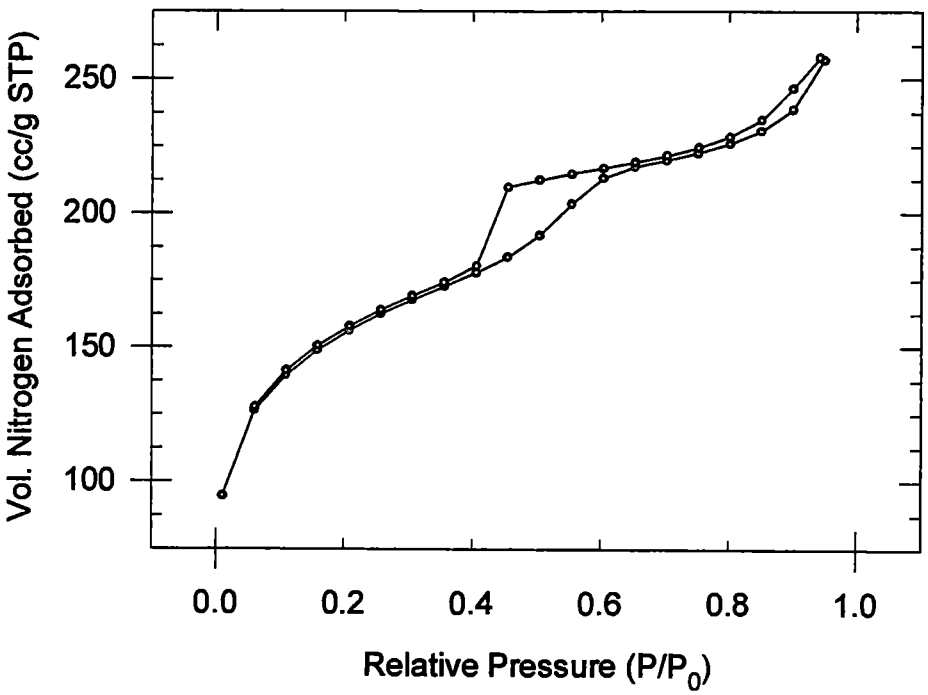


Figure 2.27 N_2 adsorption/desorption isotherm of Pluronic F127 silica.

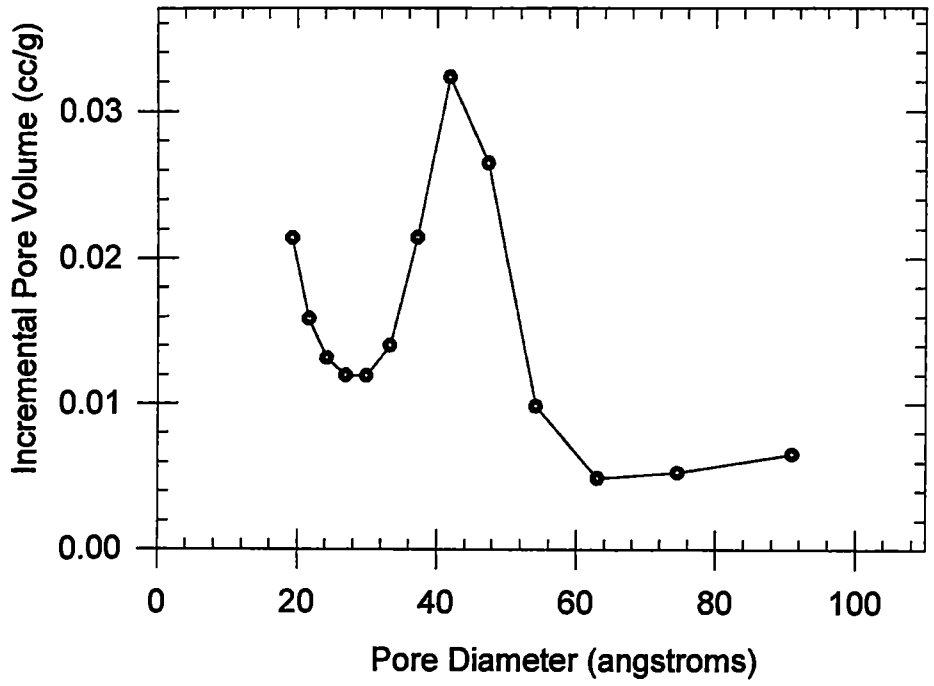


Figure 2.28 Pore size distribution of Pluronic F127 silica.

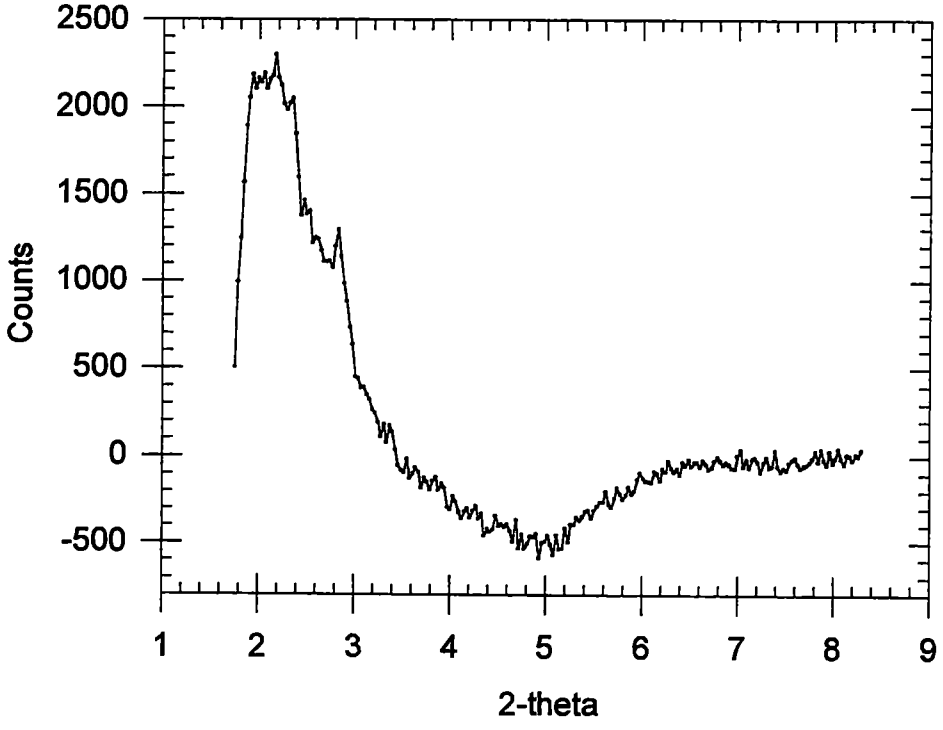


Figure 2.29 Powder X-ray diffraction pattern of Pluronic F127 silica.

the average pore diameter would give an approximate wall thickness of only 3.5 Å. This may not be a very accurate estimate in this case, since the inhomogeneous nature of the pore system in this material gave relatively broad peaks in both the pore size distribution and the X-ray diffraction pattern.

2-III.6.2 Pluronic P85 Silica

2-III.6.2.1 Synthesis

Pluronic P85 has the general formula $EO_{26}PO_{39}EO_{26}$ and an average molecular weight of 4600 a.m.u. It is a viscous, transparent liquid at S.T.P. Porous silica was synthesized using Pluronic P85 by the following procedure. Pluronic P85 (20 g) was placed in a 1 L beaker and 650 mL of deionized water and 100 mL concentrated (12.2 M) HCl were added. The mixture was stirred at 40° C for 2 h. until the surfactant was completely dissolved. TEOS (35 g) was added gradually, and the solution was covered and stirred at 40 °C for 20 h. The molar ratios of the reaction mixture were as follows:

1.0 TEOS : 0.026 P85 : 7.3 HCl : 248 H_2O

The milky white solution was then heated to 90 °C and stirred for an additional 12 h. The solid product was recovered by filtration and washed with plenty of deionized water and absolute ethanol. The surfactant was removed from the solid product by calcination in air.

2-III.6.2.2 Characterization

The nitrogen adsorption/isotherm for the calcined P85 material is shown in **Figure 2.30**. Multiple steps in the isotherm give evidence for both micropores and mesopores. The lack of a sharp step indicates a rather broad distribution of pores. The pore size distribution (**Figure 2.31**) gives a D_{max} of 30.2 Å. This sample has a calculated surface area of 858 m^2/g, micropore volume of 0.17 cm^3/g, and a total pore volume of 0.59 cm^3/g. Despite the good porosity illustrated by these results, the powder X-ray diffraction pattern (**Figure 2.32**) contains no peaks of strong intensity, indicating a lack of short-range order in this material.

2-III.6.3 Pluronic P123 Silica

2-III.6.3.1 Synthesis

Pluronic P123 has the general formula $EO_{20}PO_{70}EO_{20}$ and an average molecular weight of 5800 a.m.u. It is a sticky, transparent paste at S.T.P. Porous silica was synthesized using Pluronic P123 by the following procedure. Pluronic P123 (20 g) was placed in a 1 L round bottom flask with 650 mL of deionized water and 100 mL of concentrated (12.2 M) HCl. This mixture was heated to 50 °C and stirred for 6 h., after which the surfactant had completely dissolved. TEOS (46 mL) was then

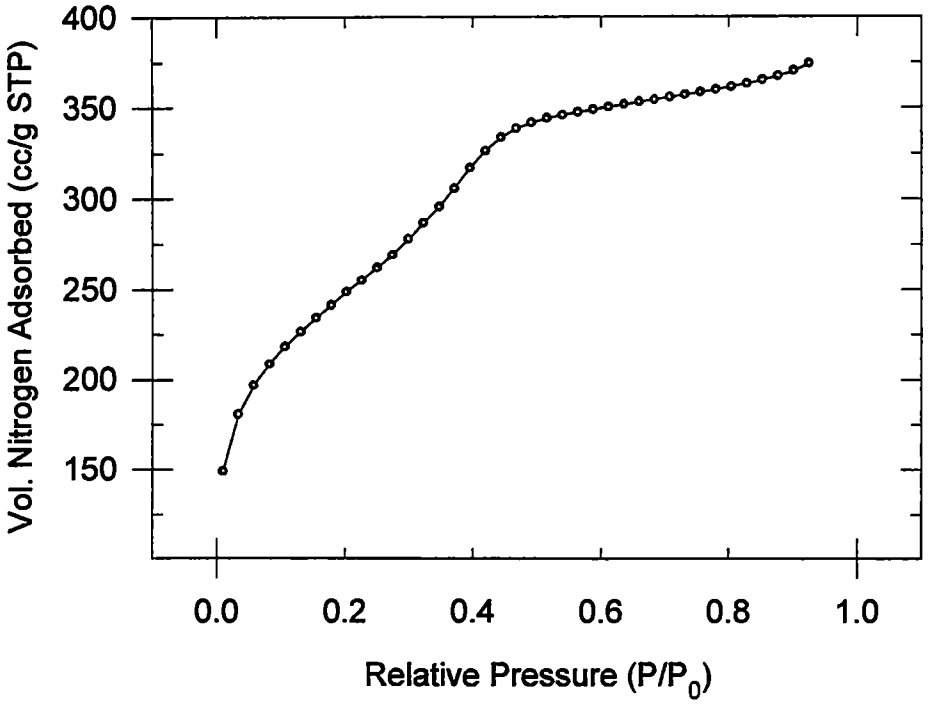


Figure 2.30 N_2 adsorption isotherm of Pluronic P85 silica.

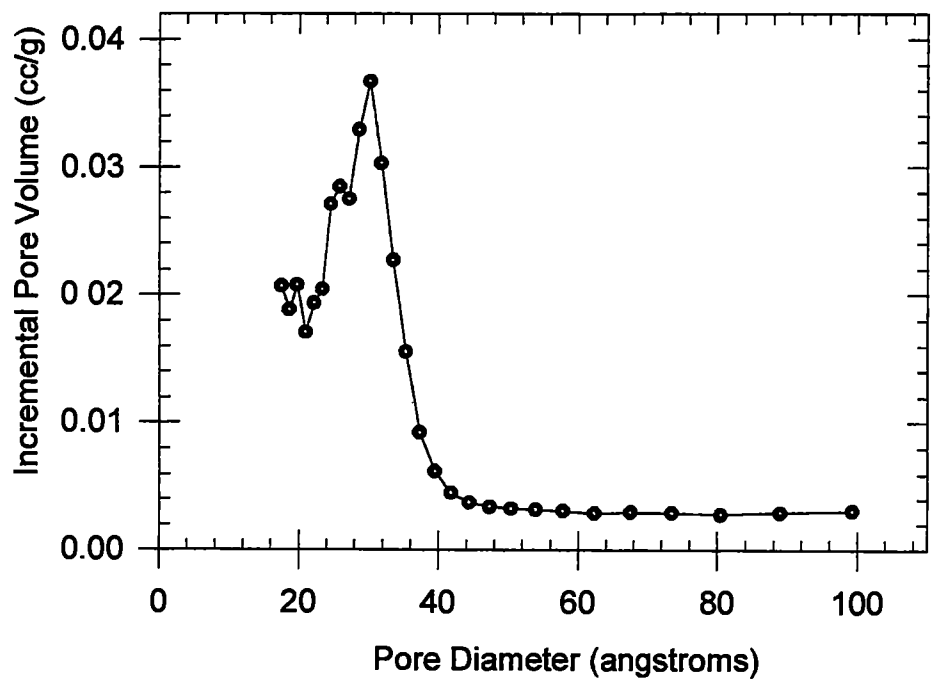


Figure 2.31 N_2 adsorption/desorption isotherm of Pluronic P85 silica.

gradually added to the solution, which was then stirred at 50 °C for 24 h. The milky white solution was then refluxed for an additional 24 h. The molar ratios of the reaction mixture were as follows:

$$1.0\ TEOS : 0.016\ P123 : 5.9\ HCl : 202\ H_2O$$

The white precipitate was recovered by filtration and washed with deionized water and absolute ethanol. The surfactant was removed from the solid product by calcination in air.

2-III.6.3.2 Characterization

The N_2 adsorption/desorption isotherm for the calcined material is shown in **Figure 2.33**. A very large step located in the relative pressure range of ca. 0.6-0.8 is due to the presence of mesopores. The isotherm shape indicates the presence of a broad distribution of micropores and little evidence of macropores. Calculated properties of the calcined product include a B.E.T. surface area of 790 m^2/g, micropore volume of 0.14 cm^3/g, and a total pore volume of 0.99 cm^3/g. The pore size distribution (**Figure 2.34**) shows a rather broad peak with very large pore volumes and a D_{max} of 73.6 Å. **Figure 2.35** shows the powder X-ray diffraction pattern of the calcined Pluronic P123-silica. A sharp peak located at $2\theta = 1.08°$ corresponds to a d-spacing of 90.6 Å. The difference between the d-spacing and the average pore diameter gives an approximate wall thickness of 17 Å. A dark field T.E.M. image (**Figure 2.36a**) of the calcined Pluronic P123-silica illustrates the long ordered

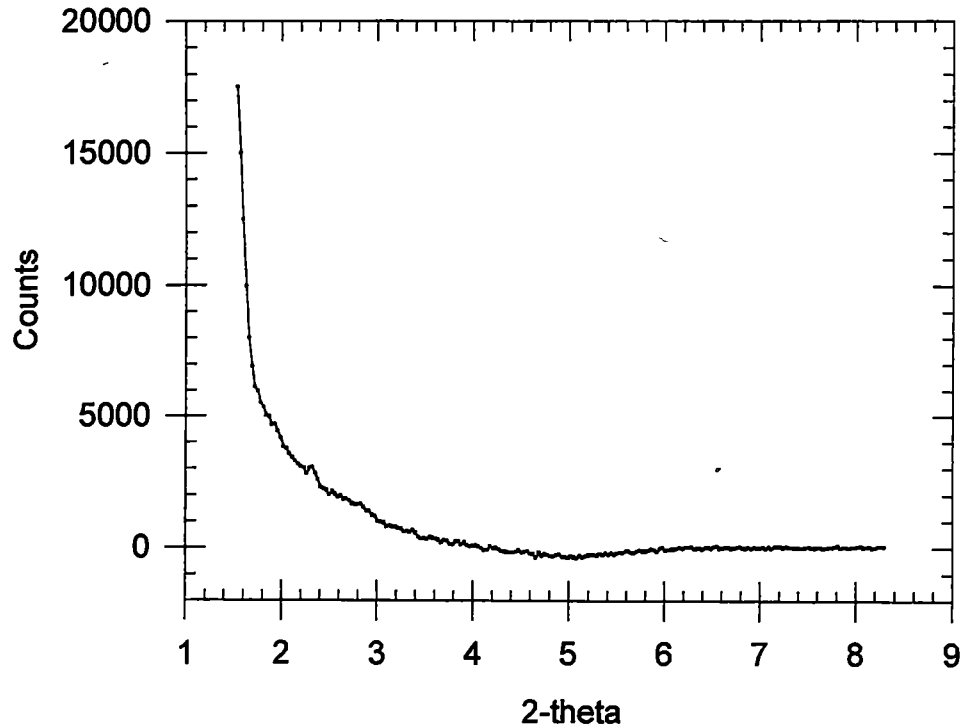


Figure 2.32 Powder X-ray diffraction pattern of Pluronic P85 silica.

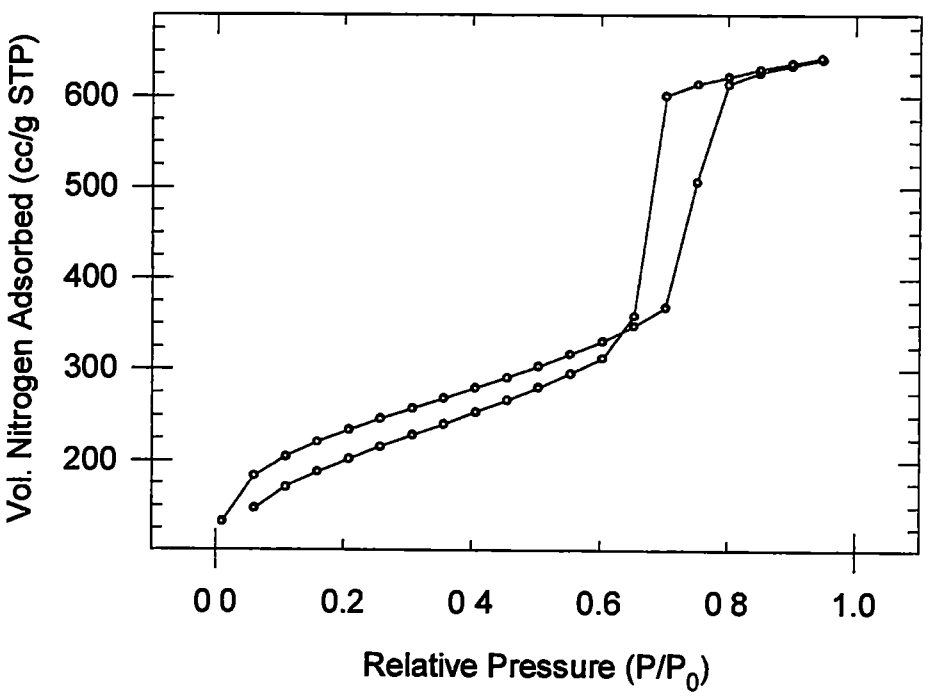


Figure 2.33 N_2 adsorption/desorption isotherm of Pluronic P123 silica.

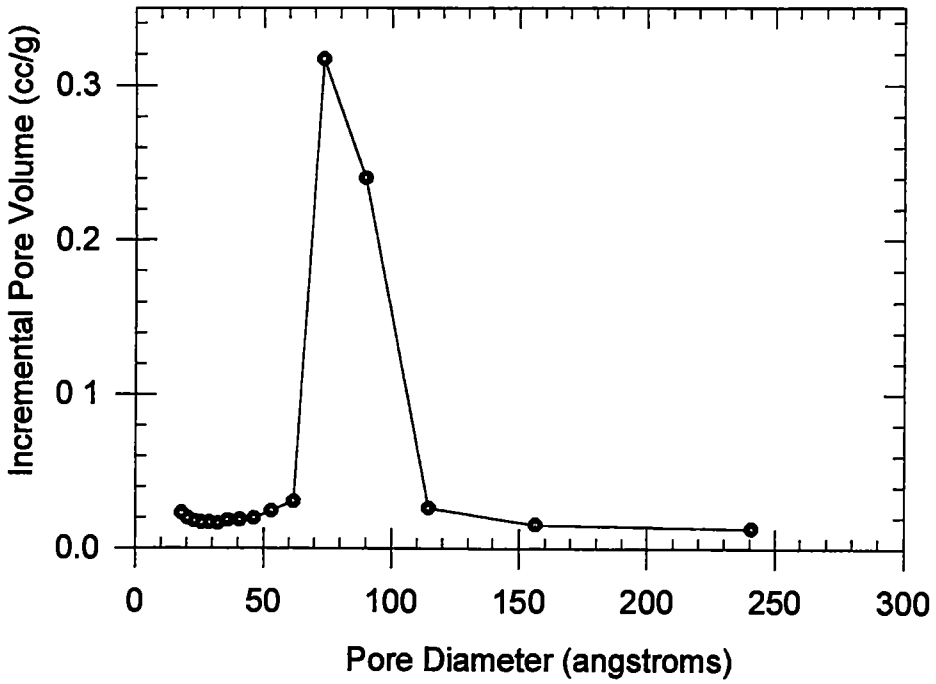


Figure 2.34. Pore size distribution of Pluronic P123 silica.

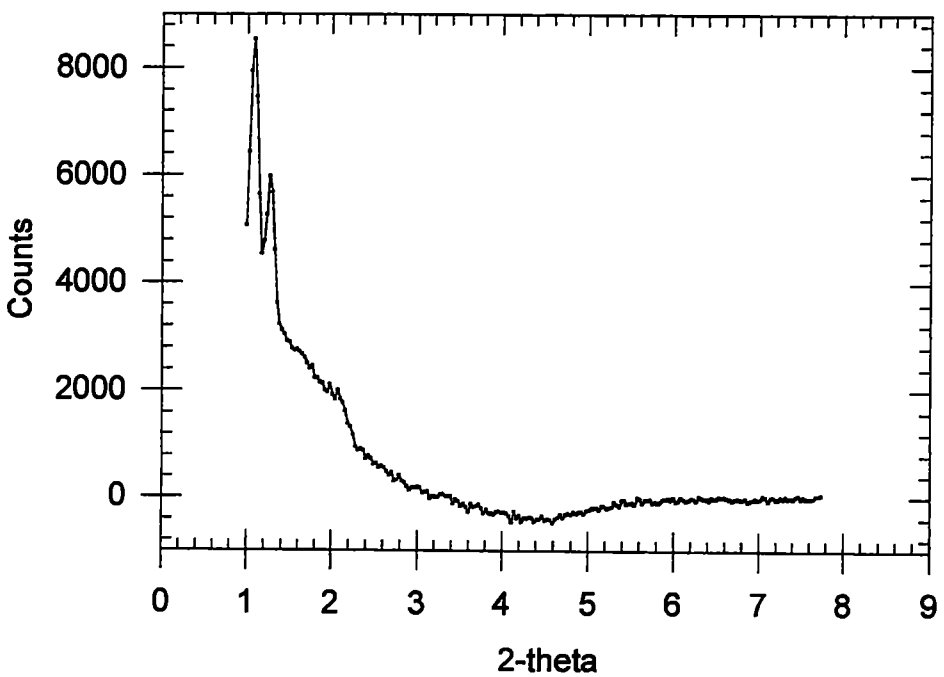


Figure 2.35 Powder X-ray diffraction pattern of Pluronic P123 silica.

channels present in the mesoporous matrix. A high field T.E.M. image of an end-on view of the same sample (**Figure 2.36b**) shows the remarkable hexagonal packing of pores in these self-assembled materials.

2-III.7 Reproducibility

All of the aforementioned syntheses were conducted three times. The reported results represent the best of the three runs. The calculated surface areas were used to determine which syntheses were the best. Powder X-ray analyses were only run on the best samples and only once due to limited instrumental access. Some of the syntheses described for mesoporous silica did not exhibit good reproducibility. **Table 2.1** lists the calculated B.E.T. surface areas from the nitrogen adsorption experiments for multiple runs of each synthesis. It should be noted that the instrumental error bar for the nitrogen adsorption experiment can be as high as two percent. For example, if a single sample with a known surface area of 1000 m^2/g is run multiple times, this value can vary as much as 20 m^2/g.

2-IV. Conclusions

The synthesis of MCM-41 by the base catalyzed proceedure produced mesoporous silica with large surface areas (~1000 m^2/g), and sharp pore size distributions. Powder X-ray diffraction results clearly show that calcination does not result in damage to the mesoporous silica matrix. The reproducibility of the product by this experimental procedure is very good. The pore size (~29 Å) and large pore

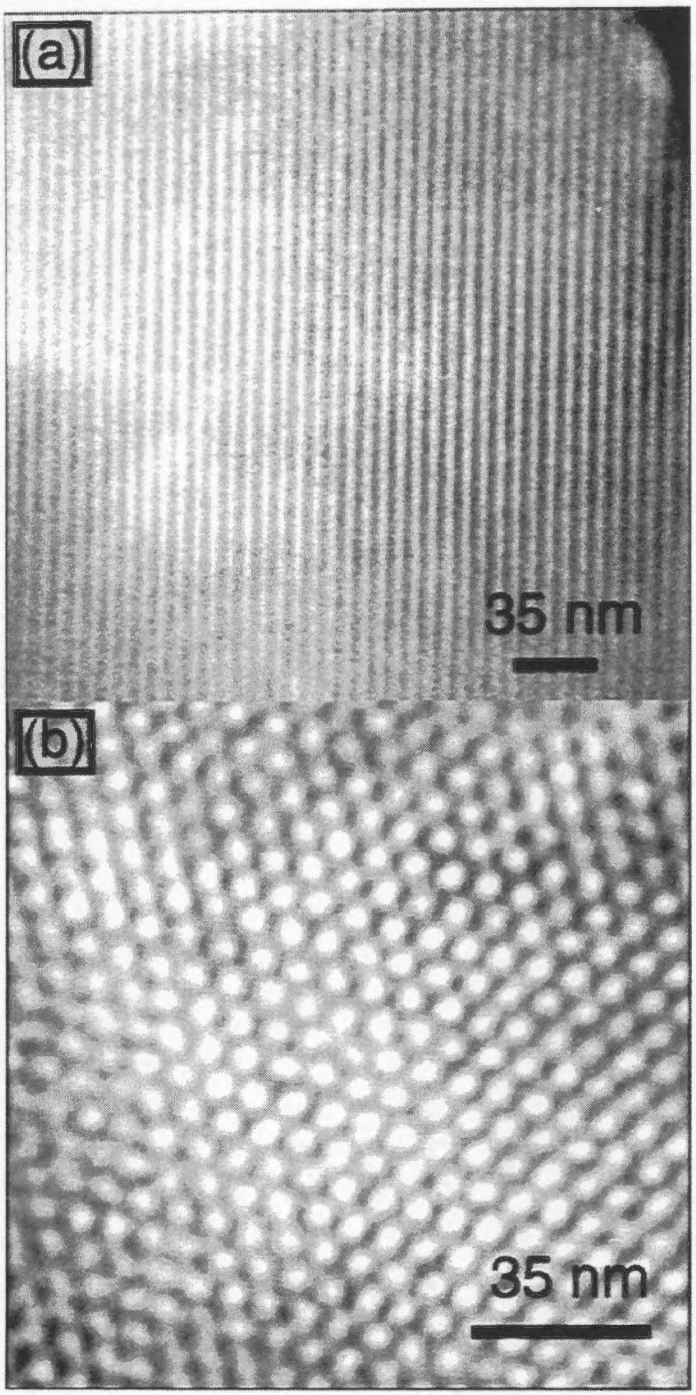


Figure 2.36 TEM image of calcined Pluronic P123 silica.

Table 2.1 Surface areas of synthesized mesoporous silicas.

Synthesis	Surface Area m^2/g
MCM-41	1034
	1010
	983
MCM-41/mesitylene	949
	939
	770
CTAB/H^+	1294
	1217
	1131
HMS	1129
	1121
	1086
Tween 80	620
	511
	288
F127	510
	385
	2.9
P85	858
	673
	609
P123	790
	652
	597

volumes make this material an ideal candidate for a sorbent support. Use of the mesitylene pore expander (CTAB/mesitylene) resulted in larger pores, but also very broad pore size distributions and a general decrease in long-range order.

A comparison of the nitrogen adsorption data for the calcined and extracted $CTAB/H^+$ silica samples clearly indicates that calcination is the more efficient process. Not only was the extraction process more laborious, but also the substantial decrease in surface area and pore sizes in the extracted sample indicates that the extraction failed to remove all of the surfactant. In addition, large amounts of ethanol/HCl/CTAB waste were produced in the process. Powder X-ray diffraction patterns show that, although a slight contraction of the pores does take place during calcination (d-spacing decreased from 40.7 Å to 38.3 Å), the sharp peak indicates that the localized order is retained in the matrix. The calcination process provides an efficient, nondestructive, and clean method for removing the CTAB template molecules from the silica. The lack of porosity and very low surface area of the as-synthesized material indicated by the nitrogen adsorption analysis highlights the importance of the surfactant template in engineering the pore structures of these materials.

This acid catalyzed pathway ($CTAB/H^+$ silica) to porous silica via hydrolytic sol-gel reaction in the presence of supramolecular assemblies of CTAB has some advantages over similar base catalyzed procedures. This reaction proceeds relatively fast and no heating is required. Although the final product is very porous and has a substantial surface area, experimental data indicate that the great majority of the pores

are actually between 10 and 15 Å in diameter. As a support in applications such as sorbents and catalysts, the pores may be too small to allow large molecules access to the inner pore spaces where the great majority of the surface area is located.

Although HMS materials have been reported as having substantially thicker pore walls than their MCM-41 counterparts, our results show that the difference in wall thickness (23.2 Å for HMS and 20.9 Å for MCM-41) is very small. The general protocol for the synthesis of HMS requires no heating and shows excellent reproducibility, but requires a longer reaction time than the CTAB/H^+ silica synthesis which was also performed at ambient temperatures.

The synthesis of mesoporous silica using Tween 80 and Pluronic surfactants as the structure directing agents exhibited a much lower reproducibility than the MCM-41 and HMS analogs. Although the Tween 80 silica showed excellent porosity, no evidence for the reported cubic structure was found. The use of Pluronic F127 resulted in a highly porous network with unusual properties as shown by the multiple steps in the N_2 adsorption isotherm of Pluronic F127 silica. Although the reported cubic structure was not elucidated, this may be an area of future study. The Pluronic P85-silica did not result in the relatively large pore size reported (38). It had a pore size similar to that of MCM-41, but with very thin (ca. 12 Å) pore walls. This could result in pore hydrothermal stability in this material. Pluronic P123 silica exhibited large pore sizes and highly ordered structures. One disadvantage of these materials is the long reaction time required for their formation.

CHAPTER 3

IMPRINT COATING OF MESOPOROUS SILICA

3-I. Introduction

Solvent extraction has been one of the most popular methods for the separation of metal ions from aqueous solutions. A major disadvantage of this technique is that the ligands are slowly absorbed into the aqueous phase(43). Covalent grafting of the ligands to a solid support alleviates this problem, since they are permanently bound and therefore cannot leach into the aqueous phase. Among the many possible substrates on which to immobilize ligands, silica gel has been of particular interest. Silica does not swell like many organic supports, has good mechanical strength, and excellent thermal stability (5). The silicon dioxide matrix is also very stable and resistant to chemical degradation. Only hydrofluoric acid and strongly basic conditions are known to destroy the silica structure (6). Silica is particularly promising as a support for metal ion sorbents in aqueous media, due to its hydrophilic character.

The general procedure for the covalent grafting of ligands to the surface of silica is shown in **Figure 3.1.** Bifunctional reagents consisting of alkoxysilyl groups, an alkyl spacer(X), and ligand(L), undergo condensation reactions with silanol groups on the silica surface (a). These reactions result in the formation of the organofunctionalized silica and alcohol (b). When placed in metal ion solutions, a metal-ligand complex is formed (c). Ligands containing a wide variety of electron

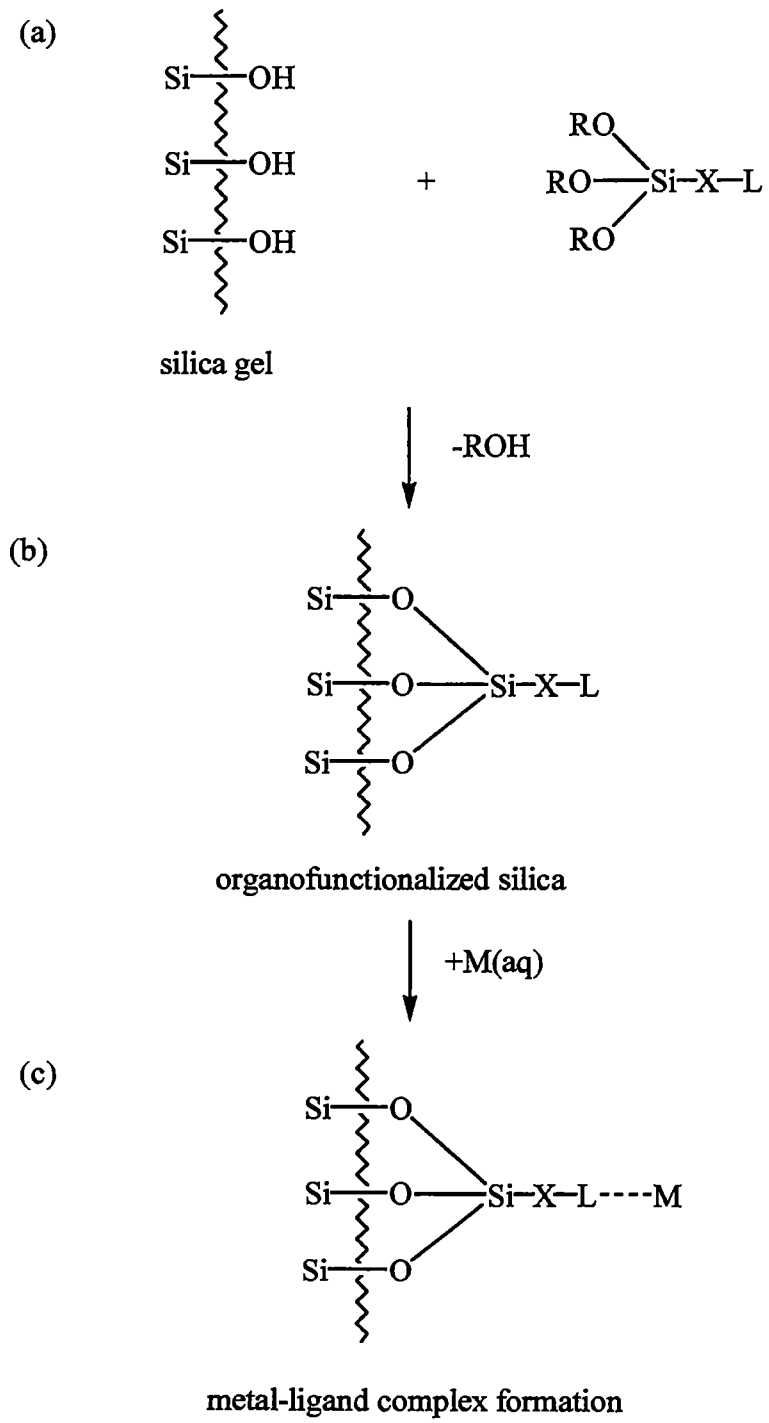


Figure 3.1 Mechanism of ligand grafting to silica surface.

donating atoms (i.e. N, O, P, S) can be used to form metal ion complexes via dative bonding. Once the metal ions are immobilized on the surface, removal of the solid sorbent results in separation.

Many researchers have grafted ligands to amorphous silica gel in order to synthesize selective metal ion sorbents. Izatt and co-workers have immobilized numerous crown ether ligands, each with a unique selectivity for specific metal ions (6-8). Thermodynamic studies have shown that the equilibrium constants for the association of metal cations with the silica gel-bound crown ethers are comparable to log K (H_2O) values for the association of the same cations with the unbound ligand (9). Koklu et al. grafted 3-aminopropyltriethoxysilane to amorphous silica for the removal of Cu(II) and Cd(II) from aqueous solutions (10-11). Airoldi and co-workers reacted silica gel with 3-mercaptopropyltrimethoxysilane to produce a thiol-modified silica material which was shown to remove a wide variety of metal cations [ie. Hg(II), Ag(I), Cu(II), Ni(II), and Zn(II)] from aqueous solutions (12-13).

Although amorphous silica has been shown to be an effective sorbent support, the development of ordered mesoporous silica described in the previous chapter has allowed the technology of functionalized silica to reach a whole new level. Mercier and Pinnavaia have synthesized metal ion sorbents by reacting 3-mercaptopropyl trimethoxysilane with calcined HMS (44-5). A sample of amorphous silica with a similar surface area (750 m^2/g), and average pore diameter (40 Å), was also treated in this way in order to compare the effectiveness of each as a sorbent for the removal of Hg(II) from aqueous solutions. Elemental analysis indicated that the two materials

exhibited a similar ligand loading (1.5 and 1.4 mmol/g, respectively) following treatment. Despite having a similar number of ligands, the HMS sample consistently absorbed more than 10 times the Hg(II) that the amorphous silica sample did. While the Hg(II) loading capacity of functionalized HMS (1.5 mmol/g) was equal to the ligand loading, the Hg(II) loading capacity of the functionalized amorphous material was found to be not more than seven percent of its total ligand loading. Like amorphous silica, ordered mesoporous silica has large enough pores to allow the bifunctional ligands access to its substantial interior pore surfaces. The principal advantage of the HMS is its uniform pore structure, which allows metal ions access to all functionalized sites. Amorphous silica consists of very irregular pore spaces containing bottlenecks which can cause pore blockage making access to the majority of grafted ligands very difficult. These concepts are illustrated in **Figure 3.2**, which shows cross-sectional views of ordered mesoporous (a,b) and amorphous (c) silica sorbents.

In work performed concurrently with that of Mercier and Pinnavaia, Liu and co-workers (46-9) reported an analogous metal ion sorbent. CTAB/mesitylene silica similar to that described in the previous chapter was used as the support for the mercaptopropylsilyl ligands. By using the larger pore (~55 Å) framework and a functionalization process involving repeated cycles of surface hydrolysis and silylation reactions, an unprecedented Hg(II) loading of >500 mg/g was achieved. Batch tests performed on aqueous Hg(II) solutions showed that the sorbent decreased mercury concentrations to less than 1 part per billion after a ten minute contact time. This

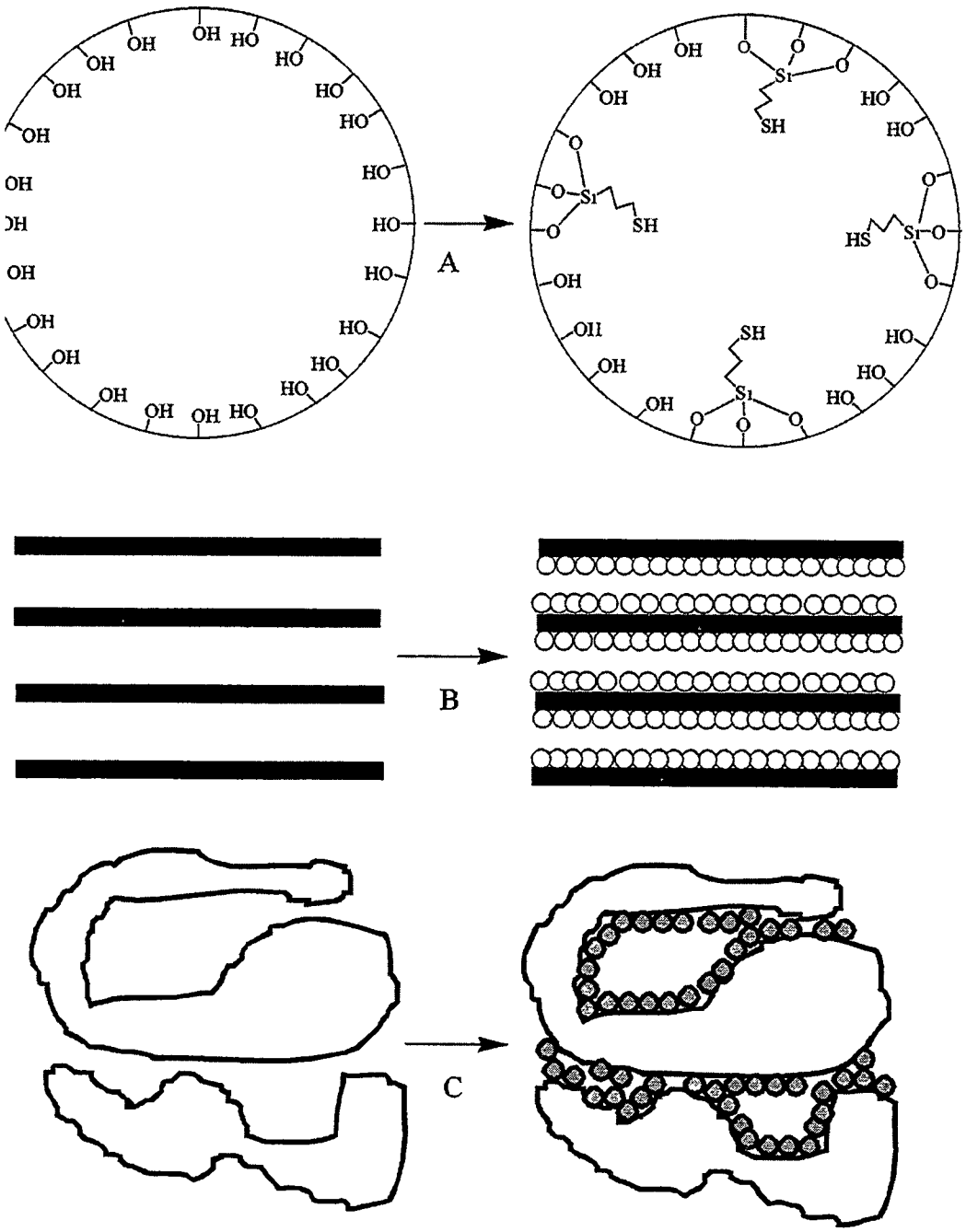


Figure 3.2 Cross-sectional views of the structures of ordered mesoporous (A,B), and amorphous (C), silicas before and after functionalization

combination of high metal ion capacities, fast uptake kinetics, and ability to "polish" solutions to very low concentrations, gives these materials superior performance over all previously developed sorbent technologies (ion exchange materials, functionalized organic polymers, functionalized amorphous silica, etc.) for the removal of metal ions from aqueous media.

With the impressive results reported for functionalized mesoporous materials, we envisioned this as a good starting point for our rational design of metal ion sorbents. Instead of simply grafting ligands to the surface of mesoporous silica, we used the technique known as molecular imprinting to enhance the metal ion selectivity of these materials. The technique of molecular imprinting involves the incorporation of a template into a host matrix by combining it with polymerizable functional groups, which are copolymerized with host monomers, surrounding the template (**Figure 3.3**). Subsequent removal of the template results in a material that contains imprints with the ideal size, shape, and chemical environment to rebind the template. The imprinting approach based on organic polymer hosts was first developed by Wulff and Sarhan (21) who used this technique to produce polymers for the resolution of racemic mixtures. It has since been utilized in the development of artificial enzymes (22), and antibodies (23-4), chromatographic resins (25), and metal ion sorbents (26). In analogies to our present work, the templates are metal ions and the polymerizable functional groups take the form of bifunctional reagents which contain both alkoxysilyl and amine groups. The amine groups form complexes with the metal ion templates via dative bonding. The alkoxysilyl groups undergo condensation reactions

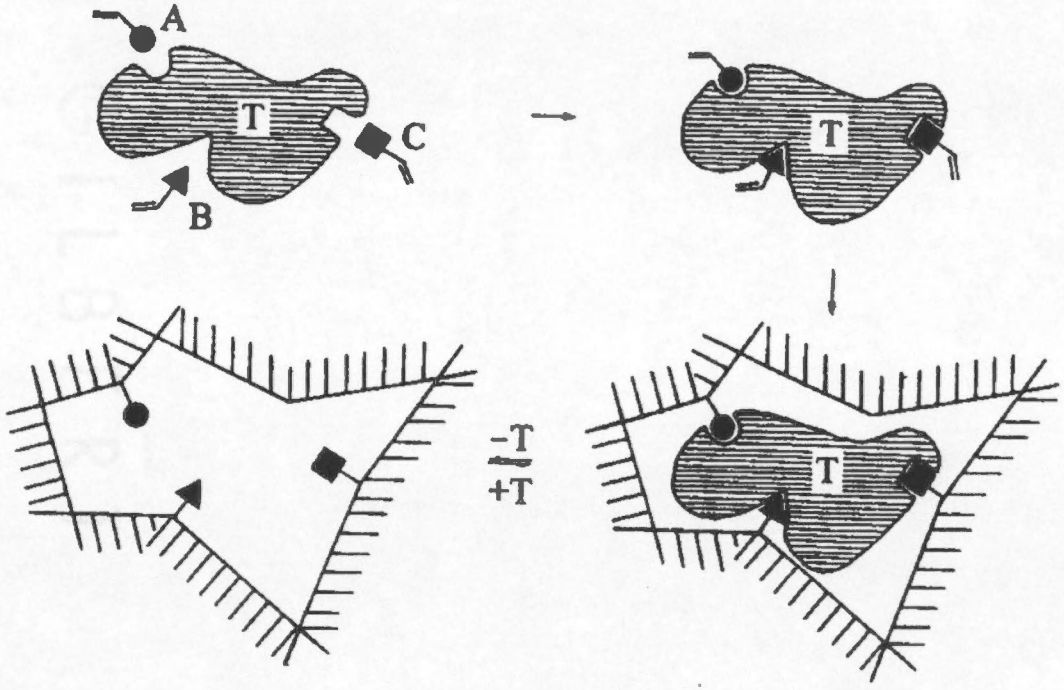


Figure 3.3 Schematic representation of molecular imprinting

with the silanol groups on the silica surface. Surface imprinting of both organic and inorganic molecules has been reported on amorphous silica and organic polymer surfaces. (50-2).

Since our methodology involves the coating of imprints on ordered mesoporous supports, it is referred to as "imprint coating." One of the keys to this approach is that the metal-ligand coordination complexes are formed prior to the surface functionalization (**Figure 3.4**). In this way the ligands are arranged in ideal conformations for metal ion binding affinity. A material prepared by conventional surface functionalization techniques, as illustrated in **Figure 3.5**, grafts ligands to the silica surface in relatively random orientations. Once the metal ion template has been removed from the imprint coated samples, a comparison of the two structures (**Figure 3.6**) shows the difference between the cavities generated by conventional coating and imprint coating. Although the flexibility of the grafted ligands may allow for reorientation in the nonimprinted materials, the resulting metal-ligand complexes would be formed in higher energy conformations than those of the imprint coated materials. This is due to the increased strain on the ligand molecules caused by the stretching or bending required for complex formation in the nonimprinted sorbents. The ligand molecules in the imprint coated materials are already in their most stable conformations because they were formed this way and therefore, no reorientation is necessary.

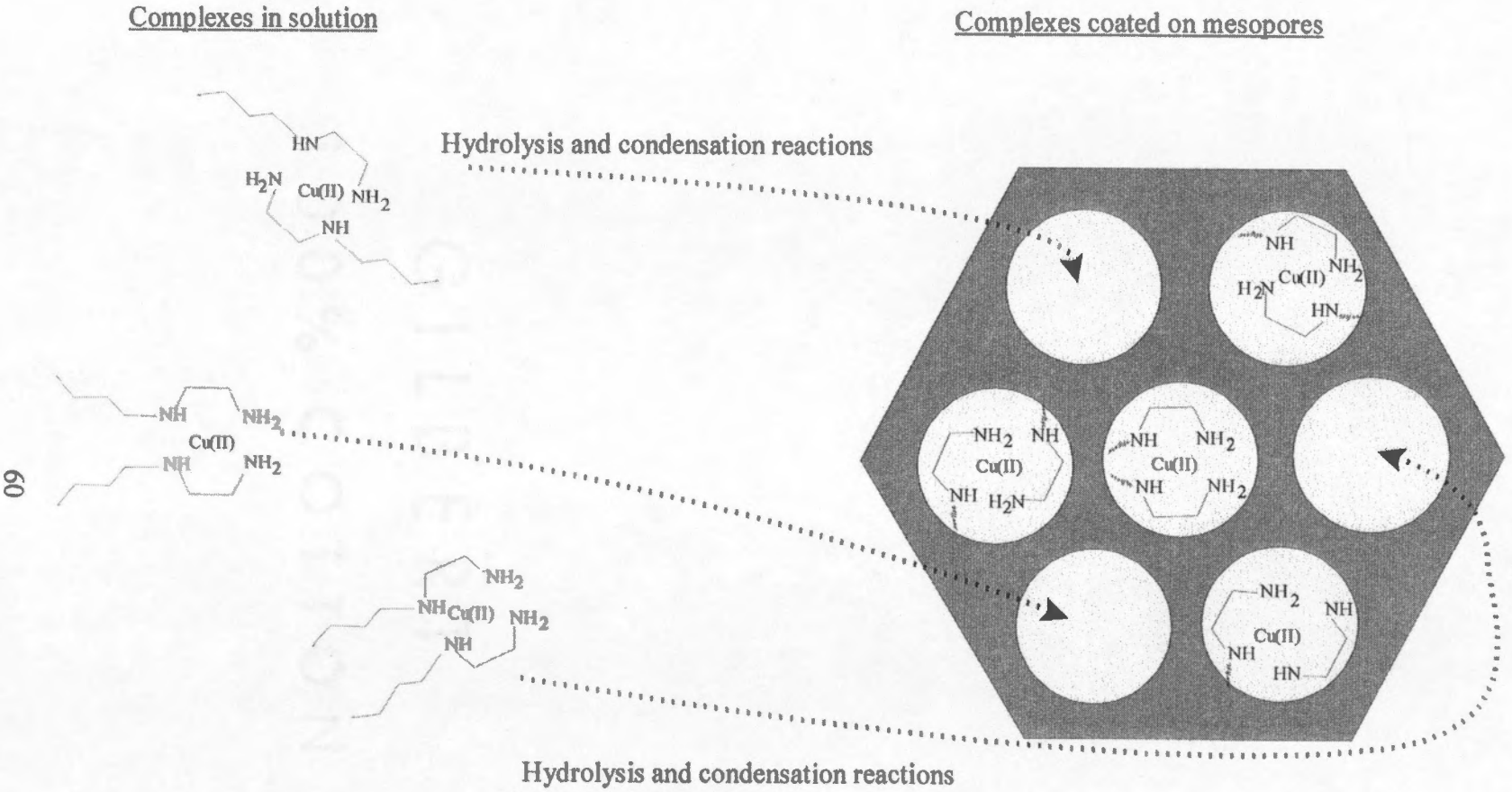


Figure 3.4 Mechanism of imprint coating functionalization

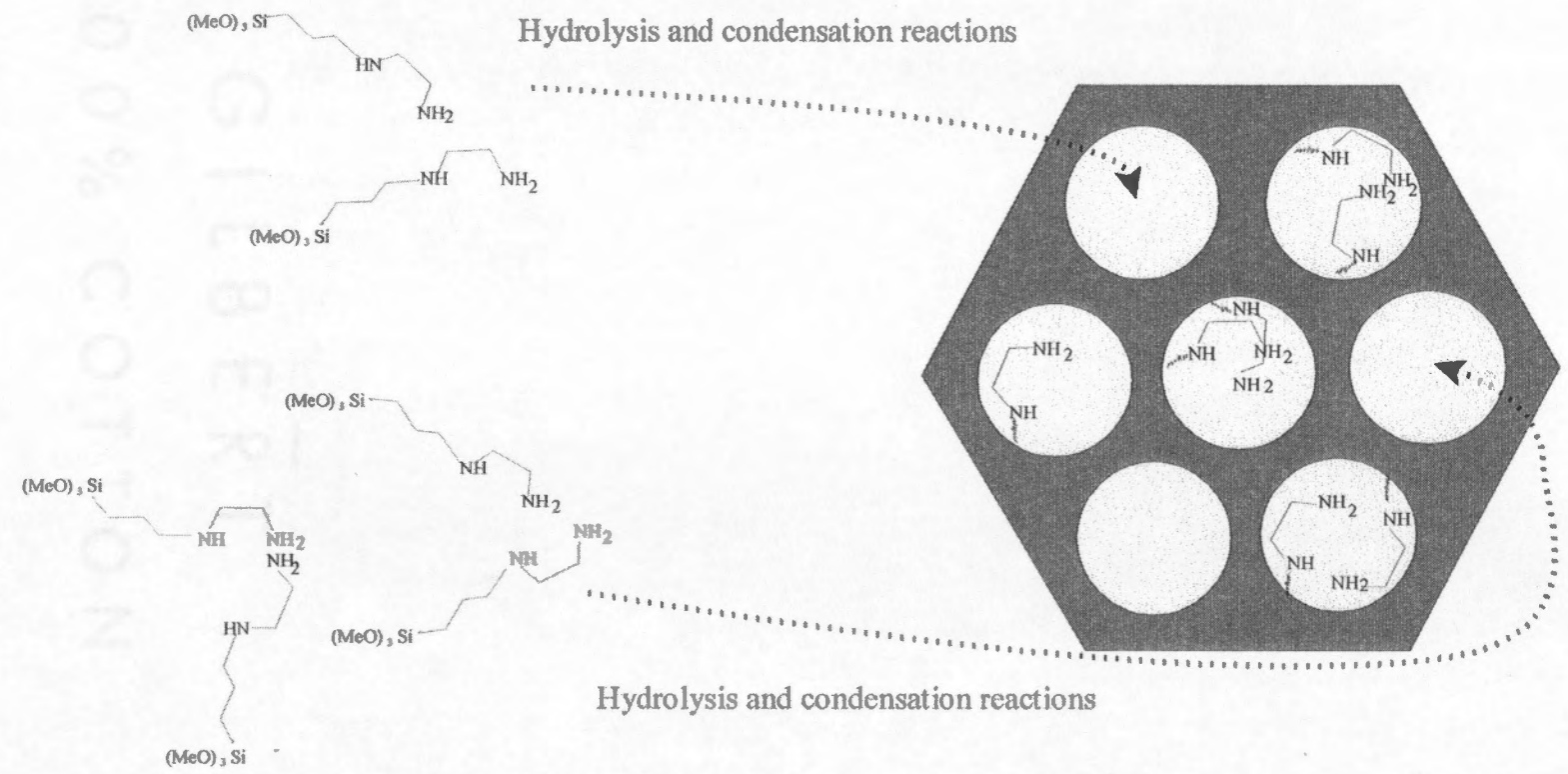
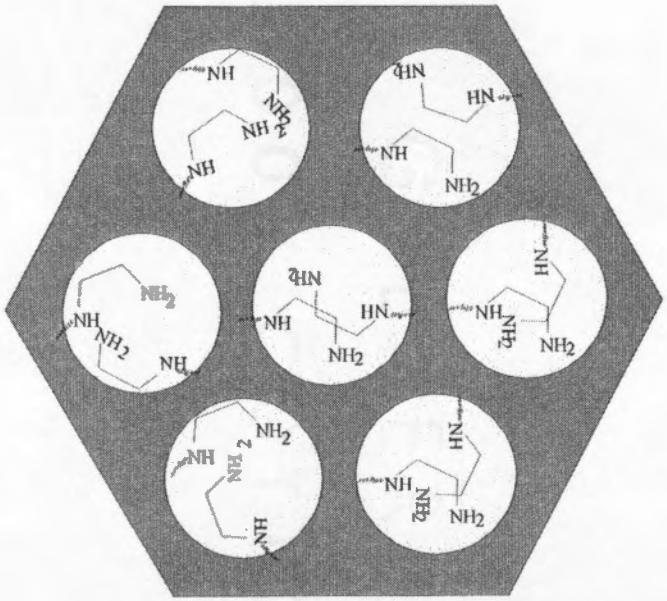
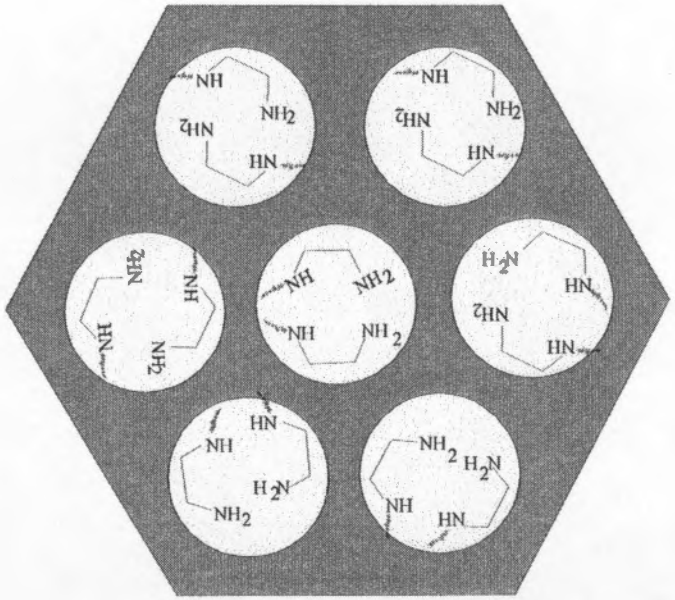


Figure 3.5 Conventional surface functionalization procedure



Ordered mesopores coated
with the conventional method



Ordered mesopores coated
with the surface imprinting method

Figure 3.6 Binding cavaties created by conventional coating and imprint coating

3-II. Preliminary Experiments

In order to demonstrate both the basic principles and the ease with which imprint coated sorbents may be prepared, amine-functionalized, ordered mesoporous sorbents were imprinted with Cu(II). Amine ligands were chosen for their versitility, since they form stable coordination complexes with a wide variety of metal ions. The pH dependence of complexation allows for a simple mechanism for template removal. Under mildly acidic conditions the amine groups are protonated and metal ions are removed. Also, the bifunctional form of various amine ligands are commercially available so that time-consuming syntheses are unnecessary. The reasons for selecting Cu(II) as the primary metal ion template are as follows. The cupric ion forms strong dative bonds with amine ligands. These copper-amine complexes absorb light in the visible region with relatively large molar absorptivity coefficients. These distinctly colored complexes (blue through dark violet), can be used as a probe at the different stages of sorbent synthesis, template removal, and reloading. Since Cu(II) has the same charge, similar size, and similar chemical reactivity as Ni(II) and Zn(II) it is well suited for the study of selective adsorption from mixed solutions.

A selective sorbent for copper(II) would have wide ranging applications. Copper is a fatal toxin for many plant and animal species at concentrations not considered harmful to humans. Because of the many concerns over environmental issues deemed more important (i.e. radioactive waste, pesticides etc.), copper pollution has been largely ignored. Human activities have resulted in the dissemination of copper throughout the world's waterways. Its presence in acid mine drainage(53),

landfill leachate(54), electroplating wastewater(55), smelting stack precipitates(56), paper mill effluents(57), and numerous municipal and industrial wastestreams, makes copper pollution a worldwide problem. Since Cu(II) is frequently present in mixed solutions with other cations which compete for sorbent coordination sites, an efficient sorbent must selectively adsorb Cu(II)

3-II.1 Synthesis

Two different bifunctional reagents, [3-(trimethoxysilyl)propylamine] (TMSA), and N-[3-(trimethoxysilyl)propyl]ethylenediamine (TMSen), were used to create metal ion sorbents via imprint coating. Calcined MCM-41 (Chapter 2, section III-1) was used as the sorbent support. Methanol was chosen as the solvent in which to conduct the imprint coating of $[Cu(TMSen)_2]^{2+}$ (11), while water was used as the solvent for the imprint coating of $[Cu(TMSA)_5]^{2+}$. The reason for choosing water for the latter is that the stability constant of Cu(II) complexed to TMSA is very small in methonal. The stoichiometric ratios of metal ion to amine ligand were chosen based on the coordination environment preferred by the cupric ion with the given ligand.

3-II.1.1 Cu(II)/TMSen/MCM-41

In a typical preparation, copper nitrate trihydrate [$Cu(NO_3)_2$ $3H_2O$, 0.576 g] was added under stirring to methanol (CH_3OH, 50 mL). After the metal salt had completely dissolved, TMSen (1.02 mL) was added. After stirring the mixture for 1 h, calcined MCM-41 (0.25 g) was added. The solution was stirred and evaporated to

dryness. A nonimprinted sample was prepared by an identical protocol with the exception that no metal salt was added. The residue was washed with nitric acid (HNO_3, excess) to remove the Cu(II) template. Excess bifunctional reagent is redissolved and washed away. The resulting gel was placed in deionized water and titrated with sodium hydroxide (NaOH, 2 N) to pH 7.5, recovered by filtration, washed with deionized water and absolute ethanol, and placed under vacuum at 80 °C for 4 h.

3-II.1.2 Cu(II)/TMSA/MCM-41

In a typical preparation, copper nitrate trihydrate [$Cu(NO_3)_2$ $3H_2O$, 0.576 g] was added under stirring to deionized water (50 mL). After the metal salt had completely dissolved, TMSA (2.57 mL) was added. After stirring the mixture for 1 h, calcined MCM-41 (0.25 g) was added. The solution was stirred and evaporated to dryness. A nonimprinted sample was prepared by an identical protocol with the exception that no metal salt was added. The residue was washed with nitric acid (HNO_3, excess) to remove all of the copper template. The resulting gel was placed in deionized water and titrated with sodium hydroxide (NaOH, 2 N) to pH 7.5, recovered by filtration, washed with deionized water and absolute ethanol, and placed under vacuum at 80 °C for 4 h.

3-II.2 Batch Tests

All metal ion solutions were buffered to pH = 5.0 (NaAc/HAc, 0.05 M). In a typical run, 0.1 g of sorbent and 10 mL of a metal ion solution were sonicated in capped PET vials for 30 min. The resulting mixture was filtered and both the filtrate

and the initial standard solutions were analyzed via ICP/OES. The overall capacity of the sorbent for a given metal has been reported as the percentage of the initial concentration that was adsorbed. Values are based on the average of six replicate measurements conducted on the filtrate and standard solutions. The detection limits of Cu(II) and Zn(II) were determined to be 2 ppb by measuring the ICP response of deionized water. Ten replicate measurements were taken following plasma stabilization on three non-consecutive days. The concentration corresponding to three times the standard deviation was taken as the limit of detection. Based on these results the error bar for the metal ion analyses is approximately +/- 0.03%. All analyses were conducted on samples which were synthesized in the same batch. Larger changes in the percentage uptake of these sorbents occur from one batch to another, but no changes in the fundamental trends were observed.

3-II.3 Analytical Techniques

All metal ion concentration analyses were performed with a Perkin-Elmer Plasma 400, inductively coupled plasma spectrometer. UV/Visible spectra were measured with a Cary 14H scanning spectrophotometer converted by On-Line Instrument Systems (OLIS) for data acquisition via PC. X-ray scattering plots of the samples were measured on the 10 m small-angle X-ray scattering camera at the SAXS user facility at the Oak Ridge National Laboratory.

3-II.4 Metal(II) Sorption Calculations

The metal ion uptake of a given sorbent material can be expressed in terms of a distribution coefficient (K_d), according to equation (3-1):

$$K_d = (C_0\text{-}C_f/C_f) * (\text{mL solution/g sorbent}) \quad (3\text{-}1)$$

Where C_0 and C_f represent the initial and final concentrations of the metal ion solution. A selectivity coefficient, *k*, for the binding of a specific metal ion in the presence of competitor species can be obtained from equilibrium binding data according to equation (3-3):

$$M_1(\text{solution}) + M_2(\text{sorbent}) \rightleftharpoons M_2(\text{solution}) + M_1(\text{sorbent}) \quad (3\text{-}2)$$

$$k = \{[M_2]_{sol}[M_1]_{sor}\} / \{[M_1]_{sol}[M_2]_{sor}\} = K_d(M_1)/K_d(M_2) \quad (3\text{-}3)$$

Comparison of the *k* values for the imprinted and nonimprinted samples can show the effect that imprinting has on the metal ion selectivity for a given sorbent (26). The selectivities of these sorbents were investigated using aqueous solutions of Zinc(II) and Cu(II). A measure of the increase in selectivity due to molecular imprinting can be defined by the ratio of the selectivity coefficients of the imprinted and nonimprinted materials, and is referred to as the relative selectivity coefficient, *k'*.

$$k' = k_{\text{imprinted}} / k_{\text{nonimprinted}} \quad (3\text{-}4)$$

3-II.5 Results and Discussion

Table 3.1 summarizes the measured adsorption capacities of imprint-coated and conventionally coated mesoporous sorbents for Cu(II). Both imprinted sorbents exhibited higher effective capacities for Cu(II) than the corresponding nonimprinted samples. The enhanced capacities of the imprinted materials for the metal ion template are illustrated by their larger distribution coefficients.

Table 3.1 Cu(II) Uptake Capacity of Cu(II) Imprint Coated and Nonimprinted Sorbents

Sorbent	C_0 (ppm)	C_f (ppb)	K_d Cu	% Cu(II) absorbed	Cu(II) capacity (mmol/g)
Nonimprinted-TMSA	63.55	1,143	5300	98.2	0.098
Imprinted-TMSA	**63.55**	**254**	**26000**	**99.6**	**0.1**
Nonimprinted-TMSen	63.55	953	6800	98.5	0.099
Imprinted-TMSen	**63.55**	**191**	**39000**	**99.7**	**0.1**
Nonimprinted-TMSen	6.35	51	14000	99.2	0.0099
Imprinted-TMSen	**6.35**	**<6**	**>105000**	**>99.9**	**0.01**

The results of competitive ion sorption experiments performed with both the Cu(II) imprinted and nonimprinted sorbents using mixed solutions containing equimolar amounts of Cu(II) and Zn(II) are listed in **Table 3.2**. The Cu(II) imprinted sorbent materials synthesized with both the TMSA and TMSen bifunctional reagents exhibited larger selectivity coefficients (k) than their nonimprinted analogs. A comparison of the K_d values for the Cu(II) imprinted samples with the nonimprinted samples for the TMSen-coated system shows a six-fold increase in K_d for Cu(II), while the K_d for Zn(II) decreases by the same amount. The value of the selectivity coefficient (k') is greater than unity for all imprint-coated sorbents. The k' value of 40 for the TMSen-imprint-coated sorbent is, to the best of our knowledge, the highest value ever reported for the molecular imprinting of metal ions (26, 59-62). The k' (1.7) for the TMSA-imprinted sorbent is smaller than that for the TMSen-imprinted material.

The UV/Vis spectra of the two imprinting precursor complexes [$Cu(TMSA)_5^{2+}$ and $Cu(TMSen)_2^{2+}$], and the corresponding diffuse reflectance spectra of washed and dried imprint coated mesoporous silicas are shown in **Figure 3.7**. The close match between the spectra of $Cu(TMSen)_2^{2+}$ and $Cu(s\text{-}TMSen)_2^{2+}$ (s-TMSen = surface coated TMSen ligand) indicates that the stereochemical environments of the copper ions in the two systems are similar and that the complex is coated on the silica surface. The absorption band in the UV/Vis spectrum of $Cu(s\text{-}TMSA)_5^{2+}$ is broader than that of the corresponding precursor complex solution. On the basis of the average environmental rule (63) this indicates that the distribution of distinct copper complexes in the solid

Table 3.2 Competitive Loading of Cu(II) and Zn(II) by Cu(II) Imprinted and Nonimprinted Sorbents

Sorbent	Initial Concentrations		% Cu(II) absorbed	% Zn(II) absorbed	K_d Cu	K_d Zn	k	k'
	Cu(II) (M)	Zn(II) (M)						
Nonimprinted TMSA	0.001	0.01	35.4	63.3	55	170	0.3	-
Imprinted TMSA	**0.001**	**0.01**	**53.2**	**68**	**110**	**210**	**0.5**	**1.7**
Nonimprinted TMSen	0.001	0.001	98.5	96.6	6500	2900	2.3	-
Imprinted TMSen	**0.001**	**0.001**	**99.8**	**82.9**	**44000**	**480**	**91**	**40**
Nonimprinted TMSen	0.001	0.005	98.5	70	6500	230	28	-
Imprinted TMSen	**0.001**	**0.005**	**99.6**	**52.6**	**2400**	**110**	**220**	**7.7**

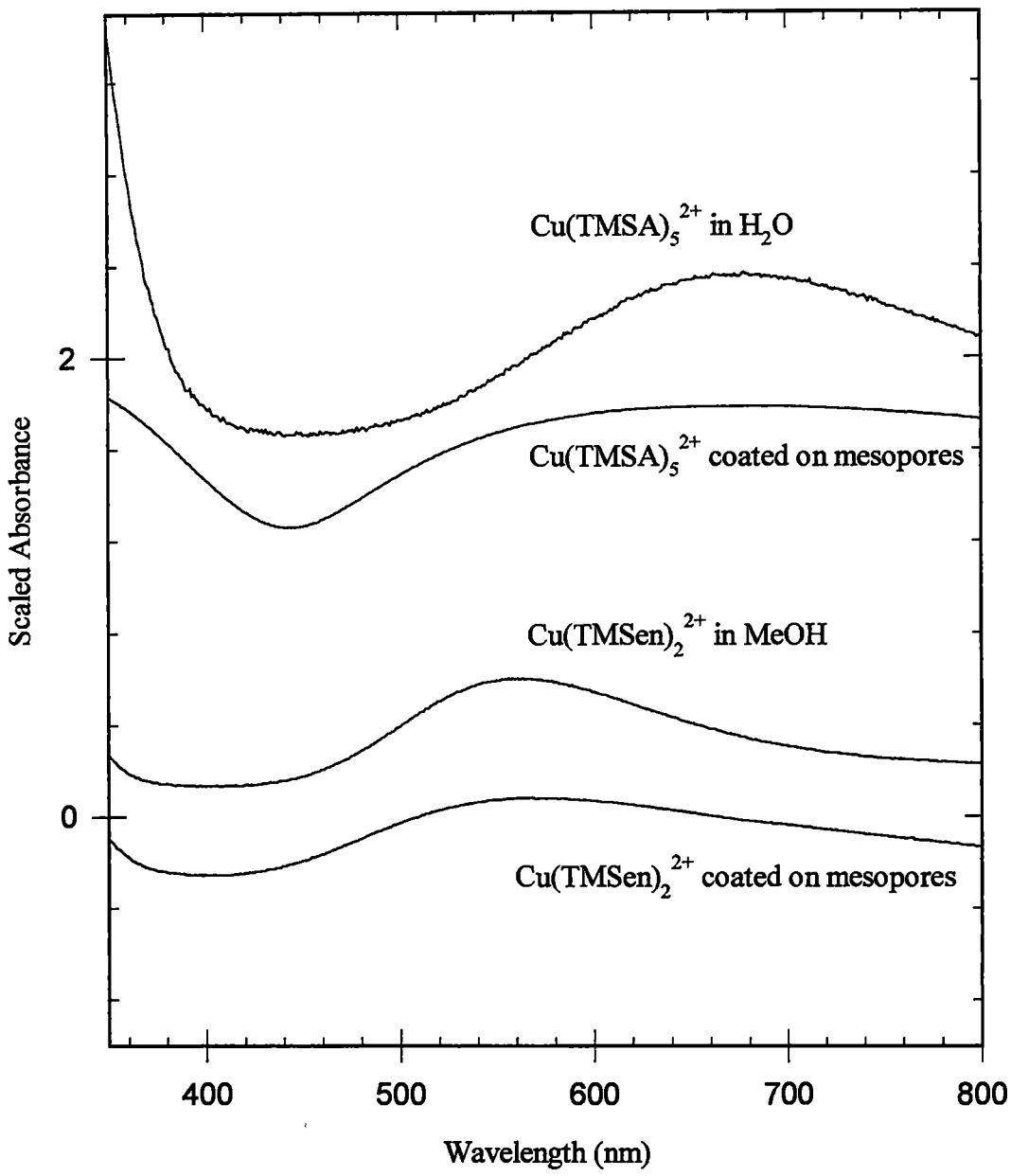


Figure 3.7 UV/Vis spectra of precursor complexes and the corresponding diffuse reflectance spectra of the complexes coated on the mesopore surfaces

phase is broader than that in the solution phase. The locations of the electronic transition bands for all the complexes agree well with those of the model complexes $Cu(en)_2^{2+}$ and $Cu(NH_3)_5^{2+}$ (64).

3-III. Imprint Coating of Amorphous Silica

Some of the advantages of using ordered, mesoporous silica as sorbent support over conventional amorphous silica were discussed earlier (Chapter 3, Section I). The inaccessibility of many of the ligands in the amorphous case (Figure 3.2 and ref. 44), results in a lower overall metal ion capacity than in ordered, mesoporous sorbents of similar surface area and ligand loading. In order to compare the performance of organofunctionalized sorbents synthesized with an amorphous silica support to those with ordered, mesoporous supports, we imprint coated a commercially available amorphous silica gel. The same ligands (TMSA and TMSen) and similar synthetic conditions were employed that we used to synthesize the Cu(II)/TMSen/MCM-41 and Cu(II)/TMSA/MCM-41 sorbents in Section II. These analogous syntheses, coupled with metal ion batch experiments similar to those performed in Section II, will allow us to compare a number of important characteristics of these two types of sorbents. The goal here is not only to compare overall metal ion capacities, but also to see what effect the support morphology has on molecular imprinting characteristics of imprinted and nonimprinted sorbents, such as differences in capacities and selectivities.

3-III.1 Synthesis

The synthetic protocols employed here are similar to those followed in Section II.1, with the exception that the commercially available amorphous silica (Aldrich, d = 60 Å, surface area = 600 m^2/g) was used as the support. Methanol was again used as the solvent for imprint coating of TMSen, while a separate experiment was carried out using water to see its effect on the resulting sorbent. The imprint coating of TMSA was also performed in water. Copper(II) was used as the metal ion template for all imprinted materials.

3-III.1.1 Cu(II)/TMSen/SG/MeOH

In a typical preparation, copper nitrate trihydrate [$Cu(NO_3)_2$ $3H_2O$, 0.576 g] was added under stirring to methanol (CH_3OH, 50 mL). After the metal salt had completely dissolved, TMSen (1.02 mL) was added. After stirring the mixture for 1 h, silica gel (0.25 g) was added. The solution was stirred and evaporated to dryness. A nonimprinted sample was prepared by an identical protocol with the exception that no metal salt was added. The residue was washed with nitric acid (HNO_3, excess) to remove all of the copper template. The resulting gel was placed in deionized water and titrated with sodium hydroxide (NaOH, 2 N) to pH 7.5, recovered by filtration, washed with deionized water and absolute ethanol, and placed under vacuum at 80 °C for 4 h.

3-III.1.2 Cu(II)/TMSen/SG/H_2O

In a typical preparation, copper nitrate trihydrate [$Cu(NO_3)_2$ $3H_2O$, 0.576 g] was added under stirring to 50 mL of deionized water. After the metal salt had completely dissolved, TMSen (1.02 mL) was added. After stirring the mixture for 1 h, silica gel (0.25 g) was added. The solution was stirred and evaporated to dryness. A nonimprinted sample was prepared by an identical protocol with the exception that no metal salt was added. The residue was washed with nitric acid (HNO_3, excess) to remove all of the copper template. The resulting gel was placed in deionized water and titrated with sodium hydroxide (NaOH, 2 N) to pH 7.5, recovered by filtration, washed with deionized water and absolute ethanol, and placed under vacuum at 80 °C for 4 h.

3-III.1.3 Cu(II)/TMSA/SG

In a typical preparation, copper nitrate trihydrate [$Cu(NO_3)_2$ $3H_2O$, 0.576 g] was added under stirring to deionized water (50 mL). After the metal salt had completely dissolved, TMSA (2.57 mL) was added. After stirring the mixture for 1 h, silica gel (0.25 g) was added. The solution was stirred and evaporated to dryness. A nonimprinted sample was prepared by an identical protocol with the exception that no metal salt was added. The residue was washed with nitric acid (HNO_3, excess) to remove all of the copper template. The resulting gel was placed in deionized water and titrated with sodium hydroxide (NaOH, 2 N) to pH 7.5, recovered by filtration,

washed with deionized water and absolute ethanol, and placed under vacuum at 80 °C for 4 h.

3-III.2 Results and Discussion

The copper(II) uptake capacities of the Cu(II) imprinted and nonimprinted sorbents coated on the amorphous silica are shown in **Table 3.3**. The results of competitive ion adsorption batch tests employing a mixed solution of equimolar (0.001 M) amounts of Cu(II) and Zn(II) are summarized in **Table 3.4**. The results of similar competitive adsorption experiments using excess zinc(II) ion (0.01 M) are summarized in **Table 3.5**.

The copper(II) uptake capacities of both the Cu(II) imprinted and nonimprinted sorbents synthesized with amorphous silica (Table 3.3) are considerably lower than those synthesized with MCM-41 as the support (Table 3.1). While all of the sorbents made with MCM-41 removed greater than 98% of the copper(II) from 63.55 ppm solutions, none of the amorphous silica-based sorbents removed as much as 90%. In addition, the significant enhancement of copper(II) capacity exhibited by the Cu(II)-imprinted MCM-41-based sorbents, that resulted in a five to eight-fold increase in K_d values over nonimprinted samples, is not exhibited by the amorphous silica imprint-coated sorbents.

The Cu(II)/TMSA/SG sorbents had the lowest Cu(II) uptake, removing less than 20% of the copper(II) from the 63.55 ppm solutions. In contrast to the sorbents synthesized with the TMSA ligand on MCM-41, the Cu(II)/TMSA/SG sorbents did

Table 3.3 Cu(II) Uptake Capacity of Cu(II) Imprinted and Nonimprinted Sorbents Coated on Amorphous Silica

Sorbent	C_0 (ppm)	C_f (ppm)	K_d Cu	% Cu(II) absorbed	Cu(II) capacity (mmol/g)
Nonimprinted-TMSA	63.55	51.70	23	18.64	0.019
Imprinted-TMSA	**63.55**	**51.25**	**24**	**19.35**	**0.019**
Nonimprinted-TMSen (MeOH)	63.55	14.66	330	76.93	0.077
Imprinted-TMSen (MeOH)	**63.55**	**10.35**	**510**	**83.71**	**0.084**
Nonimprinted-TMSen (H_2O)	63.55	6.83	830	89.26	0.089
Imprinted-TMSen (H_2O)	**63.55**	**6.53**	**870**	**89.72**	**0.090**

Table 3.4 Competitive Loading of Cu(II) and Zn(II) by Cu(II) Imprinted and Nonimprinted Sorbents Coated on Amorphous Silica

Sorbent	Initial Concentrations		% Cu(II) absorbed	% Zn(II) absorbed	K_d Cu	K_d Zn	k	k'
	Cu(II) (M)	Zn(II) (M)						
Nonimprinted-TMSA	0.001	0.001	19.58	22.33	24	29	0.85	-
Imprinted-TMSA	**0.001**	**0.001**	**14.51**	**34.80**	**17**	**55**	**0.31**	**0.4**
Nonimprinted-TMSen (MeOH)	0.001	0.001	78.67	53.10	370	110	3.3	-
Imprinted-TMSen (MeOH)	**0.001**	**0.001**	**86.73**	**24.20**	**650**	**32**	**20**	**6.2**
Nonimprinted-TMSen (H_2O)	0.001	0.001	98.27	40.34	5700	68	84	-
Imprinted-TMSen (H_2O)	**0.001**	**0.001**	**76.62**	**27.86**	**330**	**39**	**8.5**	**0.1**

Table 3.5 Competitive Loading of Cu(II) and Zn(II) by Cu(II) Imprinted and Nonimprinted sorbents Coated on Amorphous Silica

Sorbent	Initial Concentrations		% Cu(II) absorbed	% Zn(II) absorbed	K_d Cu	K_d Zn	k	k'
	Cu(II) (M)	Zn(II) (M)						
Nonimprinted-TMSA	0.001	0.01	8.76	6.83	10	7	1.3	-
Imprinted-TMSA	**0.001**	**0.01**	**8.32**	**7.59**	**9**	**8**	**1.1**	**0.9**
Nonimprinted-TMSen (MeOH)	0.001	0.01	79.55	12.46	390	14	27	-
Imprinted-TMSen (MeOH)	**0.001**	**0.01**	**74.53**	**5.99**	**290**	**6**	**46**	**1.7**
Nonimprinted-TMSen (H_2O)	0.001	0.01	88.03	8.89	740	10	75	-
Imprinted-TMSen (H_2O)	**0.001**	**0.01**	**63.66**	**10.44**	**170**	**12**	**15**	**0.2**

not exhibit selectivity for copper(II). The Cu(II) imprinted TMSA/SG material absorbed less copper(II) and more zinc(II) than the nonimprinted TMSA/SG sorbent when mixed with both the equimolar [10^{-3} M Cu(II)/10^{-3} M Zn(II), Table 3.4] and excess Zinc(II) [10^{-3} M Cu(II)/10^{-2} M Zn(II), Table 3.5] aqueous metal ion mixtures.

Although the Cu(II)/TMSen/SG/MeOH sorbents exhibit much lower copper(II) uptake capacities than their MCM-41 counterparts, they do show the best enhancement of Cu(II) capacity of the amorphous series. Furthermore, the copper(II) imprinted TMSen/SG/MeOH sorbent absorbed more Cu(II) and less Zn(II) than the nonimprinted sample in both competitive metal ion binding experiments, resulting in relative selectivity coefficients, $k' > 1$ (Tables 3.4 and 3.5). Coating the Cu(II)/TMSen/SG sorbents in water resulted in a higher TMSen ligand loading than those coated in MeOH, as indicated by the larger copper(II) uptake capacities shown in Table 3.3. Despite this, these sorbents do not exhibit any enhancement in copper(II) capacity or selectivity due to molecular imprinting.

Two key properties shown by our sorbents imprint-coated on MCM-41 (Section II) thought to be a direct result of molecular imprinting are:

(1) The imprinted sorbents have larger effective adsorption capacities than the nonimprinted sorbents for the metal ion template from solutions containing no competitor species.

(2) The imprinted sorbents remove more of the metal ion template and less of the competitor species than the nonimprinted sorbents from mixed

solutions. This results in larger selectivity coefficients (k) for the imprinted sorbents, and a relative selectivity coefficient (k') > 1.

The Cu(II)/TMSA/SG and Cu(II)/TMSen/SG/H_2O sorbents desribed and characterized above, do not exhibit either of these two properties. In fact, there is no evidence of molecular imprinting in these two systems. The Cu(II)/TMSen/SG/MeOH sorbents do exhibit both of these key properties, but have a much lower total copper(II) uptake capacity than the analogous MCM-41-coated sorbents. This is clearly evidenced by a comparison of the Cu(II) batch tests performed with an initial Cu(II) concentration of 63.55 ppm. While the concentration of the remaining copper(II) was ~190 ppb when the imprinted Cu(II)/TMSen/MCM-41 sorbent was used, over 50 times this amount ~10.3 ppm remained when the same amount of the Cu(II)/TMSen/SG/MeOH sorbent was used.

3-IV. Imprint Coating of BTMSen on CTAB/H^+ Silica

The preliminary investigations of imprint coating described in Chapter 3, Section II, showed us that the technique can be used to synthesize selective metal ion sorbents. This is somewhat surprising due to the expected flexibility (bending and stretching) of the ligands, which are connected to the silica surface via propyl groups. In an attempt to improve the metal ion selectivity of the sorbent materials, the bifunctional reagent, bis-[(trimethoxysilyl)propyl]ethylenediamine (BTMSen) was used in the imprint coating process. The two trimethoxy groups on this molecule (**Figure 3.8**), allow it to graft to the silica surface at each end. This may result in less

ligand flexibility as compared to the ligands which are grafted only at one end (i.e. TMSen and TMSA). **Figure 3.9** illustrates the expected decrease in the magnitude of motions of the ethylenediamine functionality when it is a part of a grafted BTMSen molecule as compared to a grafted TMSen molecule. This could lead to more stable imprint cavities and therefore, a sorbent with a better selectivity for metal ions. CTAB/H^+-silica (Chapter 2, Section III) was used as the support for imprint coating with BTMSen. The relatively small pore size of CTAB/H^+-silica may allow for the formation of selective sites by constraining the distances between ligand molecules during the grafting process.

3-IV.1 Synthesis

A similar procedure to that followed for the synthesis of Cu(II)/TMSen/MCM-41 and Cu(II)/TMSA/MCM-41 materials (Chapter 3, Section II) was followed here. Copper(II) was used as the metal ion template for the imprinted sorbents, methanol as the solvent, and the reaction mixtures were evaporated to dryness. A different bifunctional reagent (BTMSen) and sorbent support (CTAB/H^+ silica) were employed.

3-IV.1.1 Cu(II)/BTMSen/CTAB/H^+ Silica

In a typical preparation, copper nitrate trihydrate [$Cu(NO_3)_2$ $3H_2O$, 0.76 g] was added under stirring to methanol (CH_3OH, 50 mL). After the metal salt had completely dissolved, BTMSen (5.0 mL, 62% in MeOH) was added. After stirring the mixture for 2 min, calcined CTAB/H^+ silica (1.00 g) was added. The solution was

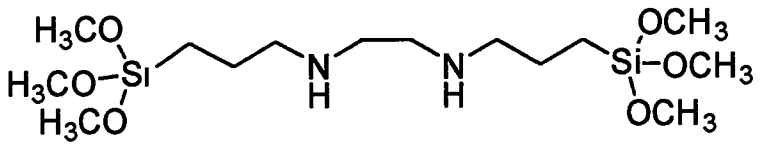


Figure 3.8 Structure of bis[(3-trimethoxysilyl)propyl]ethylenediamine

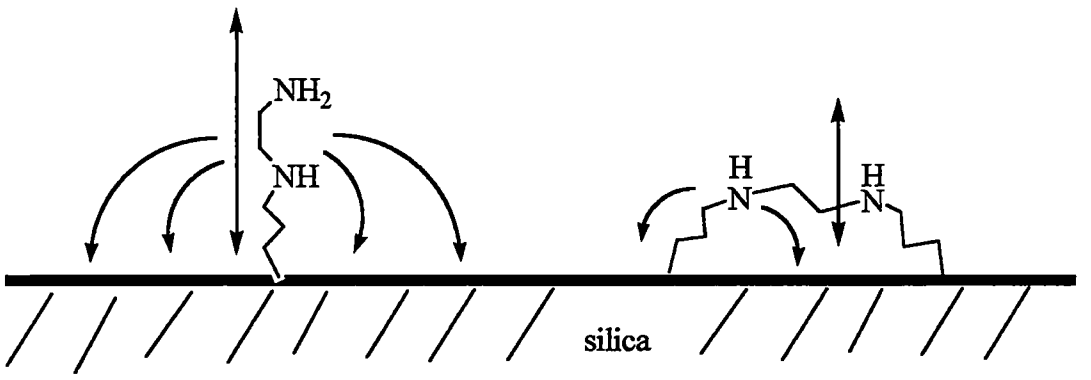


Figure 3.9 Flexibility of grafted TMSen and BTMSen

stirred and evaporated to dryness. A nonimprinted sample was prepared by an identical protocol with the exception that no metal salt was added. The residue was washed with nitric acid (HNO_3, excess) to remove all of the copper template. The resulting gel was placed in deionized water and titrated with sodium hydroxide (NaOH, 2 N) to pH 7.5, recovered by filtration, washed with deionized water and absolute ethanol, and placed under vacuum at 80 °C for 1 h.

The relatively short stirring time (2 min) allowed for the formation of the $Cu(BTMSen)_2^{2+}$ complex was required due to the fact that longer stir times resulted in precipitation. This indicates that BTMSen is more reactive than either TMSen or TMSA under similar conditions. The formation of the complex prior to the addition of the calcined CTAB/H^+ silica was evidenced by the strong navy blue color of the solution.

3-IV.2 Copper(II) Adsorption

The results of batch tests conducted with the copper(II) imprinted and nonimprinted BTMSen/CTAB/H^+ sorbents are shown in **Table 3.6**. Five different Cu(II) concentrations ranging from 10^{-5}-10^{-3} M (0.64-63.55 ppm) were used. The copper(II) imprinted sorbents removed more Cu(II) than the nonimprinted sorbents at all concentrations studied. This enhanced capacity for the template ion is substantially higher than any achieved under similar conditions with TMSen or TMSA coated on MCM-41 or amorphous silica. The Cu(II) imprinted sorbent adsorbed nearly 3 times

Table 3.6 Cu(II) Uptake Capacity of BTMSen/CTAB/H^+ Sorbents

Sorbent	C_0 (ppm)	C_f (ppm)	K_d Cu	% Cu(II) absorbed
Nonimprinted	0.64	0.20	220	69.14
Cu(II) imprinted	**0.64**	**0.10**	**520**	**83.96**
Nonimprinted	3.18	1.31	140	58.67
Cu(II) imprinted	**3.18**	**0.30**	**940**	**90.44**
Nonimprinted	6.35	3.63	80	42.85
Cu(II) imprinted	**6.35**	**1.66**	**280**	**73.86**
Nonimprinted	31.77	24.91	30	21.60
Cu(II) imprinted	**31.77**	**12.10**	**160**	**61.91**
Nonimprinted	63.55	56.79	12	10.64
Cu(II) imprinted	**63.55**	**24.68**	**160**	**61.17**

as much Cu(II) as the nonimprinted sorbent at $[Cu^{2+}] = 5 \times 10^{-4}$ M, and 6 times as much at $[Cu^{2+}] = 10^{-3}$ M.

3-IV.3 Copper(II) vs. Zinc(II) Selectivity

The results of competitive ion adsorption batch tests using mixed solutions of Cu(II) and Zn(II) are summarized in **Table 3.7**. An equimolar solution [10^{-3} M Cu(II)/10^{-3} M Zn(II)] and a solution containing excess competitor species [10^{-3} M Cu(II)/10^{-2} M Zn(II)] were both used. The copper(II) imprinted sorbents exhibited a higher selectivity for the Cu(II) ion than the nonimprinted sorbents from both mixtures. None of these sorbents synthesized with BTMSen adsorb significant amounts of Zn(II) .

3-IV.4 Discussion

The synthesis and characterization of BTMSen/CTAB/H^+ sorbents has shown us that these materials have some unique properties. During the initial synthesis, a methanol solution containing BTMSen and copper(II) formed a quantitative amount of precipitate after 5 min. This required us to change the protocol by adding the calcined CTAB/H^+ quickly, thereby allowing only 2 min for complex formation. More importantly, this showed us some important properties of the BTMSen molecules. It is safe to assume that the precipitate was a polysiloxane formed by the homocondensation of BTMSen molecules. The lack of water in the complex solution indicates that very few methoxy groups on the BTMSen molecules were hydrolyzed

Table 3.7 Competitive Loading of Cu(II) and Zn(II) by BTMSen/CTAB/H^+ Sorbents

Sorbent	Initial Concentrations		% Cu(II) absorbed	% Zn(II) absorbed	K_d Cu	K_d Zn	k	k'
	Cu(II) (M)	Zn(II) (M)						
Nonimprinted	1×10^{-3}	1×10^{-3}	9.78	0.30	11	0.3	37	-
Cu(II) Imprinted	1×10^{-3}	1×10^{-3}	**52.32**	**0.20**	**110**	**0.2**	**550**	**15**
Nonimprinted	1×10^{-3}	1×10^{-2}	7.07	-	8	-	-	-
Cu(II) Imprinted	1×10^{-3}	1×10^{-2}	**50.47**	-	**100**	-	-	-

and therefore, the primary products of the homocondensation of BTMSen were the polysiloxane and methanol. It is surprising to us that this reaction proceeded quickly at room temperature, since methanol was also the solvent.

The results of the copper(II) adsorption experiments show an unprecedented enhancement of Cu(II) capacity for the Cu(II) imprinted sorbents over the nonimprinted samples. Despite this, the overall Cu(II) uptake is very low compared to that exhibited by similar sorbents synthesized with TMSen and TMSA (Chapter 3, Sections II-III). Also, these results show a number of anomalies. For example, a common trend found with all metal ion sorbent materials is that they adsorb more metal ions when in solutions of higher concentration, but a smaller percentage of the total metal ions in the solution. This trend is not followed by the Cu(II) imprinted sorbent at a Cu(II) concentration of 3.18 ppm, since it adsorbed a higher percentage (90.44) than it did at 0.64 ppm (83.96).

The competitive metal ion batch tests between Cu(II) and Zn(II) also show some unique properties of the BTMSen/CTAB/H^+ sorbents. As was the case in the single metal ion batch tests with Cu(II) descibed above, the overall metal ion capacities were very low. Despite this, both the Cu(II) imprinted and nonimprinted materials exhibited excellent selectivity for Cu(II), since they fail to absorb any significant amount of Zn(II). But these results are very puzzling, since they indicate that both sorbents have a lower metal ion capacity in the 10^{-3} M Cu(II)/10^{-2} M Zn(II) mixture than in the 10^{-3} M Cu(II)/10^{-3} M Zn(II) mixture, even though the former has a much higher ionic strength.

Because of the many inconsistencies in the experimental results discussed above, further experiments were performed to determine whether the enhanced capacities and selectivities were a result of molecular imprinting. Small angle X-ray scattering experiments were performed on both sorbents, and no peaks were resolved. This is in stark contrast to the sharp peak observed at $2\theta = 2.56°$ for the calcined CTAB/H^+ silica support (Chapter 2, Section III.3). This shows direct evidence that both sorbents have inhomogeneous matrices. Another telling result was the large increase in the mass of the sorbents following synthesis and post-synthetic processing. Although exact masses of the two sorbents were not recorded after the imprint coating procedure, a large increase over the 1.00 g starting mass of the sorbent support was observed. This would be consistent with the formation of significant clusters of en-bridged polysiloxane throughout the sorbent materials. This may also explain the inconsistent batch test results and low overall metal ion uptake in these materials.

The experimental evidence suggests that the BTMSen ligand used in the synthesis of the Cu(II) imprinted and nonimprinted CTAB/H^+ silica sorbents may have reacted too vigorously. Although it may have coated the pores of the support, it seems likely that it may have also underwent homocondensation reactions, causing a significant decrease in the homogeneity of the sorbents. For these reasons we felt that the BTMSen bifunctional reagent may be better suited for the synthesis of a sorbent in which it serves as a part of the matrix and not simply coated on the surface of a porous silica support. See Chapter 5 for complete details.

3-V. Imprint Coating of TMSen on MCM-41

The preliminary experiments (Chapter 3, Section II) of imprint coating on calcined MCM-41 had very promising results. Copper(II) imprinted sorbents exhibited larger capacities and a better selectivity for the metal ion template than the nonimprinted samples. The sorbents imprint coated with TMSen showed a much better selectivity for copper(II) than those synthesized with the TMSA bifunctional reagent. This is clearly evidenced by the larger values of k' (Table 3.2) achieved with the TMSen/MCM-41 sorbents contacted with mixtures containing both copper(II) and the zinc(II) competitor. For these reasons, further imprint coating experiments were performed using TMSen as the ligand and calcined MCM-41 as the sorbent. One goal was to perform numerous metal ion batch tests with a range of different concentrations in order to reveal the adsorption trends shown by these sorbents.

3-V.1 Synthesis

Although a protocol similar to that used in Section II was employed here, a few changes were made. First, the mixtures were not evaporated to dryness. The idea behind this was that complete evaporation of the solvent would force the equilibrium of the condensation reactions towards the formation of the product (grafted TMSen). The relatively large amounts of TMSen in the reaction mixture and the formation of clumps in the dry material indicated that homocondensation of TMSen may have occurred. Shorter reaction times will be used to avoid this problem.

3-V.1.1 Cu(II)/TMSen/MCM-41

In a typical preparation, copper nitrate trihydrate [$Cu(NO_3)_2$ $3H_2O$, 2.26 g] was added under stirring to methanol (CH_3OH, 100 mL). After the metal salt had completely dissolved, TMSen (4.08 mL) was added. After stirring the mixture for 10 min., calcined MCM-41 (1.00 g) was added. The solution was stirred for ca. 3 h, until the total volume of the mixture reached 40 mL. A nonimprinted sample was prepared by an identical protocol with the exception that no metal salt was added. The solid product was recovered by filtration and washed with nitric acid (HNO_3, excess) to remove all of the copper template. The resulting gel was placed in deionized water and titrated with sodium hydroxide (NaOH, 2 N) to pH 7.5, recovered by filtration, washed with deionized water and absolute ethanol, and placed under vacuum at 80 °C for 4 h.

3-V.2 Copper(II) Adsorption

The results of batch tests conducted with the copper(II) imprinted and nonimprinted TMSen/MCM-41 sorbents are shown in **Table 3.8**. Six different Cu(II) concentrations ranging from 10^{-5} M (0.64 ppm) to 10^{-3} M (63.55 ppm) were used. The Cu(II) imprinted sorbent adsorbed more Cu(II) at the three lower concentrations and less Cu(II) at the three higher concentrations than the nonimprinted sorbent. The copper(II) adsorption isotherms of the TMSen/MCM-41 sorbents are shown in **Figure 3.10**.

Table 3.8 Cu(II) Uptake Capacity of TMSen/MCM-41 Sorbents

Sorbent	C_0 (ppm)	C_f (ppb)	K_d Cu	% Cu(II) absorbed
Nonimprinted	0.64	7	9000	98.9
Imprinted	**0.64**	**3**	**27100**	**99.6**
Nonimprinted	3.18	41	7800	98.7
Imprinted	**3.18**	**22**	**13900**	**99.3**
Nonimprinted	6.35	70	9000	98.9
Imprinted	**6.35**	**51**	**12200**	**99.2**
Nonimprinted	15.89	207	7600	98.7
Imprinted	**15.89**	**222**	**7000**	**98.6**
Nonimprinted	31.77	540	5800	98.3
Imprinted	**31.77**	**731**	**4200**	**97.7**
Nonimprinted	63.55	1843	3300	97.1
Imprinted	**63.55**	**2351**	**2600**	**96.3**

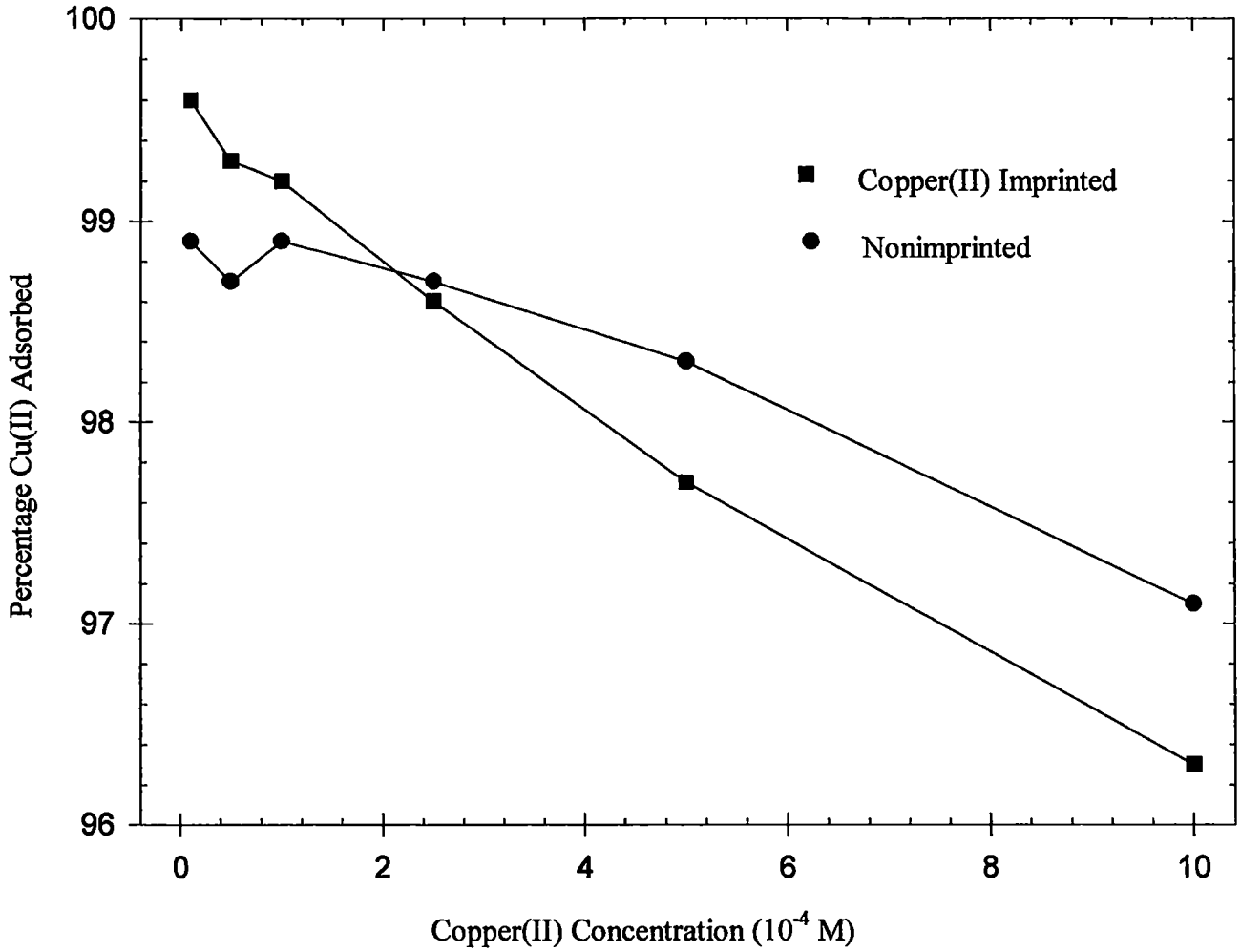


Figure 3.10 Copper(II) adsorption isotherms of TMSen/MCM-41 sorbents

3-V.3 Copper(II) vs. Zinc(II) Selectivity

The results of competitive ion adsorption batch tests employing mixed solutions of equimolar amounts of Cu(II) and Zn(II) are summarized in **Table 3.9**. The copper(II) imprinted sorbents exhibited a higher selectivity for the Cu(II) ion than the nonimprinted materials at all concentrations studied. Although all the relative selectivity coefficient (k') values > 1 reflect this, the copper(II) imprinted sorbents have the highest selectivity at the lower concentrations.

3-V.4 Adsorption of Divalent Cations on Calcined MCM-41

It has long been known that silica can act as a cation exchanger because of its hydroxylated surface (65). The mechanism of exchange has been reported by numerous researchers (66-9). It is generally agreed that the surface reaction with metal ions occurs according to equation (5), where x represents the number of silanol

$$\left(\equiv Si{-}OH\right)_x + M^{z+} \rightleftharpoons \left(\equiv Si{-}O\right)_x M^{z+} + xH^{+} \qquad (5)$$

groups and z the charge on the cation. The formation of products is favored when the value of x is large, the concentration of the metal ion is large, and at high solution pH. The practical use of equation (5) is limited because of the low solubility of metal cations at high pH.

The condensation reactions which graft our bifunctional reagents to the silica surface during the imprint coating process effectively eliminate silanol groups.

Table 3.9 Competitive Loading of Cu(II) and Zn(II) by TMSen/MCM-41 Sorbents

Sorbent	Initial Concentrations		% Cu(II) absorbed	% Zn(II) absorbed	K_d Cu	K_d Zn	k	k'
	Cu(II) (M)	Zn(II) (M)						
Nonimprinted	1×10^{-5}	1×10^{-5}	98.03	74.70	5000	300	17	-
Cu(II) Imprinted	**1×10^{-5}**	**1×10^{-5}**	**99.84**	**79.52**	**60700**	**390**	**160**	**9.3**
Nonimprinted	1×10^{-4}	1×10^{-4}	99.38	77.08	16200	340	48	-
Cu(II) Imprinted	**1×10^{-4}**	**1×10^{-4}**	**99.75**	**46.79**	**40500**	**88**	**460**	**9.6**
Nonimprinted	5×10^{-4}	5×10^{-4}	99.11	58.01	11100	140	81	-
Cu(II) Imprinted	**5×10^{-4}**	**5×10^{-4}**	**98.83**	**29.33**	**8400**	**42**	**200**	**2.5**
Nonimprinted	1×10^{-3}	1×10^{-3}	96.39	16.32	2700	20	140	-
Cu(II) Imprinted	**1×10^{-3}**	**1×10^{-3}**	**96.96**	**9.08**	**3200**	**10**	**320**	**2.3**

Despite this, even at very high ligand loading it is likely that some silanol groups are still present and could bind metal ions. To determine the adsorption behavior of Cu(II), Zn(II), Ni(II), and Cd(II) on calcined MCM-41, batch experiments were conducted at pH = 5.0.

Table 3.10 summarizes the results of the batch experiments performed using single metal ion solutions of Cu(II), Zn(II), and Ni(II), as well as a mixture of Cu(II), Zn(II), Ni(II), and Cd(II). Despite its large surface area (~1000 m^2/g) and corresponding silanol content, the adsorption of these three divalent cations was relatively low at this pH. Only about 1.6% of the Cu(II) was adsorbed from the 10^{-3} M solution, while no detectable amount of Ni(II) was adsorbed. Zinc(II) was adsorbed in the greatest quantity from both the single metal ion (6.43%) and mixed (7.62%) solutions. Calcined MCM-41 exhibited a significant selectivity for zinc(II) over the other three cations. More than 10 times as much Zn(II) was adsorbed than the other three cations combined. No detectable amount of Ni(II) or Cd(II) was adsorbed by the porous silica from the mixed solution.

3-V.5 Discussion

The copper(II) uptake capacities of the Cu(II) imprinted and nonimprinted TMSen/MCM-41 sorbents show a surprising trend. The copper(II) imprinted sorbents adsorbed more Cu(II) at the lower concentrations studied (0.64-6.35 ppm), but less at the higher concentrations (15.89-63.55 ppm). One explanation for this trend is that the nonimprinted material has more TMSen binding sites than the Cu(II) imprinted

Table 3.10 Adsorption of Divalent Cations on Calcined MCM-41 at pH = 5.0

Sorbent	Initial Concentrations				Percentage Adsorbed			
	Cu(II) (M)	Zn(II) (M)	Ni(II) (M)	Cd(II) (M)	Cu(II)	Zn(II)	Ni(II)	Cd(II)
Calcined MCM-41	1×10^{-3}	-	-	-	1.62	-	-	-
Calcined MCM-41	-	1×10^{-3}	-	-	-	6.43	-	-
Calcined MCM-41	-	-	1×10^{-3}	-	-	-	0	-
Calcined MCM-41	1×10^{-3}	1×10^{-3}	1×10^{-3}	1×10^{-3}	0.68	7.62	0	0

sorbent. Assuming a homogeneous distribution of TMSen in these sorbents and similar ligand loading, the nonimprinted material would have twice as many TMSen binding sites as the Cu(II) imprinted sorbent. This is due to the way in which the sorbents were synthesized. Since the $Cu(TMSen)_2^{2+}$ complex was formed prior to grafting, the TMSen ligands may be "paired up" in the imprinted sorbent. This results in a higher affinity for the metal ion template at low concentrations. At higher concentrations, when most of the sites in the Cu(II) imprinted sorbent are occupied the nonimprinted sorbent still has many open sites and therefore, a higher copper(II) uptake.

The results of competitive ion sorption experiments performed with both the Cu(II) imprinted and nonimprinted sorbents using mixed solutions containing equimolar amounts of Cu(II) and Zn(II) are listed in Table 3.9. The copper(II) imprinted sorbents exhibit higher selectivity coefficients for the Cu(II) ion than the nonimprinted materials at all concentrations studied. In the batch test with the lowest starting concentrations [1×10^{-5} M Cu(II)/1×10^{-5} M Zn(II)] the copper(II) imprinted sorbent absorbed more of both cations. This may be because at this low concentration there are enough "paired up" sites on the Cu(II) imprinted material for all the divalent cations. In the other three batch tests, all of which were performed with higher starting concentrations, the nonimprinted sorbent had a higher total metal ion uptake [Cu(II) + Zn(II)] than the Cu(II) imprinted material. This is mainly due to the fact that the more selective Cu(II) imprinted sorbent adsorbs much less zinc(II) than the nonimprinted TMSen/MCM-41 material at these concentrations.

3-VI. Ethylenediamine as a Competitor Species

Although many of the relatively simple laboratory experiments used to determine the effectiveness of metal ion sorbents do not employ complicated matrices, most real world applications require that sorbents perform well in complex mixtures. In addition to unwanted metal ions, which compete for sorbent binding sites, free ligands in solution compete for the template metal ion species. Chelating ligands such as ethylenediaminetetraacetic acid (EDTA) and ethylenediamine (en) have many uses, but are primarily used as the active ingredients in many industrial cleaning solutions. Because of their common use these metal ion chelators are usually present in industrial waste streams.

In order to determine its effect on the performance of imprint coated sorbents, en was added to 10^{-4} M Cu(II)/10^{-4} M Zn(II) aqueous solutions, which were used in batch experiments. The concentration of en was varied from zero to 10^{-3} M (excess). Copper(II) imprinted and nonimprinted sorbents were synthesized using TMSen as the bifunctional reagent and MCM-41 as the support. The use of en and TMSen in these experiments allowed for a direct comparison of the affinity of the grafted en moeity and the free en ligand for copper(II) and zinc(II) ions.

3-VI.1 Synthesis

Although a protocol similar to that used in Section V was employed here, a few changes were made. Due to its availability and low toxicity, absolute ethanol was used as the solvent in place of methanol. Reaction mixtures were covered to eliminate

any evaporation during the imprint coating process. Calcined MCM-41 (3.00 g) was placed in a clean beaker with 60 mL of absolute ethanol and sonicated for 10 min. In a separate beaker, 7.5 mmol of $Cu(NO_3)_2$ $3H_2O$ (1.81 g) was added to 120 mL of absolute ethanol and stirred until all the metal salt had dissolved. TMSen (15 mmol, 3.27 mL) was then slowly added upon stirring to the Cu(II) solution, forming a dark-violet colored complex. The complex solution was then added to the MCM-41 mixture. This mixture was covered and stirred at RT for 4 h. A nonimprinted sorbent was synthesized with a similar protocol, but without the addition of any metal salt. The solid product was recovered by filtration and washed with nitric acid (1 M HNO_3, excess) to remove all of the copper template. The resulting gel was placed in deionized water and titrated with sodium hydroxide (NaOH, 2 N) to pH 7.5, recovered by filtration, washed with deionized water and absolute ethanol, and placed under vacuum at 80 °C for 4 h.

3-VI.2 Copper(II) vs. Zinc(II) Selectivity with Free Ethylenediamine

The results of competitive ion adsorption batch tests employing mixed solutions of 10^{-4} M Cu(II) and 10^{-4} M Zn(II) which also contain various amounts of en are summarized in **Table 3.11**. The molar ratios of Cu(II)/Zn(II)/en in the specific solutions was varied from 1:1:0 (no en) to 1:1:6. The latter corresponds to three en for each divalent cation or coordinative saturation. One solution containing excess en (1:1:10) was also used.

Table 3.11 Competitive Loading of Cu(II) and Zn(II) by TMSen/MCM-41 Sorbents in the Presence of en. Initial Cu(II) and Zn(II) Concentrations = 10^{-4} M

Sorbent	C_0 en (10^{-4}M)	% Cu(II) absorbed	% Zn(II) absorbed	K_d Cu	K_d Zn	k	k'
Nonimprinted	-	99.63	84.52	27100	550	49	-
Cu(II) Imprinted	-	**99.87**	**89.83**	**81400**	**880**	**93**	**1.9**
Nonimprinted	1	99.64	88.76	27300	790	35	-
Cu(II) Imprinted	**1**	**99.72**	**93.23**	**35200**	**1400**	**25**	**0.7**
Nonimprinted	2	99.30	92.38	14200	1200	12	-
Cu(II) Imprinted	**2**	**99.57**	**96.90**	**23300**	**3100**	**7.5**	**0.6**
Nonimprinted	3	99.28	98.83	13700	8400	1.6	-
Cu(II) Imprinted	**3**	**99.31**	**99.83**	**14500**	**59600**	**0.2**	**0.1**
Nonimprinted	4	99.86	98.65	8700	7300	1.2	-
Cu(II) Imprinted	**4**	**99.90**	**99.57**	**9000**	**23100**	**0.4**	**0.3**
Nonimprinted	5	98.65	98.86	7300	8700	0.8	-
Cu(II) Imprinted	**5**	**98.42**	**99.75**	**6200**	**40400**	**0.2**	**0.3**
Nonimprinted	6	98.23	98.98	5500	9700	0.6	-
Cu(II) Imprinted	**6**	**97.78**	**99.98**	**4400**	**412000**	**0.01**	**0.02**
Nonimprinted	10	96.07	99.54	2400	21700	0.1	-
Cu(II) Imprinted	**10**	**94.47**	**98.79**	**1700**	**82800**	**0.02**	**0.2**

The batch test performed with 10^{-4} M Cu(II)/10^{-4} M Zn(II)/no en (1:1:0) gave results similar to those achieved in the preliminary experiments (Section II) and the imprint coating of TMSen on MCM-41 in methanol (Section V). The copper(II) imprinted sorbent adsorbed more Cu(II) than the nonimprinted sample and was selective for Cu(II) over Zn(II), giving $k' > 1$. This selectivity was not exhibited in metal ion adsorption from any of the solutions containing en. The experiment using the (1:1:1) solution shows that even a relatively small amount of the en ligand results in a lack of Cu(II) selectivity by the Cu(II) imprinted sorbent (k' = 0.7). Surprisingly, as the amount of en is increased (i.e. 1:1:2, 1:1:3, 1:1:4, etc.) the overall metal ion capacities of both the Cu(II) imprinted and nonimprinted sorbents are enhanced. This is due to an increase in Zn(II) sorption. The amount of Cu(II) absorbed by both sorbents remains relatively constant with en molar ratios in the range 0-4, while the amount of Zn(II) adsorbed increases with increasing en concentrations. When excess en is present (1:1:10) both the Cu(II) imprinted and nonimprinted materials adsorb more Zn(II) than Cu(II).

3-VI-3. Discussion

The presence of free ethylenediamine ligands in the mixed solutions of Cu(II) and Zn(II) did not inhibit, but actually enhanced the metal ion binding ability of both Cu(II) imprinted and nonimprinted TMSen/MCM-41 sorbents. This effectively reversed the selective binding properties normally exhibited by the Cu(II) imprinted sorbent in Cu(II)/Zn(II) mixed solutions that do not contain any free en.

Although these results are very puzzling to us, one possible explanation for the enhanced metal ion uptake in the Cu(II) imprinted sorbent may lie in the solution thermodynamics. If a Cu(II) ion [or Zn(II) ion] bound to two en molecules is adsorbed on the Cu(II) imprinted sorbent (**Figure 3.11**), an overall increase in entropy of the solution may result. This could make the metal ion adsorption a thermodynamically favored process. This would not however, explain the increase in overall metal ion sorption exhibited by the nonimprinted sorbent. Since the solutions were not buffered, the solution pH would be expected to increase with the addition of en. The pH effects may play an important role in the metal ion adsorption behavior of these materials.

The batch tests performed with the Cu(II)/Zn(II)/en mixed solutions of (1:1:5), (1:1:6), and (1:1:10) resulted in a higher uptake of Zn(II) than Cu(II) for both sorbents. Perhaps at these relatively high concentrations of en, the stronger affinity of en for Cu(II) inhibits its adsorption onto the sorbents. For a better of understanding of this complex system, more experiments need to be performed. Future experiments should include characterization of the solute solutions for en. This may help to explain how much ligand exchange is occuring at various concentrations of en. Also, the pH effects need to be investigated. Either the solutions can be buffered in order to stabilize the pH, or the pH of the solutions can be monitored.

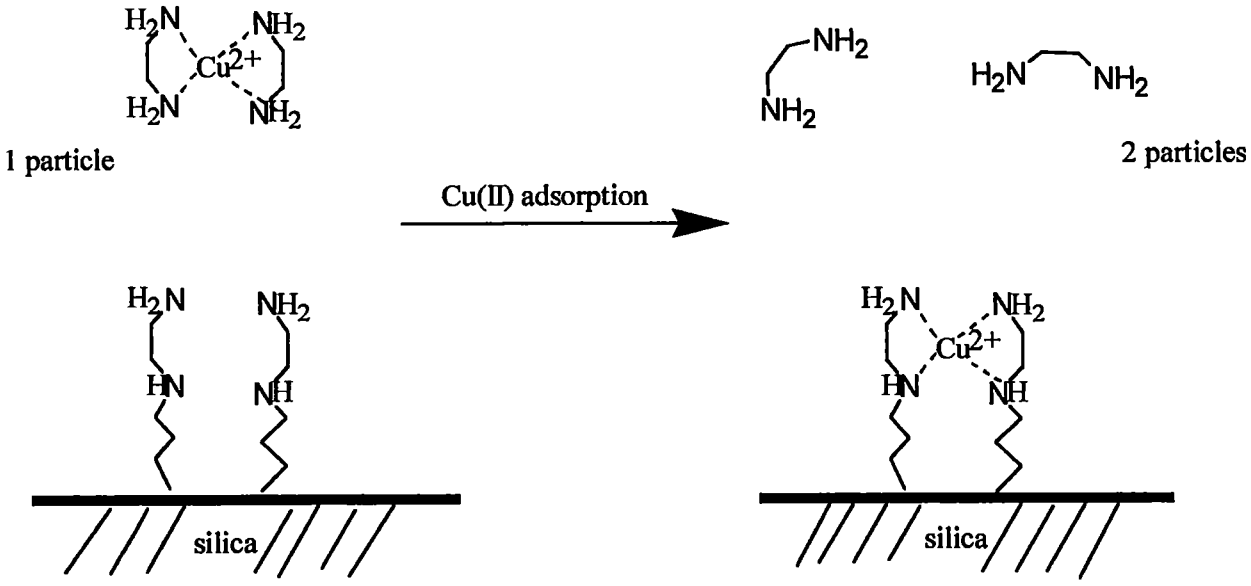


Figure 3.11 Copper(II) adsorption on Cu(II) imprint coated sorbent and the resulting increase in solution entropy

3-VII. Stability of TMSen/MCM-41 Imprint Coated Sorbents

An important property of any sorbent is its stability. For example, commercial ion exchange materials need to have a relatively long shelf life since they are not always used immediately following synthesis. We are primarily concerned with the possibility that our imprint-coated sorbents may undergo ligand rearrangement on the surface of MCM-41. Any rearrangement could cause our imprinted materials to lose their "memory", and no longer be selective. Since most of our experiments involve prompt characterization, a decrease in the overall performance of the sorbents over time would, in general not be noticed.

In order to investigate whether or not our sorbents undergo any significant changes, which could adversely effect their ability to selectively bind metal ions, the following experiments were performed. A new batch of copper(II) imprinted and nonimprinted sorbents were synthesized using a similar protocol as that used in Section VI. TMSen was used as the bifunctional reagent, MCM-41 as the support, and ethanol as the solvent. Both sorbents were divided into three portions. The first portion was characterized immediately via N_2 adsorption and batch testing. The second portion was left open to air in the laboratory hood for two weeks before it was similarly characterized. The third portion was placed in a laboratory freezer at -5 °C for two weeks and then characterized. If the second portion were to undergo any ligand rearrangement or decomposition over the two-week period, then the freezing of the third portion may hinder that process by decreasing the chemical kinetics on the sorbent surfaces.

3-VII.1 Synthesis

A protocol similar to that used in section VI was employed here. Reaction mixtures were covered to eliminate any evaporation during the imprint coating process. Calcined MCM-41 (1.50 g) was placed in a clean beaker with 60 mL of absolute ethanol and sonicated for 10 min. In a separate beaker, 3.75 mmol of $Cu(NO_3)_2\ 3H_2O$ (0.64 g) was added to 60 mL of absolute ethanol and stirred until all the metal salt had dissolved. TMSen (7.5 mmol, 1.68 mL) was then slowly added upon stirring to the Cu(II) solution, forming a dark violet colored complex. The complex solution was then added to the MCM-41 mixture. This mixture was covered and stirred at RT for 1 h. A nonimprinted sorbent was synthesized with a similar protocol, but without the addition of any metal salt. The solid product was recovered by filtration and washed with nitric acid (1 M HNO_3, excess) to remove all of the copper template. The resulting gel was placed in deionized water and titrated with sodium hydroxide (NaOH, 2 N) to pH 7.5, recovered by filtration, washed with deionized water and absolute ethanol, and placed under vacuum at 80 °C for 4 h. As mentioned previously, both sorbents were divided into three portions. The first portion was characterized immediately via N_2 adsorption and batch testing. The second portion was placed in the laboratory hood open to the atmosphere for two weeks before it was similarly characterized. The third portion was placed in a laboratory freezer at -5 °C for two weeks before characterization. Samples from all three portions to be used in the batch tests were weighed out immediately after synthesis to avoid any change in mass that could occur during curing.

In order to avoid any confusion all samples were named according to the following designations:

Stab: prefix assigned to all samples in these "**stab**ility" studies

S: samples characterized immediately following **s**ynthesis

H: samples cured in the **h**ood for two weeks prior to characterization

F: samples cured in the **f**reezer for two weeks prior to characterization

I: copper(II) **i**mprinted sorbents

N: **n**onimprinted sorbents

For example, the sample named StabHN represents the nonimprinted sorbent that was cured in the hood for two weeks.

3-VII.2 Copper(II) Adsorption

The results of batch tests performed between the Copper(II) imprinted and nonimprinted TMSen/MCM-41 sorbents and Cu(II) solutions are shown in **Table 3.12**. All solutions were buffered at pH 5.0 with NaAc/HAc (0.05 M). Two different Cu(II) concentrations, 10^{-4} M (6.35 ppm) to 10^{-3} M (63.55 ppm) were used. All sorbents adsorbed > 99% of the Cu(II) from both solutions. All copper(II) imprinted sorbents exhibited enhanced capacities for Cu(II) relative to the nonimprinted analogs. No evidence for ligand rearrangement or sorbent degradation was observed.

Table 3.12 Cu(II) Uptake Capacity of TMSen/MCM-41 Sorbents

Sorbent	C_0 (ppm)	C_f (ppb)	K_d Cu	% Cu(II) absorbed
StabSN	6.35	36	17300	99.43
StabHN	6.35	19	21100	99.70
StabFN	6.35	24	26300	99.62
StabSI	**6.35**	**27**	**23700**	**99.58**
StabHI	**6.35**	**7**	**88100**	**99.89**
StabFI	**6.35**	**4**	**175600**	**99.94**
StabSN	63.55	578	10900	99.09
StabHN	63.55	121	52400	99.81
StabFN	63.55	248	25800	99.61
StabSI	**63.55**	**515**	**12200**	**99.19**
StabHI	**63.55**	**108**	**58400**	**99.83**
StabFI	**63.55**	**83**	**76100**	**99.87**

3-VII.3 Copper(II) vs. Zinc(II) Selectivity

The results of competitive ion adsorption batch tests employing a mixed solution of 2.5 x 10^{-4} Cu(II) and 2.5 x 10^{-4} Zn(II) are summarized in **Table 3.13**. All copper(II) imprinted sorbents exhibited a higher selectivity for the Cu(II) ion than the nonimprinted materials. The sorbents that were cured for two weeks exhibited higher relative selectivity coefficients (*k'*) than the sorbents that were used immediately in the competitive ion adsorption experiments.

3-VII.4 N_2 Adsorption Analysis

The N_2 adsorption/desorption isotherm for the calcined MCM-41material is shown in **Figure 3.12**. The very large, sharp step located in the relative pressure range of 0.2-0.4 is typical of MCM-41 type materials, and indicates that this sample is primarily mesoporous. This sample has a calculated surface area of 957 m^2/g, no micropore volume, and a total pore volume of 0.86 cm^3/g. The average pore diameter is 25 Å.

The N_2 adsorption/desorption isotherms for the three different noimprinted MCM-41 sorbents used in the stability study are shown in **Figures 3.13-3.15**. The similarity of the three isotherms indicates that no significant changes occurred in the sorbent matrices cured for two weeks relative to that characterized immediately after synthesis. The porosity data of the various imprint-coated sorbents is summarized in **Table 3.14**.

Table 3.13 Competitive Loading of Cu(II) and Zn(II) by TMSen/MCM-41 Sorbents. Initial Cu(II) and Zn(II) Concentrations = 2.5×10^{-4} M

Sorbent	% Cu(II) absorbed	% Zn(II) absorbed	K_d Cu	K_d Zn	k	k'
StabSN	99.68	90.51	31400	954	33	-
StabHN	**99.85**	**97.13**	**65200**	**3400**	**19**	-
StabFN	99.86	99.07	71000	10700	7	-
StabSI	**98.93**	**47.56**	**9200**	**91**	**102**	**3.1**
StabHI	99.90	87.73	97900	710	137	7.1
StabFI	**99.89**	**94.58**	**91300**	**1700**	**52**	**7.9**

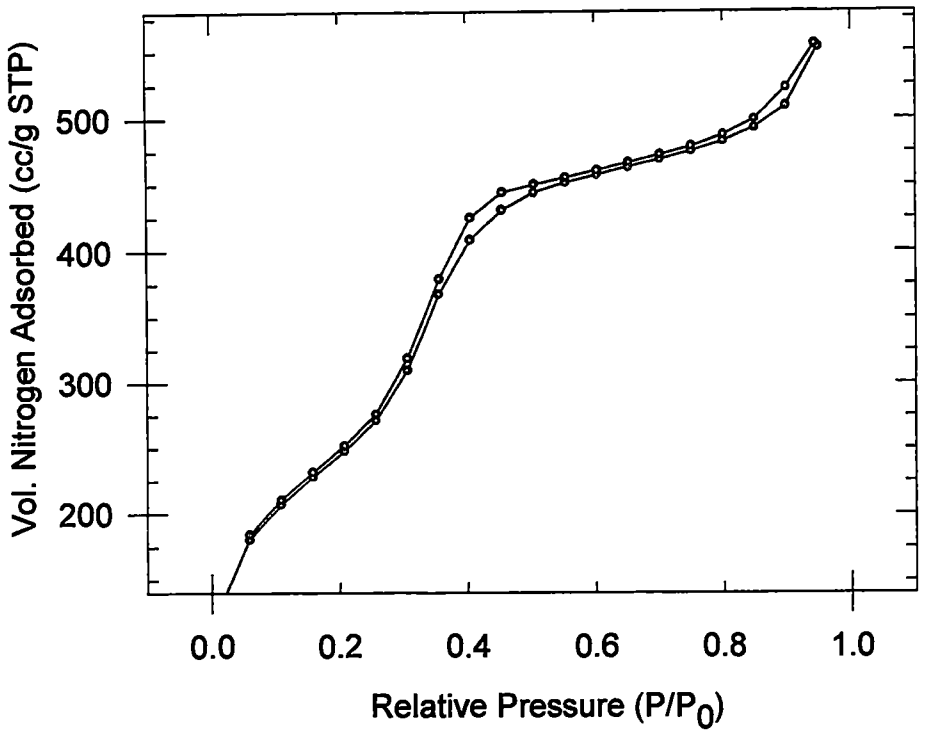


Figure 3.12 N_2 adsorption/desorption isotherm of calcined MCM-41

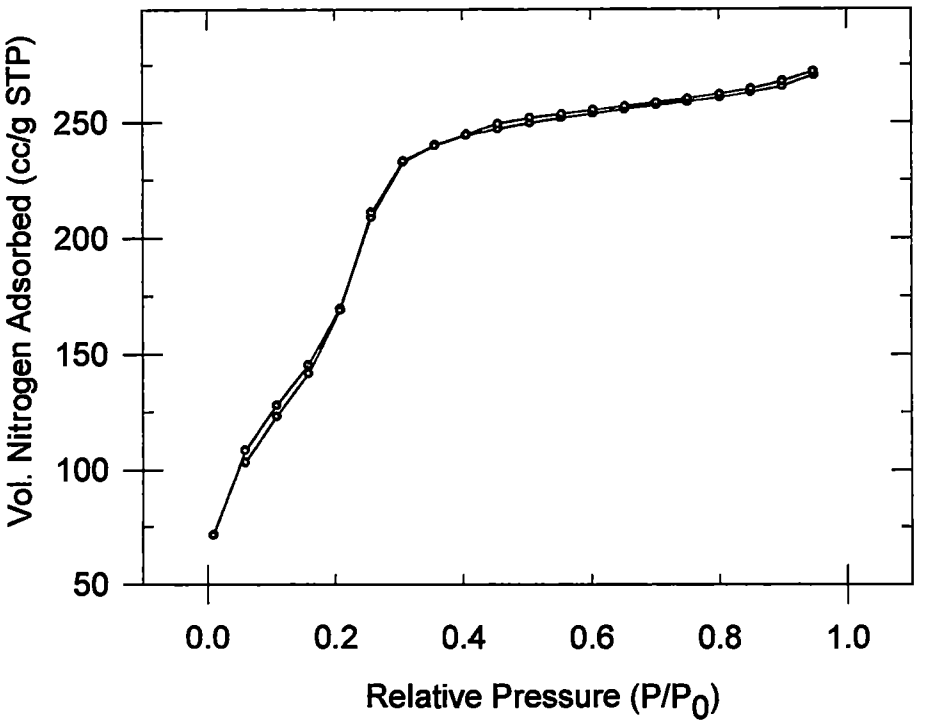


Figure 3.13 N_2 adsorption/desorption isotherm of StabSN sorbent

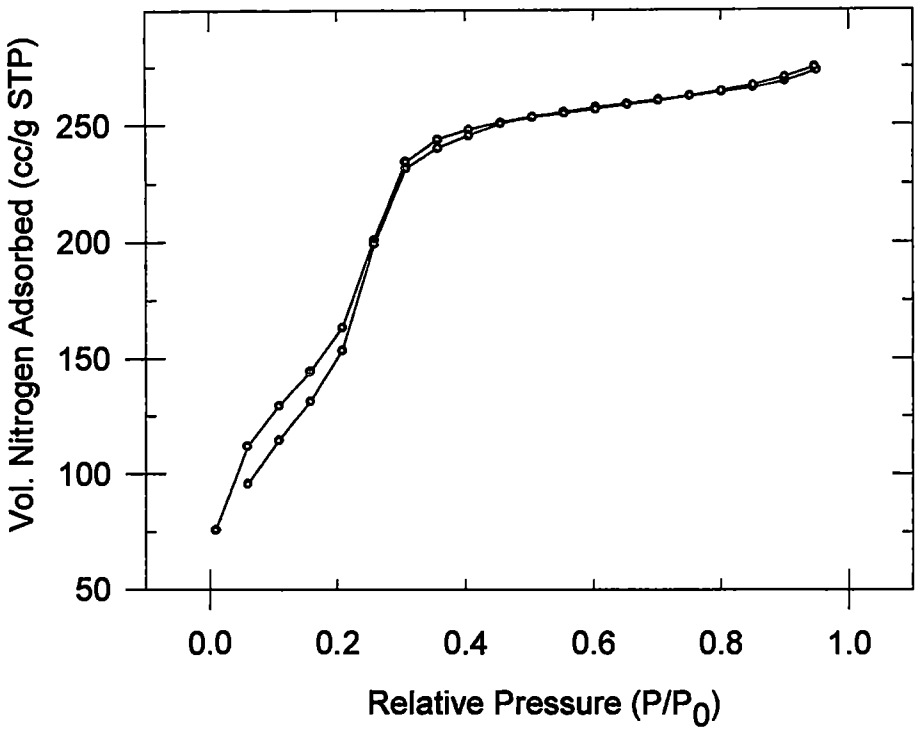


Figure 3.14 N_2 adsorption/desorption isotherm of StabHN sorbent

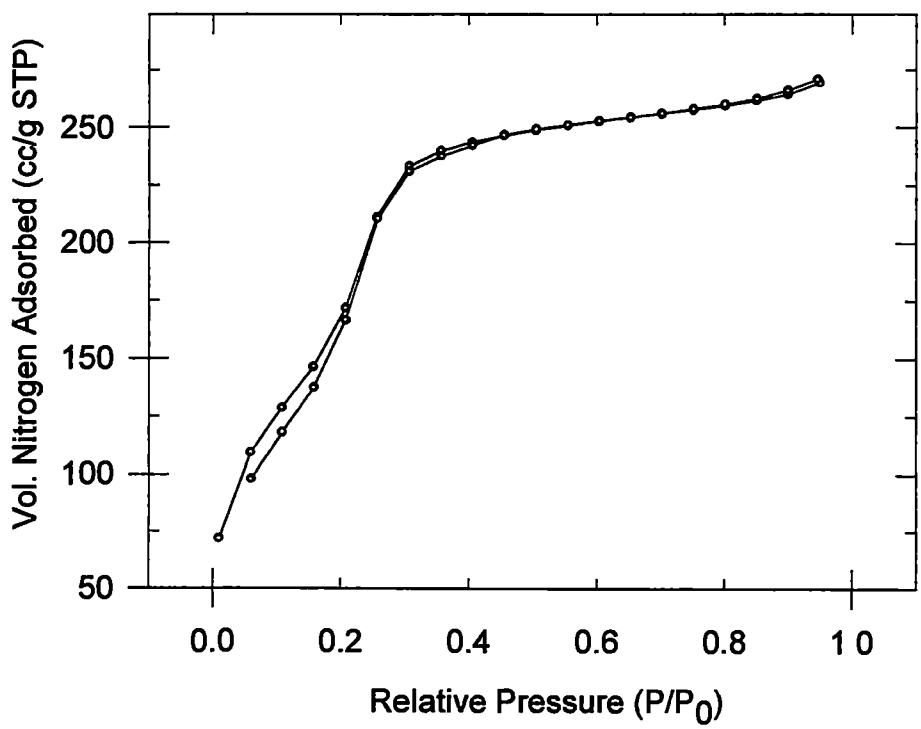


Figure 3.15 N_2 adsorption/desorption isotherm of StabFN sorbent

Table 3.14 Porosity Data of Imprint Coated Sorbents

Sample	BET Surface Area (m^2/g)	Total Pore Volume (cm^3/g)	Micropore Volume (cm^3/g)	Average Pore Diameter (Å)
Calcined MCM-41	957	0.86	-	25
StabSN	785	0.42	0.09	19
StabHN	762	0.42	0.07	17
StabFN	788	0.42	0.09	19

3-VII.5 Discussion

The results in Table 3.9 clearly illustrate that all of the copper(II) imprinted sorbents exhibited enhanced capacities for Cu(II) relative to the nonimprinted samples, when these materials were placed in copper(II) solutions. All of the sorbents, including those cured for two weeks, adsorbed over 99% of the Cu(II) from 10^{-4} M Cu(II) and 10^{-3} M Cu(II) solutions. No evidence for ligand rearrangement or a corresponding decrease in sorbent capacity was observed. Surprisingly, the sorbents cured in the laboratory hood and freezer both had a higher Cu(II) capacities than the those characterized immediately.

The data from competitive ion adsorption batch tests using a mixed solution of 2.5×10^{-4} Cu(II) and 2.5×10^{-4} Zn(II) displayed in Table 3.10, show that all three copper(II) imprinted sorbents exhibited a higher selectivity for the Cu(II) ion than the nonimprinted materials. The sorbents that were cured for two weeks again performed better than those used immediately, giving higher relative selectivity coefficients (k'). The reasons for this improvement in selectivity is not clear.

The porosity data calculated from the N_2 adsorption/desorption isotherms show that there was no significant change in the structure of the sorbents which were cured. A decrease in surface area, total pore volume, and average pore diameter is shown by all three sorbents coated with TMSen. These can be attributed to the grafting of the bifunctional reagent on the surface of the MCM-41 mesopores, which results in an overall decrease in the amount if N_2 which can be adsorbed.

The experiments conducted here indicate that the imprint-coated sorbents do not undergo ligand rearrangement on the MCM-41 surface, nor any significant structural changes within their matrices over the short term. Future studies that may lead to a better understanding of the stability of these materials could be the following. Studies similar to those described here, but much longer in duration, to determine a shelf life. Also, hydrothermal studies in which the sorbents are placed in water for various times at different temperatures may be particularly pertinent, due to the possible applications of these sorbents.

3-VIII. Imprint Coating of TMSen on Pluronic P123 Silica

Mesoporous silica has been synthesized using the block copolymer Pluronic P123 as the organic template (Chapter 2, section III.6.3). The calcined product had an average pore diameter of 74 Å. TEM images (Figure 2.36) have shown that Pluronic P123 silica has a highly ordered matrix, similar to that of MCM-41. To investigate the effect of using a "large pore support", calcined Pluronic P123 silica was imprint coated with TMSen. Copper(II) was again employed as the metal ion template and methanol as the solvent.

3-VIII.1 Synthesis

Calcined Pluronic P123-silica (1.00 g) was placed in a clean beaker with 20 mL of methanol and sonicated for 10 min. In a separate beaker, 0.200 g of $Cu(NO_3)_2$ $3H_2O$ was added to 30 mL of methanol and stirred until all the metal salt had

dissolved. TMSen (0.365 mL) was then slowly added upon stirring to the Cu(II) solution, forming a dark violet colored complex. The complex solution was then added to the Pluronic P123 silica mixture. This mixture was covered and stirred at RT for 1 h. The solid product was recovered by filtration and washed with nitric acid (1 M HNO_3, excess) to remove all of the copper template. The resulting gel was placed in deionized water and titrated with sodium hydroxide (NaOH, 2 N) to pH 7.5, recovered by filtration, washed with deionized water and absolute ethanol, and placed under vacuum at 80 °C for 1 h. A nonimprinted sorbent was synthesized with a similar protocol, but without the addition of any metal salt.

3-VIII.2 Copper(II) Adsorption

The results of batch tests conducted with the copper(II) imprinted and nonimprinted TMSen/P123 sorbents are shown in **Table 3.15**. Two different Cu(II) concentrations (6.35 and 63.55 ppm) were used. The copper(II) imprinted sorbents removed more Cu(II) than the nonimprinted sorbent at both concentrations. In the experiment with a starting Cu(II) concentration of 6.35 ppm, the final concentration left by the nonimprinted sorbent (8 ppb) is twice that left by the Cu(II) imprinted sorbent.

3-VIII.3 Copper(II) vs. Zinc(II) Selectivity

The results of competitive ion adsorption batch tests using mixed solutions of Cu(II) and Zn(II) are summarized in **Table 3.16**. An equimolar solution [10^{-3} M

Table 3.15 Cu(II) Uptake Capacity of TMSen/P123 Sorbents

Sorbent	C_0 (ppm)	C_f (ppb)	K_d Cu	% Cu(II) absorbed
Nonimprinted	6.35	8	78500	99.87
Cu(II) imprinted	**6.35**	**4**	**165400**	**99.94**
Nonimprinted	63.55	241	26300	99.62
Cu(II) imprinted	**63.55**	**184**	**34700**	**99.71**

Table 3.16 Competitive Loading of Cu(II) and Zn(II) by TMSen/P123 Sorbents

Sorbent	Initial Concentrations		% Cu(II) absorbed	% Zn(II) absorbed	K_d Cu	K_d Zn	k	k'
	Cu(II) (M)	Zn(II) (M)						
Nonimprinted	1×10^{-3}	1×10^{-3}	99.54	72.84	21900	270	82	-
Cu(II) Imprinted	1×10^{-3}	1×10^{-3}	**99.49**	**54.24**	**19600**	**120**	**160**	**2.0**
Nonimprinted	1×10^{-3}	1×10^{-2}	99.52	14.75	20900	17	1200	-
Cu(II) Imprinted	1×10^{-3}	1×10^{-2}	**99.07**	**10.64**	**10640**	**12**	**890**	**0.7**

Cu(II)/10^{-3} M Zn(II)] and a solution containing excess competitor species [10^{-3} M Cu(II)/10^{-2} M Zn(II)] were both used. The copper(II) imprinted sorbents exhibited a higher selectivity for the Cu(II) ion than the nonimprinted materials from the [10^{-3} M Cu(II)/10^{-3} M Zn(II)] mixed solution, with a k' = 2.0 despite the fact that it absorbed less Cu(II). When placed in the mixed solution containing excess Zn(II), the Cu(II) imprinted sorbent had a lower selectivity for Cu(II) than the nonimprinted materials. The total metal ion uptake [Cu(II) +Zn(II)] of the nonimprinted sorbent was greater than that of the copper(II) imprinted sorbent from both solutions.

3-VIII.4 Adsorption of Divalent Cations on Pluronic P123 Silica

To determine the adsorption behavior of Cu(II), Zn(II), and Ni(II) on calcined Pluronic P123 silica, batch experiments were conducted at pH = 5.0. **Table 3.17** summarizes the results of the batch experiments performed using Cu(II) solutions, as well as mixtures of Cu(II) with Zn(II) and Ni(II) competitor species. Despite its large surface area (790 m^2/g) and corresponding silanol content, the adsorption of these three divalent cations was relatively low at this pH. Only about 1.4% of the Cu(II) was adsorbed from 10^{-4} M and 10^{-3} M solutions. Zinc(II) was selectively adsorbed over both Cu(II) and Ni(II) species. Greater than 7.5% of the Zn(II) was adsorbed from a 10^{-3} M Cu(II)/10^{-3} M Zn(II) mixture. This represents more than 5 times the amount of Cu(II) adsorbed. No detectable amount of Ni(II) was adsorbed by the porous silica.

Table 3.17 Adsorption of Cu(II), Zn(II), and Ni(II) on Calcined Pluronic P123 Silica

Sorbent	Initial Concentrations			% Cu(II) absorbed	% Zn(II) absorbed	% Ni(II) absorbed
	Cu(II) (M)	Zn(II) (M)	Ni(II) (M)			
Calcined Pluronic P123-silica	1×10^{-4}	-	-	1.44	-	-
Calcined Pluronic P123-silica	1×10^{-3}	-	-	1.41	-	-
Calcined Pluronic P123-silica	1×10^{-3}	1×10^{-3}	-	1.43	7.52	-
Calcined Pluronic P123-silica	1×10^{-3}	1×10^{-2}	-	1.51	2.64	-
Calcined Pluronic P123-silica	1×10^{-3}	1×10^{-3}	1×10^{-3}	2.68	7.55	-

3-VIII.4 Discussion

The use of calcined Pluronic P123-silica as the support for imprint-coated sorbents has shown very promising results. A comparison of the performance of these "large pore" sorbents (74 Å), with those employing MCM-41 (28 Å) described in Section V, indicates that there may be some distinct advantages to using them as the sorbent support. Both the Cu(II) imprinted and nonimprinted TMSen/P123 sorbents (Table 3.14) adsorbed more Cu(II) than the TMSen/MCM-41 sorbents (Table 3.8) from solutions with indentical Cu(II) concentrations. Although both types of sorbent exhibit similar relative selectivity coefficients of 2.3 (TMSen/MCM-41, Table 3.9) and 2.0 (TMSen/P123, Table 3.15) when used in batch tests with mixed solutions containing 10^{-3} M Cu(II)/10^{-3} M Zn(II), the TMSen/P123 sorbents had a total metal ion uptake approximately 50% higher than the TMSen/MCM-41 materials. This is significant because the synthesis of the TMSen/P123 sorbents used less than 10% of the TMSen per gram of sorbent support than was used in the TMSen/MCM-41 materials. This clearly illustrates that the majority of the TMSen bifunctional reagent used in the synthesis of the TMSen/MCM-41 was simply an excess, and was not needed. Furthermore, the 3 h stirring time employed in the TMSen/MCM-41 synthesis may be much longer than required, since the imprint coating of calcined Pluronic P123 silica took only 1 h. It should be noted that limited availability of the surfactant and a more time consuming synthesis of the support are two disadvantages associated with Pluronic P123 silica sorbents.

The experiments involving the adsorption of Cu(II), Zn(II), and Ni(II) on Pluronic P123 silica at pH = 5.0 were designed to determine if these processes were contributing to the overall adsorption behavior of the organofunctionalized sorbents. The adsorption of Cu(II) and Ni(II) were found to be insignificant, while Zn(II) was selectively adsorbed (ca. 7.5%).

3-IX. Imprint Coating of TMSen on Pluronic P123 Silica with Low Ligand Loading

The favorable results described in the previous section indicate that the imprint coating of Pluronic P123 silica with TMSen can be used to synthesize selective metal ion sorbents. The synthesis and characterization of the various sorbents described in this chapter have led us to improve various experimental parameters which we feel will result in improved sorbent performance. The reactant concentrations, extent of solvent evaporation, and reaction times as well as our choice of support, bifunctional reagent, and solvent are examples of these parameters.

One parameter that has been held relatively constant is the initial amount of bifunctional reagent or reagent metal complex used. A large excess has been employed with the idea this will result in sorbents with very metal ion capacities. Although this has certainly been the case, a sorbent with a relatively low ligand loading may exhibit certain advantageous properties over one that is saturated with ligands. A Cu(II) imprinted sorbent prepared by our imprint coating technique contains ligands that are paired up and therefore have a higher affinity for the metal

ion template than a nonimprinted material in which each individual ligand is located too far from the next nearest ligand to form a 1:2 metal to ligand complex. If the silica surface is saturated with ligands, then the difference between the imprinted and nonimprinted sorbents comes into question. For this reason, sorbents with a relatively low ligand loading may exhibit better molecular imprinting characteristics than those synthesized with excess ligands.

3-IX.1 Synthesis

Copper(II) imprinted and nonimprinted sorbents have been synthesized by imprint coating TMSen on calcined Pluronic P123 silica. A similar protocol to that used in Section VIII was employed here, with the exception that considerably less TMSen and $CuNO_3$ $3H_2O$ are added to the initial reaction mixtures. Calcined Pluronic P123 silica (1.00 g) was placed in a clean beaker with 20 mL of methanol and sonicated for 10 min. In a separate beaker, 0.011 g of $Cu(NO_3)_2$ $3H_2O$ (0.0453 mmol) was added to 30 mL of methanol and stirred until all the metal salt had dissolved. TMSen (20 μL, 0.0906 mmol) was then slowly added upon stirring to the Cu(II) solution, forming a dark violet colored complex. The complex solution was then added to the Pluronic P123 silica mixture. This mixture was covered and stirred at RT for 1 h. The solid product was recovered by filtration and washed deionized water and then with nitric acid (1 M HNO_3, excess) to remove all of the copper template. The resulting gel was placed in deionized water and titrated with sodium hydroxide (NaOH, 2 N) to pH 7.5, recovered by filtration, washed with deionized water and

absolute ethanol, and placed under vacuum at 80 °C for 1 h. A nonimprinted sorbent was synthesized with a similar protocol, but without the addition of any metal salt.

3-IX.2 Ligand Loading Capacity via Copper(II) Leaching

In the synthetic procedure described above, the leachate from the HNO_3 wash of the Cu(II) imprinted as-synthesized material was collected. Since the as-synthesized material was washed with plenty of deionized water prior to this step, it is assumed that all of the Cu(II) was leached from grafted ligand sites. The amount of Cu(II) in the leachate can be used to estimate the total number of grafted ligands per gram of sorbent.

The leachate volume was adjusted to precisely 200 mL with deionized water and the Cu(II) concentration was determined by ICP/OES to be 1.57×10^{-4} M. This corresponds to 3.13×10^{-5} moles Cu(II) leached from 1.00 grams sorbent. This also represents an estimate of the number of imprinted sites. Since a 1:2 metal to ligand complex was formed during the synthesis, the ligand loading is approximately 6.26×10^{-5} moles per gram sorbent. N_2 adsorption studies (Section III.6.3) indicated that the calcined Pluronic P123 silica had a surface area of 790 m^2/g, or 790×10^{20} $Å^2/g$. Since 6.26×10^{-5} moles of TMSen represents 3.77×10^{19} molecules (Avogadro's Law), it follows that the sorbent contains approximately one grafted ligand per 2096 $Å^2$. Since the ligands are believed to be paired up in the imprinted material, this represents one site per 4192 $Å^2$. If evenly distributed on the silica surface this represents a separation of 65 Å between imprinted sites. Assuming that the nonimprinted sorbent has a

similar ligand loading, it would have a separation between single ligands of approximately 46 Å.

3-IX.3 Copper(II) Adsorption

The results of batch tests conducted with the copper(II) imprinted and nonimprinted TMSen/P123 sorbents with low ligand loading are shown in **Table 3.18**. Four different Cu(II) concentrations from 0.64 to 63.55 ppm were used. The lower ligand loading of these materials compared to those synthesized in Section VIII is evidenced by the lower Cu(II) uptake. The copper(II) imprinted sorbents removed more Cu(II) than the nonimprinted sorbent at the two lower Cu(II) concentrations, but less Cu(II) at the two higher concentrations. A graphical representation of this trend is illustrated in **Figure 3.16**. The "crossover point" in Figure 16 is located at ca. 3.15 x 10^{-4} M Cu(II). At initial concentrations below this, the Cu(II) imprinted sorbent adsorbed more Cu(II) than the nonimprinted sorbent. At concentrations above the crossover point the nonimprinted sorbent had a higher Cu(II) uptake than the Cu(II) imprinted material. It should be noted that since the batch experiments used 10 mL of Cu(II) solution and 0.100 g of sorbent, that the crossover point corresponds to 3.15 x 10^{-5} mol Cu(II) per gram of sorbent. This value is very close to the 3.13 x 10^{-5} mol of Cu(II) per gram of sorbent that was leached from the Cu(II) imprinted as-synthesized material.

Table 3.18 Cu(II) Uptake Capacity of TMSen/P123 Sorbents with Low Ligand Loading

Sorbent	C_0 (ppm)	C_f (ppm)	K_d Cu	% Cu(II) absorbed
Nonimprinted	0.64	0.026	2400	95.92
Cu(II) imprinted	**0.64**	**0.023**	**2700**	**96.37**
Nonimprinted	6.35	0.468	1300	92.63
Cu(II) imprinted	**6.35**	**0.424**	**1400**	**93.33**
Nonimprinted	31.78	7.24	340	77.23
Cu(II) imprinted	**31.78**	**7.43**	**330**	**76.63**
Nonimprinted	63.55	25.48	150	59.90
Cu(II) imprinted	**63.55**	**26.65**	**140**	**58.07**

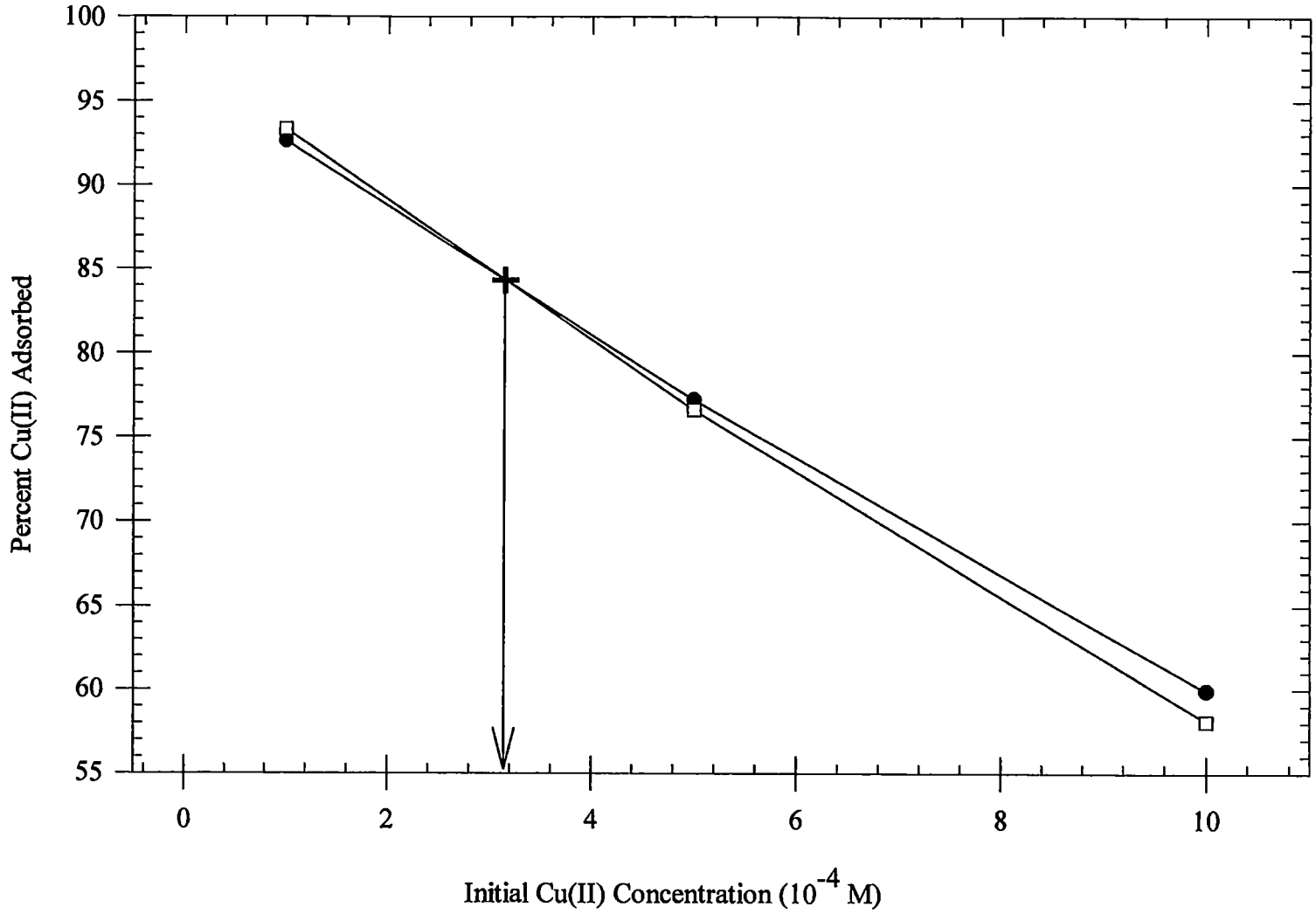


Figure 3.16 Copper(II) adsorption of TMSen/Pluronic P123-silica with low ligand loading

3-IX.4 Copper(II) Adsorption as a Function of pH

All of the solutions used in the adsorption batch tests described earlier were buffered to pH = 5.0. The reason for this is that changes in pH have a significant effect on the formation of metal ion compexes and therefore, the overall performance of our sorbents. Looking at the formation of copper(II) ethylenediamine complexes in particular, the stepwise stability constants (K_1 and K_2) can be derived from equations 6 and 7 (70). In a similar manner the stepwise stability constants (K_1 and K_{12}) for the protonation of ethylenediamine can be derived from equations 8 and 9.

$$Cu^{2+} + en \rightleftharpoons Cu(en)^{2+} \qquad K_1 = \frac{[Cu(en)^{2+}]}{[Cu^{2+}][en]} \qquad (6)$$

$$Cu(en)^{2+} + en \rightleftharpoons Cu(en)_2^{2+} \qquad K_2 = \frac{[Cu(en)_2^{2+}]}{[Cu(en)^{2+}][en]} \qquad (7)$$

$$H^{+} + en \rightleftharpoons H(en)^{+} \qquad K_1 = \frac{[H(en)^{+}]}{[H^{+}][en]} \qquad (8)$$

$$H^{+} + H(en)^{+} \rightleftharpoons H_2(en)^{2+} \qquad K_{12} = \frac{[H_2(en)^{2+}]}{[H(en)^{+}][H^{+}]} \qquad (9)$$

The affinity of en for Cu(II) ($\log K_1 \sim 11$) is higher than it is for a proton ($\log K_1 \sim 10$). Despite this, if the concentration of protons is considerably larger than Cu(II) then en is protonated. This is the case at lower pH values. When en becomes protonated the lone pairs of electrons on the nitrogen atoms are shared with the

hydrogens and no dative bonding between en and Cu(II) occurs. This is why washing of the TMSen sorbents with dilute nitric acid readily leaches out the bound metal ions. In order to determine the effect of pH on our copper(II) imprinted and nonimprinted TMSen/P123 sorbents, batch tests were conducted in the pH range 4.1-5.3. The sorbents synthesized in Section IX were used.

All solutions had a copper(II) concentration of 2.5×10^{-4} M (15.89 ppm). The solutions were buffered to specific pH values with NaAc/HAc (0.05 M). The results of the Cu(II) uptake experiments conducted at various pH values, with the Cu(II) imprinted and nonimprinted sorbents are listed in **Table 3.19**. The nonimprinted TMSen/P123 sorbent adsorbed more Cu(II) at the lower pH values (4.1-4.5), while the copper(II) imprinted material adsorbed more Cu(II) at the higher pH values (**Figure 3.17**).

3-IX.5 Discussion

The synthesis of copper(II) imprinted and nonimprinted sorbents using the TMSen bifunctional reagent coated on calcined Pluronic P123 silica described in Section VIII was modified by decreasing the initial concentration of TMSen [or $Cu(TMSen)_2^{2+}$] by more than ten-fold. The resulting sorbents exibited a lower Cu(II) uptake (Table 3.17) than those described in section VIII (Table 3.14). The low ligand loading did not result in any enhancement of molecular imprinting characteristics when compared to those sorbents prepared with higher ligand loading described in Sections V and VIII.

Table 3.19 Cu(II) Uptake Capacity of TMSen/P123 Sorbents as a Function of pH

Sorbent	pH	C_0 (ppm)	C_f (ppm)	K_d Cu	% Cu(II) absorbed
Nonimprinted	4.1	15.89	6.11	160	61.54
Cu(II) imprinted	**4.1**	15.89	**6.98**	**130**	**56.05**
Nonimprinted	4.3	15.89	5.38	200	66.16
Cu(II) imprinted	**4.3**	15.89	**5.96**	**170**	**62.49**
Nonimprinted	4.5	15.89	4.39	260	72.40
Cu(II) imprinted	**4.5**	**15.89**	**4.48**	**250**	**71.80**
Nonimprinted	4.9	15.89	2.92	440	81.60
Cu(II) imprinted	**4.9**	**15.89**	**2.79**	**470**	**82.43**
Nonimprinted	5.1	15.89	2.25	610	85.86
Cu(II) imprinted	**5.1**	**15.89**	**1.85**	**760**	**88.37**
Nonimprinted	5.3	15.89	1.80	780	88.68
Cu(II) imprinted	**5.3**	15.89	**1.39**	**1040**	**91.24**

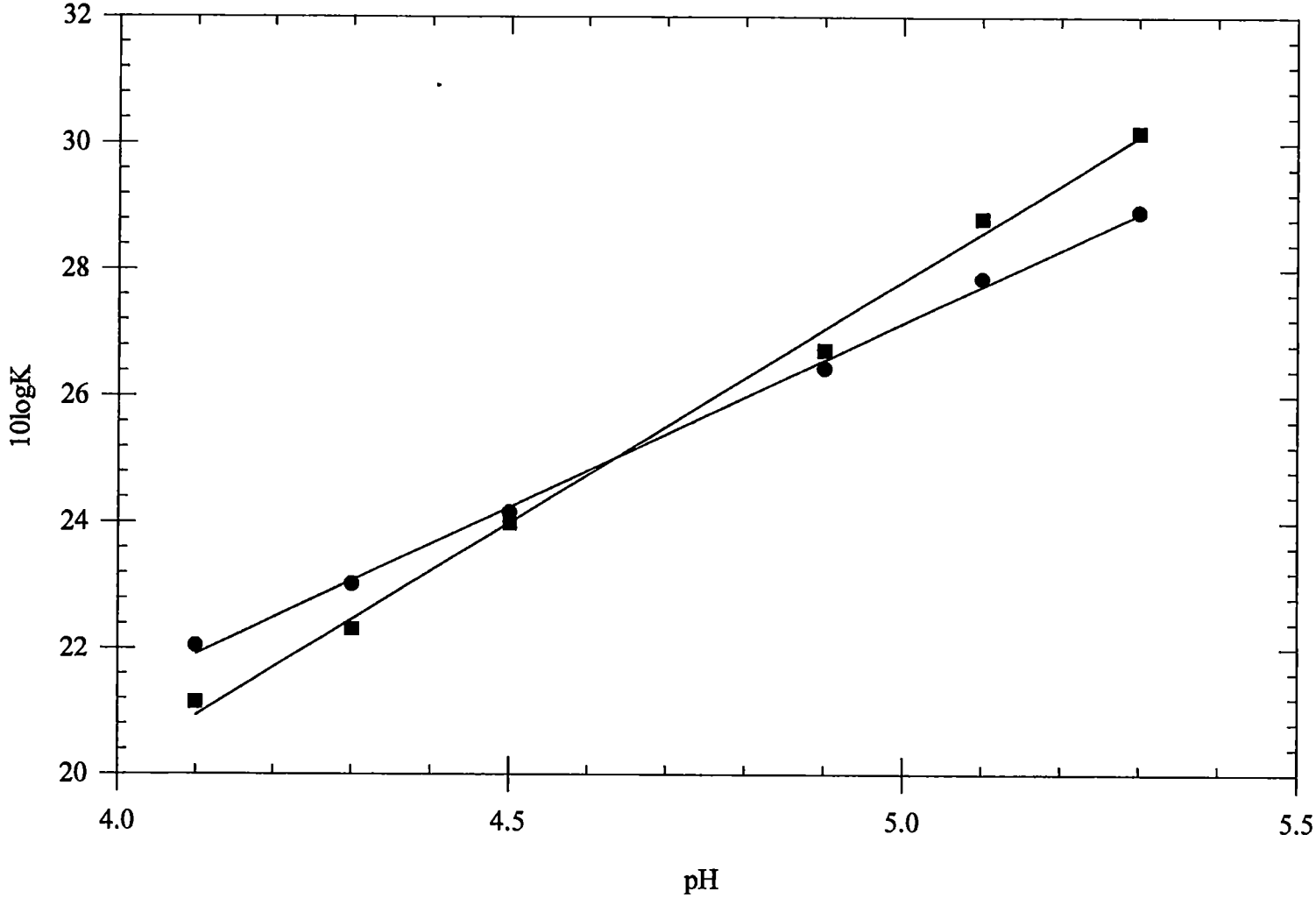


Figure 3.17 Copper(II) adsorption of TMSen/P123 sorbents as a function of pH

The copper(II) imprinted sorbent exibited an enhanced capacity for the metal ion template at low concentrations, but adsorbed less Cu(II) at the higher concentrations studied. This trend was also exhibited by the sorbents synthesized by imprint coating TMSen on calcined MCM-41 described in Section V. We believe that this trend may be due to the nonimprinted material having more TMSen binding sites than the Cu(II) imprinted sorbent. Assuming a homogeneous distribution of TMSen in these sorbents and similar ligand loading, the nonimprinted material would have twice as many TMSen binding sites as the Cu(II) imprinted sorbent. This is due to the way in which the sorbents were synthesized. Since the $Cu(TMSen)_2^{2+}$ complex was formed prior to grafting, the TMSen ligands may be "paired up" in the imprinted sorbent. This results in a higher affinity for the metal ion template at low concentrations. At higher concentrations, when most of the sites in the Cu(II) imprinted sorbent are occupied the nonimprinted sorbent still has many open sites and therefore, a higher copper(II) uptake.

The copper(II) leaching experiment in section IX-2 indicated that the as-synthesized Cu(II) imprinted sorbent contained approximately 3.13×10^{-5} mol of Cu(II) per gram of sorbent. If this value is used to approximate the number of binding sites in the Cu(II) imprinted sorbents, then the "crossover point" illustrated in Figure 3.16 takes on added significance. Since 0.100 g of sorbent and 10.0 mL of solution have been used in all batch tests, its location at 3.15×10^{-4} M Cu(II) corresponds to the point at which the sorbent has adsorbed 3.15×10^{-5} mol Cu(II) per gram. The crossover point may be used to approximate the ligand loading in these imprint coated

materials. At concentrations above the crossover point, there are more copper(II) ions in the solution than imprinted sites on the sorbent. Although the Cu(II) imprinted sorbent can continue to adsorb Cu(II) ions at concentrations above this point, this requires that 1:1 Cu(II) to ligand complexes form. The Cu(II) ions would be very close together (higher in energy) compared to those in the nonimprinted materials. This would explain the copper(II) adsorption trends shown by the imprint coated sorbents in Sections V and IX.

Batch experiments were conducted at various pH values and constant Cu(II) solution concentration in order to determine the effect of pH on the Cu(II) uptake of the imprint coated sorbents. Figure 3.17 shows that the nonimprinted TMSen/P123 sorbent adsorbed more Cu(II) at the lower pH values (4.1-4.5), while the copper(II) imprinted material adsorbed more Cu(II) at the higher pH values. The highly basic nature of the Cu(II) imprinted sorbents with the en moieties in close proximity to each other may allow for protons to share electrons from more than one ligand and reduce the affinity of the sorbent at low pH. This effect would be much less pronounced in the nonimprinted materials because of the larger number of sites and the inability of a proton to share electron density with more than one ligand. At higher pH, ligand protonation is not a significant problem and the Cu(II) imprinted sorbent adsorbs more Cu(II) than the nonimprinted sorbent.

3-X. Ion Exchange Properties of Imprint Coated Sorbents

The experiments described thus far have all included a post-synthetic step to remove the template ion from the metal ion imprinted sorbents. If the metal ions are not removed and the sorbent is placed in solutions containing metal ions with a higher affinity for the en moeity, cation exchange may occur. Ion exchange materials containing chelating groups, are called chelating or coordinating polymers, and have been developed as an alternative to polyelectrolytes for many industrial applications (71).

3-X.1 Synthesis

A protocol similar to that used in Section VII was employed here. Reaction mixtures were covered to eliminate any evaporation during the imprint coating process. Calcined MCM-41 was used as the sorbent support and absolute ethanol as the solvent. Ni(II) imprinted, Zn(II) imprinted, and nonimprinted sorbents were synthesized.

3-X.1.1 Zn(II)/TMSen/MCM-41/EtOH

Calcined MCM-41 (2.00 g) was placed in a beaker with 20 mL of absolute ethanol and sonicated for 10 min. In a separate beaker, 5.0 mmol of $Zn(NO_3)_2$ $6H_2O$ (1.49 g) was added to 40 mL of absolute ethanol and stirred until all the metal salt had dissolved. TMSen (10 0 mmol, 2.24 mL) was then slowly added upon stirring to the Zn(II) solution. The complex solution was then added to the MCM-41 mixture. This

mixture was covered and stirred at RT for 3 h. A nonimprinted sorbent was synthesized with a similar protocol, but without the addition of any metal salt. The solid product was recovered by filtration and washed with deionized water and absolute ethanol, and placed under vacuum at 80 °C for 4 h.

3-X.1.2 Ni(II)/TMSen/MCM-41/EtOH

Calcined MCM-41 (1.00 g) was placed in a clean beaker with 20 mL of absolute ethanol and sonicated for 10 min. In a separate beaker, 2.5 mmol of $Ni(NO_3)_2$ $6H_2O$ (0.727 g) was added to 40 mL of absolute ethanol and stirred until all the metal salt had dissolved. TMSen (5.0 mmol, 1.12 mL) was then slowly added upon stirring to the Zn(II) solution, forming a navy blue complex. The complex solution was then added to the MCM-41 mixture. This mixture was covered and stirred at RT for 3 h. A nonimprinted sorbent was synthesized with a similar protocol, but without the addition of any metal salt. The solid product was recovered by filtration and washed with deionized water and absolute ethanol, and placed under vacuum at 80 °C for 4 h.

3-X.2 Ion Exchange Batch Tests

All metal ion solutions were buffered to pH = 5.0 with NaAc/HAc (0.05 M). Unless stated otherwise, equilibration times of 10 min were used. The results of metal ion batch tests with Ni(II)-loaded TMSen/MCM-41 are listed in **Table 3.20**. The Ni(II) loaded sorbent adsorbed >98% of the Cu(II) from a 1 x 10^{-3} M Cu(II) solution.

Table 3.20 Ion Exchange Properties of Ni(II) loaded TMSen/MCM-41 at pH = 5.0.

Sorbent	Initial Concentrations				Percentage Adsorbed			
	Cu(II) (M)	Zn(II) (M)	Ni(II) (M)	Cd(II) (M)	Cu(II)	Zn(II)	Ni(II)	Cd(II)
Nonimprinted TMSen/MCM-41	1×10^{-3}	-	-	-	99.36	-	-	-
Ni(II) loaded TMSen/MCM-41	1×10^{-3}	-	-	-	98.44	-	Ni(II) excess	-
Nonimprinted TMSen/MCM-41	1×10^{-3}	1×10^{-3}	1×10^{-3}	1×10^{-3}	99.74	96.26	57.24	13.24
Ni(II) loaded TMSen/MCM-41	1×10^{-3}	1×10^{-3}	1×10^{-3}	1×10^{-3}	97.86	77.58	Ni(II) excess	0
Nonimprinted TMSen/MCM-41	-	1×10^{-3}	-	-	-	89.93	-	-
Ni(II) loaded TMSen/MCM-41	-	1×10^{-3}	-	-	-	60.21	Ni(II) excess	-
Nonimprinted TMSen/MCM-41	-	1×10^{-3}	1×10^{-3}	1×10^{-3}	-	95.03	77.08	15.85
Ni(II) loaded TMSen/MCM-41	-	1×10^{-3}	1×10^{-3}	1×10^{-3}	-	64.30	Ni(II) excess	0

The final Ni(II) concentration of approximately 60 ppm indicates that a 1:1 cation exchange has taken place. The exchange with the zinc(II) ion is not as pronounced, as only 60.21% of the Zn(II) is adsorbed from the 1 x 10^{-3} M Zn(II) solution. When placed in mixed solutions containing Cu(II), Zn(II), and Cd(II), a few trends are clear. The nickel(II) is readily exchanged by Cu(II) and the nickel loaded material adsorbed nearly as much Cu(II) as the nonimprinted sorbent which does not require the displacement of any divalent cation. Zn(II) ions did not exchange the nickel(II) as well as the Cu(II) did, but >77% of the Zn(II) was adsorbed. The nickel(II) ions bind to en moeities more strongly than Cd(II) ions, thereby effectively blocking the adsorption of Cd(II). While the nonimprinted sorbent removed >13% of the Cd(II) from one mixed solution and nearly 16% from the other, the nickel(II) loaded sorbent adsorbed no detectable amount of Cd(II) from either.

The kinetics of cation exchange in these materials was investigated using the Zn(II) loaded TMSen/MCM-41 sorbents. Batch tests were conducted using equilibration times of 5 min, 1 h, and 18 h. The results of batch tests using a 1 x 10^{-3} M Ni(II) solution and two mixed solutions are listed in **Table 3.21**. Although the great majority of ion exchange occurs quickly, the changes in adsorption percentages between the 1 h and the 18 h batch tests indicate that equilibrium is not reached for many hours. One particularly interesting result is that more than 4% of the Cd(II) is initially adsorbed, then exchanged out by Cu(II) and Ni(II) after a 1 h equilibration.

The adsorption behavior of Ni(II) seems to be critically dependent upon competitor species. When in solution by itself, it exchanges with Zn(II) rather quickly

Table 3.21 Ion Exchange Properties of Zn(II) Loaded TMSen/MCM-41 at pH = 5.0

Sorbent	Time	Initial Concentrations				Percentage Adsorbed		
		Cu(II) (M)	Zn(II) (M)	Ni(II) (M)	Cd(II) (M)	Cu(II)	Ni(II)	Cd(II)
Zn(II) loaded TMSen/MCM-41	5 min.	1×10^{-3}	1×10^{-3}	1×10^{-3}	1×10^{-3}	83.95	13.77	4.44
Zn(II) loaded TMSen/MCM-41	1 h.	1×10^{-3}	1×10^{-3}	1×10^{-3}	1×10^{-3}	90.46	26.04	0
Zn(II) loaded TMSen/MCM-41	18 h.	1×10^{-3}	1×10^{-3}	1×10^{-3}	1×10^{-3}	93.54	30.87	0
Zn(II) loaded TMSen/MCM-41	5 min.	-	1×10^{-3}	1×10^{-3}	1×10^{-3}	-	50.85	7.29
Zn(II) loaded TMSen/MCM-41	1 h.	-	1×10^{-3}	1×10^{-3}	1×10^{-3}	-	53.23	4.76
Zn(II) loaded TMSen/MCM-41	18 h.	-	1×10^{-3}	1×10^{-3}	1×10^{-3}	-	54.08	3.87
Zn(II) loaded TMSen/MCM-41	5 min.	-	-	1×10^{-3}	-	-	56.56	-
Zn(II) loaded TMSen/MCM-41	1 h.	-	-	1×10^{-3}	-	-	57.27	-
Zn(II) loaded TMSen/MCM-41	18 h.	-	-	1×10^{-3}	-	-	57.58	-

as 56.56% is adsorbed in 5 min compared to 57.27% in 1 h. When in solution with the weaker competitor species Cd(II), 50.85% is exchanged within 5 min, while 53.23% is adsorbed within 1 h. When in solution with the stronger competitor species Cu(II), only 13.77% is exchanged in the first 5 min and this nearly doubles to > 26% adsorption after 1 h.

3-X.3 Discussion

The experiments conducted in this section indicate that our sorbents imprint coated with TMSen readily undergo cation exchange reactions. Although these tests did not result in complete metal ion separations, they are very significant. Due to the nature of the basic research being described herein, as well as time and manpower limitations, metal ion adsorption by our sorbent materials have been measured using "static" batch tests. For real world applications such as environmental remediation and industrial separations, high throughput columns are required. The significance of these ion exchange reactions cannot be underestimated.

For example, the results listed in Table 3.9 (Section V.3) show that the Cu(II) imprinted TMSen/MCM-41 sorbent adsorbed 99.84% of the Cu(II) and 79.52% of the Zn(II) from an equimolar mixed solution of these two cations. This result may not seem impressive, but when the ion exchange properties of these materials are taken into account, many applications are possible. If the sorbent were packed into a large column and a steady flow of the Cu(II)/Zn(II) solution was eluted, the Zn(II) would be adsorbed initially as it was in the static batch test. As more Cu(II) was eluted all the

Zn(II) ions would be exchanged out, as they were in the experiments described in Section X.2 and listed in Table 3.21. In order to take this research to the next level, column testing of the sorbents developed herein must be performed.

3-XI. Ligand Loading via ^{29}Si Solid-State NMR

An estimation of ligand loading via copper(II) leaching was reported in Section IX.2. Although those results for the imprint coated TMSen/Pluronic P123 silica with low ligand loading were consistent with other experimental findings, many attempts to quantify the ligand loading in the amorphous materials described in this chapter have resulted in inconsistent results and therefore have not been reported. Characterization by UV-visible diffuse reflectance spectroscopy, infrared spectroscopy, pH titration, and HF digestion followed by carbon ICP/OES have all failed to produce consistent and/or quantifiable results. In an attempt to gain an understanding of the relative ligand loading between Cu(II) imprinted and nonimprinted sorbents, calcined MCM-41 imprint coated with TMSen has been characterized via ^{29}Si solid-state nuclear magnetic resonance spectroscopy (SSNMR).

3-XI.1 Synthesis

A protocol similar to that in Section V was followed here, with the exception that absolute ethanol was used as the solvent. In a typical preparation, copper nitrate trihydrate [$Cu(NO_3)_2$ $3H_2O$, 0.60 g, 2.5 mmol] was added under stirring to absolute ethanol (100 mL). After the metal salt had completely dissolved, TMSen (1.12 mL, 5

mmol) was added. After stirring the mixture for 10 min., calcined MCM-41 (1.00 g) was added. The solution was covered and stirred for 4 h. The solid product was recovered by filtration and washed with nitric acid (HNO_3, excess) to remove all of the copper(II) template. The resulting gel was placed in deionized water and titrated with sodium hydroxide (NaOH, 2 N) to pH 7.5, recovered by filtration, washed with deionized water and absolute ethanol, and placed under vacuum at 80 °C for 4 h. A nonimprinted sample was prepared by an identical protocol with the exception that no metal salt was added. Copper(II) imprinted and nonimprinted sorbents were also synthesized with a 8 h mixing time, for a total of 4 samples.

3-XI.2 Analytical Methods

Solid-state ^{29}Si NMR analyses were performed with a Bruker 400 MHz NMR spectrometer operating at 9.4 Tesla. The ^{29}Si Larmour Frequency was 79.49 MHz. Observations were made using single pulse excitation and magic angle spinning (SPE/MAS) with a 7.5 μs 90° pulse time and a 300 sec recycle delay. Seven mm zirconia rotors were spun at 4.1 +/- 0.1 KHz. The ^{29}Si spin lattice relaxation time of the Q_4 site was measured at 60 +/- 15 sec from a five point data set acquired using progressive saturation. This T_1 was used to determine the 300 sec recycle delay used in all experiments (5 T_1) to insure quantitative intensity response of all the ^{29}Si resonances.

3-XI.3 Results and Discussion

The coordination environment of ^{29}Si can be described in terms of the Q_n notation (72), where n represents the number of silicon atoms in the secondary coordination sphere of the ^{29}Si atom being described. Some of the possible bonding modes of ^{29}Si atoms in our organofunctionalized sorbents and the corresponding Q_n notations are shown in **Figure 3.18**. The structural characterization of a substantial series of functionalized polysiloxanes via SSNMR, including those containing TMSen pendent groups, have been reviewed in detail (73).

The ^{29}Si SPE/MAS NMR spectrum of calcined MCM-41 is shown in **Figure 3.19**. The large convoluted peak is a result of the Q_4 silicons located at ~ -111 ppm and Q_3 silicons attributed to surface silanols located at ~ -101 ppm. Relatively small spinning sidebands located at ~ -50 ppm and −155 ppm reflect the small chemical shift anisotropy around the silicon atoms. Spectra of the copper(II) imprinted and nonimprinted sorbents coated for 4 h are shown in **Figures 3.20 and 3.21**, respectively. Both exhibit a substantial decrease in the size of the silanol peak relative to that exhibited by the calcined MCM-41 sample due to the replacement of the surface silanol groups with grafted ligand. The convoluted peaks located from -50 to -80 ppm represent ligand silicon atoms, which contain an alkyl chain in place of a siloxane group (72). A direct comparison of the spectra reveals that the silanol peak of the nonimprinted sorbent is smaller than that of the copper(II) imprinted material. This indicates a higher substitution of the silanol groups and therefore, a higher ligand loading on the nonimprinted sorbent. The integrated area under the ligand peaks can

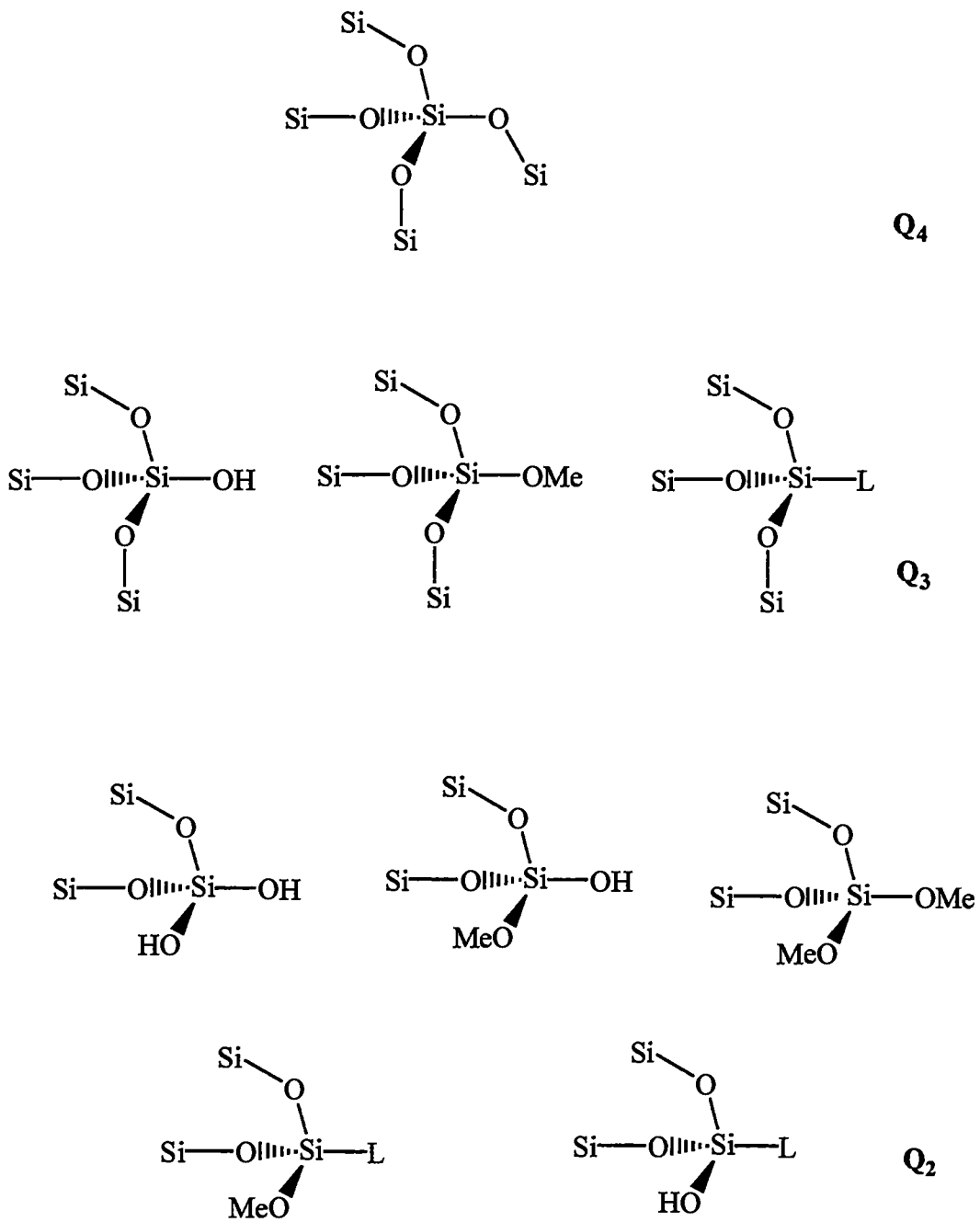


Figure 3.18 Possible bonding modes of ^{29}Si in imprint coated sorbents

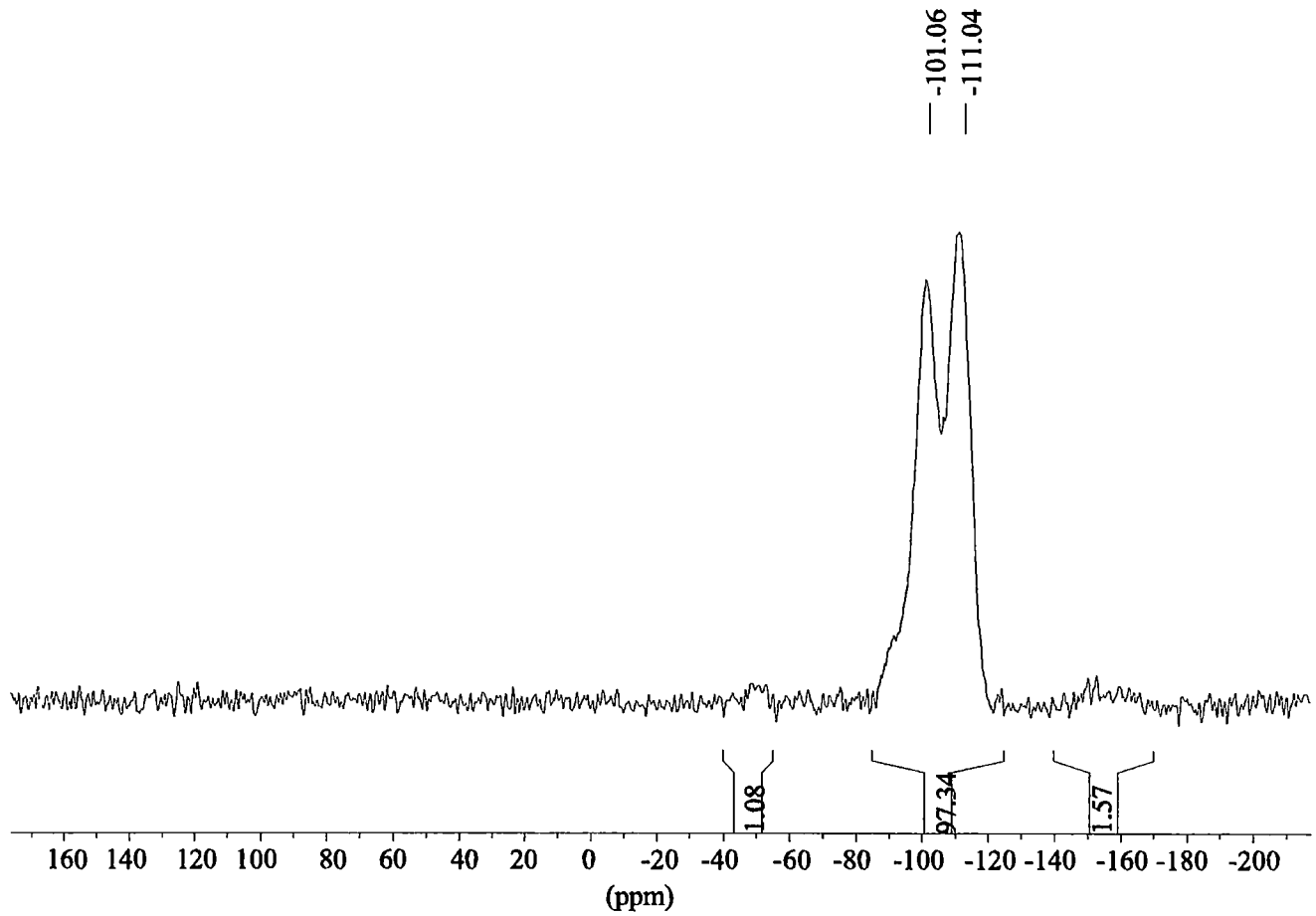


Figure 3.19 Solid-state ^{29}Si SPE/MAS NMR spectrum of calcined MCM-41

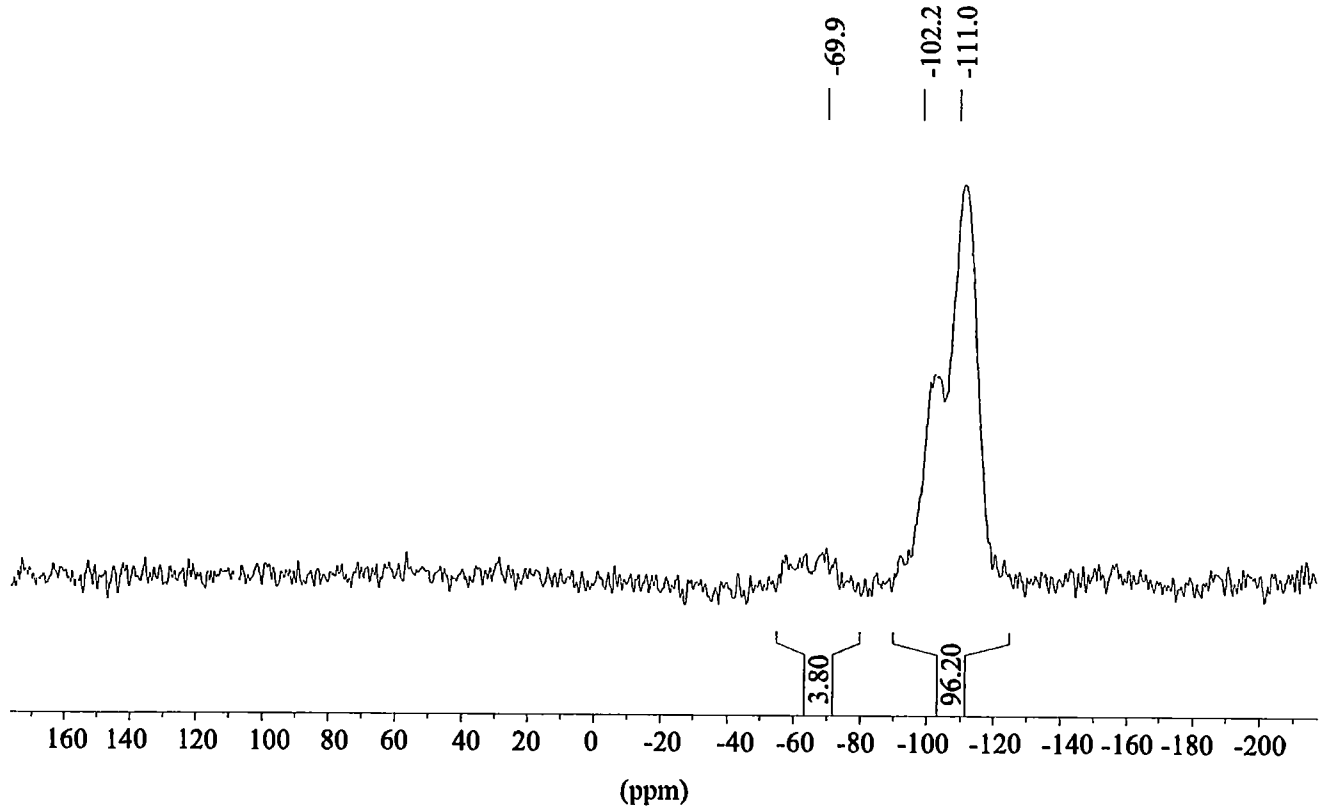


Figure 3.20 Solid-state ^{29}Si SPE/MAS NMR spectrum of copper(II) imprinted sorbent coated for 4 h

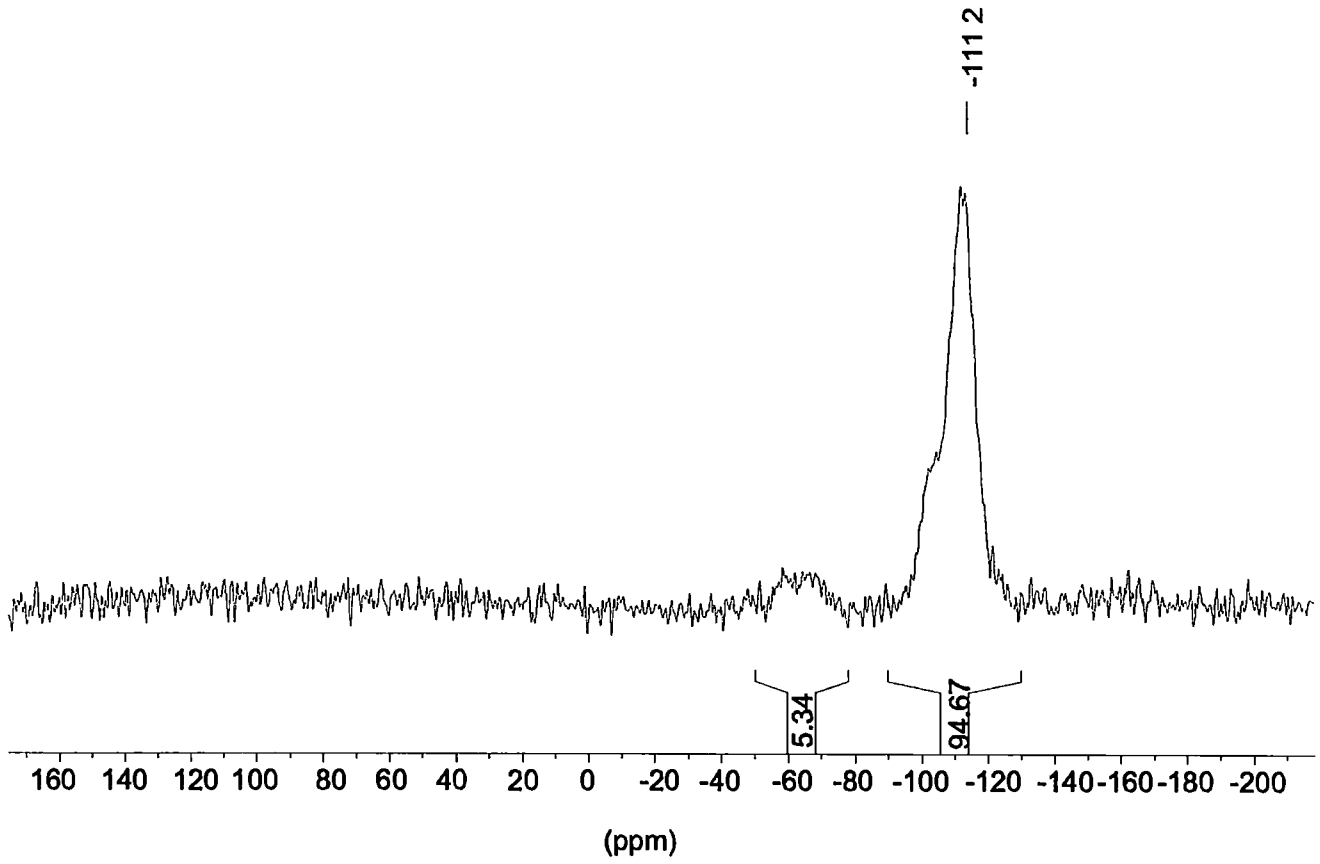


Figure 3.21 Solid-state ^{29}Si SPE/MAS NMR spectrum of nonimprinted sorbent coated for 4 h

be used to estimate the relative ligand loading in the two samples. Consistent with the observation of the magnitude of the silanol peaks, the nonimprinted sorbent has a larger ligand peak area (57% higher) than the copper(II) imprinted material. These results indicate that the nonimprinted sorbent has a higher ligand loading than the copper(II) imprinted sorbent.

The ^{29}Si MAS NMR spectra of the copper(II) imprinted and nonimprinted sorbents coated for 8 h are shown in **Figures 3.22 and 3.23**, respectively. Although these sorbents show larger overall ligand loadings than those coated for 4 h, the trend is similar with the nonimprinted material containing more (31%) grafted ligands than the copper(II) sorbent. One explanation of this trend is that during the coating process of the nonimprinted sorbents, only single TMSen molecules need to fit inside the mesopores of the support in order to undergo condensation reactions with the silica silanol groups. During the coating process of the copper(II) imprinted sorbents, the much bulkier $Cu(TMSen)_2^{2+}$ complex also needs to gain access to the interior of the mesopores and due to steric constraints, is less likely to do so.

These results indicate that despite our attempts to create nonimprinted sorbents for direct comparison, the metal ion imprinted sorbents described in this chapter have a lower ligand loading than the corresponding nonimprinted samples. This is a decided disadvantage and therefore, further indicates that the imprinted sites have a much higher affinity for the metal ion template. These results lead us to believe that if the metal ion imprinted and nonimprinted sorbents were synthesized with an identical ligand loading, the results of the metal ion adsorption batch tests would favor the

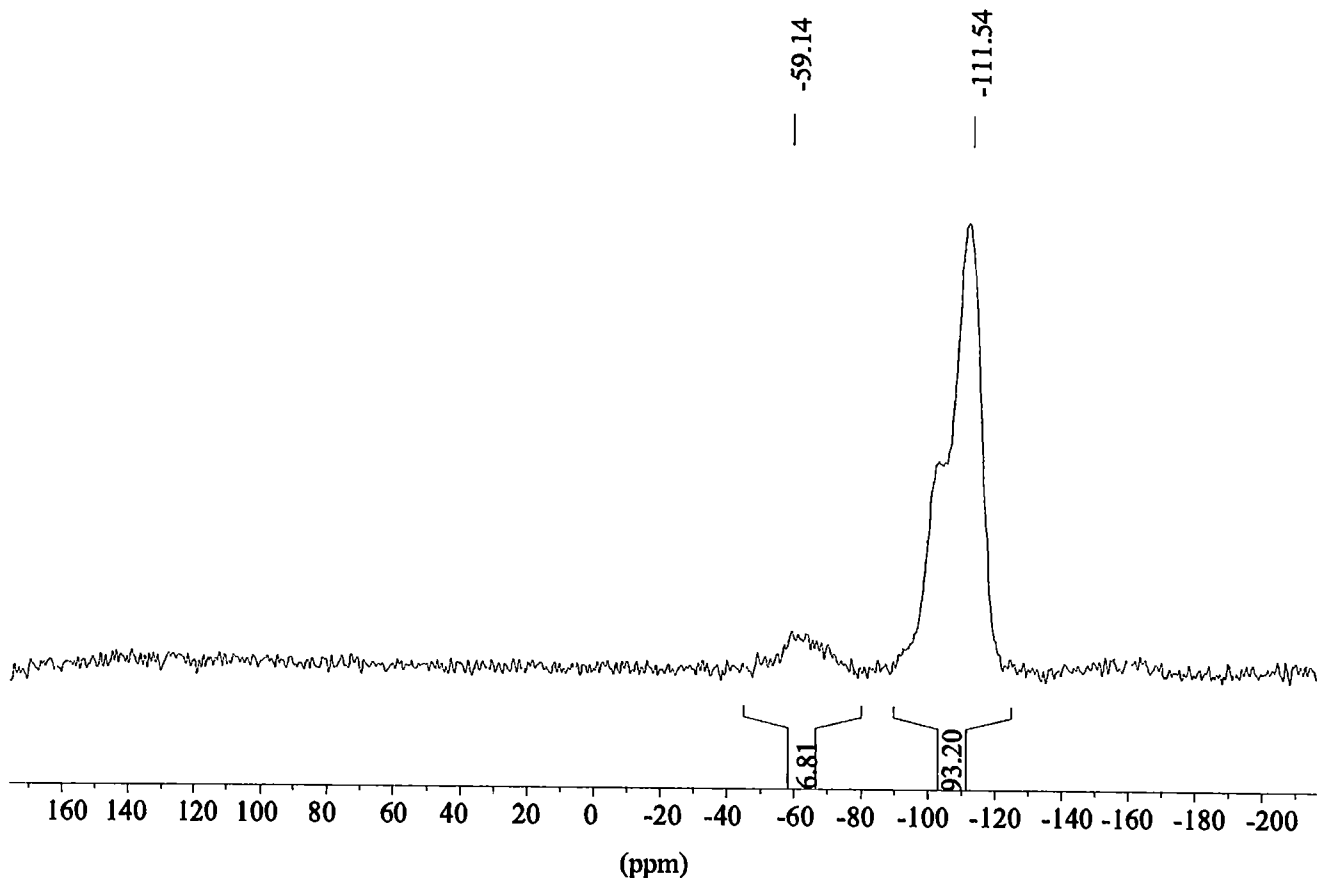


Figure 3.22 Solid-state ^{29}Si SPE/MAS NMR spectrum of copper(II) imprinted sorbent coated for 8 h

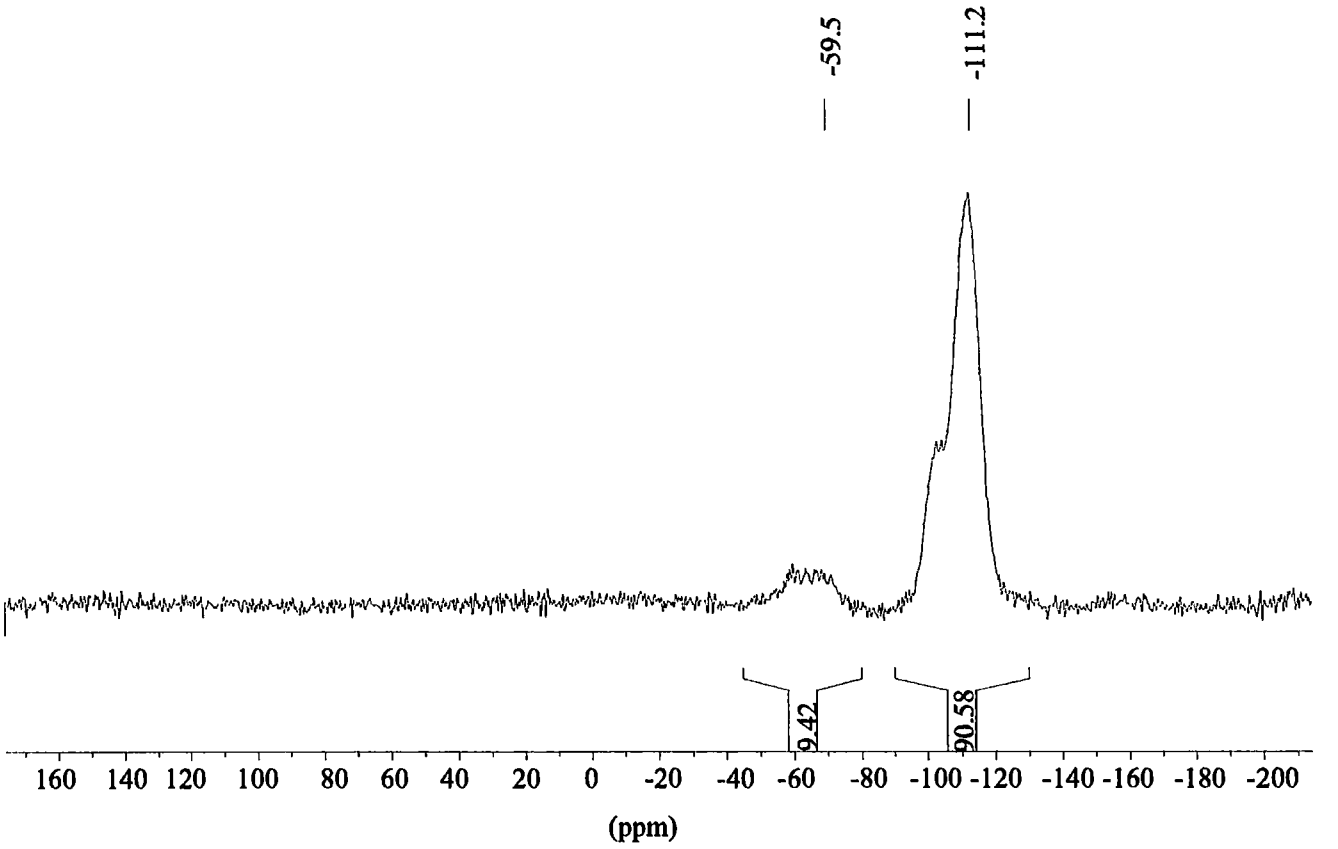


Figure 3.23 Solid-state ^{29}Si SPE/MAS NMR spectrum of nonimprinted sorbent coated for 8 h

metal ion imprinted sorbents even more than those described in this chapter. The advantages of molecular imprinting would be far better illustrated, with larger enhancements of distribution constants and selectivity coefficients for the metal ion imprinted materials.

CHAPTER 4

STEPWISE ASSEMBLY OF SURFACE IMPRINT SITES ON MESOPOROUS SILICA

4-I. Introduction

The imprint coating methodology described in Chapter 3 was used to construct binding sites on the surface of the sorbent support that were designed to have a high affinity for the metal ion template. A metal-ligand complex was formed in solution and then grafted to the surface of mesoporous silica . The ligands were arranged in a favorable configuration so that following the removal of the metal ion, the cavities that remained had a higher affinity for the metal ion template than those created by conventional surface coating. For comparison, non-imprinted sorbents were made using an identical mesoporous support and reaction conditions, except that no metal ion complex was formed prior to the grafting process. We have found that the overall ligand coverage of the imprinted sorbents can be considerably lower than that of the non-imprinted samples. This can be attributed to the increased steric hindrance experienced by the relatively large metal ion complexes when trying to incorporate them into the inner pore spaces of MCM-41 as compared to the smaller single ligands. In spite of this, the imprint coated materials exhibited a better selectivity for the metal ion template in the presence of competitor species than conventionally coated sorbents. This drawback in our original method has prompted us to seek an alternative approach to imprint coating. In order to minimize the discrepancy in

overall ligand coverage between the imprinted and non-imprinted sorbents, we have developed a stepwise assembly technique. Herein, we describe the preparation of a mesoporous sol-gel sorbent using calcined MCM-41 as the support, TMSen as the bifunctional reagent, and Cu(II) as the metal ion template via the stepwise assembly approach.

4-II. Experimental

4-II.1 Synthesis of the MCM-41 Mesoporous Support.

A protocol similar to that used in Chapter 2, Section III.1 was used to synthesize the mesoporous support. Cetyltrimethylammonium bromide (36.0 g) was added to 485 mL of deionized water. The mixture was heated gently and stirred at 60 °C to dissolve all surfactant. The clear solution obtained was then allowed to cool to room temperature. Concentrated NH_4OH (7.7 M, 109 mL) was gradually added to the stirred solution. Tetraethyl orthosilicate (TEOS, 82.0 g) was then added. The resulting molar ratios of the reaction mixture were as follows:

1.0 TEOS : 0.25 CTAB : 2.13 NH_4OH : 83.8 H_2O

The mixture was then refluxed for 16 h. The solid product was recovered by filtration, washed with deionized water and ethanol, and air-dried. In order to remove the surfactant template the product was calcined in air. The as-synthesized material is then placed in a furnace and ramped at 1° C/min to 550 °C, at which temperature it is calcined for 3 h to remove all surfactant (**Figure 4.1**).

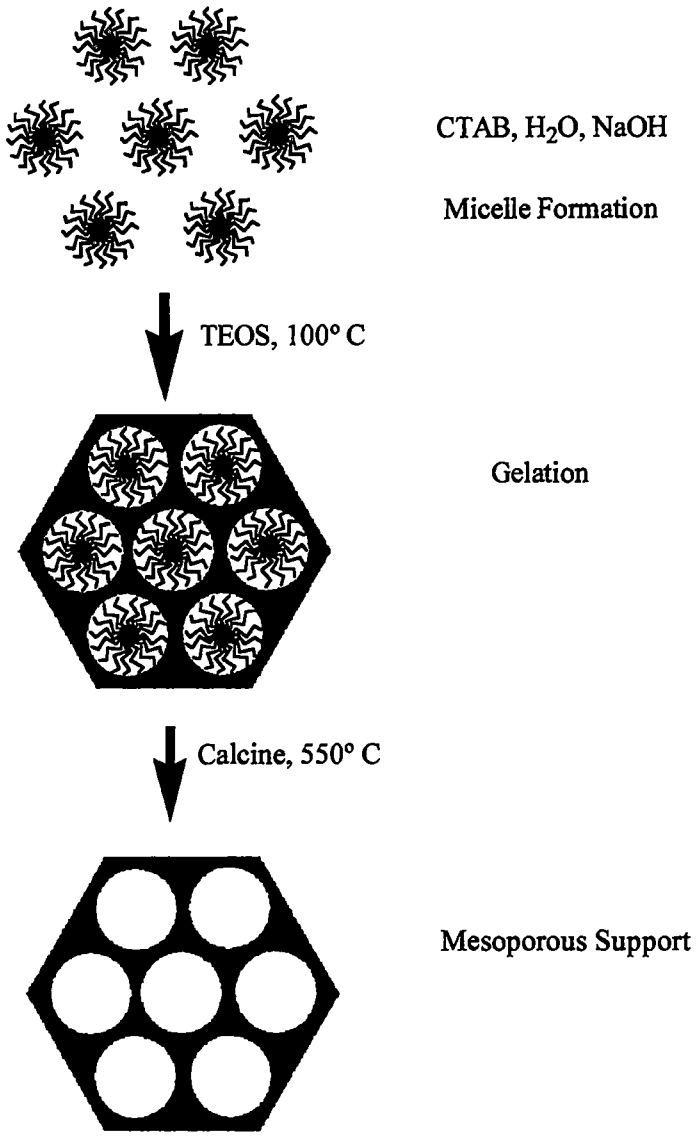


Figure 4.1 Preparation of the mesoporous support

4-II.2 Functionalization and Imprinting.

Calcined MCM-41 (1.00 g) was placed in 100 mL of toluene and 4.58 mmol of TMSen was added. The mixture was stirred and refluxed for 5 h. The sorbent was recovered by filtration and washed with ethanol and air dried. The sample was then placed in 100 mL of 10^{-2} M $Cu(NO_3)_2$ $3H_2O$ solution and sonicated for 15 min., recovered by filtration, washed with deionized water, and placed under vacuum at 90 °C for 1 h. The material was then placed in 100 mL of toluene with 4.58 mmol of TMSen and refluxed for another 5 h. The resulting material was recovered by filtration, washed with ethanol, air dried, and placed under vacuum at 90 °C for 1 h. A nonimprinted control sample was prepared by a similar protocol, without the metal salt solution step.

4-II.3 Post-synthetic Treatment

The metal ion template was then removed by mixing the sorbent in 100 ml of 8 M HNO_3 and gently heated for 1 h. The gel was recovered by filtration and placed in 100 mL of deionized water and titrated with 2 N NaOH to pH 7.0. The neutralized material is filtered, washed with plenty of deionized water, and placed under vacuum at 90 °C for 1 h. The nonimprinted control sample is treated in an identical manner to ensure experimental consistency.

4-II.4 Batch Procedures

All metal ion solutions were buffered to a specific pH with sodium acetate/acetic acid (0.05 M). In a typical run, 0.1 g of sorbent and 10 mL of metal ion solution were placed in a capped plastic vials and sonicated for 30 min. The resulting mixture was filtered and the filtrate was analyzed via ICP/AE spectroscopy in order to measure the metal ion concentration. The overall capacity of the sorbent for a given metal ion was then calculated by the change in concentration between the filtrate and the original metal ion solution.

4-II.5 Analytical Methods

All metal ion concentration analyses were performed with a Thermo Jarrel Ash Iris inductively coupled plasma optical emission spectrometer (ICP/OES). Surface areas and pore volumes were measured on a Micromeritics Gemini 2375 surface area analyzer. Nitrogen (N_2) was used as the adsorbent. Adsorption isotherms were measured at 77 K after degassing the samples at 80° C for 4 h. Small angle X-ray scattering of the mesoporous samples was conducted at the SAXS user facility of the Oak Ridge National Laboratory. Solid-state ^{29}Si NMR analyses were performed with a Bruker 400 MHz NMR as described in Chapter 3, Section XI.

4-III. Results and Discussion

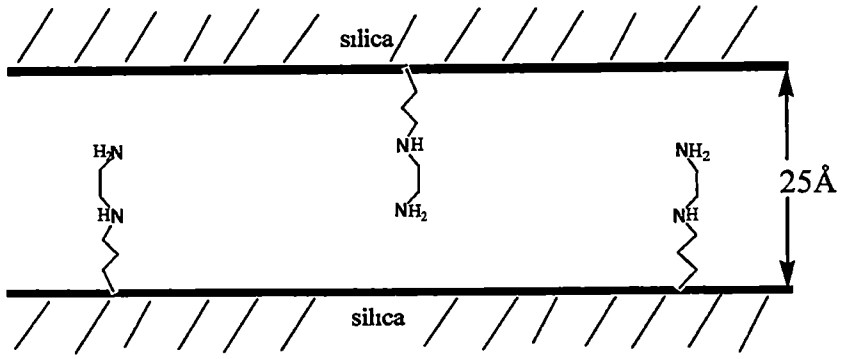
4-III.1 MCM-41 Characterization

N_2 adsorption analysis was performed on the mesoporous support following the calcination step. A B.E.T.(39) surface area of 1030 m^2/g , a total pore volume of 1.0 cc/g, and a narrow B.J.H.(40) pore size distribution with a peak at 28 Å were calculated from the isotherm. Small angle X-ray scattering data shows a peak at 2θ = 2 deg, characteristic of hexagonally packed mesoporous materials. The d-spacing value is 35 Å. Subtracting the average pore diameter from the B.J.H. data from the d-spacing gives an approximate wall thickness of 10 Å.

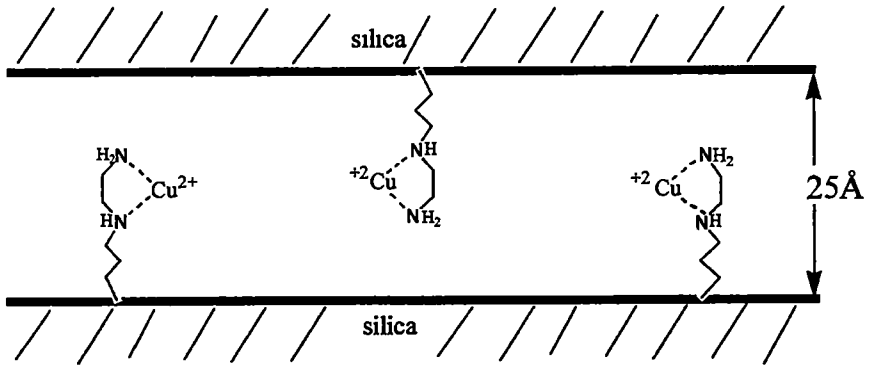
4-III.2 Stepwise Methodology.

The stepwise assembly approach involves three principal steps (**Figure 4.2**). In the primary step, the mesoporous support is coated with the bifunctional ligand by refluxing in toluene. During this step, the ligand concentration and reflux time are used to control the ligand coverage. Secondly, the sorbent is placed in an aqueous solution of the metal salt and allowed to absorb the metal ion template. The relatively high Cu(II) concentration and 100 mL volume of the metal salt solution ensures that there are enough copper ions to form a 1:1 complex with all of the ligands in the sample. In the final step, the sorbent is again coated with the bifunctional ligand, which first forms a 1:2 metal:ligand complex and then grafts to a nearby silanol group on the silica surface. The Cu(II) ions act as a catalyst for this step due to the high affinity it has for the ethylenediamine functional group on the ligand molecules. The

(a). Reflux calcined MCM-41 in toluene/TMSen



(b). Place sorbent in aqueous Cu(II) solution



(c). Reflux in toluene/TMSen

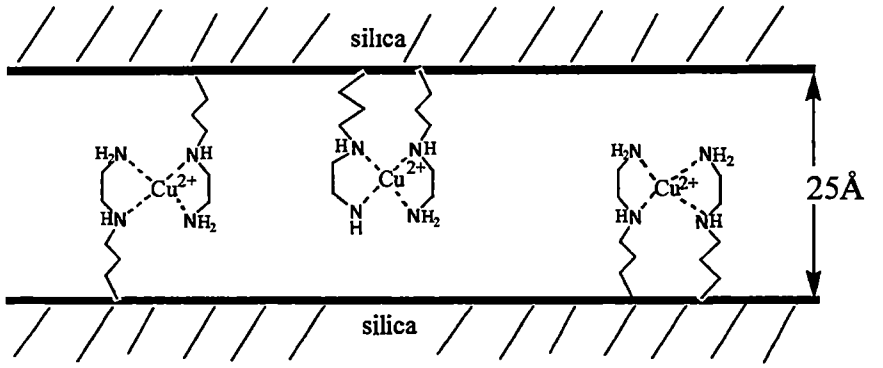


Figure 4.2 Mechanism of stepwise assembly

solubility characteristics of toluene make it an appropriate solvent since the ligand molecules are quite soluble in toluene while copper and the copper:ligand complexes involved here are not. The condensation reaction between the ligand and the surface silanol groups produces methanol. The high solubility of methanol in toluene may help to drive this reaction which is required to graft the ligand to the silica support. A non-imprinted control sample is synthesized by excluding the second step in this process. Therefore, it is important not to attain too high a coverage during the primary step, so that silanol sites remain for the final step and ligand coverages for the copper-imprinted and non-imprinted materials are similar. With a similar number of surface grafted ligands, the metal ion sorption behavior of these two materials can be compared to give the effect of imprinting.

4-III.3 Copper(II) Adsorption

The copper(II) imprinted sol-gel showed an enhanced capacity relative to the nonimprinted gel for the absorption of copper(II) ions from aqueous solutions. **Table 4.1** summarizes the copper(II) uptake of the sorbents from solutions ranging from 6.35-63.55 ppm Cu(II). A direct comparison shows the higher affinity of the imprinted gel for the Cu(II) ion at concentrations up to 31.77 ppm. The non-imprinted sample absorbed more copper at the higher concentrations studied. A simple depiction of the probable arrangement of ligands in the mesoporous channels of these sorbents is shown in **Figure 4.3**. On the nonimprinted sorbent the ligands are homogeneously distributed throughout the channels. Due to the grafting locations of

Table 4.1 Cu(II) Uptake of Cu(II) Imprinted and Nonimprinted Sorbents

Sorbent	C_0 Cu^{2+} (ppm)	C_f Cu^{2+} (ppb)	Cu^{2+} K_d (ml/g)
Nonimprinted	6.35	166	3,730
Cu(II) imprinted	**6.35**	**6**	**109,000**
Nonimprinted	15.89	280	5,580
Cu(II) imprinted	**15.89**	**14**	**115,000**
Nonimprinted	31.77	585	5,340
Cu(II) imprinted	**31.77**	**127**	**25,000**
Nonimprinted	47.66	505	9,340
Cu(II) imprinted	**47.66**	**4220**	**1,030**
Nonimprinted	63.55	769	8,170
Cu(II) imprinted	**63.55**	**7000**	**808**

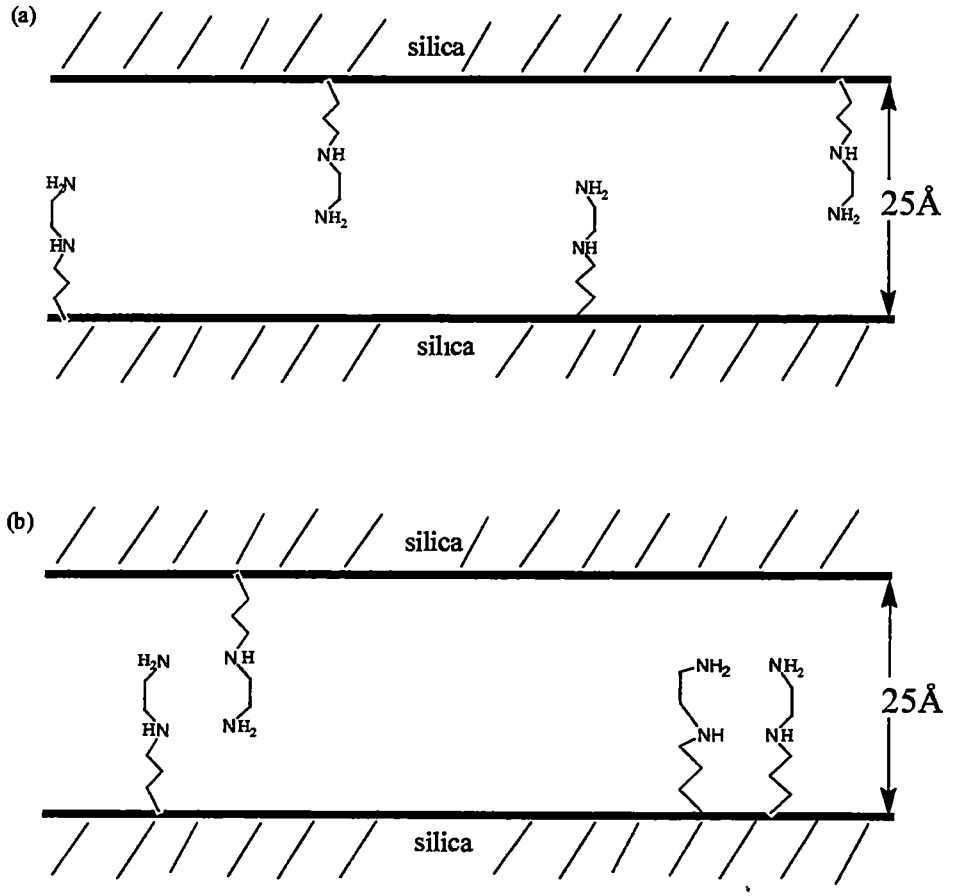


Figure 4.3 Structures of imprinted and nonimprinted TMSen sorbents

the ligands, the formation of a 1:2 metal to ligand complex is unlikely. In contrast to this, the ligands on the copper-imprinted sorbent are "paired up," making a 1:2 metal to ligand complex the most likely configuration upon metal ion sorption. The relatively large stability constant associated with the addition of a second diamine moiety to metal ions (70) gives the imprinted material a much higher affinity for Cu(II) ions. This can explain the enhancement of Cu(II) capacity by the imprinted material at the lower concentrations. A consequence of this arrangement of ligands is that although the non-imprinted sites may not have the great affinity for the metal ion that the imprinted sites have, there are approximately twice as many of them. This explains the larger distribution coefficients for the non-imprinted materials for Cu(II) at the higher solution concentrations.

4-III.4 Metal Ion Selectivity

Competitive ion binding studies were conducted with Cu(II) and Zn(II) ions in order to measure the selectivity of the imprinted material. Zinc(II) was chosen as the competitor species since it has the same charge, nearly identical size, and also binds well with the diamine ligand. Zinc(II) is also usually present in industrial effluents containing copper, such as electroplating waste, landfill leachate, and acid mine drainage (53). The results of competitive ion binding batch tests at pH 5.0 are summarized in **Table 4.2**. The copper(II) imprinted sorbents absorbed more Cu(II) and less Zn(II) than the nonimprinted material at all concentrations studied. The separation factors (k) of ~ 150-400 and the selectivity coefficients (k') of ~ 850-2,500

Table 4.2 Sorbent Metal Ion Selectivity (Cu^{2+} Vs. Zn^{2+}).

Sorbent	C_0 Cu^{2+} (ppm)	C_f Cu^{2+} (ppb)	Cu^{2+} K_d (ml/g)	C_0 Zn^{2+} (ppm)	C_f Zn^{2+} (ppb)	Zn^{2+} K_d (ml/g)	k	k'
Nonimprinted	6.35	125	4,980	6.54	16	42,200	0.118	
Cu(II) imprinted	**6.35**	**15**	**42,100**	**6.54**	**1770**	**269**	**156**	1,330
Nonimprinted	15.89	210	7,470	16.35	101	16,000	0.466	
Cu(II) imprinted	**15.89**	**32**	**49,100**	**16.35**	**7300**	**124**	**396**	850
Nonimprinted	63.55	269	2,260	65.39	229	28,500	0.079	
Cu(II) imprinted	**63.55**	**10**	**67,100**	**65.39**	**15,100**	**334**	**201**	2,540

for our copper(II) imprinted materials synthesized via stepwise assembly show a considerable improvement over the values of k (0.5-220) and k'(1.7-40) achieved previously with imprint coated sorbents under similar experimental conditions (Chapter 2, Section III).

4-III.5 Solid-state ^{29}Si NMR Analyses of Sorbents

Solid-state ^{29}Si single pulse excitation magic angle spinning (SPE/MAS) NMR spectra of the copper(II) imprinted and nonimprinted sorbents prepared via stepwise functionalization are shown in **Figures 4.4 and 4.5**, respectively. Integration of the ligand peaks located ~ -50 to -80 ppm indicate that the nonimprinted sorbent has a ligand loading approximately 14% higher than that of the copper(II) imprinted sorbent. This is a much smaller percentage difference than those found for imprint coated sorbents characterized in Chapter 3. Perhaps the most significant difference between the SSNMR spectra of the imprint coated sorbents and the stepwise sorbents is the total ligand loading. For both stepwise sorbents over 20% of the silicon atoms are in the ligands. This is more than twice the ligand loading of the imprint coated materials. The spectrum of the nonimprinted material synthesized by stepwise functionalization (Figure 4.5) is nearly identical to that reported by Liu and co-workers (46) for "76% coverage" of trimethoxymercaptopropylsilane coated on MCM-41. To our knowledge, this is the highest loading of organofunctional ligands on mesoporous silica ever reported.

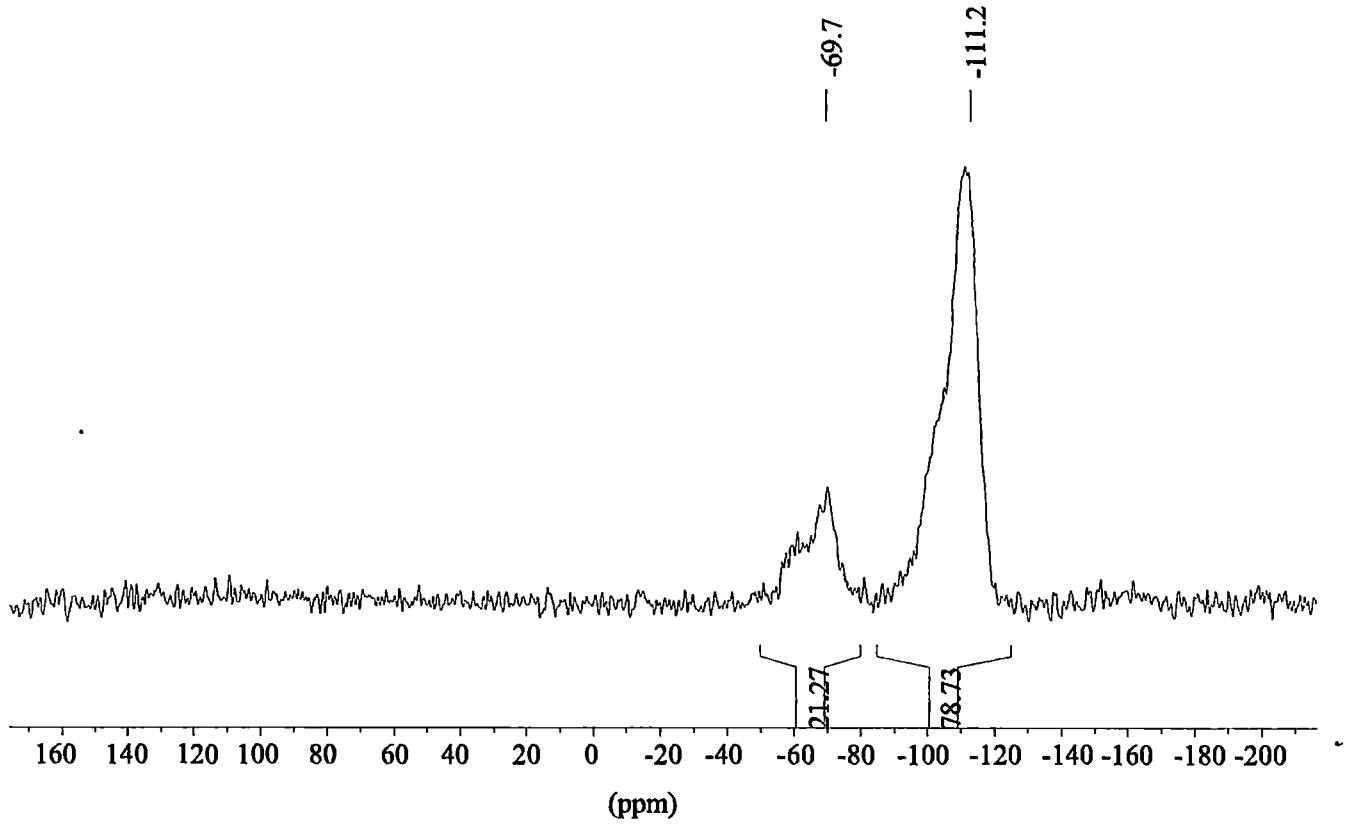


Figure 4.4 Solid-state ^{29}Si SPE/MAS NMR spectrum of copper(II) imprinted stepwise sorbent

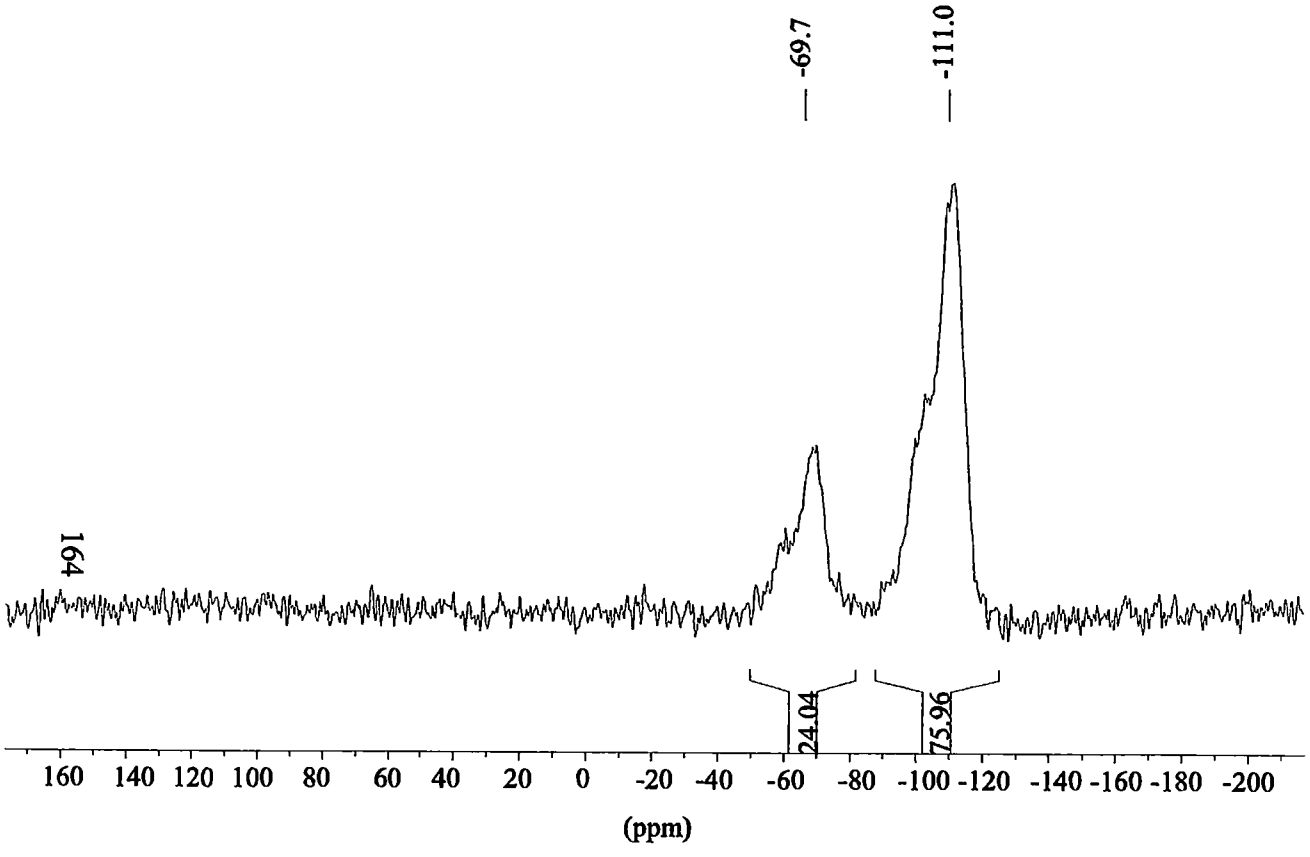


Figure 4.5 Solid-state ^{29}Si SPE/MAS NMR spectrum of nonimprinted stepwise sorbent

4-IV. Conclusions

A new stepwise surface functionalization methodology has been developed to synthesize mesoporous sol-gel sorbents containing the ethylenediamine functionality. The N-[3-(trimethoxysilyl)-propyl]ethylenediamine (TMSen) ligand is first coated on MCM-41, followed by sorption of Cu(II). A second exposure to TMSen may result in the formation of a 2:1 TMSen:Cu(II) complex on the surface of the mesopores. Acid washing protonates the amino groups which release the copper(II) ions. This results in the formation of binding sites that are uniquely designed with the coordination environment Cu(II) prefers. The mesoporous MCM-41 used for coating was synthesized under basic conditions using cetyltrimethylammonium bromide (CTAB) as the structure directing agent. Mesopores are formed by the calcination of the surfactant micelles giving this material relatively large surface areas and good mass transfer. A copper(II) imprinted sorbent has shown significant enhancement of copper(II) uptake capacities at various concentrations relative to a nonimprinted material made without the metal ion template. The imprinted material also exhibits improved selectivity for removal of copper(II) ions from Cu(II)/Zn(II) aqueous solutions. This material has copper(II) distribution coefficients (K_d) > 100,000 at concentrations less than 20 ppm. Separation factors, k > 100 w.r.t. copper(II), were achieved with an aqueous Cu(II)/Zn(II) system at pH 5.0.

Solid-state ^{29}Si NMR results indicate that, like the imprint coated sorbents characterized in Chapter 3, the nonimprinted stepwise sorbents have a higher ligand loading than the corresponding copper(II) imprinted sorbents. It is important to note

that the difference in ligand loading is much smaller in the case of the stepwise materials. We attribute the better ionic recognition characteristics of the sorbents prepared by stepwise functionalization to this smaller difference.

CHAPTER 5

DOUBLE IMPRINTING OF AN ORGANOFUNCTIONALIZED SOL-GEL FOR SELECTIVE METAL ION SEPARATIONS

5-I. Introduction

The methodologies discussed in Chapters 3 and 4 created organofunctionalized sol-gel materials by the immobilization of bifunctional reagents on silica. Condensation reactions between the silanol groups on the silica surface and alkoxy groups of the bifunctional reagent resulted in the covalent grafting of the ligand. The value of these materials as selective metal ion sorbents was demonstrated via adsorption studies. Another route to organofunctionalized sol-gel materials is the incorporation of the bifunctional reagent into a siloxane polymer by co-condensation with TEOS.

Parish and co-workers (74-7) incorporated a number of amine and phosphine ligands into a polysiloxane network by co-condensation with TEOS. The amine-functionalized materials prepared by this method were compared with those prepared by surface functionalization via copper(II) and proton uptake experiments. The sorbents prepared by direct incorporation contained more ligand groups. Both EPR and visible spectra indicated that 1:1 and 1:2 metal to ligand complexes were formed with Co(II), Ni(II), and Cu(II) in aqueous solutions. Unfortunately, these sorbents exhibit poor uptake kinetics (>24 h equilibration time) and low metal ion capacities. This is primarily the result of the lack of porosity in these materials.

As described in Chapter 2, surfactants can be used in conjunction with sol-gel techniques to engineer the porosity of silica. The porosity of a siloxane polymer synthesized by co-condensation of a bifunctional reagent with TEOS can also be created with surfactants. The use of a micellar solution of surfactants in the original reaction mixture with a bifunctional reagent and TEOS can lead to incorporation of the micelles into organofunctionalized sol-gel materials. Water serves as both a medium for micelle formation and as a hydrolyzing agent. The extraction of the surfactant molecules with an appropriate solvent leads to the formation of many pores throughout the sorbent.

Macquarrie (78) reported porous organofunctionalized sol-gels prepared in this way. Dodecylamine, TMSA, and TEOS were used as the surfactant, bifunctional reagent, and sol-gel precursor, respectively. Specific surface areas >500 m^2/g were achieved. Mann and co-workers (79-80) have synthesized organofunctionalized materials with a variety of bifunctional reagents and CTAB surfactant. Characterization via N_2 adsorption, TEM, and XRD indicate that these materials contain ordered arrays of mesopores, with large surface areas and pore volumes.

The work of Parish and co-workers was hindered by the lack of porosity in their sorbent materials. Although neither Mann nor Macquarrie used their materials as sorbents, their findings clearly indicate that surfactants can be used to engineer the porosity of organofunctionalized sol-gel materials. This porosity could lead to better accessibility to the internal functional sites of a sorbent prepared in this way. This

may improve sorbent properties such as metal ion uptake kinetics and metal ion capacities.

Herein, we describe the preparation of metal ion sorbents synthesized by the co-condensation of the bifunctional reagent BTMSen with TEOS, in a micellar solution of dodecylamine surfactant. Molecular imprinting techniques are used to create specific binding sites for Cu(II) and Zn(II) species. Metal ion-BTMSen complex formation prior to condensation arranges the en moeities in the conformation prefered by the given metal ion. We refer to this methodology as double imprinting since both the metal ions and surfactant micelles act as templates in this system. Acid leaching of the metal ions and solvent extraction of the surfactant micelles results in the formation of different sized imprints, each with a specific function. On the microporous level, the removal of the metal ions gives tailored binding sites ideal for rebinding the metal ion template. These pores give the sorbent enhanced selectivity for the target ion. On the mesoporous level, the removal of the surfactant micelles results in the formation of relatively large pores which give the sorbent an overall porosity which includes large surface areas and excellent metal ion transfer kinetics.

5-II. Synthesis

Dodecylamine was selected as the surfactant since it is neutral and its use as a template for the formation of mesoporous materials are well documented (35-7). The hydrogen bonding between the head groups of dodecylamine and the silicate is a weaker interaction than the coulombic interactions between a charged surfactant and

the silicate. This may lead to a relatively facile solvent extraction step. BTMSen has been used to synthesize selective metal ion sorbents via imprint coating of porous silica (Chapter 3, Section IV). Cu(II) and Zn(II) have been employed as the metal ion templates because their identical charges, similar sizes and strong dative bonding with ethylenediamine make them a stringent test for sorbent selectivity studies.

In a typical preparation of the copper(II) imprinted sorbent, dodecylamine (0.803 g) was added to a beaker containing deionized water (8.67 mL) and absolute ethanol (6.67 mL). The mixture was stirred for 5 min until all of the surfactant was dissolved. In a separate beaker $Cu(NO_3)$ $3H_2O$ (0.338 g) is added to 3.33 mL of absolute ethanol. This mixture was stirred for 5 min until all the metal salt had completely dissolved. BTMSen (2.04 mL, 48% in methanol) is slowly added. A navy blue complex forms. TEOS (3.57 mL) is then added upon stirring. The dodecylamine solution was then added to the TEOS/metal complex mixture, which was covered and stirred until gelation (~ 10 min) and cured at ambient temperature for 12 h (**Figure 5.1**). The molar ratios of the reaction mixture were as follows:

480 H_2O : 170 EtOH : 16 TEOS : 4.3 DDA : 2.8 BTMSen : 1.4 $Cu(NO_3)_2$ $3H_2O$

The gel was then placed under vacuum at 80 °C for an additional 12 h. A nonimprinted sample was made with the identical procedure with the exception that no metal salt was added. A zinc(II) imprinted sorbent was synthesized with $Zn(NO_3)_2$

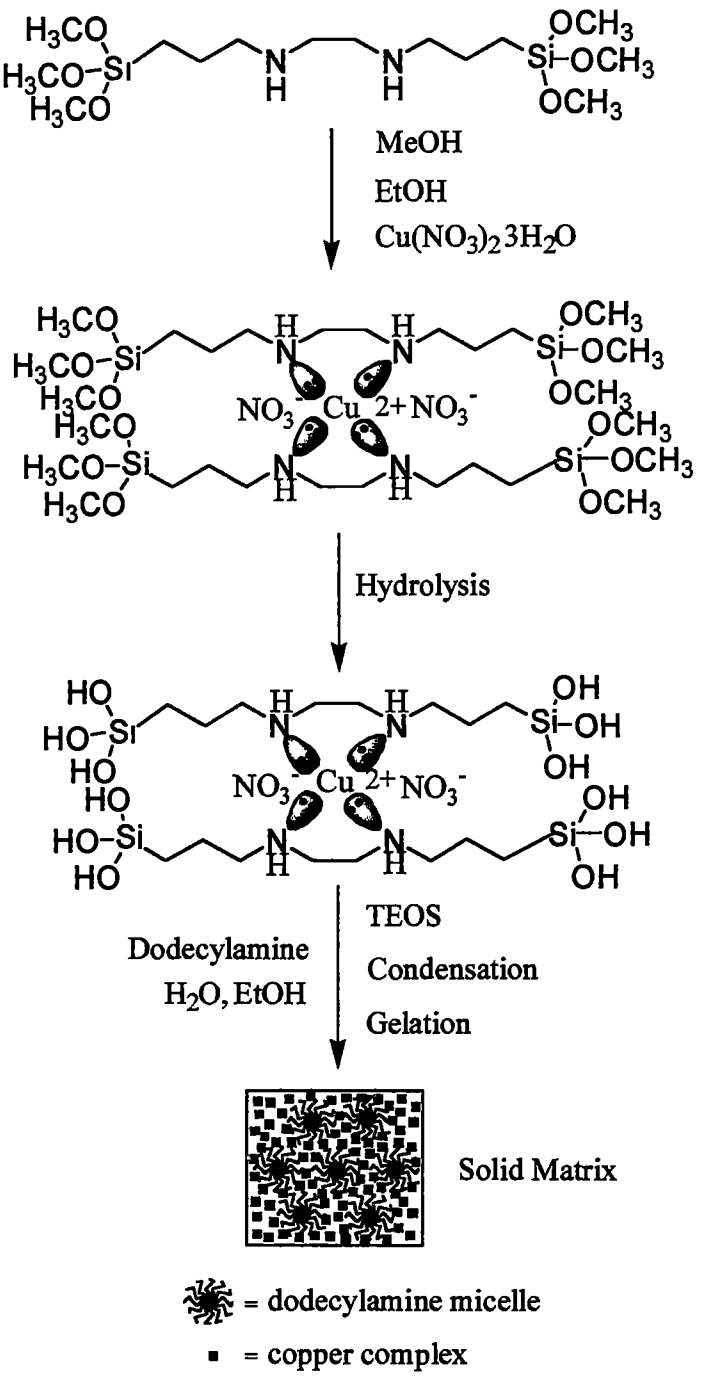


Figure 5.1 Preparation of copper(II) imprinted sorbent via double imprinting

$6H_2O$, but less metal salt was used, yielding the 1:3 metal to ligand complex, $[Zn(BTMSen)_3]^{2+}$. All sorbents were synthesized using the same amount of BTMSen.

Following the vacuum drying, samples were placed in excess 1 M HNO_3 and stirred for 1 h. This resulted in protonation of the ligand amino groups and leaching of the metal ions from the gel. Although it contained no metal salt, the nonimprinted material was treated in an identical manner to insure the accuracy of the experimental results. Samples were then recovered by vacuum filtration and refluxed in excess EtOH/HCl solution (1 M w.r.t. HNO_3) for 12 h in order to extract all the surfactant (**Figure 5.2**). The gels were then recovered and washed with plenty of EtOH. The resulting powders were placed in deionized water and titrated with 1 N NaOH to pH of 7.5. The neutralized sorbents were then placed under vacuum at 80 °C for 3 h.

The metal ion uptake of the sorbents was determined by batch testing. All metal ion solutions were buffered to a specific pH with sodium acetate/acetic acid (0.05 M). In a typical run, 0.1 g of the sorbent and 10 mL of the metal ion solution were placed in a capped plastic vial and sonicated for 1 h. The resulting mixture was filtered and the filtrate was analyzed via ICP/OE spectroscopy in order to measure the metal ion concentration. The overall capacity of the sorbent for a given metal ion was then calculated by the change in concentration between the filtrate and the original metal ion solution.

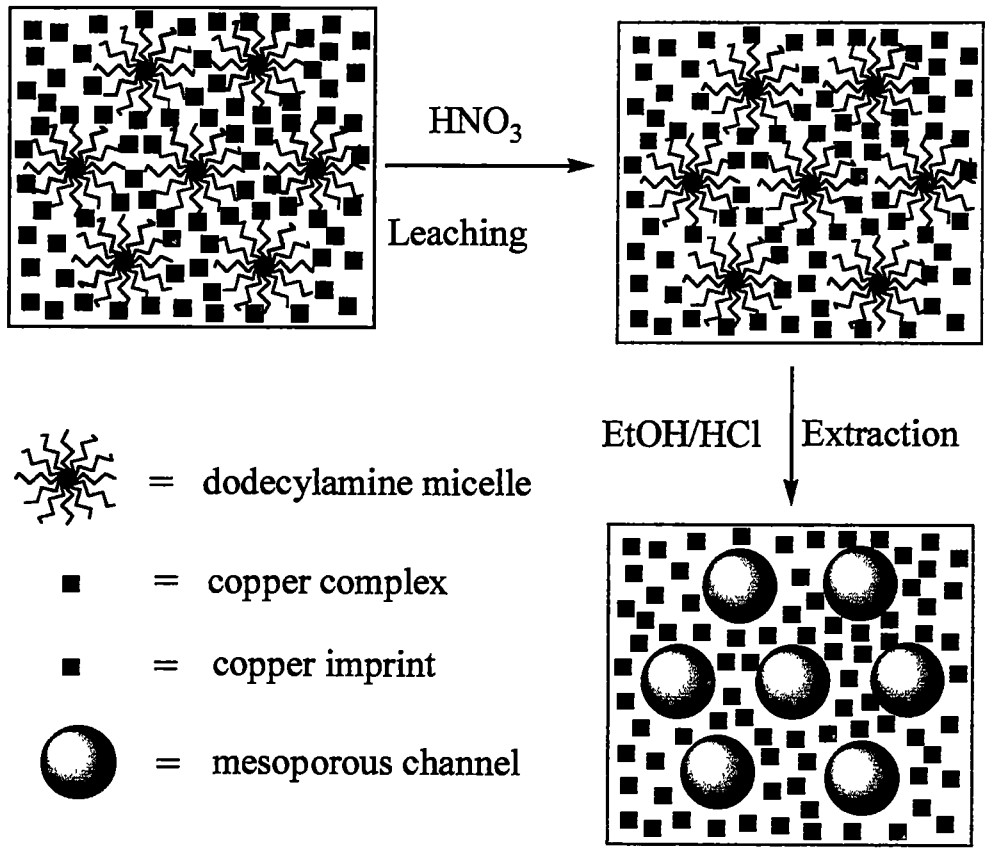


Figure 5.2 Post-synthetic processing of sorbents created via double imprinting

5-III. Copper(II) Adsorption

The results of batch tests conducted with the copper(II) imprinted and nonimprinted sorbents are shown in **Table 5.1**. Five different Cu(II) concentrations ranging from 10^{-4}-10^{-3} M (6.35-63.55 ppm) were used. The copper(II) imprinted sorbents removed more Cu(II) than the nonimprinted sorbents at all concentrations studied. The remaining copper(II) concentration left by the Cu(II) imprinted sorbent is always less than half that left by the nonimprinted sorbent.

5-IV. Copper(II) Uptake Kinetics

The copper(II) adsorption study showed that 0.1 g of the Cu(II) imprinted sorbent removed 99.17% of the Cu(II) from 10 mL of a 1 x 10^{-4} M solution (Table 5.1). Since all the batch tests involved a one hour contact time, a series of tests were run with shorter contact times in order to deduce how fast the adsorption process occurs. The results (**Figure 5.3**) show that approximately 84% of the copper(II) was absorbed in the first five minutes and that over 95% absorption occurred within 15 minutes.

5-V. Copper(II) vs. Zinc(II) Selectivity

Competitive metal ion binding studies were conducted with mixed solutions of Cu(II) and Zn(II) at pH = 5.0. The results of the batch experiments are listed in **Table 5.2**. When equilibrated with solutions containing the same concentration of both ions, the amount of copper(II) absorbed by the Cu(II) imprinted sorbent increased over the

Table 5.1 Copper(II) Adsorption of Cu(II) Imprinted and Nonimprinted Sorbents Prepared via Double Imprinting

Sorbent	Copper(II) C_0 (ppm)	Copper(II) C_f (ppm)	% Cu(II) Absorbed	Copper(II) Kd
Nonimprinted	6 35	0.180	97.92	4700
Cu(II) imprinted	**6.35**	**0.053**	**99.17**	**12000**
Nonimprinted	15 89	1.473	90.73	980
Cu(II) imprinted	**15.89**	**0.305**	**98.08**	**5110**
Nonimprinted	31.78	5 22	83.57	510
Cu(II) imprinted	**31.78**	**1.70**	**94.65**	**1770**
Nonimprinted	47.66	7 84	83.54	500
Cu(II) imprinted	**47.66**	**3.33**	**93.01**	**1330**
Nonimprinted	63.55	15 25	75.99	320
Cu(II) imprinted	**63.55**	**7.51**	**88.18**	**750**

Table 5.2 Competitive loading of Cu(II) and Zn(II) by Sorbents Prepared via Double Imprinting

Sorbent	Conc.(M)		% Abs.		K_d		k	k'
	Cu(II)	Zn(II)	Cu(II)	Zn(II)	Cu(II)	Zn(II)		
Nonimprinted	0005	.0005	93.51	28 48	1,430	40	36	-
Cu(II) imprinted	**.0005**	**.0005**	**97.42**	**30.04**	**3,780**	**40**	**88**	**2.4**
Nonimprinted	001	001	85 27	16 43	580	20	30	-
Cu(II) imprinted	**.001**	**.001**	**90.12**	**17.70**	**910**	**20**	**42**	**1.4**
Nonimprinted	.001	01	82 22	6 11	460	7	71	-
Cu(II) imprinted	**.001**	**.01**	**86.59**	**5.62**	**640**	**6**	**110**	**1.5**

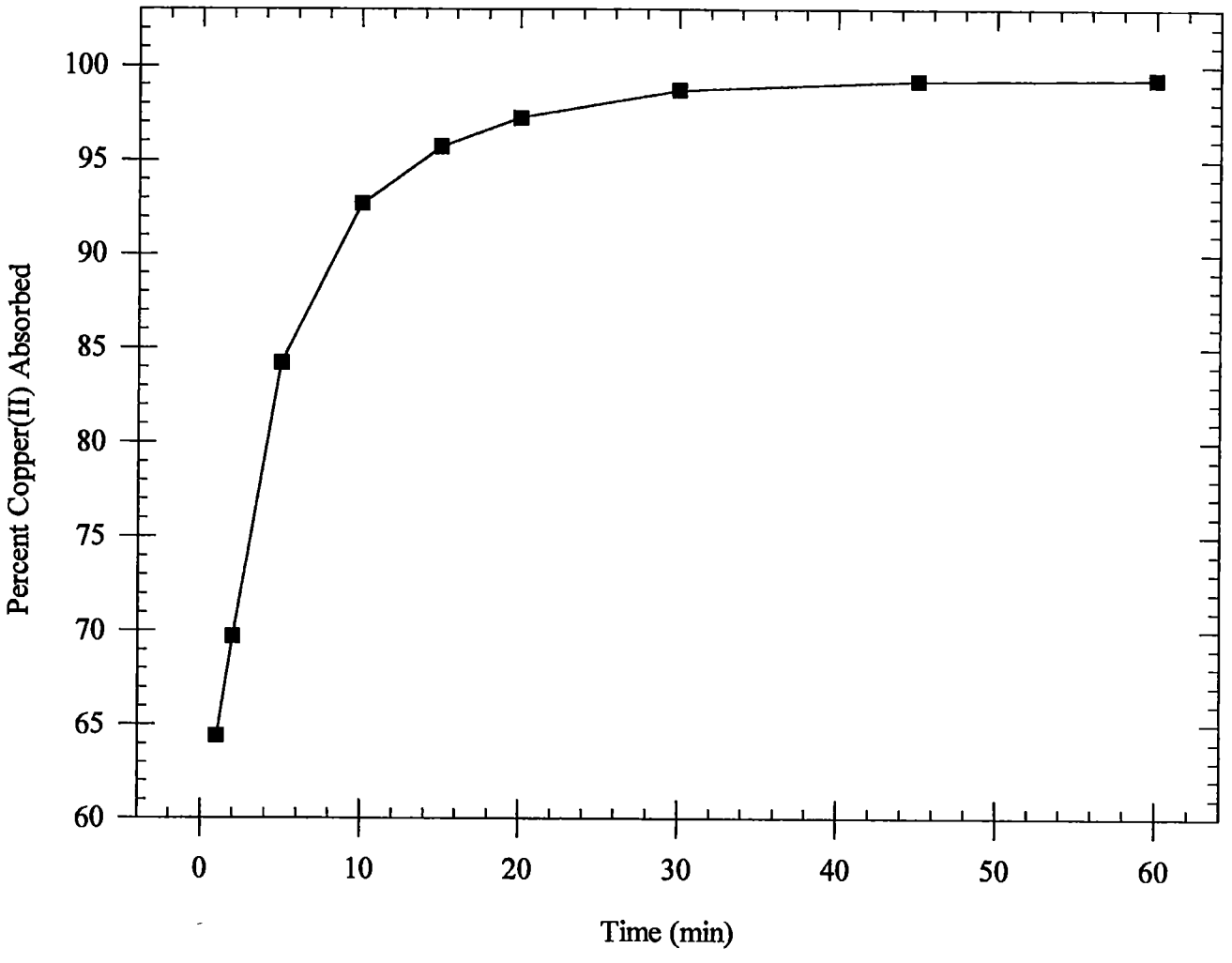


Figure 5.3 Copper(II) uptake kinetics of Cu(II) imprinted sorbent prepared via double imprinting.

nonimprinted sorbent more than the amount of zinc(II) absorbed. This results in a substantial increase in the copper(II) distribution coefficient for the imprinted material, while the K_d's for zinc(II) stay nearly the same. The values of k show that the copper(II) imprinted sample was more selective for the Cu(II) ion than the nonimprinted sample. It should be noted that when placed in a solution that contains a large excess of zinc ions [0.001M Cu(II)/0.01M Zn(II)], the copper(II) imprinted material absorbed less zinc(II) than the nonimprinted sorbent. In this case the total number of ions in solution exceeds the number of binding sites so the increased affinity for copper(II) is more pronounced, resulting in a lower K_d for zinc(II).

5-VI. Copper(II) vs. Zinc(II) Selectivity as a Function of pH

The pH dependence for sorption of Cu(II) and Zn(II) was investigated over the pH range 3.0-5.5 (**figure 5.4**). The concentrations of all solutions were 5×10^{-3}M w.r.t. both copper(II) and zinc(II). The metal ion absorption was enhanced for both metals by increasing the pH. Both the copper(II) imprinted and nonimprinted gels absorbed more Cu(II) than Zn(II) over the entire pH range. At pH values less than 5.0 no detectable amount of zinc(II) ions were absorbed.

5-VII. N_2 Adsorption

Following the post-synthetic processing, a N_2 adsorption analysis was performed on each sample. The adsorption isotherms of the copper(II) imprinted and nonimprinted sorbents (**Figure 5.5**) are very similar. The surface areas, as calculated

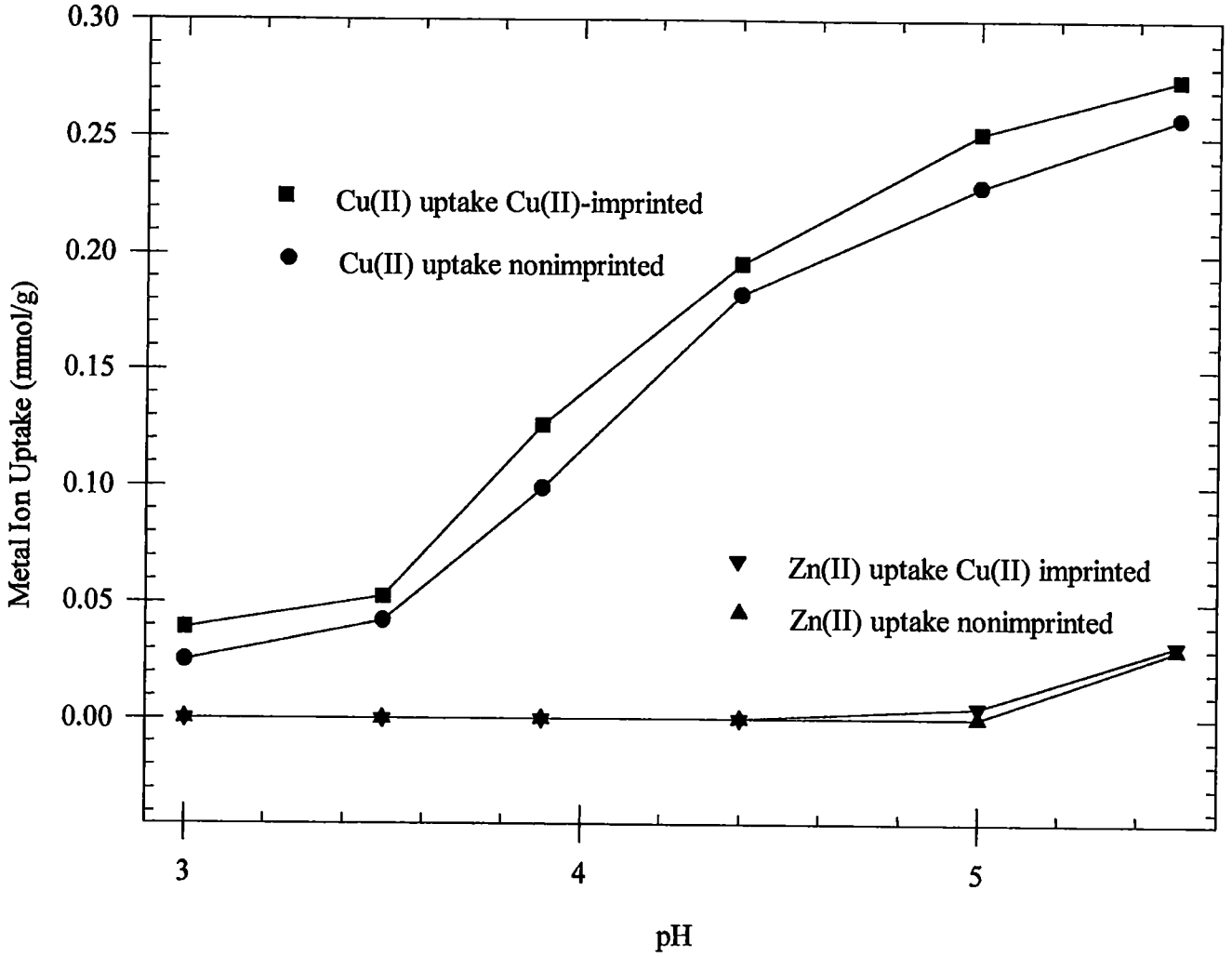


Figure 5.4 Copper(II) vs. Zinc(II) selectivity of sorbents prepared by double imprinting.

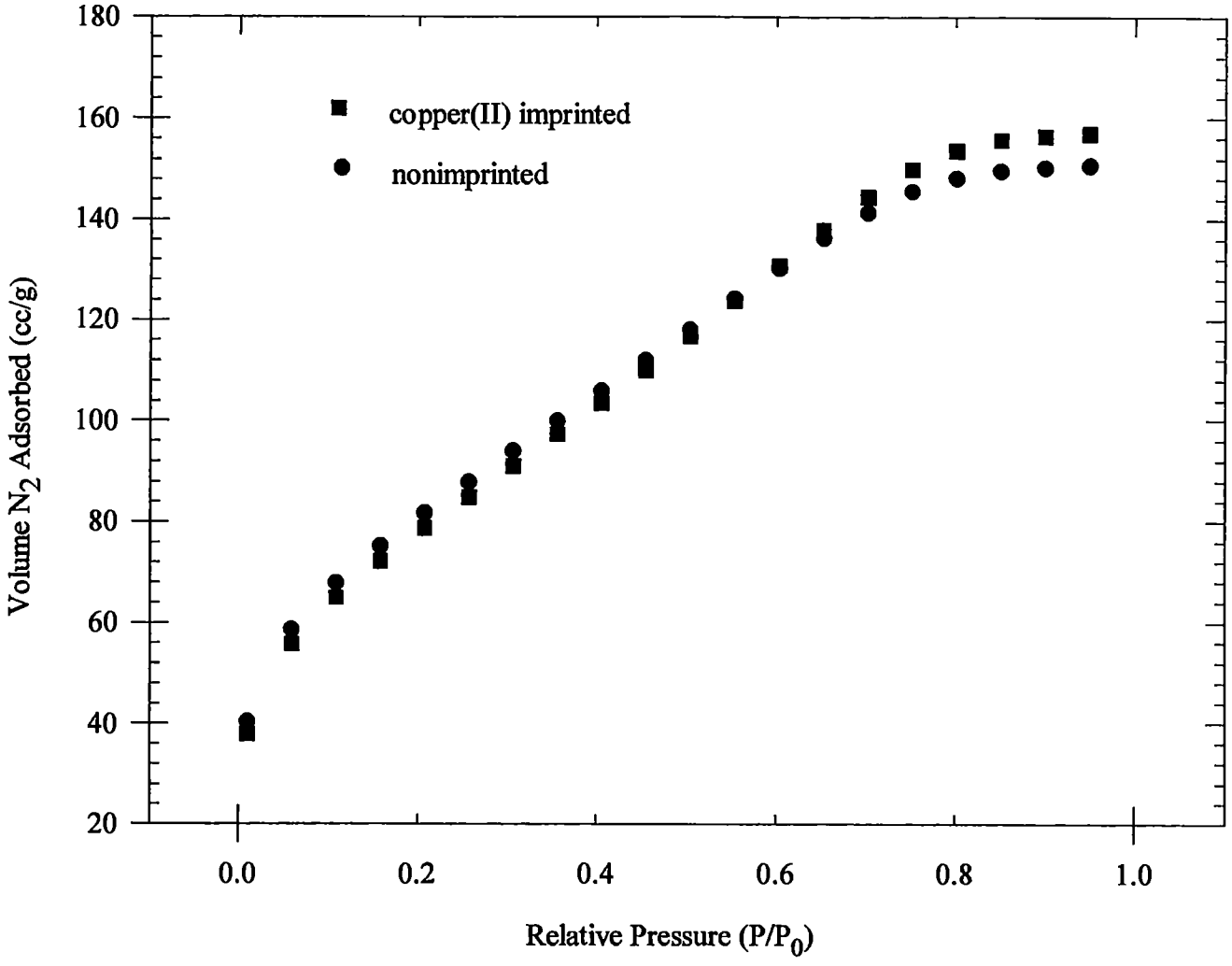


Figure 5.5 N_2 adsorption isotherms of Cu(II) imprinted and nonimprinted sorbents.

from the isotherms were 286 and 294 m^2/g for the copper(II) imprinted and nonimprinted sorbents, respectively. The nearly identical overall surface areas indicate that the increased affinity of the copper(II) imprinted sample for the Cu(II) ion is not due to a larger available surface area. The average pore diameter is slightly larger for the copper(II) imprinted gel, but both show a rather broad distribution in the mesoporous range. A summary of the nitrogen adsorption data is shown in **Table 5.3.**

5-VIII. Ligand Loading Capacity

Based on the mass of the solid as synthesized copper imprinted material (2.43 g) and the original amount of BTMSen added (2.8 mmol), the total ligand in the material is 1.03 mmol/g. This makes the assumption that 100% of the ligand polymerized and that none was lost during the post-synthetic treatments. The total copper(II) loading in the material was 0.52 mmol/g. In a batch test with relatively concentrated Cu(II) solution (0.02 M), the sorbents are effectively "flooded." All of the available sites are filled with Cu(II) ions. This can give a rough estimate of the total number of sites and therefore the ligand content. In this batch test the Cu(II) capacity of the copper(II) imprinted gel was 0.49 mmol/g, while the nonimprinted was 0.46 mmol/g. Assuming that a 2:1 ligand to metal complex is formed, this corresponds to 0.98 and 0.92 mmol BTMSen per gram of gel, or 95% and 89% of the total ligand initially added that became incorporated into the material.

5-IX. Zinc(II) Imprinted Sorbent

The synthesis of the zinc(II) imprinted sorbent was similar to that of the copper imprinted sample, with the exception of the complex stoichiometery. While the copper(II) imprinted material utilized a 2:1 ligand to metal complex, the zinc(II) imprinted gel was synthesized using a 3:1 BTMSen to metal complex, giving zinc the octahedral coordination environment that it prefers(92). **Table 5.4** summarizes the results of competitive ion binding tests between Cu(II) and Zn(II) at a concentration of 10^{-4} M with the three different sorbents used in the study. The zinc(II) imprinted sample demonstrates a dramatic enhancement in zinc(II) uptake over the nonimprinted sample as demonstrated by an increase in K_d of nearly two orders of magnitude. Despite this, the thermodynamic advantage of copper(II) over zinc(II) w.r.t. ethylenediamine complexation (70) cannot be overcome via metal ion imprinting, as the zinc(II) imprinted sample was unable to preferentially bind Zn(II) over Cu(II).

5-X. Conclusions

A double imprinting methodology has been used to synthesize organofunctionalized mesoporous sol-gel sorbents which exhibit enhanced ionic recognition. Metal ions and supramolecular assemblies of sufactant molecules are both used as templates in this system. Removal of the templates creates two types of pores, each with a specific function. Acid washing removes the metal ions and creates micropores which contain binding sites with the size, shape, and coordination environment that the metal ion prefers. Extraction of surfactant micelles results in the

Table 5.3 Porosity Data for Cu(II) Imprinted and Nonimprinted Sorbents Prepared via Double Imprinting.

Sorbent	Surface Area (m^2/g)	Total Pore Volume (cc/g)	Pore Size (Å)
nonimprinted	294	0.23	40
Copper(II) imprinted	**286**	**0.24**	**45**

Table 5.4 Cu(II) vs. Zn(II) Selectivity of Nonimprinted, Cu(II) Imprinted, and Zn(II) Imprinted Sorbents

Sorbent	Conc. (M)		% Absorbed		K_d	
	Cu(II)	Zn(II)	Cu(II)	Zn(II)	Cu(II)	Zn(II)
Nonimprinted	1×10^{-4}	1×10^{-4}	97.21	36.38	3,500	60
Cu(II) imprinted	1×10^{-4}	1×10^{-4}	98.07	54.13	5,100	120
Zn(II) imprinted	1×10^{-4}	1×10^{-4}	99.03	98.11	9,500	5,100

formation of mesoporous channels throughout the sorbent matrix, giving the material good metal ion transfer kinetics.

CHAPTER 6

MOLECULAR IMPRINTING OF AN ORGANIC-INORGANIC HYBRID POLYMER FOR THE ENHANCED RECOGNITION OF METAL IONS

6-I. Introduction

Organic-inorganic hybrid polymers can be synthesized by hydrolytic sol-gel reactions of organic poly(alkoxysilyl) monomers (81-3). These materials are distinguished from organically functionalized inorganic polymers since the organic moeity is part of the crosslinked network and not simply a side chain. The organic portion of the sol-gel precursors must be covalently bonded via carbon-silicon bonds to at least two alkoxysilyl groups. These materials have been synthesized with monomers containing a wide variety of organic functional groups (84-8). The use of a single precursor allows the organic-inorganic ratio to be fixed. Polymers which exhibit specific properties can be designed by selecting monomers containing the appropriate organic group. What makes this family of materials particularly exciting, is the ability to engineer polymeric materials which exhibit the right combination of organic and inorganic properties for a particular application.

Although it has been used primarily to synthesize metal oxides, the surfactant template approach is a very attractive route to engineer the porosity of a wide variety of new and novel materials. Recently, three groups have combined the principles of hydrolytic sol-gel formation of organic-inorganic polymers with the surfactant template method to synthesize ordered, mesoporous organic-inorganic polymers.

Inagaki et al. (89) used 1,2-bis(trimethoxysilyl)ethane as the sol-gel precursor and octadecyltrimethylammonium chloride as the surfactant to synthesize ordered, mesoporous hybrids under basic conditions. Stein and co-workers (90) reported the synthesis of similar ordered materials by using both 1,2-bis(triethoxysilyl)ethane and 1,2-bis(triethoxysilyl)ethylene and CTAB surfactant. The ethyl-bridged material exhibited better hydrothermal stability than a pure silica MCM-41 sample. Ozin and co-workers (91), compared the properties of mesoporous organic-inorganic polymers which were synthesized using various ratios of 1,2-bis(triethoxysilyl)ethylene and tetraethylorthosilicate, with CTAB surfactant.

Herein, we describe a new approach for the synthesis of selective metal ion sorbents. This methodology combines the principles of molecular imprinting, hydrolytic sol-gel formation, and the surfactant template approach. Copolymerization of the sol-gel precursor 1,2-bis(trimethoxysilyl)ethane (BTSE), with metal ion complexes of N-[3-(trimethoxysilyl)-propyl]ethylenediamine (TMSen) around supramolecular assemblies of cetyltrimethylammonium chloride (CTAC) gives the organic-inorganic polymer. Extraction of the surfactant micelles and metal ions results in a porous material with a high affinity for the metal ion template. Both the metal ions and the surfactant micelles act as templates in this system. Removal of the surfactant leaves a network of pores which give these sorbents large surface areas and excellent metal ion transfer kinetics. Removal of the metal ions results in the formation of tailored binding sites made up of ethylenediamine functionalities which

are ideally designed to rebind the specific metal ion. Selective sorbents have been synthesized for Cu(II), Ni(II), and Zn(II).

6-II. Experimental

6-II.1 Synthesis

The hybrid materials in this study were synthesized according to the following procedures.

6-II.1.1 Blank Hybrid

The appropriate amount of 25% w/w cetyltrimethylammonium chloride solution was added to deionized water. Sodium hydroxide was added upon stirring, followed by the addition of BTSE. The resulting reaction mixture had the following molar composition:

1.0 BTSE:0.12 CTAC: 1.0 NaOH:230 H_2O

The reaction mixture was stirred in a closed vessel at RT for 24 h and the solid precipitate was recovered via vacuum filtration.

6-II.1.2 Nonimprinted Hybrid

A protocol similar that of the blank hybrid was used, with the addition of the bifunctional ligand, TMSen, after the BTSE. The molar composition of the reaction mixture was:

1.0 BTSE:0.12 CTAC:0.15 TMSen:1.0 NaOH:230 H_2O

6-II.1.3 Copper Imprinted Hybrid

The appropriate amount of 25 wt % cetyltrimethylammonium chloride solution was added to deionized water. $Cu(NO_3)$ $3H_2O$ was then dissolved in the micellar solution. TMSen was then added while stirring, followed by the BTSE. NaOH was then added to the reaction mixture, which had the following molar composition:

1.0 BTSE:0.12 CTAC:0.15 TMSen:0.075 $Cu(NO_3)_2$ $3H_2O$:1.0 NaOH:230 H_2O

6-II.1.4 Nickel and Zinc Imprinted Hybrids

A similar procedure to that described above for the copper imprinted material was followed, except that the amount of metal salt used ($Ni(NO_3)_2$ $6H_2O$ or $Zn(NO_3)_2$ 6 H_2O) was decreased, so that the TMSen:metal ion molar ratio was 3:1. This resulted in the following reaction mixture molar ratios:

1.0 BTSE:0.12 CTAC:0.15 TMSen:0.05 $M(II)(NO_3)_2$ $3H_2O$:1.0 NaOH:230 H_2O

6-II.2 Post-synthetic Processing

After recovery via vacuum filtration, the solid precipitates were rinsed with deionized water and ethanol, and placed under vacuum at 80 °C for 4 h. At this point, the materials are dubbed "as-synthesized", and the appropriate amounts needed for characterization are removed. The remaining material is placed in excess 1.0 molar HNO_3, and stirred for 15 min. This material is recovered by vacuum filtration, rinsed with deionized water, and placed in a large excess (~150 mL/g) of EtOH/HCL (1.0 molar w.r.t. HCl). This mixture is stirred well under gentle heating (50 °C) for 8 h. The sorbent is again recovered by vacuum filtration, washed with plenty of EtOH, and dried under vacuum at 80 °C for 1 h.

6-II.3 Batch Procedures

All metal ion solutions were buffered to a specific pH with sodium acetate/acetic acid (0.05 M). In a typical run, 0.1 g of sorbent and 10 ml metal ion solution were placed in a capped P.E.T. vials and sonicated for 30 min. The resulting mixture was filtered and both the filtrate and the initial standard solutions were analyzed via ICP/OE spectroscopy in order to measure the initial and final metal ion concentrations. The overall capacity of the sorbent for a given metal ion was then calculated by the change in concentration between the filtrate and the initial metal ion solution.

6-II.4 Analytical Techniques

All metal ion concentration analyses were performed with a Thermo Jarrel Ash Iris inductively coupled plasma spectrometer. N_2 adsorption isotherms were measured on a Micromeritics Gemini 2375 surface area analyzer. UV/Visible spectra were measured with a Cary 14H scanning spectrophotometer converted by On-Line Instrument Systems (OLIS) for data acquisition via PC. X-ray scattering plots of the hybrid samples were measured on the 10 m small-angle X-ray scattering camera at the SAXS user facility of the Oak Ridge National Laboratory.

6-III. Results and Discussion

6-III.1 Synthesis

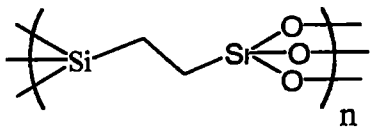
The BTSE monomer undergoes polymerization by base catalyzed hydrolysis and condensation reactions, as shown in equations (6.1) and (6.2):

(6.1) Base catalyzed Hydrolysis·

$$(EtO)_3SiCH_2CH_2Si(OEt)_3 \xrightarrow{H_2O/OH^-} (HO)_n(EtO)_{3-n}SiCH_2CH_2Si(OEt)_{3-n}(OH)_n$$

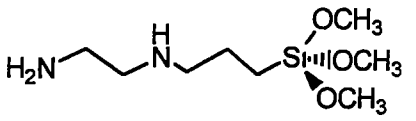
(6.2) Condensation:

$$(HO)_n(EtO)_{3-n}SiCH_2CH_2Si(OEt)_{3-n}(OH)_n \xrightarrow{-H_2O}$$



6-III.2 Functionalization

The polymer is functionalized by incorporation of the bifunctional reagent, TMSen, into the reaction mixture.



The methoxy groups on one end of TMSen readily undergo the hydrolysis and condensation reactions, which anchor it to the polymer. The ethylenediamine moeity contains nitrogen donor atoms which can sequester metal ions from aqueous solutions by forming stable complexes via dative bonding.

6-III.3 Surfactant Templating

A supramolecular assembly of sufactant molecules is formed by adding CTAC to the initial solution. Polymerization of BTSE or the copolymerization of BTSE and TMSen during the next step results in the incorporation of the surfactant structures within the organic-inorganic matrix. Post-synthetic extraction with acidified ethanol removes the surfactant molecules, leaving behind a network of pores which can result in large surface areas and pore volumes. More importantly, since these pores were templated by the relatively large surfactant assemblies, they are large enough to allow fast metal ion access to the functional groups located throughout the inner pore spaces of the sorbent. This leads to a high capacity for metal ions as well as good metal ion

transfer kinetics. It should be noted that if the organic portion of the polymer is too long, surfactant extraction leads to collapse of the pore network, due to the lack of structural rigidity of the matrix.

6-III.4 Molecular Imprinting

In order to create ideal binding sites for specific metal ions within the sorbent, the metal ion complex must be formed with the bifunctional ligand prior to polymerization. The nitrate salt of the metal ion template is dissolved in the micellar solution and TMSen is added. Knowledge of the coordination environment preferred by each metal ion with the ligand is used to make the most stable complex. For example, en forms very stable 1:2 complexes, β_2~20 (70), with Cu(II) (92). A look at the stepwise stability constants shows that K_3 is negative for this system (93). For these reasons, the appropriate amounts of the metal salt and TMSen are added to the initial solution, so that a 1:2 complex is formed. Similar reasoning is used in the preparation of the Ni(II) and Zn(II) imprinted materials, in which 1:3 complexes are used due to the fact that these ions form stable octahedral complexes with en. Once the metal ion complexes are formed, BTSE and base are added. Polymerization results in the covalent bonding of the silyl group on TMSen to the solid matrix. The ligands are fixed in this ideal geometry. Metal ions are easily removed by protonation of the TMSen nitrogens with 1 M HNO_3. Template removal and neutralization gives the material adsorption sites that are ideally suited for to rebind the specific metal ion.

6-III.5 Metal Ion Sorption

6-III.5.1 Metal(II) Uptake Capacity

The metal ion imprinted hybrids have shown an enhanced capacity relative to the nonimprinted material for the adsorption of metal ions from aqueous solutions.

6-III.5.1.1 Copper(II) Imprinted Hybrids

Table 6.1 summarizes the Cu(II) uptake of the copper imprinted and nonimprinted hybrid materials from solutions ranging from 6.35-63.55 ppm Cu(II) during a standard batch procedure at pH 5.0. A direct comparison shows that the copper imprinted material removed more of the copper ions than the nonimprinted hybrid at every concentration. **Figure 6.1** shows how the percentage of metal ion removed by the nonimprinted sorbent decreases considerably at higher concentrations, while the imprinted material does not show a marked decrease. This is a clear example of the increased affinity of the imprinted sorbent for the metal ion template. **Figure 6.2** shows the more than tenfold increase in the distribution coefficients achieved by this molecular imprinting technique.

6-III.5.1.2 Nickel(II) Imprinted Hybrids

Unlike the Cu(II) ion, which generally forms a 1:2 metal to ligand complex with the ethylenediamine moeity, the Ni(II) ion preferentially forms a 1:3 complex, resulting in an octahedral coordination environment, where the metal ion is surrounded by six nitrogen donor atoms. For this reason, we altered the reaction

Table 6.1 Copper(II) Uptake of Cu(II) Imprinted and Nonimprinted Hybrid Sorbents

Sorbent	Initial Conc. (ppm)	Final Conc. (ppb)	% Cu Absorbed	Copper Kd
Nonimprinted	6.35	56	98.12	11,300
Cu(II) imprinted	**6.35**	**4**	**99.94**	**174,100**
Nonimprinted	15.89	294	98.15	5,300
Cu(II) imprinted	**15.89**	**14**	**99.91**	**108,200**
Nonimprinted	31.77	1,200	96.07	2,400
Cu(II) imprinted	**31.77**	**44**	**99.86**	**70,500**
Nonimprinted	47.66	4,200	91.24	1,000
Cu(II) imprinted	**47.66**	**167**	**99.65**	**28,700**
Nonimprinted	63.55	10,000	84.31	540
Cu(II) imprinted	**63.55**	**381**	**99.40**	**16,560**

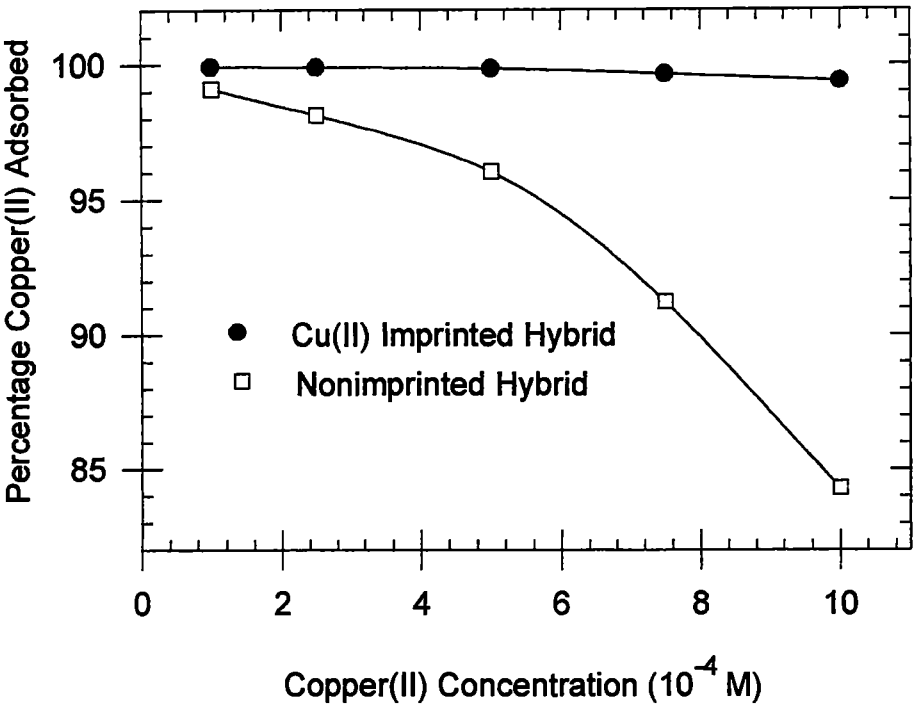


Figure 6.1 Copper percentage sorption isotherm.

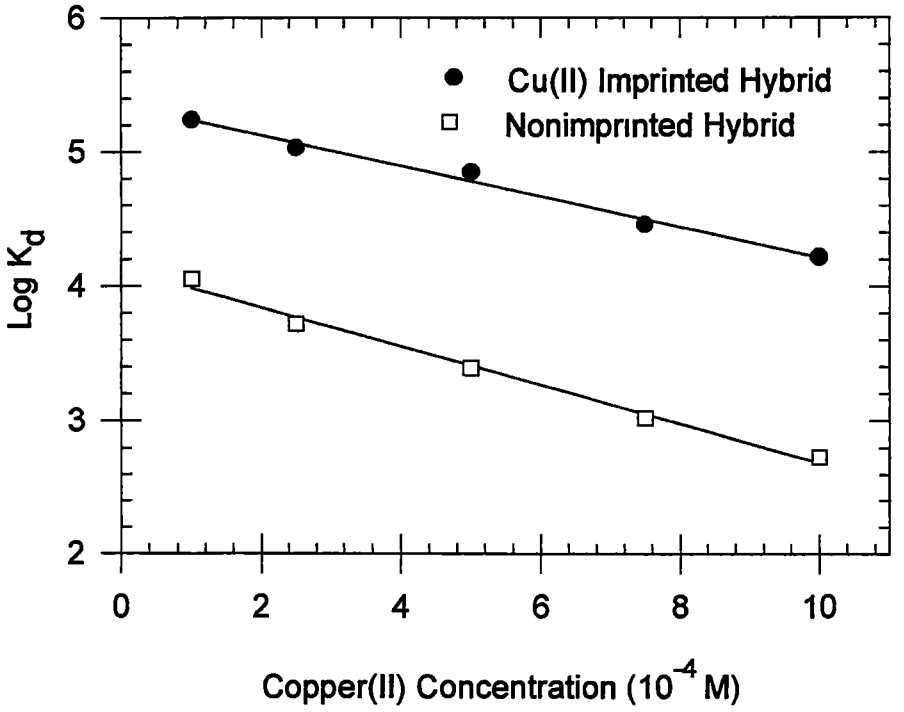


Figure 6.2 Copper K_d sorption isotherm

mixture stoichiometry from that used for the Cu(II) imprinted hybrid by reducing the molar ratio of the nitrate salt used, thereby forming the 1:3 Ni(II):en complex. The resulting imprinted material should contain binding sites tailored for this cation. **Table 6.2** shows the uptake of nickel(II) by both nickel imprinted and nonimprinted hybrids during a standard batch test at pH 6.0. The nickel imprinted sorbent removed more Ni(II) than the nonimprinted sorbent at all concentrations. **Figure 6.3** clearly illustrates the overall trend. As the percentage of Ni(II) adsorbed by the nonimprinted material decreases to below 50% at the higher concentrations, the nickel imprinted sorbent continues to remove over 90%. **Figure 6.4** shows the dramatic increase in the Ni(II) distribution coefficients as a result of molecular imprinting.

6-III.5.1.3 Zinc(II) Imprinted Hybrids

The synthetic procedure for the zinc imprinted hybrid material was similar to that of the nickel imprinted hybrid, since it also preferentially forms a 1:3 complex with the ethylenediamine moeity. **Table 6.3** summarizes the Zn(II) uptake of the zinc imprinted and nonimprinted hybrid materials from solutions ranging from 6.54-65.39 ppm Zn(II) during a standard batch procedure at pH 6.0. Like the copper and nickel imprinted sorbents, the zinc imprinted hybrid removed more Zn(II) than the nonimprinted material at all concentrations studied. **Figure 6.5** shows similar trends, as the percentage Zn(II) adsorbed by the nonimprinted sorbent is over 98% at the lowest concentration and decreases substantially to less than 65%, while the zinc imprinted sorbent still removes nearly 90% at the higher concentration. **Figure 6.6**

Table 6.2 Nickel(II) Uptake of Ni(II) Imprinted and Nonimprinted Hybrid Sorbents

Sorbent	Initial Conc. (ppm)	Final Conc. (ppb)	% Ni(II) Absorbed	Nickel Kd
Nimp	5.87	526	91.04	1,000
Ni(II) imprinted	**5.87**	**3**	**99.95**	**216,900**
Nonimprinted	14.67	3,250	77.88	350
Ni(II) imprinted	**14.67**	**12**	**99.92**	**127,400**
Nonimprinted	29.35	11,690	60.14	150
Ni(II) imprinted	**29.35**	**100**	**99.66**	**29,500**
Nonimprinted	44.02	23,590	46.41	90
Ni(II) imprinted	**44.02**	**436**	**99.01**	**10,100**
Nonimprinted	58.69	37,690	35.78	60
Ni(II) imprinted	**58.69**	**3600**	**93.92**	**1,500**

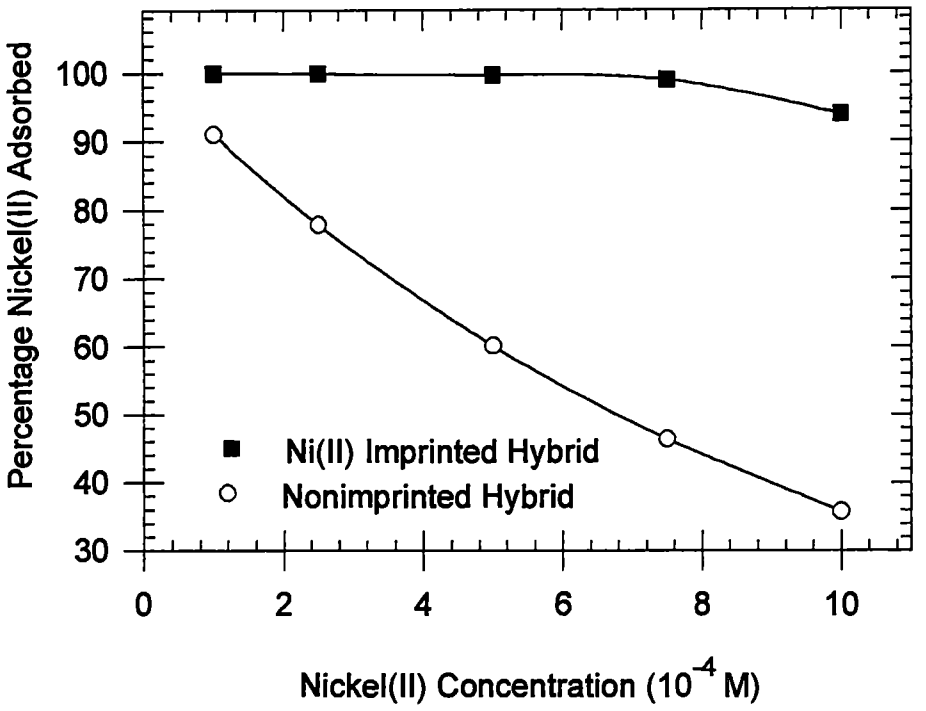


Figure 6.3 Nickel percentage sorption isotherm.

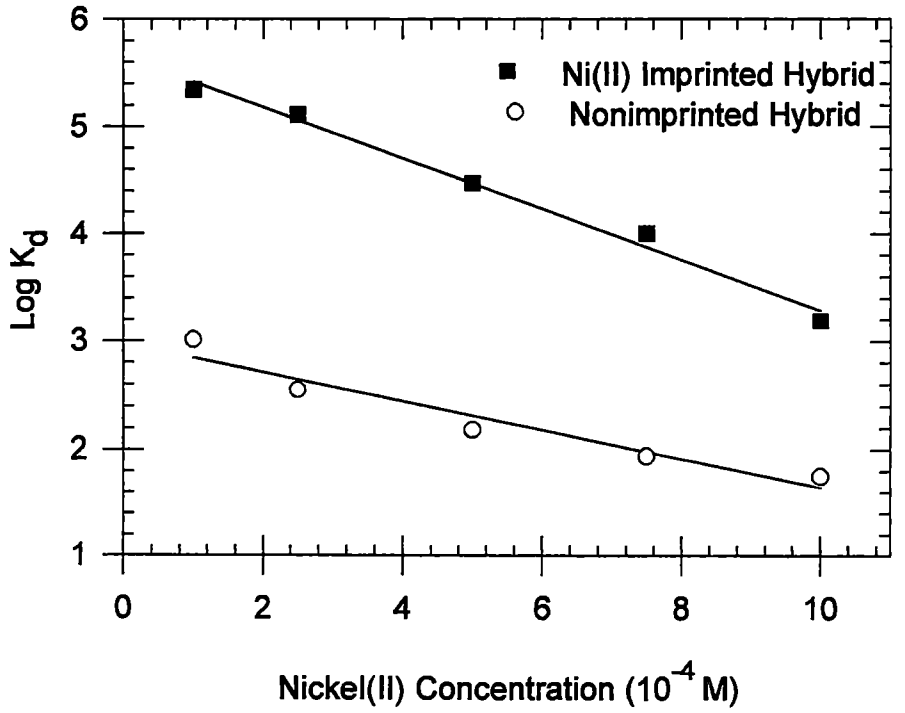


Figure 6.4 Nickel K_d sorption isotherm

Table 6.3 Zinc(II) uptake of Zn(II) imprinted and nonimprinted hybrid sorbents.

Sorbent	Initial Conc. (ppm)	Final Conc. (ppb)	% Zn Absorbed	Zinc Kd
Nonimprinted	6.54	90	98.63	7,200
Zn(II) imprinted	**6.54**	**20**	**99.70**	**33,800**
Nonimprinted	16.35	713	95.64	2,200
Zn(II) imprinted	**16.35**	**91**	**99.44**	**17,800**
Nonimprinted	32.70	4,550	86.10	620
Zn(II) imprinted	**32.70**	**1,600**	**95.21**	**2,000**
Nonimprinted	49.04	11,600	76.32	320
Zn(II) imprinted	**49.04**	**2,900**	**94.04**	**1,600**
Nonimprinted	65.39	24,100	63.20	170
Zn(II) imprinted	**65.39**	**7,800**	**88.07**	**740**

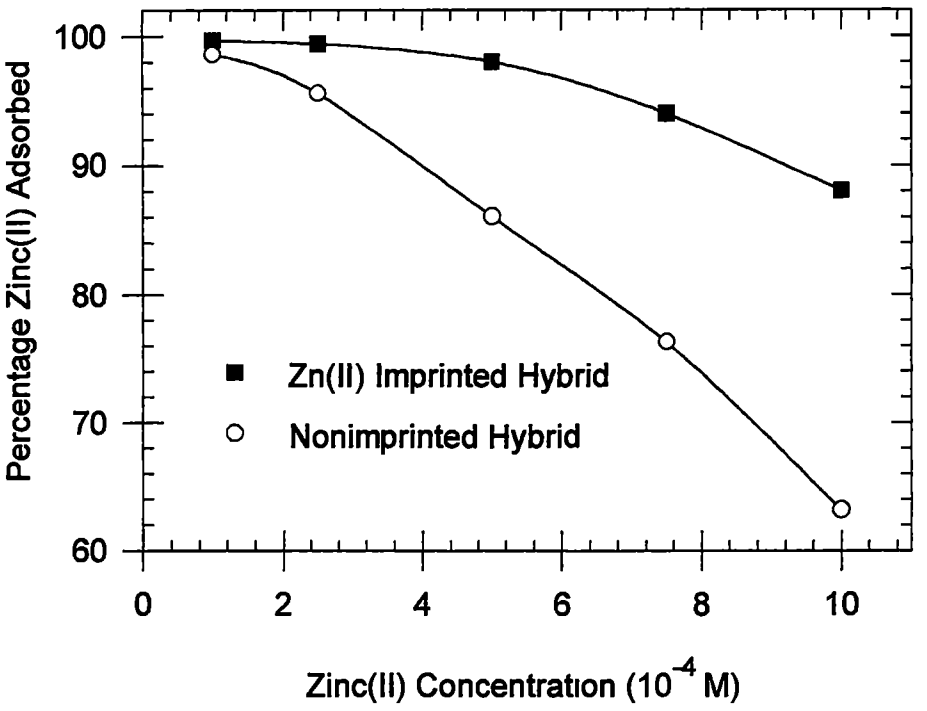


Figure 6.5 Zinc percentage sorption isotherm.

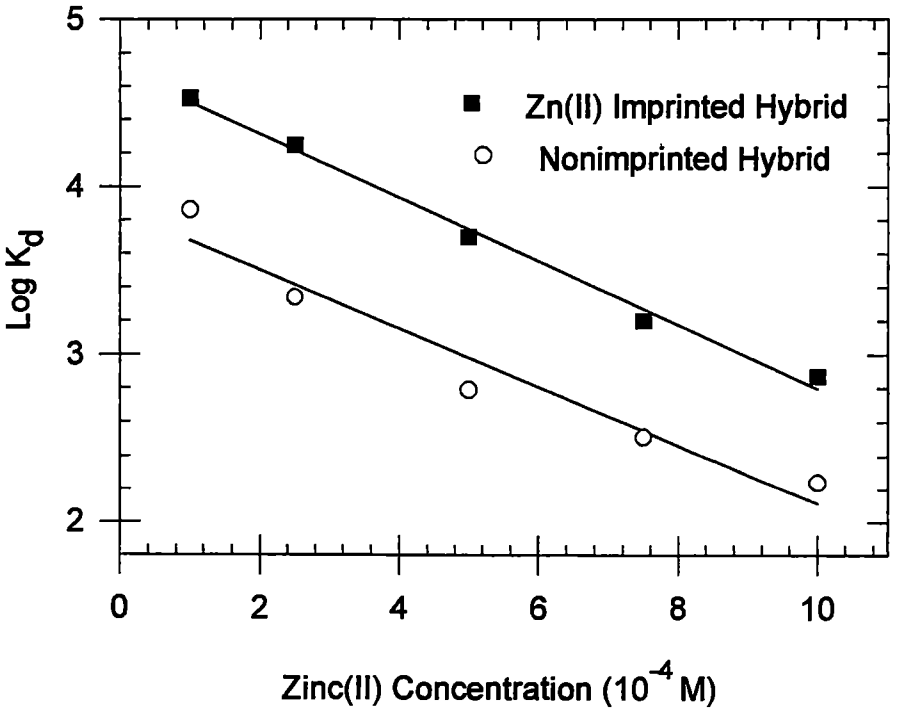


Figure 6.6 Zinc K_d sorption isotherm

shows the enhancement of the Zn(II) distribution coefficients for the zinc imprinted sorbent at all concentrations studied.

6-III.5.2 Metal(II) Selectivity

Although the results of the single metal ion batch tests described above clearly illustrate how molecular imprinting techniques can be utilized to create materials which exhibit enhanced recognition for specific metal ions, the vast majority of metal ion sorbent applications require selective separations. Therefore, the sorbent must be able to selectively bind the metal ion of choice from a mixture containing various competitor species. A selectivity coefficient, *k*, for the binding of a specific metal ion in the presence of competitor species can be obtained from equilibrium binding data according to equation (6.4):

$$M_1(\text{solution}) + M_2(\text{sorbent}) \rightleftharpoons M_2(\text{solution}) + M_1(\text{sorbent}) \qquad (6.3)$$

$$k = \{[M_2]_{\text{solution}}[M_1]_{\text{sorbent}}\} / \{[M_1]_{\text{solution}}[M_2]_{\text{sorbent}}\} = K_d(M_1)/K_d(M_2) \qquad (6\ 4)$$

Comparison of the *k* values for the imprinted and nonimprinted samples can show the effect that imprinting has on the metal ion selectivity for a given sorbent (26). A measure of the increase in selectivity due to molecular imprinting can be defined by

the ratio of the selectivity coefficients of the imprinted and nonimprinted materials, and is referred to as the relative selectivity coefficient, k'.

$$k' = k_{\text{imprinted}} / k_{\text{nonimprinted}} \tag{6.5}$$

6-III.5.2.1 Cu(II) vs. Zn(II) Selectivity

In order to test the selectivity of the copper imprinted hybrid sorbents, competitive ion binding batch studies were undertaken, with Zn(II) as the competitor species. All standard solutions were made with equimolar amounts of Cu(II) and Zn(II) at five different concentrations from 10^{-4}-10^{-3} M and pH 5.0. Identical tests were run with the nonimprinted hybrid sorbent for comparison. The results of competitive ion binding batch tests are summarized in **Tables 6.4 and 6.5.** The nonimprinted sorbent absorbed more Cu(II) than Zn(II) at all concentrations. This is an expected result, due to the larger stability constants associated with the formation of ethylenediamine : copper(II) complexes relative to those of zinc(II) at pH 5.0. The copper imprinted hybrid absorbed more Cu(II) and more Zn(II) than the nonimprinted material at all concentrations. The enhanced capacity of Cu(II) due to molecular imprinting is expected, while the increased uptake of the Zn(II) competitor species is less clear. The imprinting seems to create electron-rich, hydrophilic sites in the relatively hydrophobic organic-inorganic matrix. These sites may increase the sorbent's affinity for a wide variety of hydrated metal ions. An important concept here is that the imprinting enhances the affinity of the sorbent for the target Cu(II)

Table 6.4 Cu(II) vs. Zn(II) Selectivity of Cu(II) Imprinted and Nonimprinted Hybrid Sorbents

Sorbent	C_o(M) Cu/Zn	% Cu(II) Abs.	% Zn(II) Abs.	Copper Kd	Zinc Kd	k	k'
Nonimprinted	10^{-4}	98.99	20.20	9,700	25.3	386	
Cu(II) imprinted	**10^{-4}**	**99.93**	**85.47**	**153,000**	**588**	**260**	**0.67**
Nonimprinted	$2.5x10^{-4}$	96.60	20.08	2,840	25.1	113	
Cu(II) imprinted	**$2.5x10^{-4}$**	**99.92**	**74.68**	**129,700**	**295**	**440**	**3.9**
Nonimprinted	$5.0x10^{-4}$	92.69	14.33	1270	16.7	76	
Cu(II) imprinted	**$5.0x10^{-4}$**	**99.88**	**60.38**	**85,400**	**152.4**	**561**	**7.4**
Nonimprinted	$7.5x10^{-4}$	89.81	6.71	880	7.2	122	
Cu(II) imprinted	**$7.5x10^{-4}$**	**99.80**	**43.63**	**48,800**	**77.4**	**631**	**5.2**
Nonimprinted	10^{-3}	80.84	4.30	420	4.5	94	
Cu(II) imprinted	**10^{-3}**	**99.58**	**31.62**	**23,500**	**46**	**507**	**5.4**

Table 6.5 Cu(II) vs. Zn(II) Selectivity of Cu(II) Imprinted and Nonimprinted Hybrid Sorbents

Sorbent	C_o Cu (ppm)	C_f Cu (ppb)	C_o Zn (ppm)	C_f Zn (ppb)	C_fZn/C_fCu
Nonimprinted	6.35	64	6.54	5,220	81.6
Cu(II) imprinted	**6.35**	**4**	**6.54**	**950**	**238**
Nonimprinted	15.89	540	16.35	13,070	24.2
Cu(II) imprinted	**15.89**	**13**	**16.35**	**4,140**	**318**
Nonimprinted	31.77	2,320	32.70	28,010	12.1
Cu(II) imprinted	**31.77**	**38**	**32.70**	**12,960**	**341**
Nonimprinted	47.66	4,860	49.04	45,750	9.4
Cu(II) imprinted	**47.66**	**95**	**49.04**	**27,640**	**291**
Nonimprinted	63.55	12,180	65.39	62,580	5.1
Cu(II) imprinted	**63.55**	**267**	**65.39**	**44,710**	**167**

more than that of the Zn(II) competitor. This is shown by the larger selectivity coefficients, (k), and relative selectivity coefficients, (k'), greater than unity for the copper imprinted sorbent at all solution concentrations with the exception of the lowest [10^{-4}Cu(II)/10^{-4}Zn(II)]. At this low concentration the imprinted material has enough binding sites to remove most of both metal species, decreasing its calculated selectivity. The linear regressions in **Figure 6.7** show a larger increase in the distribution coefficients for Cu(II) relative to Zn(II) for the copper imprinted material than the nonimprinted sorbent. **Figure 6.8** shows the percentage of each metal ion absorbed by the two sorbents. The linear regressions of the Cu(II) uptake and the Zn(II) uptake by the nonimprinted materials have the same slope. Although the nonimprinted material removes nearly all the Cu(II) and only about 20 percent of the Zn(II) at the lowest concentration, both values decrease approximately the same amount (17 percent) over the entire concentration range. This is not the case with the metal ion sorption trend of the copper imprinted material. At the higher concentrations, where the competition for adsorption sites is high, the percentage of the Cu(II) absorbed remains over 99.5%, while the percentage of the Zn(II) competitor decreases substantially.

Another parameter used to describe the selectivity of a given sorbent for a target metal ion over a competitor species is the ratio of the final concentrations of the two species. In this instance, the larger the value of C_f Zn(II)/C_f Cu(II), the higher the selectivity of the sorbent for Cu(II). Table 6.5 shows that the value of this ratio is considerably higher for the copper imprinted sorbent at all concentrations.

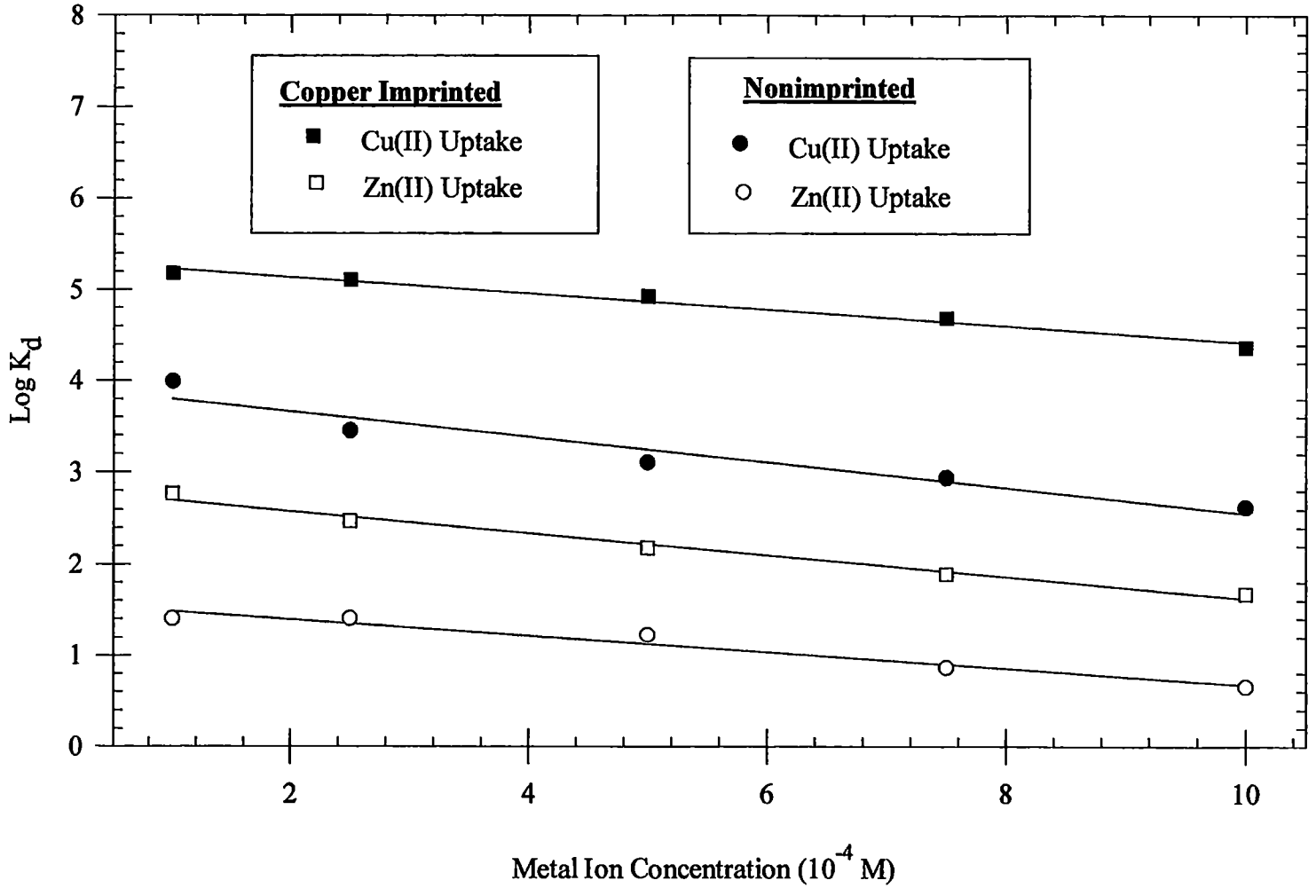


Figure 6.7 Copper(II) vs. Zinc(II) selectivity.

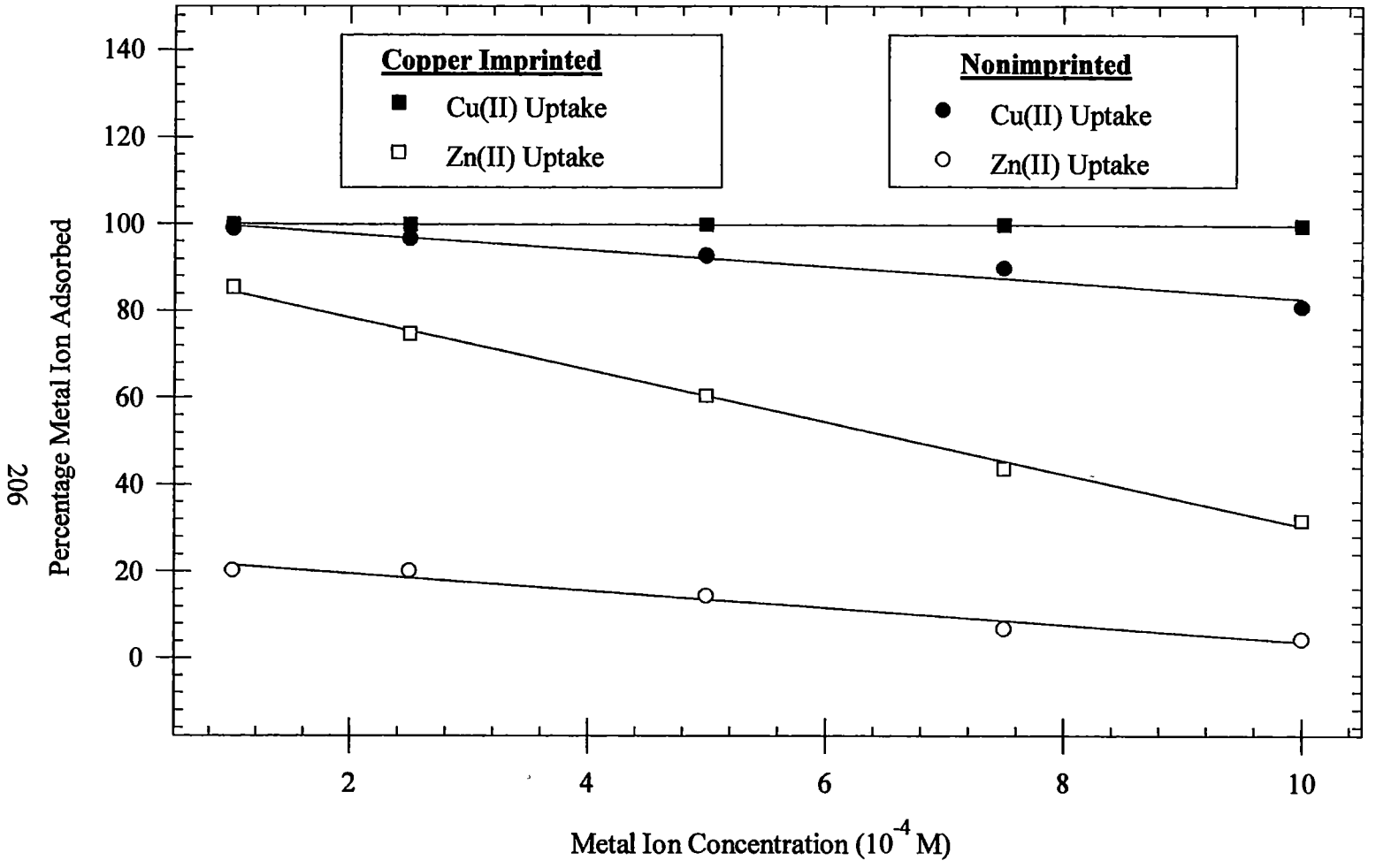


Figure 6.8 Copper(II) vs. Zinc(II) selectivity.

6-III.5.2.2 Ni(II) vs. Zn(II) Selectivity

The selectivities of the nickel(II) and zinc(II) imprinted sorbents were investigated by competitive ion binding batch tests. All initial solutions contained equimolar amounts of Ni(II) and Zn(II) at five different concentrations from 10^{-4}-10^{-3} M and pH 6.0. **Table 6.6** summarizes the results the batch test results. The nickel(II) imprinted sorbent absorbed more Ni(II) than Zn(II) at all concentrations. **Figure 6.9** illustrates the higher distribution coefficients achieved for Ni(II) with the nickel imprinted material. This sorbent removed nearly all of both metal ion species from the 10^{-4} M Ni(II)/10^{-4} M Zn(II) mixed solution. This lack of selectivity at very low concentrations may be due to the high number of imprinted sites relative to the total number of metal ions. In direct contrast to the adsorption behavior of the nickel imprinted material, the zinc imprinted sorbent absorbed more Zn(II) than Cu(II) at all concentrations studied. **Figure 6.10** shows the higher distribution coefficients achieved for Zn(II) with respect to Ni(II) by the zinc(II) imprinted sorbent. This illustration of reversible imprinting shows the utility of molecular imprinting techniques in the synthesis sective metal ion sorbents.

6-III.5.2.3 Divalent Cation Mixture

The divalent cations of copper, nickel, zinc, and cadmium are common constituents of man-made waste. They are often present together in municipal wastewater, electroplating waste, acid mine drainage, and landfill leachates (53, 94-5). In order to determine the adsorption selectivity characteristics of the copper(II)

Table 6.6 Ni(II) vs. Zn(II) Uptake of Ni(II) Imprinted and Zn(II) Imprinted Hybrid Sorbents

Sorbent	C_o Ni (ppm)	C_f Ni (ppb)	% Ni Abs.	C_o Zn (ppm)	C_f Zn (ppb)	% Zn Abs.	Nickel Kd	Zinc Kd
Ni(II) imprinted	5.87	5	99.92	6.54	6	99.91	126,800	116,600
Zn(II) imprinted	**5.87**	**29**	**99.50**	**6.54**	**1.3**	**99.98**	**20,100**	**411,200**
Ni(II) imprinted	14.67	16	99.89	16.35	26	99.84	90,100	61,000
Zn(II) imprinted	**14.67**	**293**	**98.00**	**16.35**	**20**	**99.88**	**4,900**	**82,500**
Ni(II) imprinted	29.35	360	98.77	32.70	1,000	96.90	8,000	3,100
Zn(II) imprinted	**29.35**	**4,300**	**85.44**	**32.70**	**481**	**98.53**	**590**	**6,700**
Ni(II) imprinted	44.02	3,120	92.91	49.04	6,560	86.62	1,300	650
Zn(II) imprinted	**44.02**	**16,380**	**62.80**	**49.04**	**3,710**	**92.43**	**170**	**1,200**
Ni(II) imprinted	58.69	9,180	84.35	65.39	17,700	72.88	540	270
Zn(II) imprinted	**58.69**	**32,100**	**45.30**	**65.39**	**11,490**	**82.43**	**83**	**470**

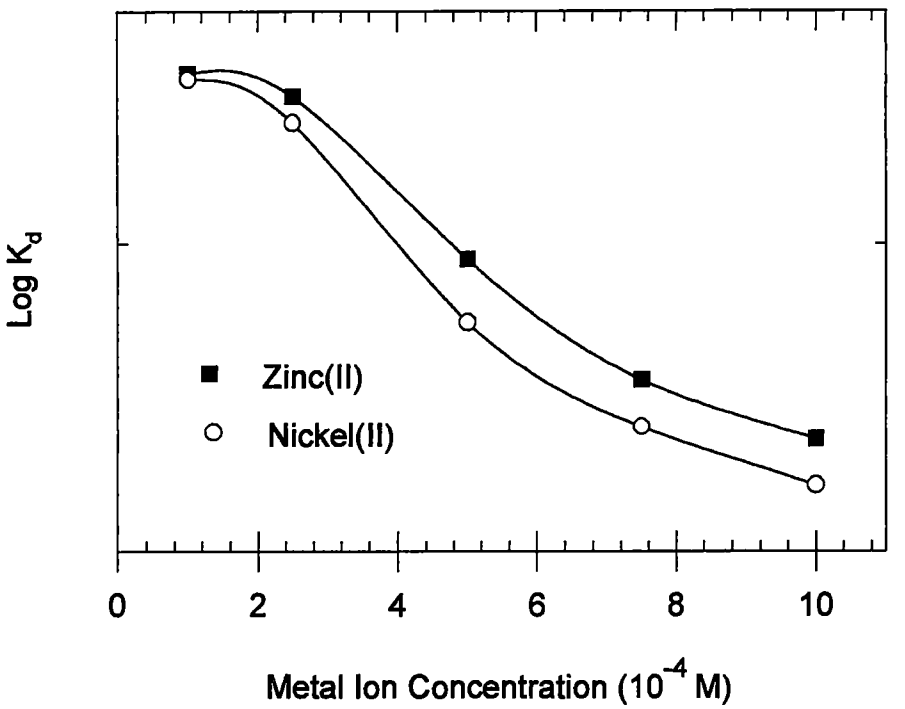


Figure 6.9 Nickel(II) vs. Zinc(II) on Nickel Imprinted Hybrid.

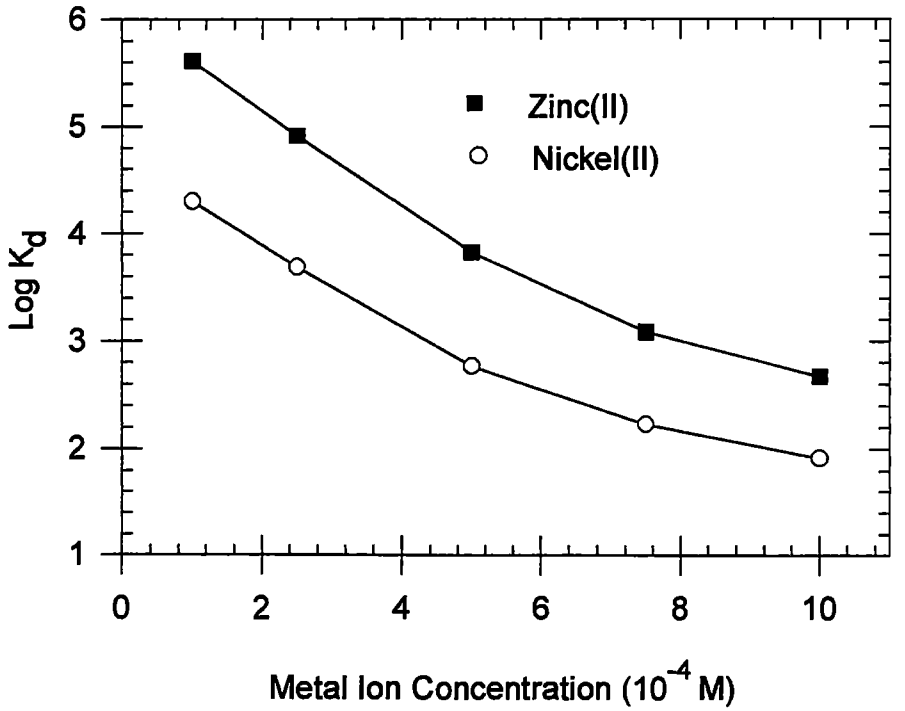


Figure 6.10 Nickel(II) vs. Zinc(II) on Zinc Imprinted Hybrid.

imprinted hybrid sorbent in these complex matrices, a metal ion solution, 10^{-3} M with respect to Cu(II), Ni(II), Zn(II), and Cd(II), was prepared at pH 5.0 and used as waste simulent. The results of a batch test with the copper imprinted sorbent are shown in **Figure 6.11**. Over 93 percent of the copper was absorbed, while the amount of zinc, nickel, and cadmium absorbed was approximately 15, 5, and 1 percent respectively.

6-III.6 Adsorption Kinetics

A very important attribute of any sorbent is the time required for the absorption process to take place. Many potential applications such as product or waste stream purification, require relatively fast uptake kinetics for the sorbent technology to be a viable option. The copper absorption study (Table 6.1) showed that 0.1 g of the copper(II) imprinted sorbent removed over 99.8% of the copper(II) from 10 mL of a $5x10^{-4}$ M solution at pH 5.0. Since all the batch tests involved a 30 min contact time, a series of tests were run with lower contact times in order to deduce how fast the adsorption process occurs in the organic-inorganic matrix. **Figure 6.12** illustrates the adsorption percentage as a function of the contact time. The copper imprinted hybrid removed over 99.5% of the Cu(II) during the first minute. During this time the initial copper concentration (31.77 ppm) is reduced to 130 ppb.

6-III.7 Multiple Use Cycles

One factor which determines the economic feasibility of any sorbent is the ease by which it can be regenerated. The ability to recycle a sorbent can offset initial costs.

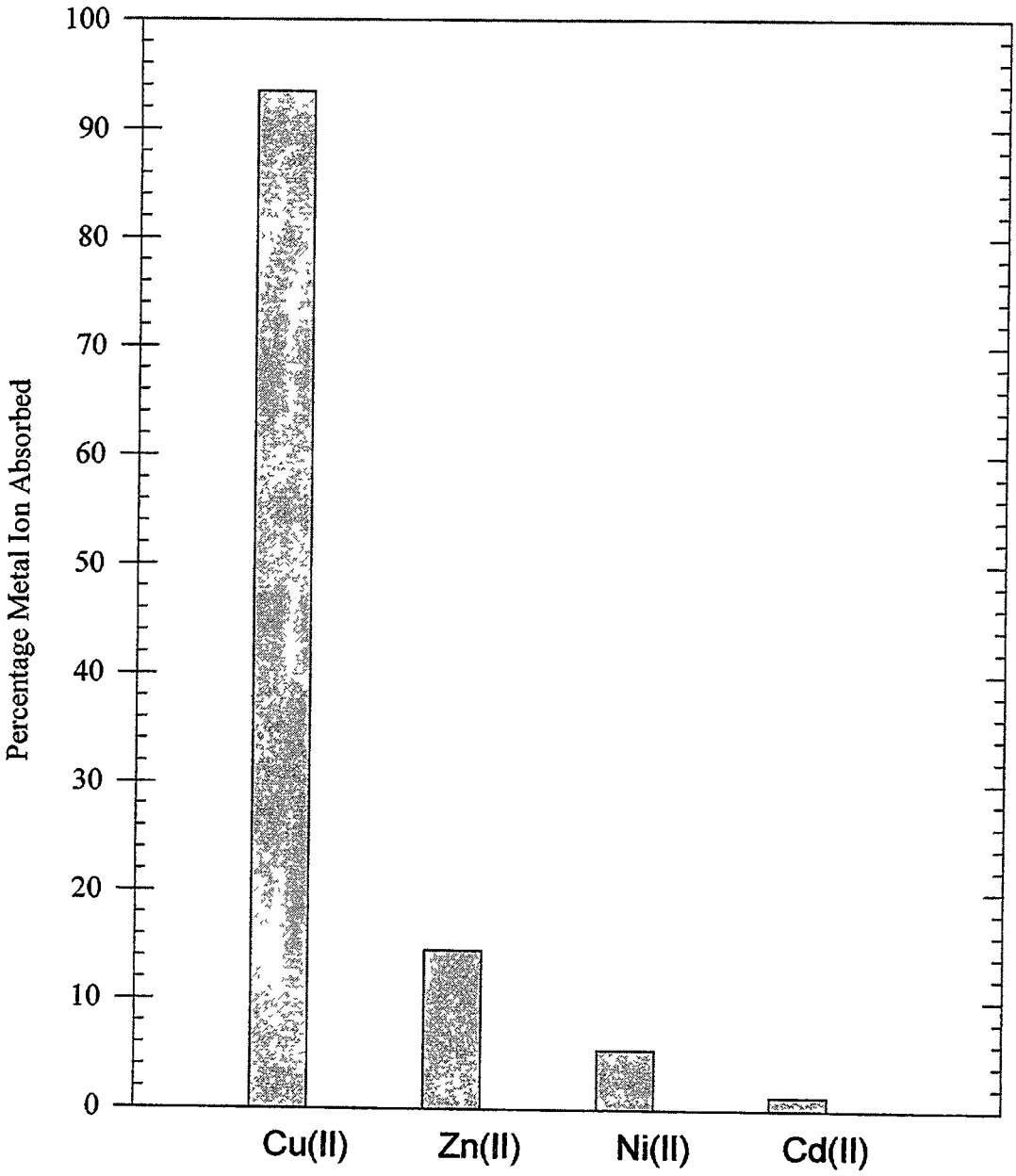


Figure 6.11 Metal ion adsorption on copper(II) imprinted hybrid.

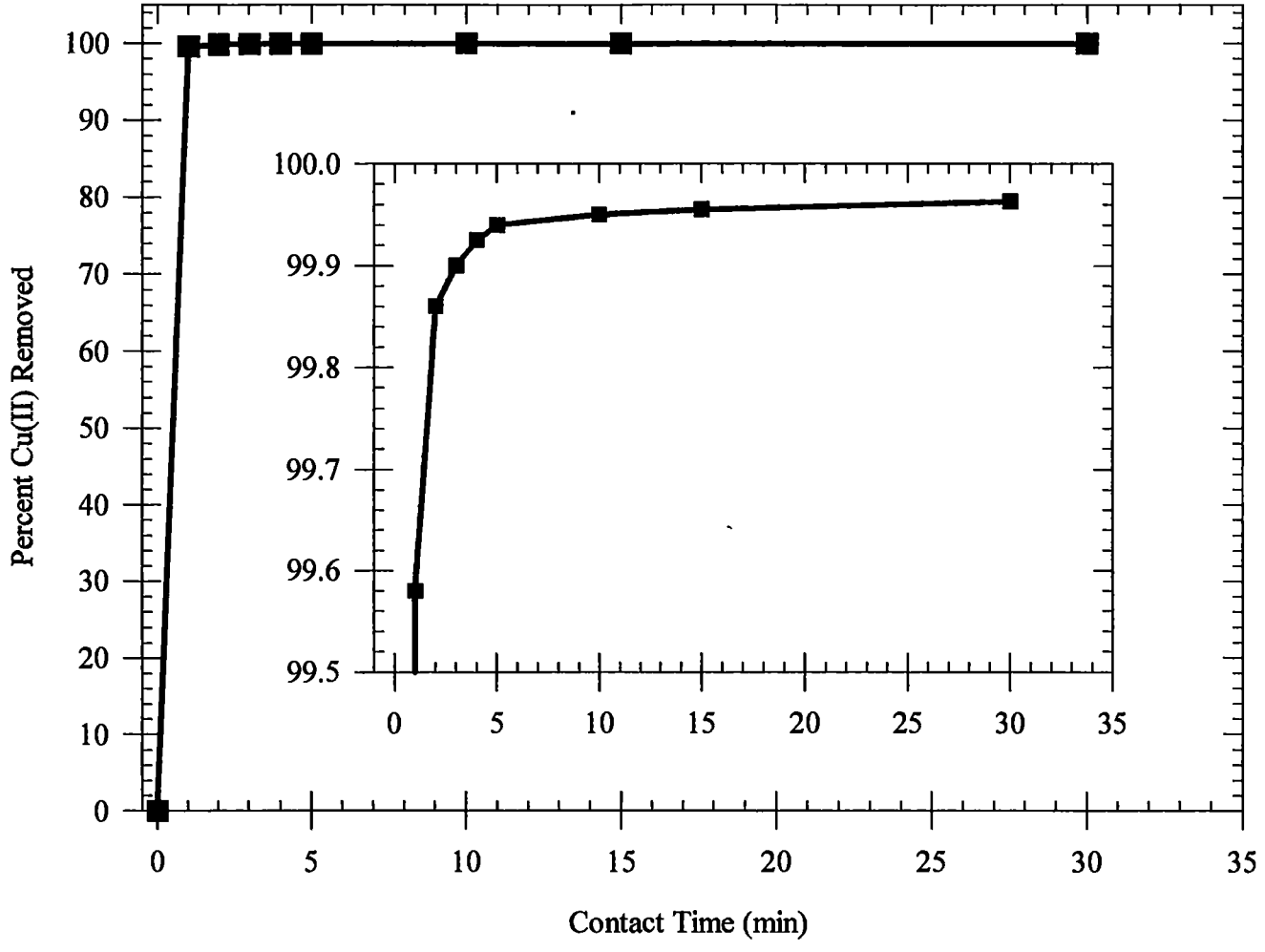


Figure 6.12 Copper(II) adsorption kinetics of hybrid sorbent.

A series of Cu(II) batch experiments were carried out with the copper(II) imprinted and nonimprinted sorbents in which copper(II) loaded sorbents were washed with 1 M HNO_3 to remove the metal ions, neutralized, and used to removed Cu(II) again. These multiple use cycles were used in order to determine a number of key factors, such as the ability of the acid to remove the metal ions, and whether the sorbents would retain their Cu(II) uptake capacities after numerous cycles. In a typical run, 0.50 g of sorbent was placed in 50 mL of $5x10^{-4}$ M Cu(II) solution and sonicated for 30 min. The sorbent was then recovered by filtration and placed in 10 mL of 1M HNO_3, stirred for 5 min, and then recovered by vacuum filtration. The sorbent was then placed in 50 mL of deionized water and titrated to neutral pH with 1 M NaOH. Following another filtration step, the sorbents were dried, weighed, and reused. Due to the number of steps involved, approximately 5% of the total mass of the sorbents were lost during each cycle. The amount of the initial Cu(II) solution was adjusted (i.e. 0.485 g/48.50 mL) to take this into account. These procedures were then repeated four more times. **Figure 6.13** shows the values of the distribution coefficients for both the copper(II) imprinted and nonimprinted sorbents for five multiple use cycles. A slight decrease in K_d is shown by both sorbents for each successive use. Despite this small decrease, the copper(II) imprinted hybrid removed greater than 99.70 percent of the Cu(II) during the fifth and final cycle. Filtrate analyses show that the simple acid washing removed greater than 98 percent of the Cu(II) from the loaded sorbents.

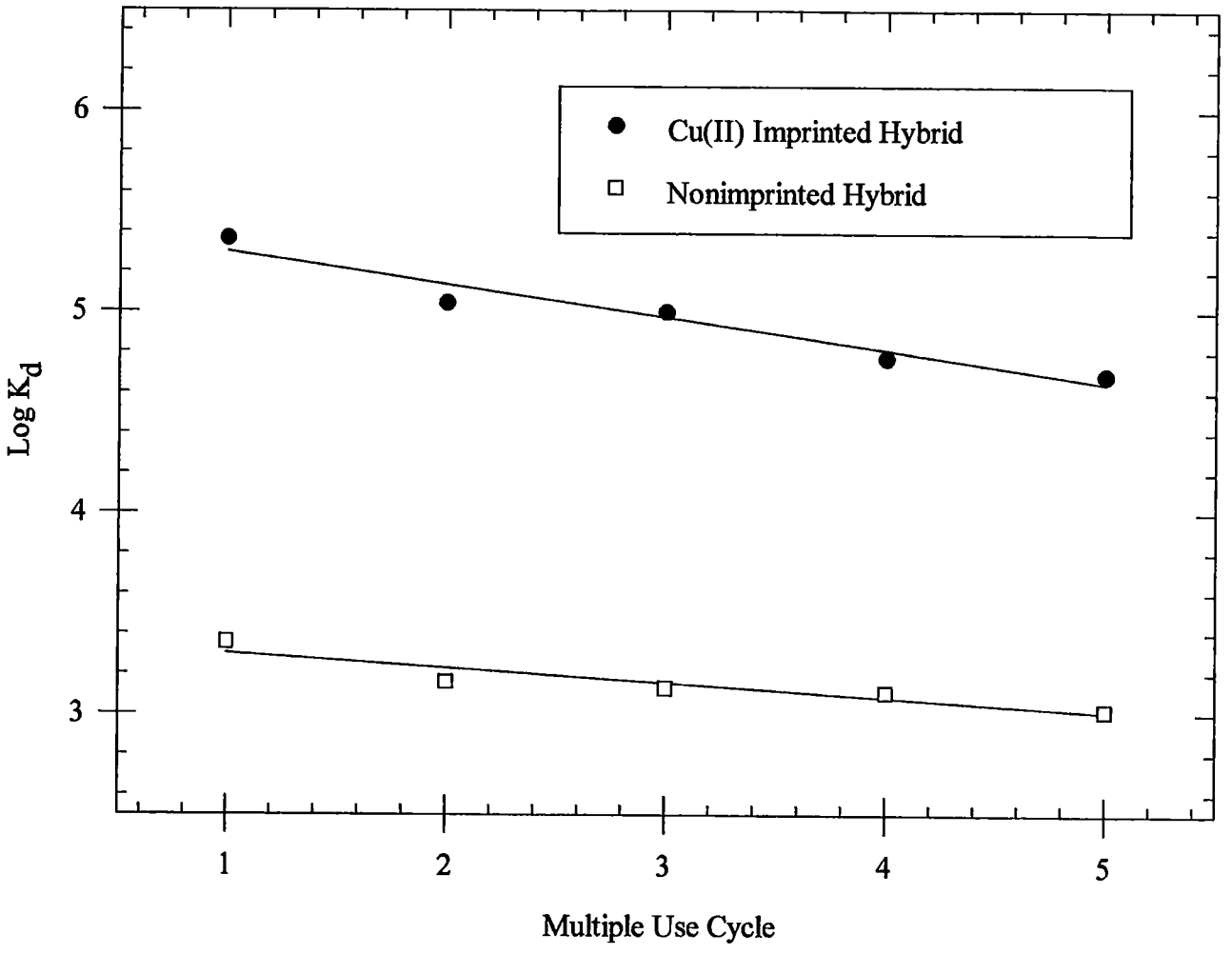


Figure 6.13 Recycleability of hybrid sorbents.

6-III.8 Small Angle X-ray Scattering

Small angle X-ray scattering plots of both the as-synthesized and extracted samples of the blank, nonimprinted, and copper(II) imprinted hybrid materials are shown in **Figure 6.14.** All samples exhibit single d_{100} reflections. Higher order Bragg reflections are not resolved. The extracted samples exhibit a much higher intensity due to the larger change in electron densities caused by removal of the surfactant assemblies. The as-synthesized materials, which still contain CTAC, show much lower intensities. The remarkable similarity of all three extracted samples suggests that incorporation of TMSen into the nonimprinted sorbent and copper:TMSen complexes into the copper(II) imprinted sorbent does not diminish the local order in these materials. Furthermore, these plots show very little change in the location of the d_{100} reflection due to the removal of the surfactant template and, therefore, no evidence of any collapse of the porous network. The presence of copper(II) in the Cu(II) imprinted as-synthesized material may account for the inconsistencies shown by this plot. Values of the structural parameters Q_{max}, $2\theta_{max}$, d_{100}, and a_o are listed in **Table 6.7**. Although no reflections higher than d_{100} have been resolved, Pinnavaia and co-workers have shown that similar single reflection materials can still exhibit local hexagonal symmetry (96-7).

6-III.9 Nitrogen Adsorption

Following the post-synthetic processing, a nitrogen adsorption analysis was performed on each sample. **Figure 6.15** shows the N_2 adsorption isotherms for the

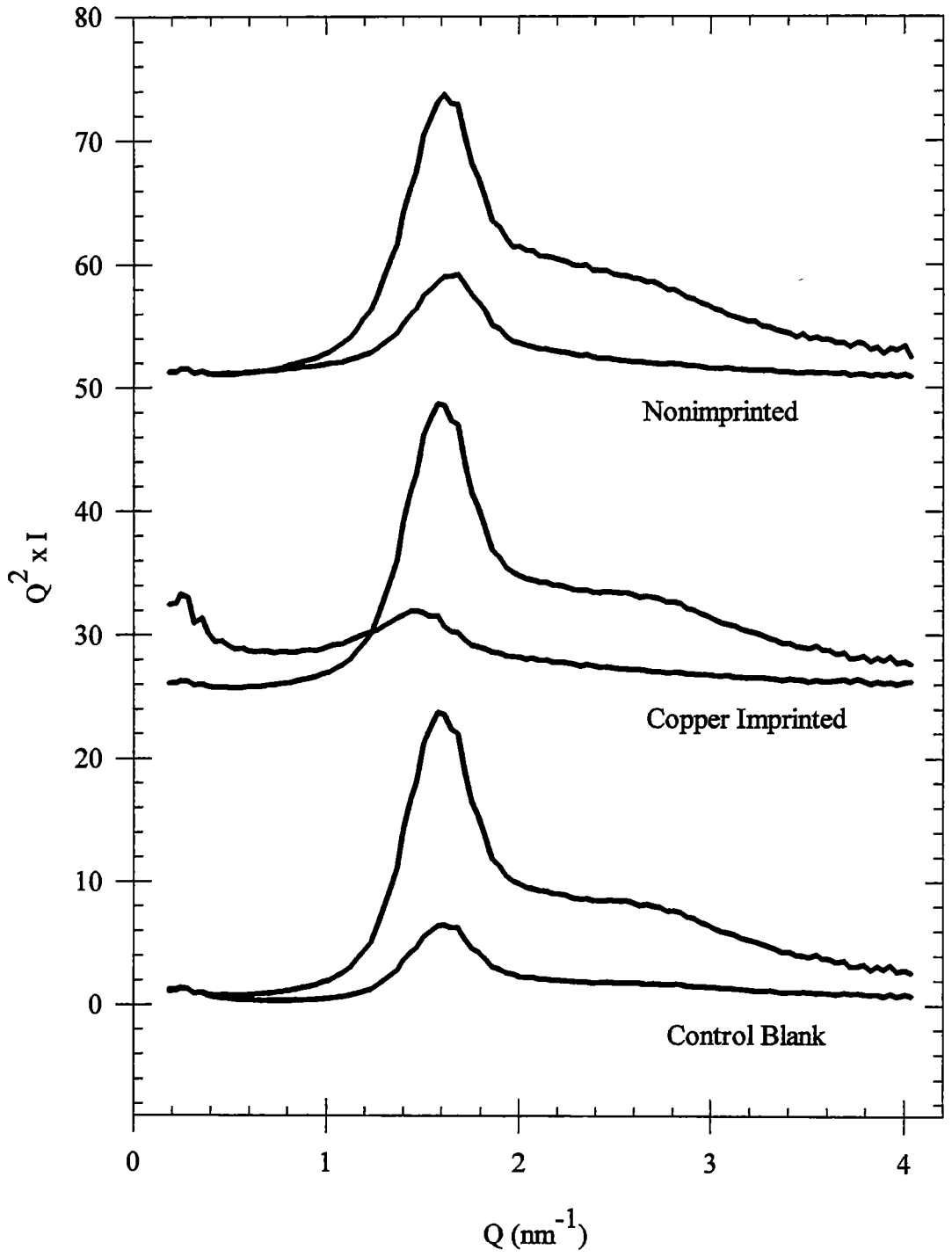


Figure 6.14 Hybrid SAXS plots of hybrid sorbents.

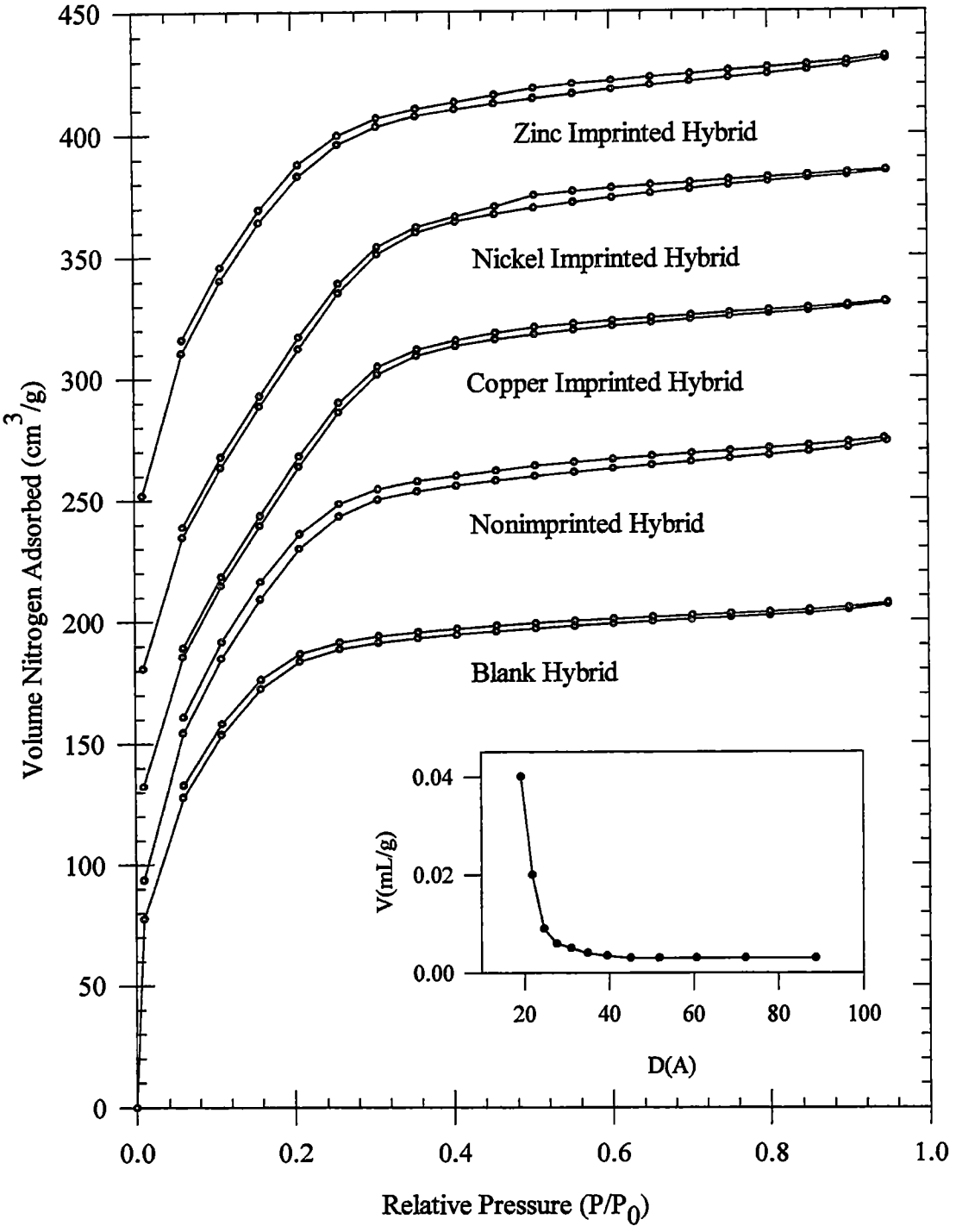


Figure 6.15 Nitrogen adsorption isotherms.

metal ion imprinted, nonimprinted, and blank hybrid sorbents after post-synthetic processing. All sorbents exhibit type I isotherms according to the BDDT classification (98), indicating a microporous structure. Linear regions from $P/P_o = 0.1\text{-}0.3$ indicate supermicroporosity (99). **Table 6.8** contains the porosity data of the extracted hybrid sorbents. Surface areas were obtained using the B.E.T. method (39). The total pore volumes of the hybrid samples simply represent the volume of the liquid equivalent of the total nitrogen absorbed. Micropore surface areas and micropore volumes were calculated by using the *t*-method (100). The d-spacings were calculated from small angle X-ray scattering data. All sorbents exhibit large surface areas and pore volumes. A distinguishing feature of these materials is the large micropore volumes. Typical B.J.H. pore size distributions (40), of these materials (Figure 6.15, inset) indicate that the few mesopores present in these samples are ~20 Å. The large micropore volumes of these sorbents, along with the similar d-spacings of the as-synthesized and extracted materials gives evidence that the surfactant molecules formed assemblies with diameters in the high microporous range (10-20 Å). In addition to these samples, a nitrogen adsorption analysis was performed on an as-synthesized sample (blank as-synthesized). It exhibited a B.E.T. surface area of 0.3 m^2/g and a total pore volume of only 0.002 cm^3/g. These results clearly indicate the important role of surfactant assemblies in creating porosity in these materials.

Table 6.7 Small Angle X-ray Scattering Data of Hybrid Sorbents

Sample	Qmax (nm^{-1})	2Θmax (deg)	d_{100} (Å)	a_o (Å)
Blank as-synthesized	1.614	2.266	38.93	44.95
Blank extracted	1.580	2.219	39.77	45.92
Nonimprinted as-synthesized	1.649	2.316	38.10	43.99
Nonimprinted extracted	1.614	2.266	38.93	44.95
Copper(II) imprinted as-synthesized	1.469	2.063	42.77	49.39
Copper(II) imprinted extracted	1.505	2.114	41.75	48.21

Table 6.8 Porosity Data of Hybrid Sorbents

Sample	BET Surface Area (m^2/g)	Total Pore Volume (cm^3/g)	Micropore Area (m^2/g)	Micropore Volume (cm^3/g)	d-spacing (Å)
Blank	600	0.32	475	0.22	39.8
Nonimprinted	826	0.43	593	0.26	38.9
Cu(II) Imprinted	823	0.43	473	0.18	41.8
Ni(II) Imprinted	821	0.44	454	0.17	
Zn(II) Imprinted	802	0.43	564	0.25	

6-III.10 UV-Visible Spectroscopy

Amine complexes of Cu(II) are more intensely blue than the hydrated cation. The stronger ligand field produced by amines cause the absorption bands of the electronic spectra to shift to shorter wavelengths (92). This characteristic of copper(II) amine complexes, coupled with relatively large extinction coefficients, has allowed us to probe the nature of the imprinting effect in the copper(II) imprinted sorbents via UV-visible spectroscopy. Since a 1 to 2, Cu(II) to TMSen complex was formed prior to polymerization and incorporated into the sorbent by copolymerization of BTSE and TMSen, the ethylenediamine moeities are thought to be "paired up." Following the removal of the metal ion and surfactant molecules, the TMSen ligands are grafted close enough throughout the organic-inorganic matrix that a 1 to 2 complex is likely to form (**Figure 6.16a**). In contrast, the TMSen ligands in the nonimprinted sorbent are believed to be homogeneously distributed. This would result in the ligands being too far apart to form the 1 to 2 complex (**Figure 6.16b**). The relatively large stability constant associated with the addition of a second diamine moeity to metal ions (70), would give the copper(II) imprinted material a much higher affinity for Cu(II). **Figure 6.17** shows the solution spectra of $[Cu\ TMSen(H_2O)_4]^{2+}$ (λ_{max} = 651 nm), and $[Cu\ TMSen_2(H_2O)_2]^{2+}$ (λ_{max} = 547 nm). The wavelength shift of 104 nm clearly illustrates the ligand field effect. Batch tests were run with the nonimprinted and copper imprinted sorbents using Cu(II) solutions at concentrations $5x10^{-4}$, $5x10^{-3}$, and 10^{-2} M. Diffuse reflectance spectra of the loaded sorbents were then recorded.

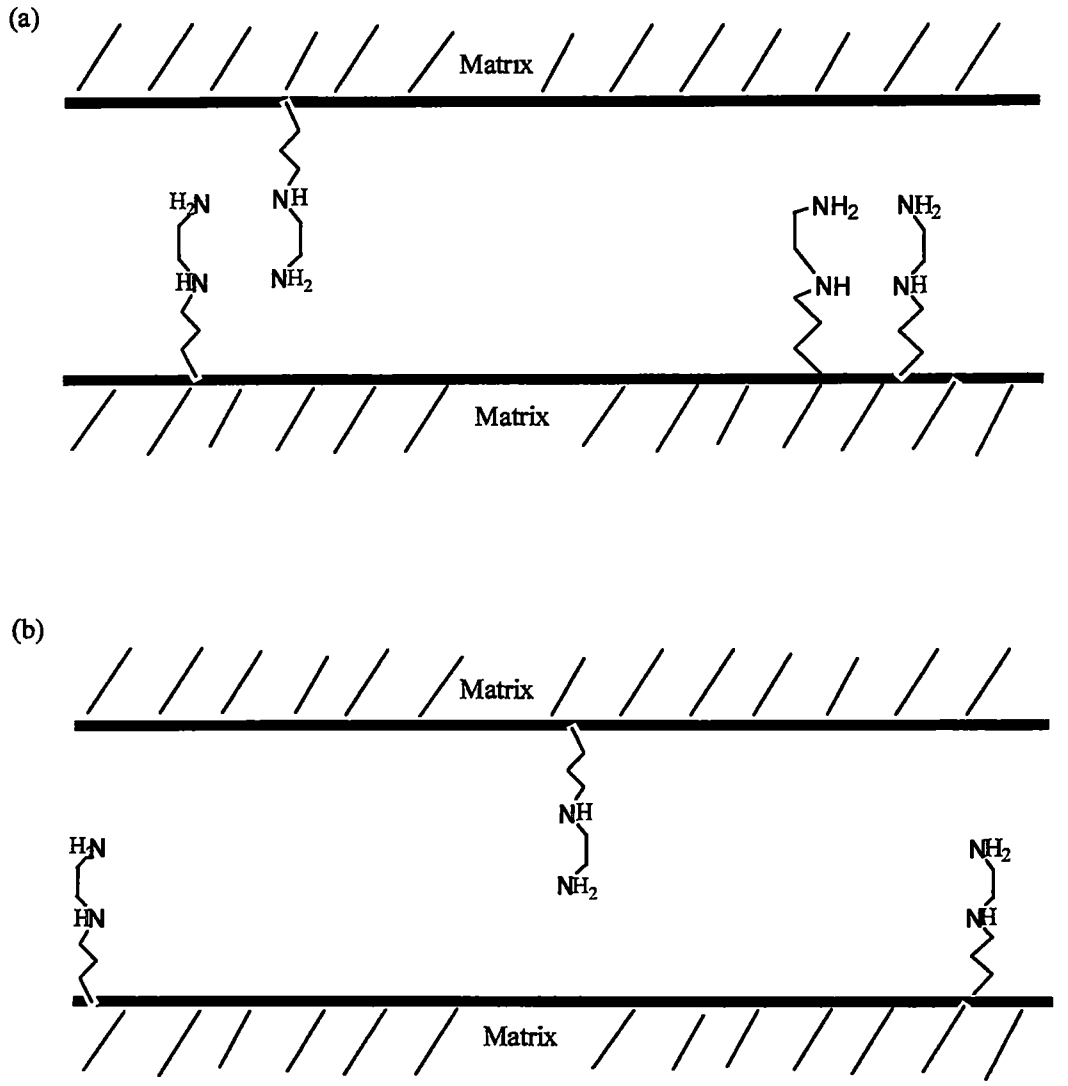


Figure 6.16 Probable arrangement of TMSen ligands in hybrid sorbents.

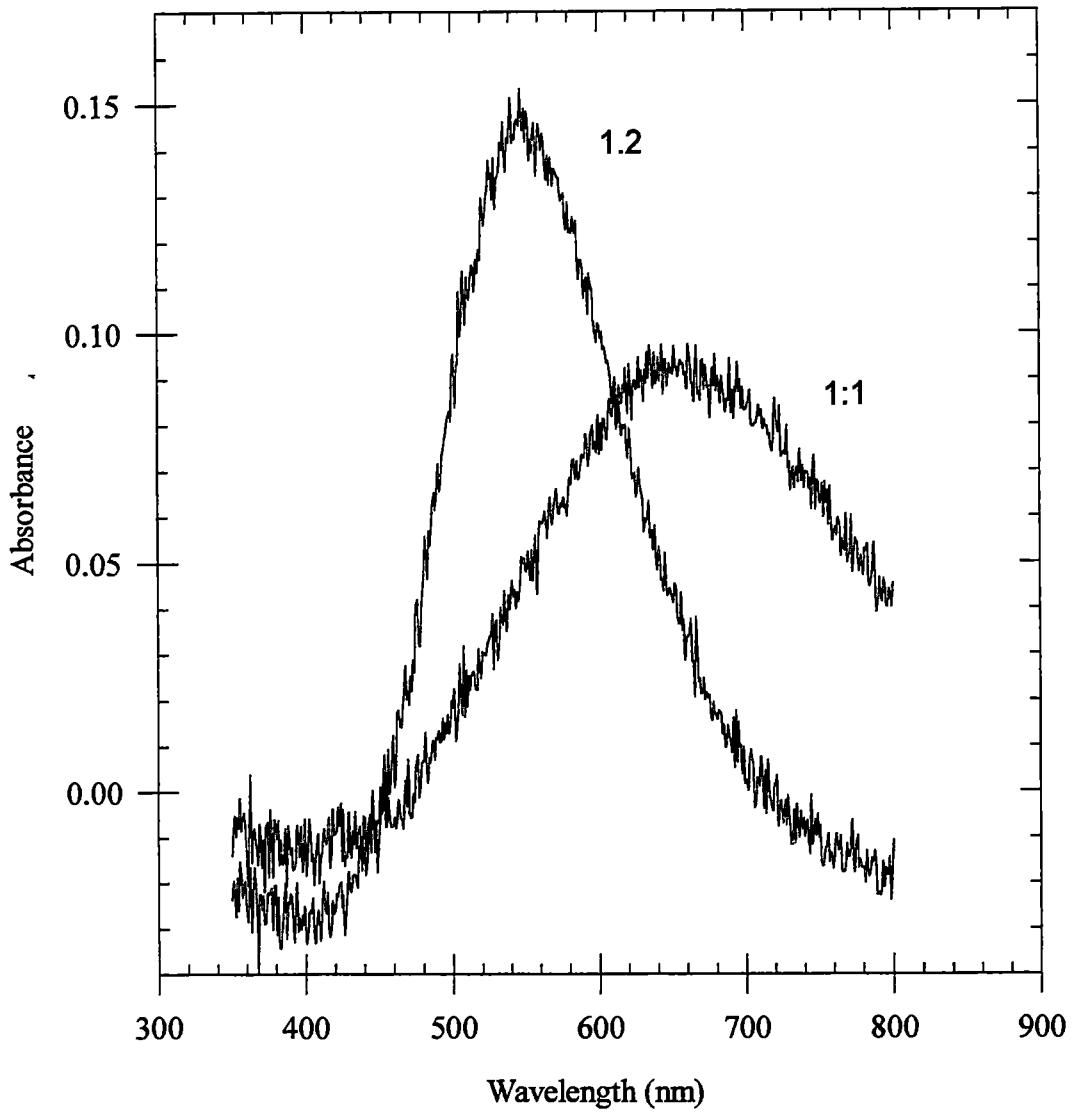


Figure 6.17 UV-visible solution spectra of Cu(II):TMSen complexes.

6-III.10.1 Nonimprinted Hybrid

Figure 6.18 shows the electronic spectra of the copper(II) loaded nonimprinted material. At the lowest concentration (5×10^{-4} M), the λ_{max} is 623 nm, while at the two higher concentrations λ_{max} shifts to 647 and 648 nm. These later two values are very close to the value recorded for the 1:1 complex in solution (651 nm). Since the electronic spectra represent the overall distribution of coordination environments, it can be inferred from these results that the nonimprinted material formed only a small percentage of 1:2 complexes at the lower concentration and nearly all 1:1 complexes at the higher two concentrations.

6-III.10.2 Copper Imprinted Hybrid

Figure 6.19 shows the diffuse reflectance spectra of the copper(II) loaded, copper(II) imprinted sorbent. As the concentration is increased the λ_{max} shifts from 595 nm, to 622 nm, and then to 638 nm. At the lowest concentration, the λ_{max} is midway between the values recorded for the 1:1 and 1:2 complexes. This indicates that approximately half of Cu(II) is bound to the imprinted sorbent as a 1:2 complex. As the concentration is increased, the percentage of Cu(II) absorbed as a 1:1 complex increases. The difference in λ_{max} values of 28 nm for the copper(II) loaded nonimprinted and copper(II) imprinted sorbents using 5×10^{-4} M Cu(II) solutions shows that the imprinted material does in fact bind more copper ions as the 1:2 complex. The copper imprinted sorbent may bind more Cu(II) in the 1:2 mode at lower concentrations, but concentrations lower than 5×10^{-4} M Cu(II) did not result in

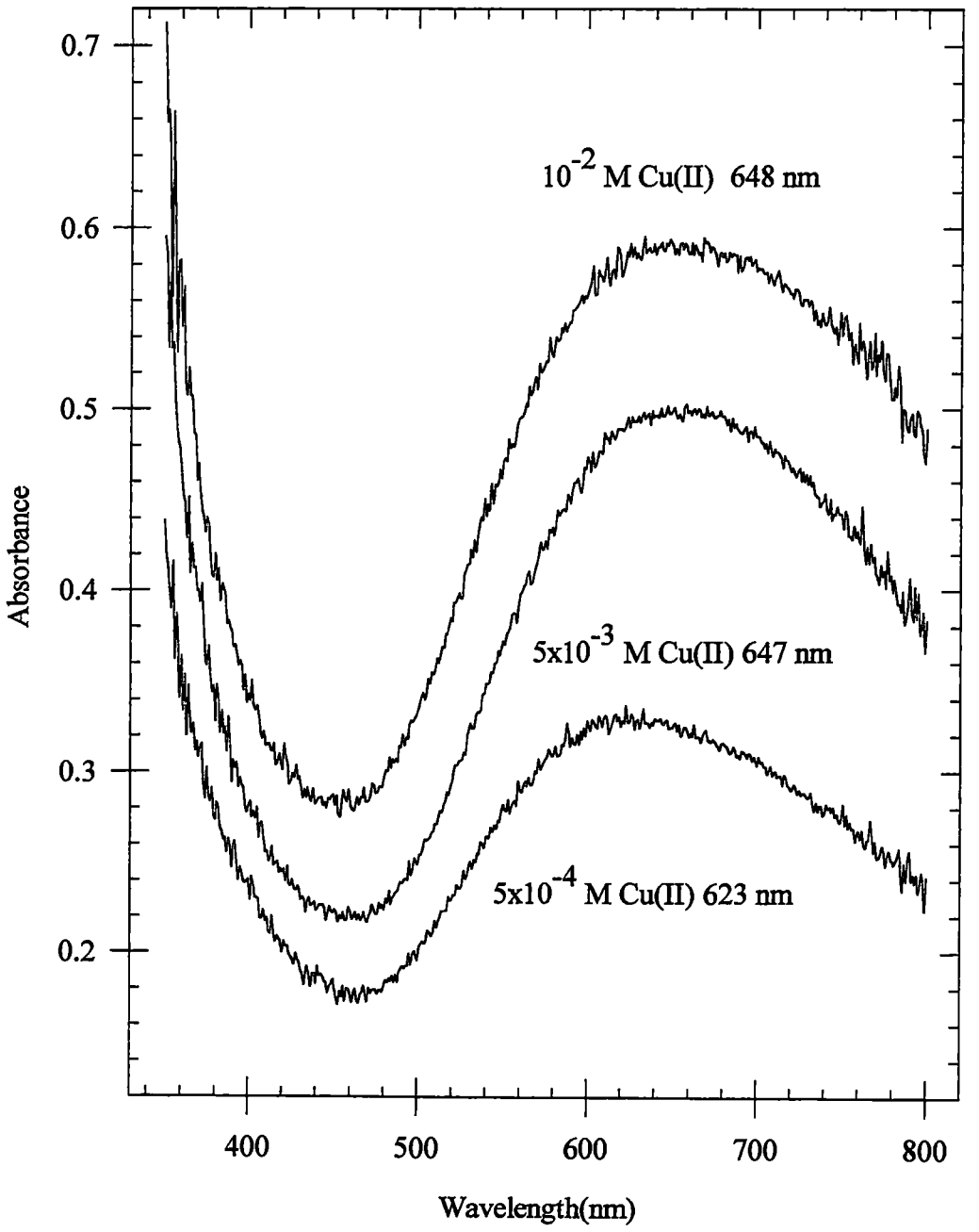


Figure 6.18 UV-visible diffuse reflectance spectra of reloaded nonimprinted hybrid sorbent.

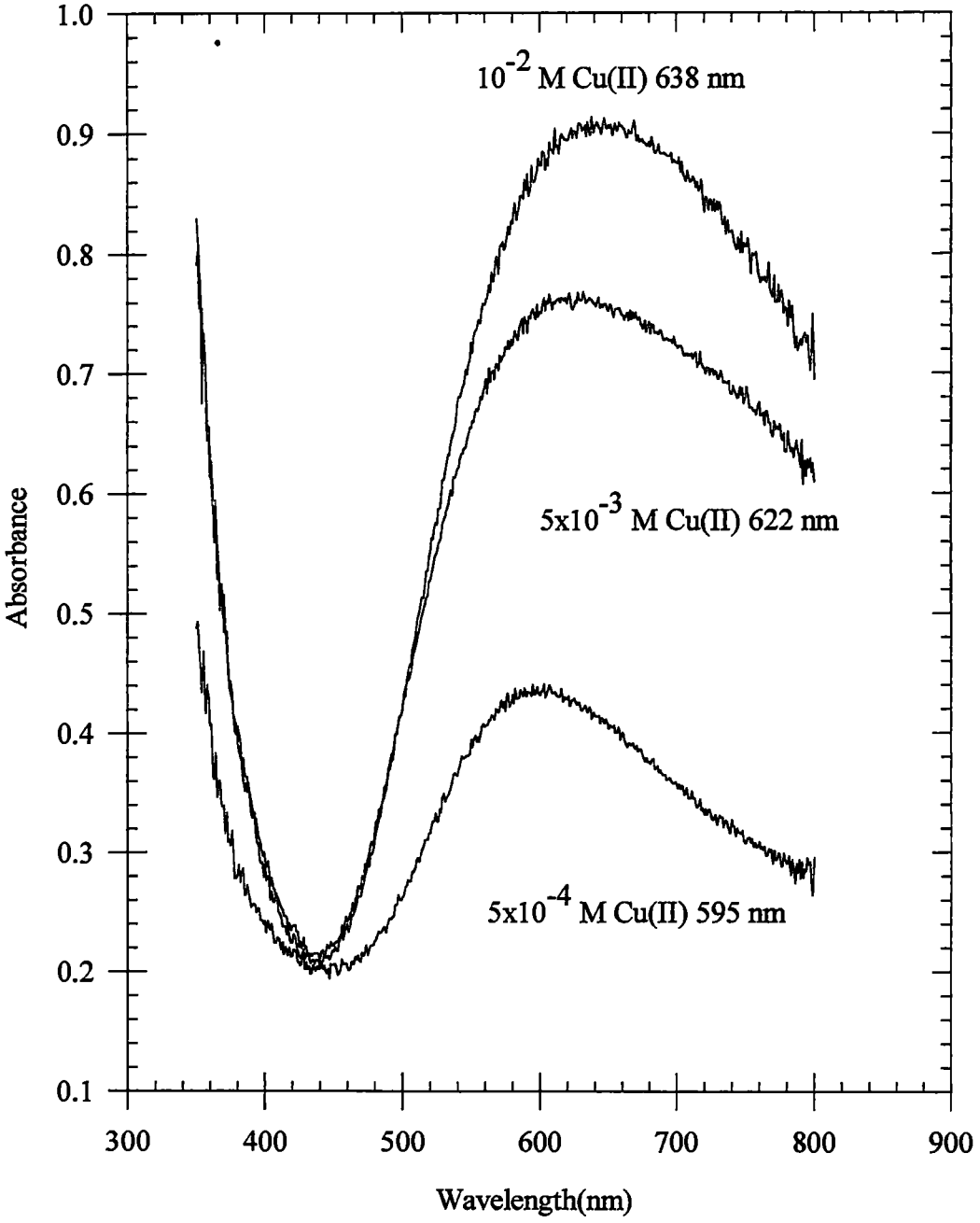


Figure 6.19 UV-visible diffuse reflectance spectra of reloaded Cu(II) imprinted sorbent

sorbents with a high enough absorbance to record meaningful results. The increase in the amount of 1:1 binding for both sorbents at higher concentrations can be explained by the stepwise stability constants for ethylenediamine with copper(II) (70). Since $K_1 > K_2$, the 1:1 binding mode is favored whenever the Cu(II) concentration is high enough.

6-IV. Conclusions

Molecular imprinting techniques have been used to synthesize organic-inorganic hybrid polymers with ionic recognition characteristics. 1,2-bis(triethoxysilyl)ethane (BTSE) monomers were copolymerized with metal ion complexes of N-[3-(trimethoxysilyl)-propyl]ethylenediamine (TMSen) in the presence of supramolecular assemblies of cetyltrimethylammonium chloride (CTAC), via room temperature, hydrolytic, sol-gel procedure. Subsequent extraction of the surfactant micelles and metal ions resulted in porous materials with a high affinity for the metal ion template. Selective sorbents were synthesized specifically for Cu(II), Ni(II), and Zn(II) cations. Adsorption studies indicate that these materials preferentially sequester the metal ion template from mixed solutions and exhibit fast uptake kinetics.

These materials have been characterized via nitrogen adsorption, small angle X-ray scattering, and UV-visible spectroscopy. Nitrogen adsorption indicates that these sorbents contain considerable porosity in the supermicoporous range. Small angle X-ray scattering plots contain peaks of high intensity corresponding to the (100) reflection, indicative of a hexagonally packed structure, but with the absence of any

higher order reflections typical of MCM-41 materials. These results seem to indicate that these materials have a pore structure with a wormhole motif with an average pore diameter of 10-15 Å. UV-Visible spectra show that at lower concentrations the copper(II) imprinted sorbents bind to the metal ions as both 1:1 and 1:2 metal to ligand complexes, while the nonimprinted sorbents bind primarily in a 1:1 configuration.

Future experiments that may reinforce these results are characterization via electron paramagnetic resonance spectroscopy (EPR) and transmission electron microscopy (TEM). EPR can be used to deduce the coordination environment of paramagnetic species such as Cu(II). A TEM image would be able to confirm the presence of a wormhole pore structure in these sorbent materials.

CHAPTER 7

CONCLUSIONS

7-I. Introduction

The synthesis and characterization of new metal ion sorbent materials have been described. Sorbents have been synthesized that selectively adsorb Cu(II), Zn(II), and Ni(II) cations. Four new methodologies have been developed and described herein: imprint coating, stepwise assembly, double imprinting, and organic-inorganic polymer imprinting. The imprint coating technique involves grafting of metal ion complexes of bifunctional reagents to the surface of mesoporous silica. Acid leaching of the metal ion template results in the formation of selective binding sites in which the ligands are arranged in a conformation well suited to rebind the template. In stepwise assembly, the bifunctional reagent is first grafted to mesoporous silica, followed by metal ion complex formation and the addition of more bifunctional reagent. In the double imprinting methodology, metal ion complexes of bifunctional reagents undergo copolymerization with silicon alkoxide precusors in the presence of supramolecular assemblies of surfactant molecules in a single step synthesis. Surfactant extraction gives a porous matrix with a large surface area. Hybrid organic-inorganic sorbents were synthesized using a protocol similar to double imprinting, except that the sol-gel precursor used was a bridged silicon alkoxide containing an ethylene group.

These sorbent materials have been characterized by a variety of techniques including: ^{29}Si solid-state nuclear magnetic resonance spectroscopy, N_2 adsorption, powder X-ray diffraction, UV/visible spectroscopy, and batch testing with subsequent ICP/OES analysis. These organofunctionalized sol-gel materials have been shown to exhibit a number of favorable properties including enhanced capacities for the target metal ion, selective adsorption of the target metal ion from mixed solutions containing competitor species, fast metal ion uptake kinetics, and easy regeneration.

7-II. Mesoporous Silica

The synthesis of MCM-41 by the base catalyzed procedure produced mesoporous silica with large surface areas (~1000 m^2/g) and sharp pore size distributions. Powder X-ray diffraction results clearly show that calcination does not result in damage to the mesoporous silica matrix. The reproducibility of the product by this experimental procedure is very good. The pore size (~29 Å) and large pore volumes make this material a good candidate for a sorbent support. Use of the mesitylene pore expander (CTAB/mesitylene) resulted in larger pores, but also very broad pore size distributions and a general decrease in long-range order.

A comparison of the nitrogen adsorption data for the calcined and extracted $CTAB/H^+$ silica samples clearly indicates that calcination is the more efficient process for surfactant removal. Powder X-ray diffraction patterns show that, although a slight contraction of the pores does take place during calcination (d-spacing decreased from 40.7 Å to 38.3 Å), the sharp peak indicates that the localized order is retained in the

matrix. The lack of porosity and very low surface area of the as-synthesized material indicated by the nitrogen adsorption analysis highlight the importance of the surfactant template in engineering the pore structures of these materials.

The acid catalyzed pathway ($CTAB/H^+$ silica) to porous silica has some advantages over similar base catalyzed procedures. This reaction proceeds relatively fast and no heating is required. Although the final product is very porous and has a substantial surface area, experimental data indicate that the great majority of the pores are actually between 10 and 15 Å in diameter. As a support in applications such as sorbents and catalysts, the pores may be too small to allow large molecules access to the inner pore spaces where the great majority of the surface area is located.

Although HMS materials were reported as having substantially thicker pore walls than their MCM-41 counterparts, our results show that the difference in wall thickness (23.2 Å for HMS and 20.9 Å for MCM-41) is very small. The general protocol for the synthesis of HMS requires no heating and shows excellent reproducibility, but requires a longer reaction time than the $CTAB/H^+$ silica synthesis which was also performed at ambient temperatures.

The synthesis of mesoporous silica using Tween 80 and Pluronic surfactants as the structure directing agents exhibited a much lower reproducibility than the MCM-41 and HMS analogs. Although the Tween 80 silica showed excellent porosity, no evidence for the reported cubic structure was found. The use of Pluronic F127 resulted in a highly porous network with unusual properties as shown by the multiple steps in the N_2 adsorption isotherm of Pluronic F127 silica. Although the reported

cubic structure was not elucidated, this may be an area of future study. The Pluronic P85 silica did not result in the relatively large pore sizes reported. It had a pore size similar to that of MCM-41, but with very thin (ca. 12 Å) pore walls. This could result in poor hydrothermal stability in this material. Pluronic P123 silica exhibited large pore sizes and highly ordered structures. One disadvantage of these materials is the long reaction time required for their formation.

7-III. Imprint Coating

The copper(II) uptake capacities of both the Cu(II) imprinted and nonimprinted sorbents synthesized with amorphous silica are considerably lower than those synthesized with MCM-41 as the support. While all of the sorbents made with MCM-41 removed greater than 98% of the copper(II) from 63.55 ppm solutions, none of the amorphous silica-based sorbents removed as much as 90%. In addition, the significant enhancement of copper(II) capacity exhibited by the Cu(II)-imprinted MCM-41-based sorbents, which resulted in a five to eight-fold increase in K_d values over nonimprinted samples, is not exhibited by the amorphous silica imprint-coated sorbents.

Key properties of our sorbents imprint-coated on MCM-41 thought to be a direct result of molecular imprinting are:

(3) The imprinted sorbents have larger effective adsorption capacities than the nonimprinted sorbents for the metal ion template from solutions containing no competitor species.

(4) The imprinted sorbents remove more of the metal ion template and less of the competitor species than the nonimprinted sorbents from mixed solutions. This results in larger selectivity coefficients (k) for the imprinted sorbents, and a relative selectivity coefficient (k') > 1.

The synthesis and characterization of BTMSen/CTAB/H^+ sorbents have shown that these materials have some unique properties. The results of the copper(II) adsorption experiments show an unprecedented enhancement of Cu(II) capacity for the Cu(II) imprinted sorbents over the nonimprinted samples. Despite this, the overall Cu(II) uptake is very low compared to that exhibited by similar sorbents synthesized with TMSen and TMSA. The competitive metal ion batch tests between Cu(II) and Zn(II) also show some unique properties of the BTMSen/CTAB/H^+ sorbents. As was the case in the single metal ion batch tests with Cu(II) descibed above, the overall metal ion capacities were very low. Despite this, both the Cu(II) imprinted and nonimprinted materials exhibited excellent selectivity for Cu(II), since they fail to absorb any significant amount of Zn(II). The experimental evidence suggests that the BTMSen ligand used in the synthesis of the Cu(II) imprinted and nonimprinted CTAB/H^+ silica sorbents may have reacted too vigorously. Although it may have coated the pores of the support, it seems likely that it may have also undergone homocondensation reactions, causing a significant decrease in the homogeneity of the sorbents. For these reasons we felt that the BTMSen bifunctional reagent may be better suited for the synthesis of a sorbents via double imprinting.

The copper(II) uptake capacities of the Cu(II) imprinted and nonimprinted TMSen/MCM-41 sorbents show a surprising trend. The copper(II) imprinted sorbents adsorbed more Cu(II) at the lower concentrations studied (0.64-6.35 ppm), but less at the higher concentrations (15.89-63.55 ppm). One explanation for this trend is that the nonimprinted material has more TMSen binding sites than the Cu(II) imprinted sorbent. Assuming a homogeneous distribution of TMSen in these sorbents and similar ligand loading, the nonimprinted material would have twice as many TMSen binding sites as the Cu(II) imprinted sorbent. This is due to the way in which the sorbents were synthesized. Since the $Cu(TMSen)_2^{2+}$ complex was formed prior to grafting, the TMSen ligands may be "paired up" in the imprinted sorbent. This results in a higher affinity for the metal ion template at low concentrations. At higher concentrations, when most of the sites in the Cu(II) imprinted sorbent are occupied, the nonimprinted sorbent still has many open sites and therefore, a higher copper(II) uptake.

The results of competitive ion sorption experiments performed with both the Cu(II) imprinted and nonimprinted sorbents using mixed solutions containing equimolar amounts of Cu(II) and Zn(II) show that the copper(II) imprinted sorbents exhibit higher selectivity coefficients for the Cu(II) ion than the nonimprinted materials at all concentrations studied.

The presence of free ethylenediamine ligands in the mixed solutions of Cu(II) and Zn(II) did not inhibit, but actually enhanced the metal ion binding ability of both Cu(II) imprinted and nonimprinted TMSen/MCM-41 sorbents. This effectively

reversed the selective binding properties normally exhibited by the Cu(II) imprinted sorbent in Cu(II)/Zn(II) mixed solutions that do not contain any free en.

N_2 adsorption and batch testing experiments indicate that the imprint-coated sorbents do not undergo ligand rearrangement on the MCM-41 surface, nor any significant structural changes within their matrices over the short term.

The use of calcined Pluronic P123-silica as the support for imprint-coated sorbents has shown very promising results. A comparison of the performance of these "large pore" sorbents (74 Å), with those employing MCM-41 (28 Å) indicate that there may be some distinct advantages to using them as the sorbent support. Both the Cu(II) imprinted and nonimprinted TMSen/P123 sorbents adsorbed more Cu(II) than the TMSen/MCM-41 sorbents from solutions with identical Cu(II) concentrations. Although both types of sorbent exhibit similar relative selectivity coefficients of 2.3 and 2.0 when used in batch tests with mixed solutions containing 10^{-3} M Cu(II)/10^{-3} M Zn(II), the TMSen/P123 sorbents had a total metal ion uptake approximately 50% higher than the TMSen/MCM-41 materials. This is significant because the synthesis of the TMSen/P123 sorbents used less than 10% of the TMSen per gram of sorbent support than was used in the TMSen/MCM-41 materials. This clearly illustrates that the majority of the TMSen bifunctional reagent used in the synthesis of the TMSen/MCM-41 was simply an excess, and was not needed. It should be noted that limited availability of the surfactant and a more time consuming synthesis of the support are two disadvantages associated with Pluronic P123 silica sorbents.

The experiments involving the adsorption of Cu(II), Zn(II), and Ni(II) on Pluronic P123 silica at pH = 5.0 were designed to determine if these processes were contributing to the overall adsorption behavior of the organofunctionalized sorbents. The adsorption of Cu(II) and Ni(II) were found to be insignificant, while Zn(II) was selectively adsorbed (ca. 7.5%).

Batch tests indicate that our sorbents imprint coated with TMSen readily undergo cation exchange reactions. Although these tests did not result in complete metal ion separations, they are very significant. Due to the nature of the basic research being described herein, as well as time and manpower limitations, metal ion adsorption by our sorbent materials were measured using "static" batch tests. For applications such as environmental remediation and industrial separations, high throughput columns are required. The significance of these ion exchange reactions cannot be underestimated.

For example, the Cu(II) imprinted TMSen/MCM-41 sorbent adsorbed 99.84% of the Cu(II) and 79.52% of the Zn(II) from an equimolar mixed solution of these two cations. This result may not seem impressive, but when the ion exchange properties of these materials are taken into account, many applications are possible. If the sorbent were packed into a large column and a steady flow of the Cu(II)/Zn(II) solution was eluted, the Zn(II) would be adsorbed initially as it was in the static batch test. As more Cu(II) was eluted all the Zn(II) ions would be exchanged out, leading to a much more efficient separation. In order to take this research to the next level, column testing of the sorbents developed herein must be performed.

^{29}Si solid –state NMR spectra indicate that despite our attempts to create nonimprinted sorbents for direct comparison, the metal ion imprinted sorbents synthesized via imprint coating have a lower ligand loading than the corresponding nonimprinted samples. This is a decided disadvantage and therefore, further indicates that the imprinted sites have a much higher affinity for the metal ion template. These results lead us to believe that if the metal ion imprinted and nonimprinted sorbents were synthesized with an identical ligand loading, the results of the metal ion adsorption batch tests would favor the metal ion imprinted sorbents even more than those described herein. The advantages of molecular imprinting would be far better illustrated, with larger enhancements of distribution constants and selectivity coefficients for the metal ion imprinted materials.

7-IV. Stepwise Assembly

A copper(II) imprinted sorbent synthesized via stepwise assembly has shown significant enhancement of copper(II) uptake capacities at various concentrations relative to a nonimprinted material made without the metal ion template. The imprinted material also exhibits improved selectivity for removal of copper(II) ions from Cu(II)/Zn(II) aqueous solutions. This material has copper(II) distribution coefficients and selectivity coefficients much larger than the imprint coated analog. ^{29}Si solid-state NMR results indicate that, like the imprint coated sorbents, the nonimprinted stepwise sorbents have a higher ligand loading than the corresponding copper(II) imprinted sorbents. It is important to note that the difference in ligand

loading is much smaller in the case of the stepwise materials. We attribute the better ionic recognition characteristics of the sorbents prepared by stepwise functionalization to this smaller difference.

7-V. Double Imprinting

A double imprinting methodology has been used to synthesize organofunctionalized mesoporous sol-gel sorbents which exhibit enhanced ionic recognition. Metal ions and supramolecular assemblies of sufactant molecules are both used as templates in this system. Removal of the templates creates two types of pores, each with a specific function. Acid washing removes the metal ions and creates micropores which contain binding sites with the size, shape, and coordination environment that the metal ion prefers. Extraction of surfactant micelles results in the formation of mesoporous channels throughout the sorbent matrix, giving the material good metal ion transfer kinetics. Batch tests conducted with Cu(II) imprinted and nonimprinted sorbents at five different Cu(II) concentrations ranging from 10^{-4}-10^{-3} M showed that the Cu(II) imprinted sorbent adsorbed more Cu(II) at all concentrations. A copper(II) adsorption study showed that 0.1 g of the Cu(II) imprinted sorbent adsorbed >95% of the Cu(II) from 10 mL of a 10^{-4} M Cu(II) solution within 15 min.

7-VI. Organic-Inorganic Hybrid

Organic-inorganic hybrid sorbents have been synthesized with Cu(II), Zn(II), and Ni(II) as the metal ion templates. All three sorbents exhibited enhanced capacities

for the metal ion template relative to a nonimprinted sorbent at the five concentrations studied in the range from 1 x 10^{-4} M to 1 x 10^{-3} M. The percentage of metal ion removed by the nonimprinted sorbent decreases considerably at higher concentrations, while the imprinted materials do not show a marked decrease. This is a clear example of the increased affinity of the imprinted sorbents for the metal ion template.
In order to test the selectivity of the copper imprinted hybrid sorbents, competitive ion binding batch studies were undertaken, with Zn(II) as the competitor species. The copper imprinted hybrid absorbed more Cu(II) and more Zn(II) than the nonimprinted material at all concentrations.

The selectivities of the nickel(II) and zinc(II) imprinted sorbents were investigated by competitive ion binding batch tests. The nickel(II) imprinted sorbent absorbed more Ni(II) than Zn(II) at all concentrations. In direct contrast to the adsorption behavior of the nickel imprinted material, the zinc(II) imprinted sorbent absorbed more Zn(II) than Ni(II) at all concentrations studied. This illustration of reversible imprinting shows the utility of molecular imprinting techniques in the synthesis of selective metal ion sorbents.

A very important attribute of any sorbent is the time required for the absorption process to take place. Many potential applications such as product or waste stream purification require relatively fast uptake kinetics for the sorbent technology to be a viable option. Batch testing showed that the copper(II) imprinted hybrid removed over 99.5% of the Cu(II) during the first minute. During this time the initial copper concentration (31.77 ppm) is reduced to 130 ppb.

A series of Cu(II) batch experiments were carried out with the copper(II) imprinted and nonimprinted hybrid sorbents in which copper(II) loaded sorbents were washed with 1 M HNO_3 to remove the metal ions, neutralized, and used to remove Cu(II) again. A slight decrease in K_d is shown by both sorbents for each successive use. Despite this small decrease, the copper(II) imprinted hybrid removed greater than 99.70 percent of the Cu(II) during the fifth and final cycle. These experiments illustrate the facile removal of the metal ion template and regeneration of these sorbent materials.

7-VII. Future Studies

Future experiments that may reinforce these results are characterization via electron paramagnetic resonance spectroscopy (EPR) and transmission electron microscopy (TEM). EPR can be used to deduce the coordination environment of paramagnetic species such as Cu(II). More TEM images would allow for better characterization of the pore structures in these sorbent materials, particularly for the confirmation of a wormhole motif in the hybrid sorbents.

Although static batch testing has served us well in performing this basic research, high throughput columns need to be used for adsorption studies if research is to be conducted at the applied level. Protocols developed here could be utilized for the synthesis of selective metal ion sorbents, which could be packed into columns. Sorbent capacities and selectivities for specific metal ions could then be measured using breakthrough curves, which plot the relative concentration versus the number of

bed volumes. Parameters could then be determined which are important on the industrial scale such as optimum flow rates and pressures. This could eventually lead to a number of practical applications for molecularly imprinted organofunctionalized sol-gel materials.

LIST OF REFERENCES

1. Ritcey, J.M.; Ashbrook, A.W.; *Solvent Extraction Principles and Applications to Process Metallurgy*, Part I. Elsevier, Amsterdam, **1984**.

2. Walsh, D.J.; Crosby, P.; Dalton, R.S.; *Polymer* **1983**, *24*, 423.

3. Helfferich, F. *Ion Exchange* McGraw-Hill, New York, **1962**.

4. Sahni, S.K.; Reedijk, J. *Coord Chem Rev.* **1984**, *59*, 1.

5. Landing, W.M.; Haraldsson, C.; Paxeus, N. *Anal Chem.* **1986**, *58*, 3031.

6. Bradshaw, J.S.; Bruening, R.L.; Krakowiak, K.E.; Tarbet, B.J.; Bruening, M.L.; Izatt, R.M.; Christensen, J.J. *J Chem. Soc , Chem. Commun.* **1988**, 812.

7. Izatt, R.M.; Bradshaw, J.S.; Bruening, R.L.; Krakowiak, K.E.; Tarbet, B.J.; Bruening, M.L.; Christensen, J.J. *Anal. Chem* **1988**, *60*, 1825.

8. Bradshaw, J.S.; Izatt, R.M. *Acc Chem. Res.* **1997**, *30*, 338.

9. Bradshaw, J.S.; Izatt, R.M.; Christensen, J.J.; Krakowiak, K.E.; Tarbet, B.J.; Bruening, R.L. *J. Inclusion Phenom.* **1989**, *7*, 127.

10. Akman, S.; Ince, H.; Koklu, U. *Anal Sci.* **1991**, *7*, 799.

11. Ince, H.; Akman, S.; Koklu, U. *Fresnius J. Anal Chem.* **1992**, *342*, 560.

12. Vieira, E.F.; Simoni, J.A.; Airoldi, C. J. *Mater. Chem.* **1997**, *7*, 2249.

13. Cestari, A.R.; Airoldi, C. *J. Coll. Inter Sci.* **1997**, *195*, 338.

14. Sing, K.S.W.; Everett, D.H.; Haul, R.A.W.; Moscou, L.; Pierotti, R.A.; Rouquerol, J.; Siemieniewska, T. *Pure Appl. Chem.* **1985**, *57*, 603.

15. Lao, H. In *Comprehensive Supramolecular Chemistry*; Atwood, J.L.; Davies, J.E.; Macnicol, D.D.; Vogtle, F., Eds.; Pergamon: New York, **1996**; Vol. 8, Chapter 6.

16. Kresge, C.T.; Leonowicz, M.E.; Roth, W.J.; Vartuli, J.C.; Beck, J.S. *Nature* **1992**, *359*, 710.

17. Beck, J.S.; Vartuli, J.C.; Roth, W.J.; Leonowicz, M.E.; Kresge, C.T.; Schmitt, K.D.; Chu, C.T.; Olsen, D.H.; Sheppard, E.W.; McCullen, S.B.; Higgens, J.B.; Schlenker, J.L. *J Am. Chem. Soc* **1992**, *114*, 10834.

18. Vartuli, J.C.; Schmitt, K.D.; Kresge, C.T.; Roth, W.J.; Leonowicz, M.E.; McCullen, S.B.; Hellring, S.D.; Beck, J.S.; Schlenker, J.L.; Olsen, D.H.; Sheppard, E.W. *Chem Mater.* **1994**, *6*, 2317.

19. Vartuli, J.C.; Kresge, C.T.; Leonowicz, M.E.; Chu, A.S.; McCullen, S.B.; Johnson, I.D.; Sheppard, E.W. *Chem Mater.* **1994**, *6*, 2070.

20. Beck, J.S.; Vartuli, J.C.; Kennedy, G.J.; Kresge, C.T.; Roth, W.J.; Schramm, S.E. *Chem Mater.* **1994**, *6*, 1816.

21. Wulff, G.; Sarhan, A. *Angew. Chem Int Ed Engl* **1972**, *11*, 341.

22. Robinson, D.K.; Mosbach, K.J. *Chem Soc., Chem Commun* **1989**, 969.

23. Vlatakis, G.; Andersson, L.I.; Muller, R.; Mosbach, K. *Nature* **1993**, *361*, 645.

24. Wulff, G. *Angew. Chem Int. Ed. Engl.* **1995**, *34*, 1812.

25. Takeuchi, T.; Matsui, J. *Acta Polymer* **1996**, *47*, 471.

26. Kuchen, W.; Schram, J. *Angew. Chem Int Ed Engl.* **1988**, *27*, 1695.

27. Dai, S.; Burleigh, M.C.; Shin, Y.S. *Imprint-Coating Synthesis of Selective Functionalized Ordered Mesoporous Sorbents for Separations and Sensors.* (patent applied for **1999**).

28. Dai, S.; Burleigh, M.C.; Shin, Y.; Morrow, C.C.; Barnes, C.E.; Xue, Z. *Angew Chem. Int. Ed.* **1999**, *38*, 1235-1239.

29. Burleigh, M.C.; Dai, S.; Hagaman, E.W.; Barnes, C.E.; Xue, Z.L. *ACS Symposium Series* (accepted for publication)

30. Burleigh, M.C.; Dai, S.; Barnes, C.E.; Xue, Z.L. *Separ Sci. Tech* (accepted for publication).

31. Dai, S.; Burleigh, M.C.; Ju, Y.H.; Gao, H.J.; Lin, J.S.; Pennycook, S.; Barnes, C.E.; Xue, Z.L. *J. Amer. Chem Soc* **2000**, *122*, 992.

32. Burleigh, M.C.; Dai, S.; Hagaman, E.W. *Chem. Mater* (submitted).

33. Corma, A. *Chem. Rev* **1997**, *97*, 2373.

34. Huo, Q.; Margolese, D.I.; Stucky, G.D. *Chem. Mater.* **1996**, *8*, 1147.

35. Bagshaw, S.A.; prouzet, E,; Pinnavaia, T.J. *Science* **1995**, *269*, 1242.

36. Bagshaw, S.A.; Pinnavaia, T.J. *Angew. Chem., Int. Ed Engl.* **1996**, *35*, 1102.

37. Prouzet, E.; Pinnavaia, T.J. *Angew. Chem., Int. Ed Engl.* **1997**, *36*, 516.

38. Zhao, D.; Huo,Q.; Feng, J.; Chmelka, B.F.; Stucky, G.D. *J. Am Chem. Soc.* **1998**, *120*, 6024.

39. Brunauer, S.; Emmett, P.H.; Teller, E *J. Amer. Chem Soc* **1938**, 60, 309.

40. Barrett, E.P.; Joyner, L.G.; Halenda, P.P. *J. Amer. Chem. Soc* **1951**, 73, 373.

41. Azaroff, L.V. *X-ray Diffraction*; McGraw-Hill: New York, **1974**.

42. Beck, J.S. *U S.Patent No.* 5,057,296 (**1991**).

43. Izatt, R.M. *J Inclusion Phenom.* **1997**, *29*, 197.

44. Mercier, L.; Pinnavaia, T.J. *Adv Mater.* **1997**, *9*, 500.

45. Mercier, L.; Pinnavaia, T.J. *Environ Sci. Technol..* **1998**, *32*, 2749.

46. Feng, X.; Fryxell, G.E.; Wang, L.Q.; Kim, A.Y.; Liu, J.; Kemner, K.M. *Science* **1997**, *276*, 923.

47. Liu, J.; Feng, X.; Fryxell, G.E.; Wang, L.Q.; Kim, A.Y.; Gong, M. *Adv Mater.* **1998**, *10*, 161.

48. Chen, X.B.; Feng, X.D.; Liu, J.; Fryxell, G.E.; Gong, M.L. *Separ Sci Technol.* **1999**, *34*, 1121.

49. Mattigod, S.V.; Feng, X.D.; Fryxell, G.E.;Liu, J.; Gong, M.L. *Separ. Sci Technol.* **1999**, *34*, 1121.

50. Wulff, G.; Heide, B.; Helfmeier, G. *J. Am. Chem Soc.* **1986**, *108*, 1089.

51. Shea, K.J.; Dougherty, T.K. *J Am Chem. Soc.* **1986**, *108*, 1091.

52. Yu, K.Y.; Tsukagoshi, K.; Maeda, M.; Takagi, M. *Anal Sci.* **1992**, *8*, 701.

53. Banks, D.; Younger, P.L.; Arnesen, R.T.; Iversen, E.R.; Banks, S.B. *Environ Geol.* **1997**, *32*, 157.

54. Mantei, E.J.; Sappington, E.J. *Environ. Geol* **1994**, *24*, 287.

55. Brower, J.B.; Ryan, R.L.; Pazirandeh, M. *Environ. Sci. Tech* **1997**, *31*, 2910.

56. De Caritat, P.; Danilova, S.; Jaeger, O.; Reimann, C.; Storro, G. *J. Hydrol.* **1998**, *208*, 92.

57. Fazeli, M.S.; Sathyanarayan, S.; Satish, P.N.; Muthanna, L. *Environ Geol Water Sci* **1991**, *17*, 47.

58. Shriver, D.F.; Atkins, P.; Langford, C.H. *Inorganic Chemistry*, 2nd ed., Freeman: New York, **1994**.

59. Tsukagoshi, K.; Yu, K.Y.; Maeda, M.; Takagi, M. *Bull Chem Soc Jpn.* **1993**, *66*, 114.

60. Tsukagoshi, K.; Yu, K.Y.; Maeda, M.; Takagi, M.;Miyajima, T. *Bull Chem. Soc Jpn.* **1995**, *68*, 3095.

61. Kabanov, V.A.; Efendiev, A.A.; Orujev, D.D. *J. Appl Polym. Sci.* **1979**, *24*, 259.

62. Nishide, H.; Deguchi, J.; Tsuchida, E. *J Polym. Sci.* **1977**, *15*, 3073.

63. Lever, A.P.B. *Inorganic Electronic Spectroscopy*, Elsiever, New York, **1968**.

64. Baker, A. *J Chem. Edu.* **1998**, *75*, 98.

65. Amphlett, C.B. *Inorganic Ion Exchangers*, Elsevier, Amsterdam, **1964**.

66. Burwell, R.L.; Chack, S.P.; Haller, G.L.; Pearson, R.G.; Tjok, P.B *Inorg. Chem.*, **1965**, *4*, 1123.

67. Markova, V.; Vydra, F. *J Inorg. Nuclear Chem.*, **1964**, *26*, 1319.

68. Kozawa, A. *J Inorg Nuclear Chem.*, **1961**, *21*, 315.

69. Cummings, W.W.; Dugger, D.L.; Irby, B.N.; Maatman, R.W.; McConnell, B.L.; Stanton, J.H. *J Phys Chem.*, **1964**, *68*, 757.

70. Smith, R.M.; Martell, A.E. In *Critical Stability Constants*, Plenum: New York **1975**, Vol. 2.

71. Warshawsky, A. In *Ion Exchange and Sorption Processes in Hydrometallurgy*, Wiley: New York, **1987**, Chapter 4.

72. Maciel, G.E. In *Solid State NMR Spectroscopy of Inorganic Materials*, ACS: Washington, D.C., **1998**, Chapter 12.

73. Maciel, G.E. *Solid State NMR of Polymers*, Elsevier: Amsterdam, **1999**.

74. Khatib, I.S.; Parish, R.V. *J Organomet. Chem* **1989**, *369*, 9.

75. Parish, R.V.; Habibi, D.; Mohammadi, V. *J. Organomet. Chem* **1989**, *369*, 17.

76. El-Nahhal, I.M.; Parish, R.V. *J. Organomet Chem.* **1993**, *452*, 19.

77. Ahmed, I.; Parish, R.V. *J. Organomet. Chem.* **1993**, *452*, 23.

78. Macquarrie, D.J. *Chem Comm.* **1996**, 1961.

79. Burkett, S.L.; Sims, S.D.; Mann, S. *Chem Comm.* **1996**, 1367.

80. Fowler, C.E.; Burkett, S.L.; Mann, S. *Chem. Comm.* **1997**, 1769.

81. Loy, D.A.; Shea, K.J. *Chem Rev.* **1995**, *95*, 1431.

82. Corriu, R.J.P.; Leclercq, D. *Angew Chem Int. Ed. Engl* **1996**, *35*, 1420.

83. Cerveau, G.; Corriu, R.J.P. *Coord Chem. Rev.* **1998**, *178-80*, 1051.

84. Shea, K.J.; Loy, D.A. *Chem. Mater.* **1989**, *1*, 572.

85. Shea, K.J.; Loy, D.A.; Webster, O. *J. Am. Chem Soc* **1992**, *114*, 6700.

86. Corriu, R.J.P.; Moreau, J.J.E.; Thepot, P.; Man, M.W.C. *Chem. Mater* **1992**, *4*, 1217.

87. Oviatt, H.W.; Shea, K.J.; Small, J.H. Chem. Mater. **1993**, *5*, 943.

88. Corriu, R.J.P.; Moreau, J.J.E.; Thepot, P.; Man, M.W.C. *Chem Mater* **1994**, *6*, 640.

89. Inagaki, S.; Guan, S.; Fukushima, Y.; Ohsuna, T.; Terasaki, O. *J. Am Chem. Soc* **1999**, *121*, 9611.

90. Melde, B.J.; Holland, B.T.; Blanford, C.F.; Stein, A. Chem. Mater. **1999**, *11*, 3302.

91. Asefa, T.; MacLachlan, M.J.; Coombs, N.; Ozın, G.A. Nature **1999**, *402*, 867.

92. Cotton, F.A.; Wilkinson, G.; Murillo, C.A.; Bochmann, M. *Advanced Inorganic Chemistry*, 6th ed., Wıley & Sons, Inc. New York, **1999**.

93. Shriver, D.F.; Atkins, P.; Langford, C.H. *Inorganic Chemistry*, 2nd ed., Freeman and Company, new York, **1994**.

94. Brower, J.B.; Ryan, R.L.; Pazirandeh, M. *Envıron Sci Tech* **1997**, *31*, 2910.

95. Mantei, E.J.; Sappington, E.J. *Envıron. Geol* **1994**, *24*, 287.

96. Tanev, P.T.; Chibwe, M.; Pinnavaia, T.J. *Nature* **1994**, *368*, 321.

97. Tanev, P.T.; Pinnavaia, T.J. *Science* **1995**, *267*, 865.

98. Brunauer, S.; Deming, L.S.; Deming, W.S.; Teller, E. *J. Amer Chem Soc.* **1940**, 62, 1723.

99. Gregg, S.J.; Sing, K.S.W. *Adsorptıon, Surface Area, and Porosity*, 2nd ed., Academic Press, New York, **1983**.

100. Lippens, B.C.; De Boer, J.H. *J Catal.* **1965**, *4*, 319.

VITA

Mark Charles Burleigh was born in Oneida, New York, on April 14, 1967. He attended Morrisvile-Eaton Central School in Morrisville, New York. In May 1985, he graduated from Morrisville-Eaton High School. He recieved an A.A.S. in Chemical Technology from the State University of New York, Agricultural and Technical College at Cobleskill in May 1993. In May 1996, he recieved his B.S. in Chemistry from Beloit College, Beloit Wisconsin. He then entered the graduate program in the Department of Chemistry, The University of Tennessee, Knoxville, and received his Ph.D. degree in August 2000.